Friends of the Pleistocene
Yucca Mountain, Nevada
October 9-11, 1998

Quaternary Geology of the Yucca Mountain Area, Southern Nevada

Field Trip Guide

Editor: Emily M. Taylor

Coleader: Ralph E. Klinger

Prepared for the 1998 annual meeting of the
Friends of the Pleistocene, Pacific Cell
October 9-11, 1998

List of Coleaders (underlined) and Coauthors

Larry Anderson
U.S. Bureau of Reclamation
Geophysics, Paleohydrology, and Seismotectonics Group
Box 25007, D-8330
Denver, Colorado 80225-0007
landerson@do.usbr.gov

Brian J. Andraski
U.S. Geological Survey
333 W. Nye Lane
Carson City, Nevada 89706
andraski@usgs.gov

David A. Beck
U.S. Geological Survey
6770 S. Paradise Rd.
Las Vegas, Nevada 89119
dabeck@usgs.gov

John W. Bell
Nevada Bureau of Min
es and Geology
University of Nevada, Reno
Reno, Nevada 89557-0088
jbell@nbmg.unr.edu

James Brune
Seismology Laboratory 174
University of Nevada
Reno, Nevada 89557

James Budahn
U.S. Geological Survey, MS 974
Denver Federal Center, Box 25046
Denver, Colorado
jbudahn@usgs.gov

Jeffrey A. Coe
U.S. Geological Survey, MS 966
Denver Federal Center, Box 25046
Denver, Colorado
jcoe@usgs.gov

Richard Craun
U.S. Department of Energy
Yucca Mountain Site Characterization Office
MS 523, Box 30307
North Las Vegas, Nevada 89036-0307

Warren C. Day
U.S. Geological Survey, MS 421
Denver Federal Center, Box 25046
Denver, Colorado

Heather Huckins Gang
Bechtel
Las Vegas, Nevada
ganghh@nv.doe.gov

Patrick A. Glancy
U.S. Geological Survey
333 W. Nye Lane
Carson City, NV 89706
paglancy@usgs.gov

John Gosse
Quaternary Surface Processes
Department of Geology
120 Lindley Hall
University of Kansas
Lawrence, Kansas 66045
gosse@ukans.edu

William Guertal
U.S. Geological Survey
1261 Town Center Drive
Las Vegas, NV 89134
wguertal@usgs.gov

Charles Harrington, J521
Los Alamos National Lab, EES-13
Los Alamos, NM 87545
charrington@lanl.gov

Michael J. Johnson
U.S. Geological Survey
333 W. Nye Lane
Carson City, NV 89706
johnsonm@usgs.gov

Ralph Klinger
U.S. Bureau of Reclamation
Geophysics, Paleohydrology, and Seismotectonics Group
Box 25007, D-8330
Denver, Colorado 80225-0007
rklinger@do.usgr.gov

Scott Lundstrom
U.S. Geological Survey, MS 951
Denver Federal Center, Box 25046
Denver, Colorado
sclundst@usgs.gov

Shannon Mahan
U.S. Geological Survey, MS 963
Denver Federal Center, Box 25046
Denver, Colorado 80225
smahan@usgs.gov

Chris M. Menges
U.S. Geological Survey MS 423
1261 Town Center Cr.
Las Vegas, Nevada 98134
cmmenges@usgs.gov

Fred Peterson
Professor Emeritus
University of Nevada
Reno, Nevada
ffpeters@scs.unr.edu

Silvio Pezzopane
U.S. Geological Survey, MS 425
Denver Federal Center, Box 25046
Denver, CO 80225-0046
spezzo@usgs.gov

Christopher J. Potter
U.S. Geological Survey, MS 421
Denver Federal Center, Box 25046
Denver, CO 80225-0046
cpotter@usgs.gov

Alan R. Ramelli
Nevada Bureau of Mines and Geology
Mackay School of Mines
University of Nevada, MS 178
Reno, Nevada 89557-0088
ramelli@nbmg.unr.edu

Marith C. Reheis
U.S. Geological Survey, MS 980
Denver Federal Center, Box 25046
Denver, CO 80225
mreheis@usgs.gov

Daniel Soeder
U.S. Geological Survey
1289 McD Drive
Dover, DE 19901
dsoeder@usgs.gov

David A. Stonestrom
U.S. Geological Survey MS 421
345 Middlefield Road
Menlo Park, CA
dastones@usgs.gov

J. Timothy Sullivan
US Department of Energy
Yucca Mountain Site Characterization Office
MS 523, Box 30307
North Las Vegas, Nevada 89036-0307
tim_sullivan@notes.ymp.gov

Don S. Sweetkind
U.S. Geological Survey MS 421
Denver Federal Center, Box 25046
Denver, CO 80225
dssweetk@usgs.gov

Emily M. Taylor
U.S. Geological Survey MS 425
Denver Federal Center, Box 25046
Denver, Colorado 80225
emtaylor@usgs.gov

Andrew Thomas
Geomatrix Consultants Inc.
100 Pine Street
San Francisco, California 94111

John Wesling
Geomatrix Consultants Inc.
100 Pine Street
San Francisco, California 94111
jwesling@geomatirx.com

John W. Whitney
US Geological Survey, MS 425
Box 25046
Denver, Colorado 80225
jwhitney@usgs.gov

James Yount
US Geological Survey, MS 980
Box 25046
Denver, Colorado 80225
jyount@usgs.gov

Quaternary Geology of the Yucca Mountain Area, Southern Nevada

Friends of the Pleistocene, Pacific Cell
1998 Annual Meeting

Table of Contents

ROAD LOG FOR FIELD TRIP IN THE YUCCA MOUNTAIN AREA, SOUTHERN NEVADA

Friends of the Pleistocene, Pacific Cell, October 9th- 11th

Mileage Cum.	Int.	Driving directions are underlined

DAY ONE--Friday October 9th, East Side of Yucca Mountain

0.0 0.0 Return to the paved road from the camping area at Big Dune.

1.4 1.4 Turn north (left) on Valley View Dr. Straight ahead is the southern extent of Yucca Mountain; just to the west lies the Lathrop Wells cinder cone, which represents the youngest center of basaltic volcanism in the area. The age and number of eruptions at this cone has been the center of controversy over the last decade. Original K-Ar dating by B. Turrin, D. Champion, and R. Fleck of the U.S. Geological Survey suggested a single eruption with an age of 120 ka which was later refined to a 130-140 ka interval by Ar/Ar and paleomagnetic work (Turrin and others, 1991). Geochemical analyses of different mapped flows and tephra units were interpreted by B. Crowe and F. Perry to indicate multiple (possibly as many as four) eruptions at the center (Crowe and others, 1995). This was supported by a wide range of geochronologic data, spanning an age range of 130 to 25 ka, based on many different methods, including Ar/ Ar and cosmogenic exposure dating of the volcanics, plus U-series and TL dating of soils and interbedded eolian sands. S. Wells and L. McFadden estimated multiple eruptions with a 20-ka age for the youngest eruption based on geomorphic-soil analyses of cone morphology and stratigraphy (Wells and others, 1990). The recently completed Probabilistic Seismic Hazard Analysis has accepted the single-eruption hypothesis with a preferred age of 75±10 ka, based primarily on a general convergence in this age range of numerous additional Ar/Ar ages of flows and tephra, as well as many of the earlier TL, U-series, and cosmogenic dating results. However, there are still a large amount of variation both within and among the various methods used to date volcanic, sedimentary, and pedogenic features at this site, which is a very important lesson in the application of existing geochronologic methods to date late to middle Pleistocene landforms, volcanism, and deposits.

3.6 2.2 Turn southeast (right) on Hwy 95.

8.1 4.5 Crossing the medial facies of Fortymile Wash. This is one of two major tributaries of the Amargosa River (the other being the drainage in Oasis Valley to the northeast of Beatty). Fortymile Wash heads in the mountainous area of Timber Mountain caldera, one of the large eruptive centers for the late Miocene volcanism located north and northeast of Yucca Mountain. Stratigraphic and

geomorphic evidence suggests a latest Miocene to Pliocene establishment for the present south-flowing drainage (see Lundstrom, this volume). Upon leaving bedrock, Fortymile Wash drains southward along the eastern flank of Yucca Mountain and forms the principal drainage for the eastern side of the mountain. The wash is deeply incised into alluvium along this reach (see Stop 3 later in the day) before it develops downstream into the broad distributary fan system observed at this highway crossing.

11.6 3.5 Turn north (left) just before the cattle guard onto the Lathrop Wells Gate (Gate 511) road Just west of the town of Amargosa Valley, formerly called Lathrop Wells. The main gate to the Nevada Test Site is located about 25 miles to the southwest on Hwy 95 at Mercury.

13.4 1.8 Stop at the Lathrop Wells Gate to complete the badging and security checks. Security at the Test Site is taken very seriously by the guards. Your cooperation and patience may help speed the process of badging.

16.4 3.0 These are MX missile silos on your left.

17.2 0.8 Turn off on the right to the X-tunnel and Little Skull Mountain. The hypocenter for the Little Skull Mountain earthquake (June 29, 1992; magnitude = 5.6) was located near the west end of this topographic high. The hypocenter for this earthquake, which is the largest magnitude historically-recorded event in the site area, occurred at a depth of approximately 9 km. Focal mechanisms indicate predominantly normal slip, with a subordinate left-oblique component, that probably occurred on northeast-striking fault that dips steeply (50°-70°) to the southeast. No surface displacements or ground cracking were observed during extensive post-earthquake investigations, although the FOC, which lies directly on the updip projection of the fault surface, did suffer considerable damage from vibratory ground motions.

20.7 3.5 Skull Mountain, straight ahead, is capped by a 10 million year old basalt that is used to constrain the regional basin and range faulting, although timing of faulting in the South Western Nevada Volcanic Field (SWNVF) is highly variable. Varnish on stone stripes on the hill slopes of this mountain have been dated by the varnish cation technique at more than 500 ka. Based on these ages and current morphology, erosion rates of < 1 cm/k.y. have been calculated (Whitney and Harrington, 1993).

24.1 3.4 Turn north (left) just before the large building. This building is the Yucca Mountain Field Operations Center (FOC) where "You Make Safety Ours"(?). The USGS, in its heyday at Yucca Mountain, had large spacious working areas in this building, which have since been filled with contractors. This building suffered extensive damage as a result of the 1992 Little Skull Mountain earthquake. The Nevada Test Site is subdivided into areas, the most famous of which is Area 51,

many miles to the northeast. This is Area 25, originally developed as a testing area for nuclear propelled rockets. We will pass a few of the test pads on the way to Yucca Mountain.

24.3 0.2 The building on your right is the USGS Hydrologic Research Facility (HRF, pronounce "hurf"). Properties of rock and sediment samples from both the saturated (SZ) and unsaturated zone (UZ) are tested in at this facility. The geologist are allowed to store a few shovels in the trailers in the back. Across the street is the Sample Management Facility (SMF, pronounced "smurf") where conceivably every rock and sediment sample collected in connection to the Yucca Mountain project, analyzed or not, is stored.

26.4 2.1 Turn west (left) following the signs to Yucca Mountain. Straight ahead is elongate north-trending series of ridges of Yucca Mountain, which the potential site for the high-level radioactive waste repository. The brightly-colored hydrothermally-altered late Miocene volcanic rocks of the Calico Hills are to the north of the road (at 3:00). We are driving across Jackass Flats which slopes southward from the Calico Hills. The Death Valley Emigrant Trail went through here. It was a shortcut into southern California in the late 1840's, but lack of water and difficult terrain caused it to be abandoned within a few years. Jackass Flats is a low-relief alluvial piedmont which slopes southward to southwestward from the Calico Hills subparallel to Fortymile Wash, which is incised below our line of sight along the base of Yucca Mountain in the middle foreground.

32.2 5.8 On the south side of the road is one of a number of borrow pits that provided aggregate used in the construction of surface facilities and concrete for inverts used in the Exploratory Studies Facility (ESF; see stop 6; Soeder, this volume). This is a horseshoe-shaped tunnel approximately 8 km in length and 7.9 m in diameter that has been constructed to study geologic, hydrologic, and geomechanical conditions at the subsurface level of the potential repository (see Soeder, this volume).

32.7 0.5 We are dropping into Fortymile Wash (see earlier discussion at mileage 8.1; also Lundstrom, this volume). Early work suggested that the upper part of this wash incised into alluvium (from approximately where we are northward to the bedrock canyon) was fault controlled, but geophysical studies (particularly seismic reflection profiles) have failed to confirm the presence of a significant subsurface fault.

33.2 0.5 Turn south (left) onto the dirt road before you begin to climb out of Fortymile Wash into Sever Wash, following the sign to the Crest of Yucca Mountain.

34.5 1.3 On the west side of the road you can see a cube draped in a white cover. It is not an NEA funded project, but in fact a bedrock cube excavated for a study of the change in hydrologic and rock properties as a function of temperature. Busted

Butte is straight ahead. We will visit the sand ramps on the west side later today at stop 2. These ramps are cut by the Paintbrush Canyon fault, a major Quaternary fault on the eastern flank of the mountain, and preserve a 740 ka history of fault displacement.

38.7 4.2 Crossing above the ESF tunnel.

39.3 0.6 Crossing above the ESF again.

41.2 1.9 **Stop 1 (9-10:00 am) Top of Yucca Mountain overlooking Crater Flat.**

Sullivan--Yucca mountain selected as a possible site to locate a high level nuclear waste site, presence of DOE--Site Characterization of Yucca Mountain, including Quaternary geology/Regional fault studies, Excavation of trenches across projections of bedrock faults

Potter--Geologic mapping investigations (see Potter and others, this volume summary of mapping of bedrock faults in area of the central repository block)

Guertal--Summary of Hydrologic investigations, including studies of the Saturated Zone, Unsaturated Zone, and Surface runoff

Pezzopane--Paleoseismic synthesis of Quaternary faulting at Yucca Mountain (see below and Pezzopane and others, this volume)

Standing on Yucca Crest, with the Solitario Canyon fault at the base of the escarpment beneath our toes, looking to the east, one can see the tops of several parallel ridges and plateaus that trend northward, similar to the ridge we are standing on and to the Bare Mountain range in the distance. One can see and feel how Neogene and Quaternary faulting along the six or eight principal normal faults has split the Yucca Mountain area into a series of north-striking, gently east-dipping structural blocks. The faults strike approximately north, dip moderately to steeply west, and are commonly spaced only a few km apart.

The USGS efforts focused at providing the geologic, geophysical, and paleoseismic data necessary to characterize the Quaternary fault activity and Neogene tectonics for use in a probabilistic seismic hazard analysis (PSHA). The faults closest to Yucca Mountain are most important to two types of seismic hazard: vibratory ground-motion and fault displacement. Input to the PSHA required characterization of earthquake magnitude and recurrence interval, which are commonly revealed from the geological record of the size and timing of pre-historical earthquakes that ruptured faults at the surface. In all, 52 trenches or natural exposures across faults were examined and logged; 40 (of 52) are across the 6-to-8 principal Quaternary faults; and 28 (of 40) show displaced or deformed Quaternary deposits.

Our compilation (Pezzopane, Whitney, and Dawson, figures 1, 2 and 3) of paleoseismic displacement and timing data from all trenches or natural exposures across faults reveals that in the past 500 ka geologic record, 39 paleoevents were recognized on faults located within a 15-km radius (includes Bare Mountain fault, but not Rock Valley fault), disregarding the age of the paleoevents. The 150 ka record, a subset of the data, reveals 26 paleoevents. In the simplest recurrence model, if each paleoevent is an individual paleoearthquake, these values indicate one surface-rupturing earthquake occurs on average about every 6 ka to 13 ka. However, this is accurate only if each paleoevent is an individual paleoearthquake, which is likely not the case -- we have double-counted some paleoevents (i.e. could double-count if one paleoevent is same paleoevent on same fault, or, if one paleoevent is same paleoevent on another fault). If one assumes that only the relatively large displacements (one-half to 1 meter) correspond to independent earthquakes (considers that smaller displacements are the product of secondary or distributed faulting), the past 150-ka record is marked by 8 large-displacement events, for an average recurrence interval of approximately 19 ka. These values, although not very accurate or precise, represent how often one would have felt a surface-rupturing earthquake if they had been sitting on Yucca crest since the middle Pleistocene. Recurrence intervals for individual faults are much longer.

Our preferred model correlates the paleoevents in time using stratigraphic and geochronological constraints from the trench studies to produce paleoearthquake rupture scenarios for Yucca Mountain faults. We used geological constraints to aggregate the probability density functions of paleoevent ages and their uncertainties, relying exclusively on the past 150-ky paleoseismic record. Here we assume distributed faulting has occurred on the basis of: 1) close spacing between faults, 2) the interconnectedness of many faults, 3) the overlap of timing data for events, and 4) the patterns of principal and distributed faulting observed during historical earthquakes on faults in the Great Basin. Using geological constraints to plot probability density functions of paleoevent ages and timing uncertainties indicate 9 paleoearthquakes occurred in the past 150 ky providing an average interevent return time of approximately 12 to 25 ka. Individual interevent return times measured peak-to-peak from the probability density functions range from approximately 7 ± 3 ka to 25 ± 10 ka. Uncertainties in dating a paleoearthquake are always present because the age can, except in a couple of unusual cases, only be bounded by dates on the deposits or soils associated with or effected by the paleoevent. Geological constraints on the correlation of events indicate some of the paleoevents, particularly those associated with volcanic ash in fault-related fissures and deposits, appear related to each other and are closely related in time, perhaps occurring simultaneously. Paleoseismic data cannot, however, prove simultaneous rupture.

Paleoearthquake magnitudes are derived from paleoevent displacement data, and whether a given trench has a given paleoevent and that trenches along-strike

A) Paleoseismic Study Sites and Mapped Faults at Yucca Mountain

EXPLANATION

- Paleoseismic Trench Locations
- Faults; Quaternary and suspected Quaternary age of last movement
- Faults; pre-Quaternary or undetermined age of last movement
- Approximate Potential Repository Area and Exploratory Studies Facility
- Approximate Controlled Area Boundary

Fault Abbreviations

BR =	Bow Ridge
DW =	Dune Wash
FW =	Fatigue Wash
GD =	Ghost Dance
IR =	Iron Ridge
NCF =	Northern Crater Flat
PC =	Paintbrush Canyon
SD =	Sundance
SC =	Solitario Canyon
SCF =	Southern Crater Flat
SCR =	Stagecoach Road
WW =	Windy Wash

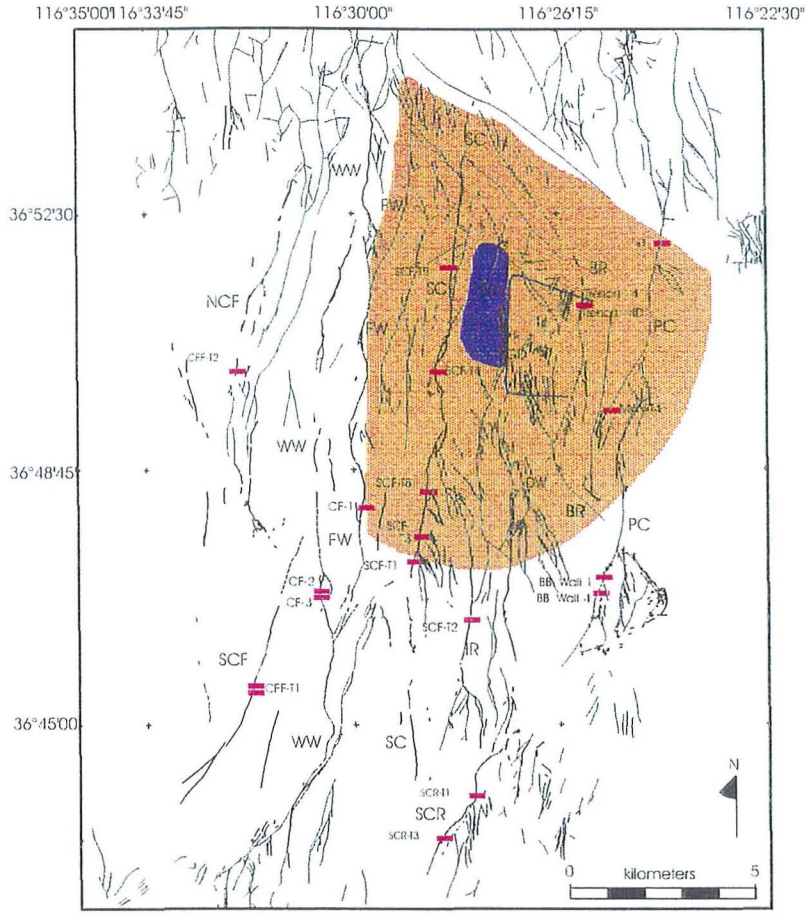

Map of late Tertiary and younger faults and paleoseismic study sites at Yucca Mountain. Fault traces with evidence of Quaternary scarps are shown with bolder and darker lines. Fault map modified from Simonds and others (1995).

B)

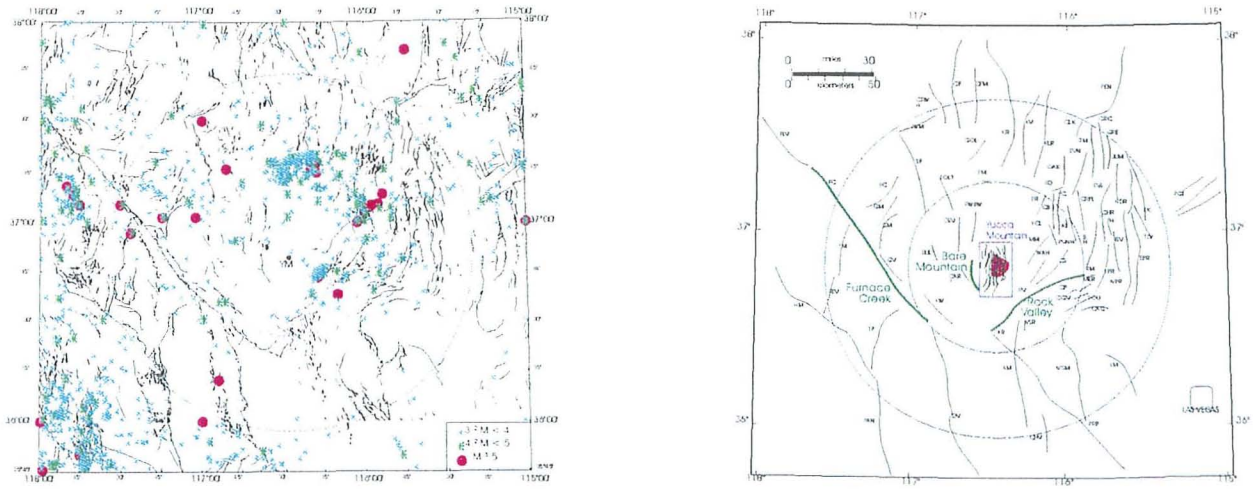

Maps of historical seismicity and known and suspected Quaternary faults within 100 km of Yucca Mountain. Earthquakes of magnitude greater than 3 (USGS–University Nevada-Reno catalog 1868-1995) are plotted with Quaternary faults (Piety, 1996) (left), idealized into fault zones (right). Plots are approximately same scale. Radii of circles are 50 and 100 km from Yucca Mountain. Rectangle enclosing Yucca Mountain (right) is shown in figure above.

Figure 1

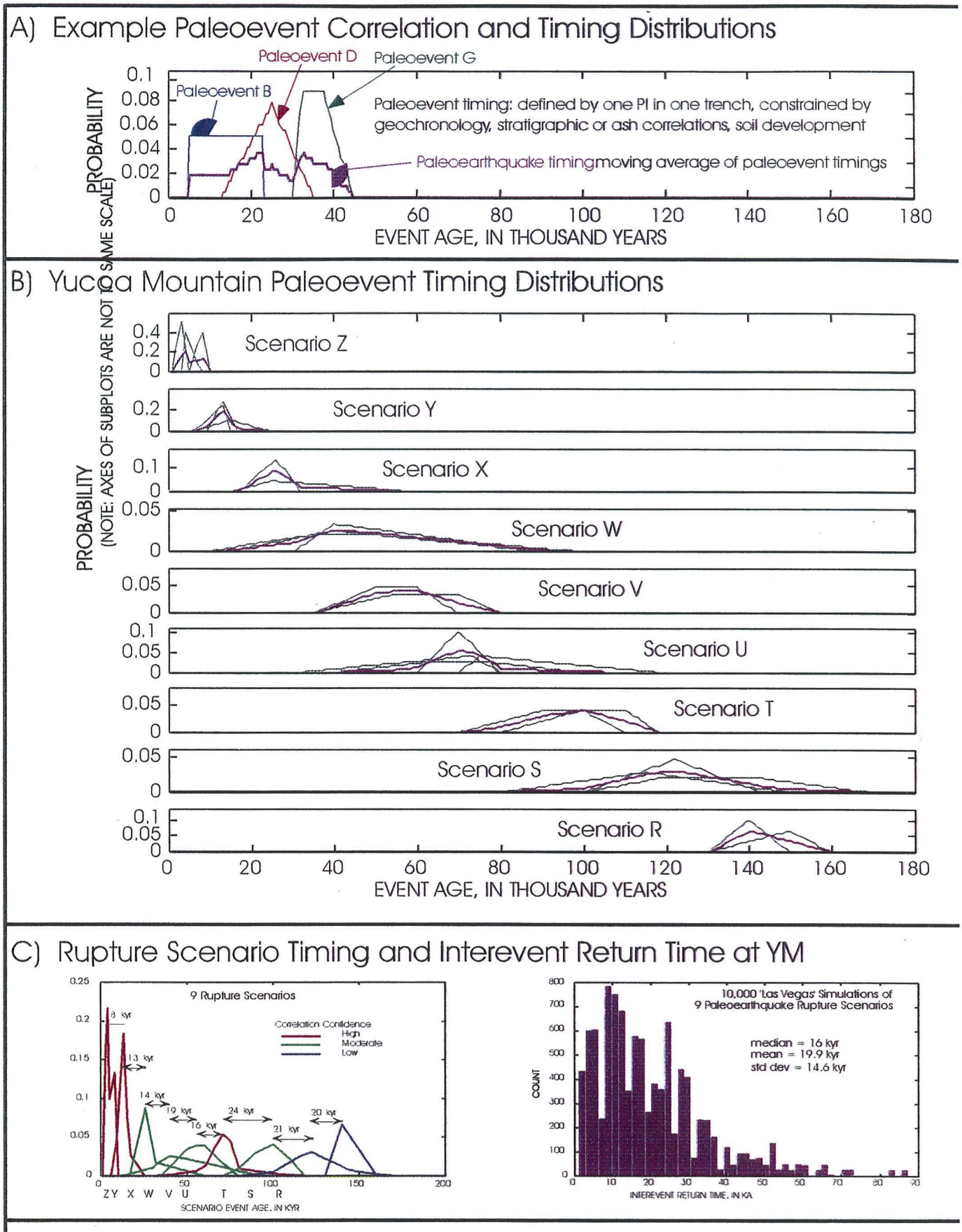

Figure 2. A) Example probability density function for the timing distributions of paleoevents. The cumulative distribution resulting from the summed average of the superposed individual peleoevent timing distributions defines the rupture scenario timing. B) Paleoearthquake rupture scenarios for Yucca Mountain faults are arranged from youngest (Z) to oldest (R), top to bottom. Note: the probability axes for individual scenarios are not to same scale. C) Left: Paleoearthquake timing distributions for 9 scenario ruptures showing peak-to-peak interevent return times and correlation confidence. Right: A histogram produced from 10,000 random samples "Vegas style" of the interevent return times randomized from the scenario timing distributions.

Figure 2

Yucca Mountain Paleoearthquake Rupture Scenarios

Scenario Z
age = 5 ± 2 ka (H)
Mw = 6.2 ± 0.3

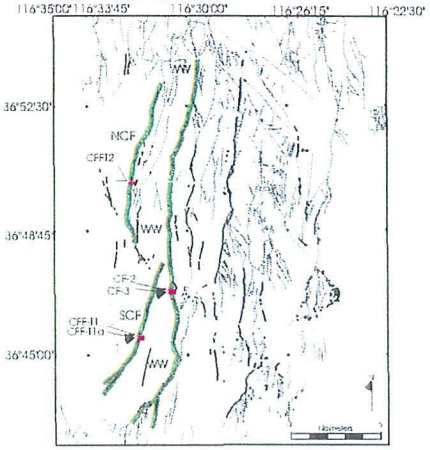

Scenario Y
age = 13 ± 3 ka (H)
Mw = 6.5 ± 0.3

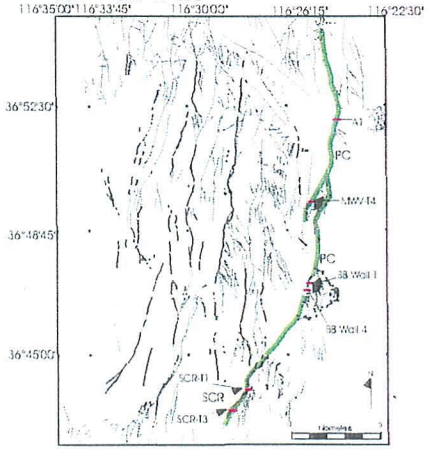

Scenario X
age = 26 ± 5 ka (M)
Mw = 6.4 ± 0.3

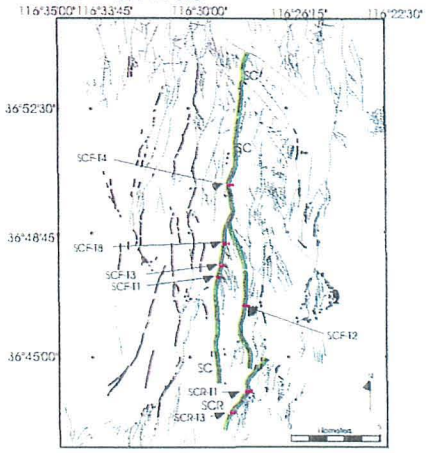

Scenario W
age = 40 ± 5 ka (M)
Mw = 6.8 ± 0.3

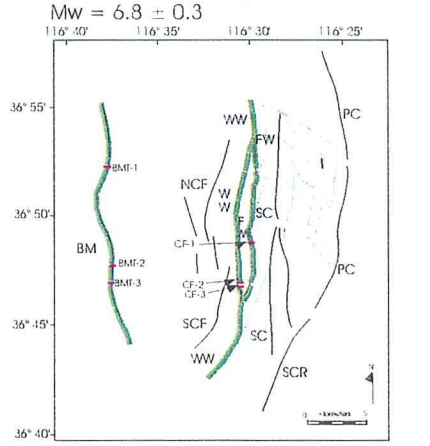

Scenario V
age = 59 ± 5 ka (M)
Mw = 6.5 ± 0.3

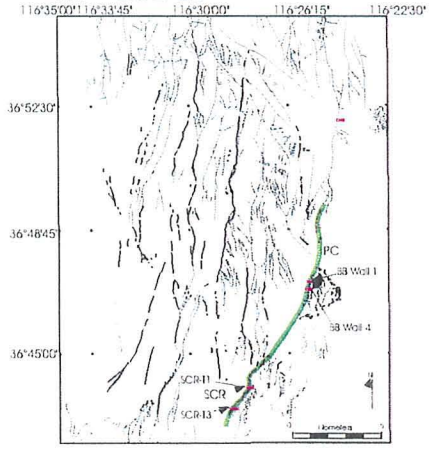

Scenario U "the ash event"
age = 75 ± 10 ka (H)
Mw = 6.7(SRL),6.9(ΣD) ± 0.3

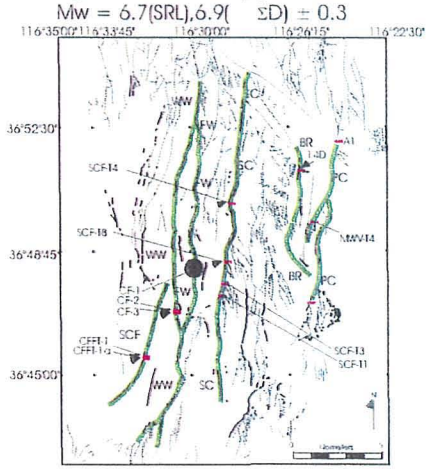

Scenario T
age = 99 ± 10 ka (M)
Mw = 6.6 ± 0.3

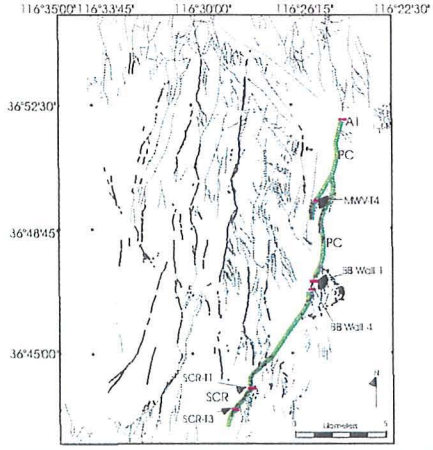

Scenario S
age = 120 ± 15 ka (L)
Mw = 6.6 ± 0.3

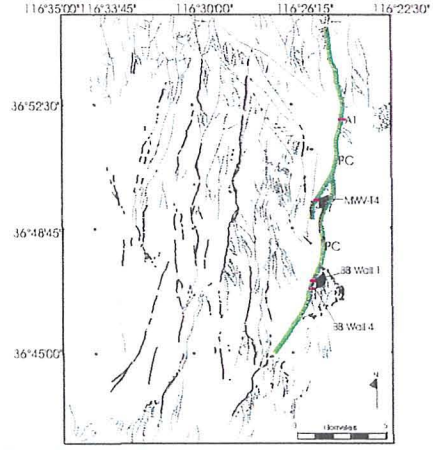

Scenario R
age = 140 ± 15 ka (L)
Mw = 6.5 ± 0.3

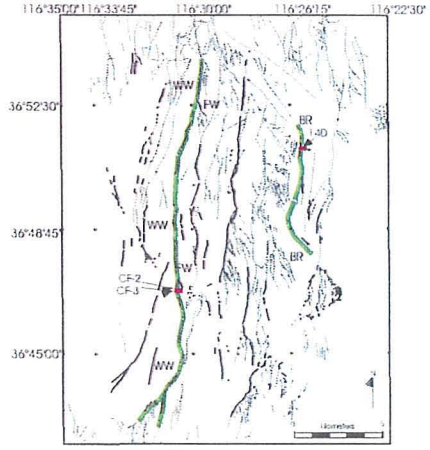

EXPLANATION

- Minimum scenario rupture length
- Maximum scenario rupture length
- Paleoseismic Trench Locations
- Faults; Quaternary and suspected Quaternary age of last movement
- Faults; pre-Quaternary or undetermined age of last movement

Fault Abbreviations

BR =	Bow Ridge	SC =	Solitario Canyon
FW =	Fatigue Wash	SCF =	Southern Crater Flat
NCF =	Northern Crater Flat	SCR =	Stagecoach Road
PC =	Paintbrush Canyon	WW =	Windy Wash

Maps of Yucca Mountain rupture scenarios. Trenches that constrain rupture lengths are labeled. The minimum and maximum rupture lengths are shown in bold and shaded lines. Plots arranged from youngest (Z) to oldest (R); left to right, top to bottom. The estimated age (in ka, thousands of years ago), confidence estimates, (Low, Medium, and High) and earthquake moment magnitude (Mw) are listed above each map. Faults are simplified from Simonds and others (1995).

Figure 3

location places constraints on paleorupture length. Rupture lengths are estimated for the 9 paleoearthquakes using a scheme where the along trace fault lengths and the paleoseismic study sites were projected onto a north-south plane using a join line at 36' 50" N. so as to obtain rupture lengths for scenario events that span more than one Yucca Mountain fault. Minimum rupture length is derived from the projected distance between the northern-most and southern-most trenches that exhibit a particular scenario paleoearthquake. Maximum rupture length is measured from the longest fault or combination of faults involved in that scenario. Moment magnitudes of the 9 scenario paleoearthquakes range from about M 6.2 to 6.9 using these methods and published empirical relations.

Our results indicate that most fracturing and small displacement paleoevents in the Yucca Mountain area correlate with relatively larger-displacement paleoevents. Because earthquakes have occurred at different times on the numerous Quaternary faults in the Yucca Mountain site area, the potential repository site experiences local surface-faulting earthquakes, on average, more frequently than the average recurrence interval of a given fault in the area. Accounting for possible distributed faulting can lengthen interevent return times by as much as a factor of 4 and increase maximum magnitudes 0.1-0.3 moment magnitude unit for cases where the distributed single-event displacements must be summed across two or more adjacent parallel faults. Surface-rupturing paleoearthquakes at the Yucca Mountain site likely produces distributed faulting on two to four nearby faults. As a result, for relatively short time periods of engineering significance, ground motion and especially fault displacement hazard levels are relatively low because distributed faulting makes for larger magnitude events that occur less frequently and thus have a low contribution to overall hazard. Over longer time periods, however, hazard levels are relatively higher, in part because the distributed faulting earthquake has a relatively higher contribution to the overall seismic hazard, especially for fault displacement.

Turn the cars around on the drill pad and drive back down the mountain.

45.2 4.0 **Stop 2 (10:00 am -12:00) Busted Butte Sand Ramps.** Park the cars along the road and prepare to walk about 20 minutes to the west side of Busted Butte. We will be gone for about an hour and a half.

> Menges and Coe--Middle and late Quaternary paleoseismic history of the Paintbrush Canyon fault; Sand ramp stratigraphy and soils; eolian history/paleoclimatic implications (see Menges and others, this volume).

The Paintbrush Canyon fault (fig. 4) runs along the western base of the series of bedrock ridges, including Busted Butte, which define the eastern margin of Yucca Mountain. At the Busted Butte site the fault displaces a series of eolian strata and buried stonelines or soils which are spectacularly exposed in the walls of 25-m

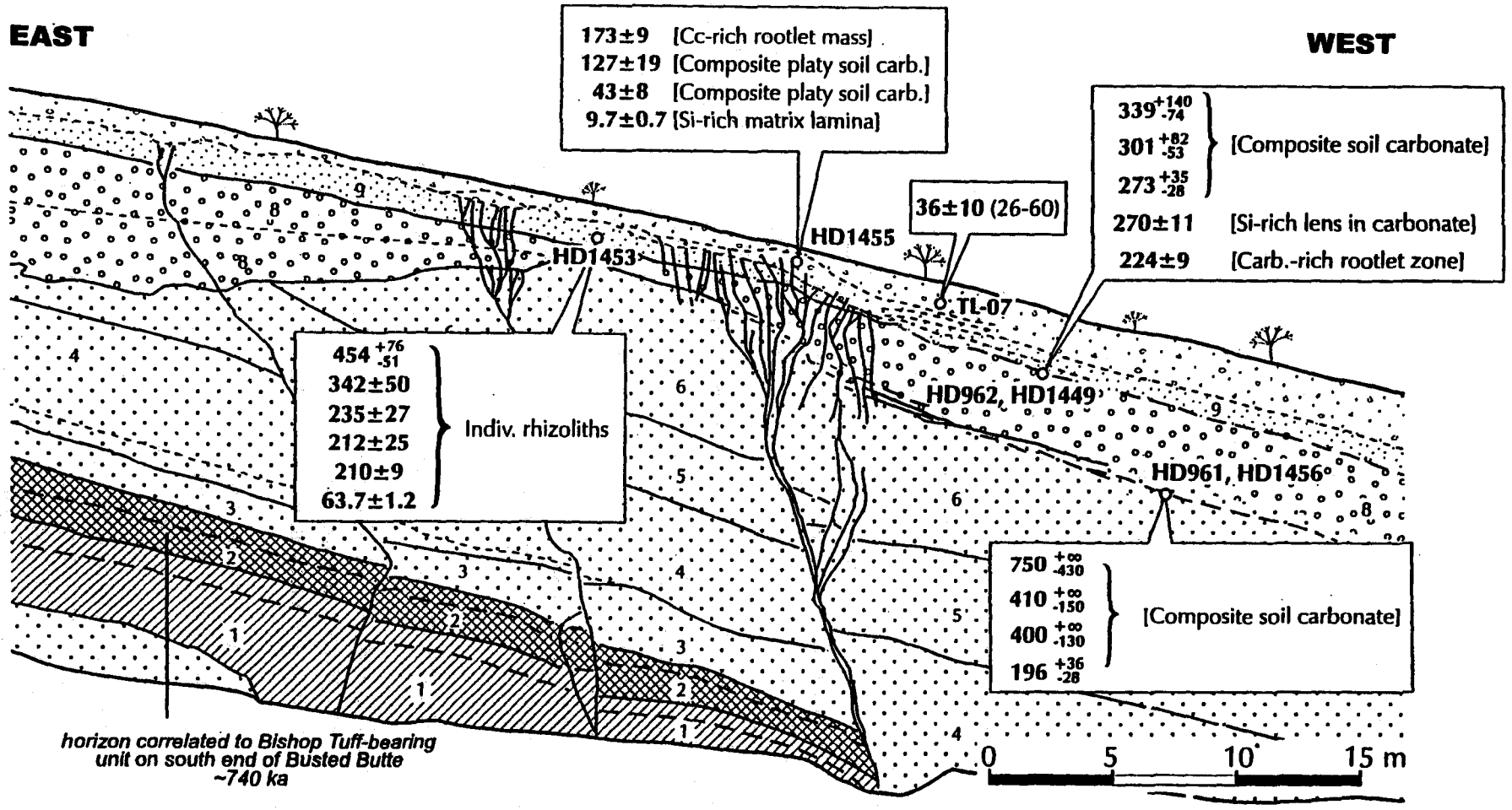

Figure 4: Generalized geology of Wall 4, west side of Busted Butte sand ramps exposing the Paintbrush Canyon fault. The geochronological data is shown in ka. Uranium series data (HD-) and thermoluminescence data (TL-) are shown for each layer. The lower dates are susceptible to uranium loss (after 300 ka), some in the extreme. Data that yields $^{230}TH/U$ ages with a calculated initial of $^{232}U/^{238}U$ greater than 2 or less than 1.2 are generally considered suspect until additional information can confirm these anomalies.

deep gullies incised into the sand ramps flanking the butte. The presence of the Bishop ash near the base of the eolian section establishes an overall 740 k.y. interval for the displacement record, which includes stratigraphic evidence for 6 to 7 paleoevents. Two buried soils near the top of the sand-ramp section have estimated ages of 400 ka and 300-150 ka, based on U-series ages of secondary carbonate, which suggests that the bulk of the eolian accumulation in this sand ramp occurred in the middle Pleistocene.

Return to the cars and continue straight ahead toward the road crossing at Fortymile Wash. Turn east (right), cross Fortymile Wash, and drive up on the road that goes due south on the upper terrace ridge.

48.3 3.1 **Stop 3 (Lunch-2:00) East Terrace overlooking Fortymile Wash.** Park the cars along the road and walk to the terrace edge. Look across the wash to the exposed stratigraphy in the bank. We will walk into the wash and to the low inset terraces, and the terraces north of the road crossing. The cars will be driven down to the parking area west of Fortymile Wash.

Lundstrom, Spaulding, Mahan--Fortymile wash--age of terraces and evolution of wash (see Lundstrom, this volume)

Glancy--Modern flooding and runoff of the Amargosa River, emphasizing contributions of Fortymile Wash (see Glancy and Beck, this volume)

Stamatakos--Gravity and magnetic data

48.9 0.6 Return to the cars and drive west toward Yucca Mountain.

50.4 1.5 Make a turn, northwest (right), onto the well used gravel road up into Yucca Wash. This wash trends northwest, subparallel to several predominantly faults which control northwest-tending canyons towards the north end of Yucca Mountain (e.g., Pagony, Sever, and Drill Hole Washes). Yucca Wash also separates bedrock of very different lithologies and structural styles. Thus most workers considered Yucca Wash to be controlled by a probable strike-slip fault, but several recent geologic and geophysical studies have failed to document any the presence of any significant faulting beneath the wash. Indeed recent geologic mapping suggest that most of the north-trending faults in Midway Valley to the south (e.g., Bow Ridge fault) continue northward without disruption across the wash.

50.7 0.3 Turn north (right), rather than continuing up Yucca Wash.

51.0 0.3 Stay to the east (right), the west road goes to the top of Alice Ridge.

52.0 1.0 Dropping onto an inset Q4 terrace.

52.5 0.5 Crossing the confluence of Yucca Wash and Fortymile Wash.

53.8 1.3 **Stop 4 (2:00-3:00) Jake's Ridge** (turn around and reset odometer)

Coe, Glancy--erosional/mass movement history, hydrologic/flood history at Jake's Ridge, the hillslope on your left. (See Coe and others, this volume).

In July 1984, debris flows on this hillslope deposited material about 1 m deep on the road where we are standing. The flows were triggered by severe thunderstorms over a two-day period. The most intense period of rainfall occurred during a two-hour period on July 21 when about 60 mm of rainfall was recorded. The maximum and mean depths of erosion on the hillslope were about 1.8 m and 5 cm, respectively. Debris movement was probably initiated by streams of water flowing from the caprock, like from a fire hose.

Glancy--discussion and oral presentation of erosional/mass movement history, hydrologic/flood history at Coyote Wash, a small drainage on the east central side of Yucca Mountain. (see Glancy, this volume).

In 1983 two trenches were excavated in the flood plain to interpret the flood potential in the drainage. The trenches exposed stratigraphically intermixed flood deposits of both Newtonian and debris-flow origin which reveal a complex flood and depositional history. Lithologic and pedogenic characteristics suggest at least two groups of deposits, an upper unconsolidated set above lower more indurated sediments, which TL analysis of the fine-grained silty fraction suggest probable minimum age ranges of mid Holocene (3-5 ka) and latest Pleistocene (25-32 ka), respectively, assuming the fine fractions are post-depositional eolian additions. Several empirical techniques were used to estimate maximum peak-flows rates of 900 to 2600 ft^3/s.

Return to the main road that crosses Fortymile Wash.

3.3 3.3 Turn west (right) toward the ESF.

3.8 0.5 Entering Midway Valley

4.6 0.8 Turnoff to right to North Portal to the ESF. This is the northern entrance to the exploratory tunnel where excavation by a tunnel boring machine (TBM) started in September, 1994. The large pile of rocks and debris visible to the right (north) is the "muck" extracted during excavation of the tunnel. There is large pad and complex of buildings adjacent to the muck pile and tunnel portal.

5.1 0.5 Turn south (left) following the signs toward the South Portal of the ESF. This is

the southern end of the tunnel where the TBM "daylighted" or exited from the ESF in April 1997. The partially disassembled TBM still lies adjacent to the South Portal.

5.8 0.7 Curve toward the west (right), do not turn east toward the South Portal, and continue up the wash.

6.2 0.4 Continue southwest (left), following the signs to drill pad UZ-7A.

6.8 0.6 **Stop 5 (3:00-4:00) Ghost Dance fault.** Park the cars on the UZ-7A drill pad. This pad was prepared as the site for an Unsaturated Zone borehole (UZ-7A) which was drilled in part to investigate the hydrology of the Ghost Dance fault, the largest and most prominent intrablock normal fault in the central repository area. The Ghost Dance fault is very well exposed in the bedrock on the south wall of the drill pad. There are two principal strands exposed here within the overall steeply west-dipping fault zone: the main fault on the east and a secondary fault on the west, which bound a large intervening area of highly fractured rock. Subsurface data, including a detailed seismic reflection profiles in the pad area, as well as the intersection of the fault in both the borehole and alcove of the ESF, indicates that the overall Ghost Dance fault zone maintains a steep dip through at least the shallow subsurface.

> Potter--Expression of the Ghost Dance fault in the drill pad exposure of UZ 7A and Whale Back Ridge

Prepare to walk to the top of Whale Back Ridge, to the north of the UZ-7A pad.

> Taylor, Menges--Trench exposure of the Ghost Dance fault on Whale Back Ridge (see Taylor and others, this volume).

A variety of geomorphic and stratigraphic studies were conducted along the Ghost Dance fault in attempt to determine whether significant Quaternary displacement has occurred on the structure. This is very important input to both vibratory ground motion and especially fault displacement elements of the seismic hazard analysis because of the faults position within the central repository block. These investigations included excavation of series of trenches across the fault. Most of these are located in undisturbed Holocene to late Pleistocene alluvium and colluvium burying the fault in the canyon bottom; however, one trench which we will visit was excavated on the ridgecrest of Whale Back Ridge across shallow Holocene to latest Pleistocene colluvium and subjacent late Pleistocene ($\leq$ 89-90 ka) carbonate platelets which mantle bedrock exposures of both traces of the fault zone (fig. 5). Only one fracture, with no detectable displacement, was observed in the carbonate coatings above a subsidiary strand of the fault in this trench. At this site and on the crest of Antler Ridge to the north, a series of ^{10}Be and ^{26}Al exposure dates collected in a transect across the gently-sloping bedrock

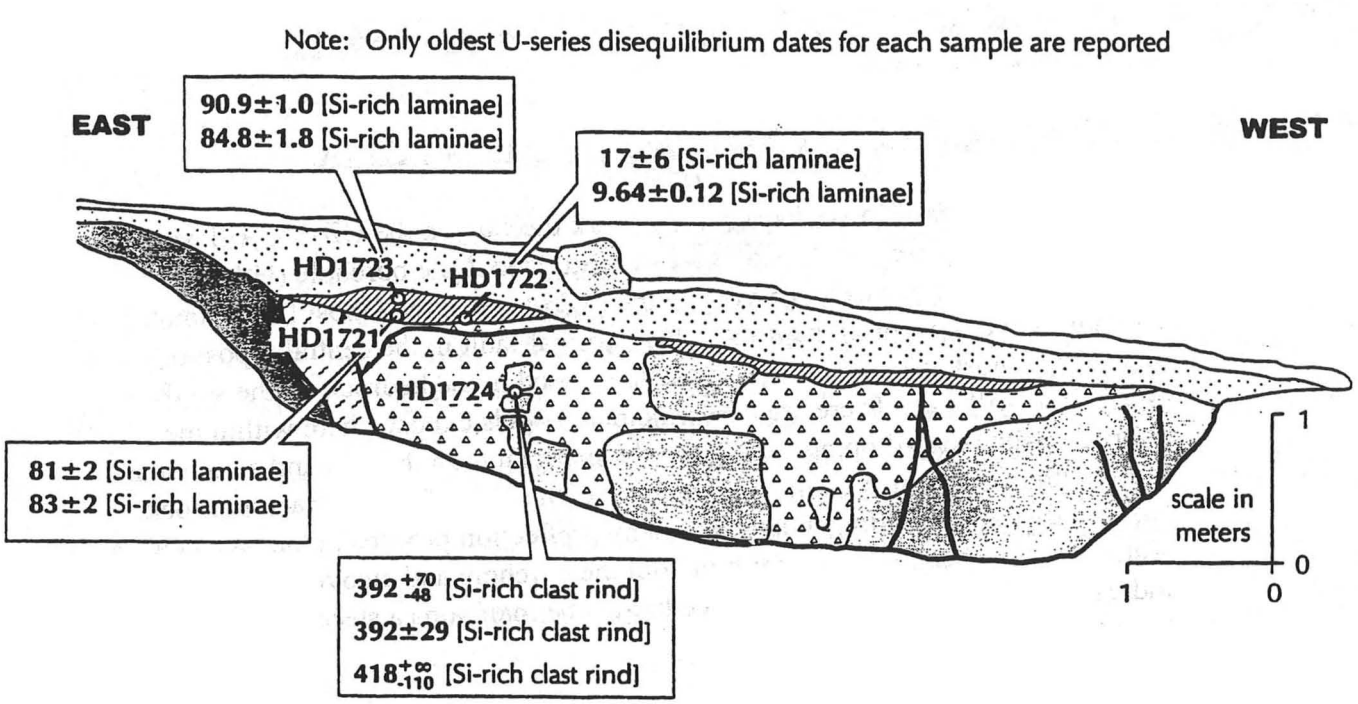

igure 5: Generalized geological log showing data of the south wall, east end, of the Whale Back Ridge exposing the ult. No TL data was collected at this site.

escarpment of the Ghost Dance fault zone indicate that this fault-line feature is very old (0.75- 1 myb) and has experienced very little erosional modification in middle and late Quaternary time.

Harrington, Whitney, and Gosse-- ^{10}Be, ^{26}Al exposure dates on bedrock scarps developed across the fault on the crest of Whale Back and Antler Ridges (see Taylor and others, this volume).

The gradual buildup of rare isotopes from interactions between cosmic rays and atoms in an exposed rock provides a method of directly determining the exposure age of rock surfaces (typically minimum ages). Cosmogenic nuclide methods can also provide constraints on erosion rates and the length of time surface exposure was interrupted by burial. Several applications of the technique have been useful to the surface geologic characterization of Yucca Mountain. The ^{10}Be exposure age of Black Cone lava, within a ten mile radius of the proposed repository site, is 910±230 ka (in agreement with previous K/Ar dates of 1.0±0.1 Ma). Ages of boulder deposits on the slopes of Yucca Mountain and surrounding hills yield an average of 0.5 Ma, suggesting the slopes have been stable through the late Quaternary. Rates of erosion of the tuff bedrock (< 0.3 cm/kyr from 7 ^{10}Be measurements) and of hillslope colluvium (< 0.5 cm/ka from ^{10}Be dates coupled with cosmogenic ^{36}Cl exposure dates) preclude denudation of the mountain as a regulatory concern. Exposure samples collected along the crests of Whale Back and Antler Ridge were measured to help characterize the stability of slopes forming the colluvium above the Ghost Dance Fault and associated fracture zone.

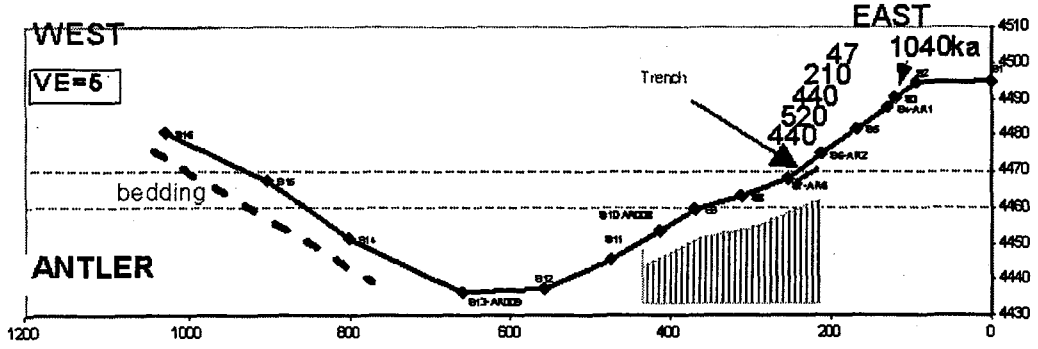

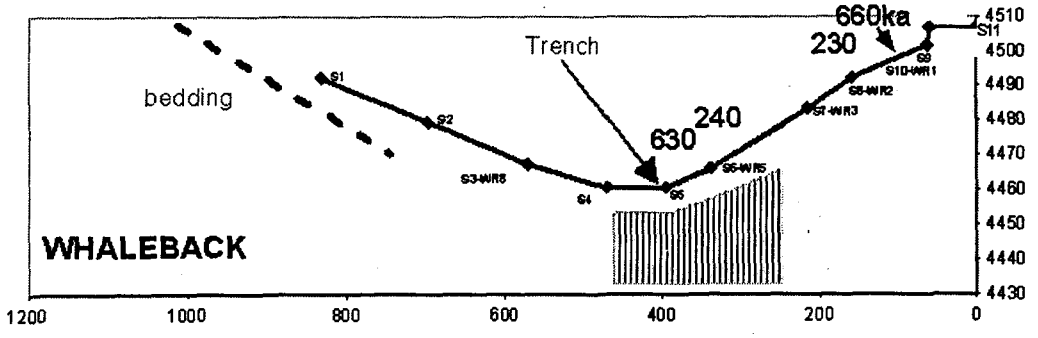

Return to the cars and drive back to the main road that crosses Fortymile Wash. Cross the road, go straight ahead (north) toward the complex of trenches (trench 14 and trenches 14A to 14D excavated across the Quaternary Bow Ridge fault at the western base of the low bedrock hill (Exile Hill) to the east (right) of the road.

7.3 0.5 **Stop 6 (4:00-5:30) Trench 14 and Exile Hill overlooking Midway Valley.** Turn east (right) to Trench 14.

Taylor, Huckins--Trench 14--Pedogenic versus thermal spring origin for secondary calcium carbonate in the Bow Ridge fault exposure (see Taylor and Huckins, this volume).

Menges, Taylor--Trench 14D---Late to middle Quaternary paleoseismic history of the Bow Ridge fault; colluvial deposition, hillslope erosion, and soil formation at the base of the ridge (see Menges and Taylor, this volume).

These first two parts of this stop examine two of the five trenches excavated at Exile Hill across the buried trace of the Bow Ridge fault, which is a Quaternary fault that crosses the ESF tunnel near the North Portal entrance. Trench 14 is the original trench excavated in the early 1980's which exposed the fault in bedrock and colluvium at the base of the hill. The fault zone in this trench is extensively coated and filled with secondary carbonate and opaline silica which generated a heated scientific debate concerning pedogenic origins from atmospheric dust versus deposition from thermally upwelling springs.

Trench 14 did not provide very good paleoseismic resolution on Quaternary fault history; and thus another series of trenches were excavated in the late 1980's and modified in 1992. Walk southward from trench 14 to the box-shaped trench 14D which contains the best record of Quaternary displacements; paleoseismic interpretation of several trench exposures indicate that two and possibly three surface ruptures on the fault displace a stacked sequence of middle to late Pleistocene colluvial deposits and soils (fig. 6).

Lundstrom--Quaternary Stratigraphy of Midway Valley and Surficial geologic mapping of the east side of Yucca Mountain--evolution of stratigraphic mapping units

Climb up to the top of Exile Hill for an view of Midway Valley which is small alluviated basin within the northeastern corner of Yucca Mountain. Quaternary deposits and soils in this valley have been extensively studied and mapped by a number of workers, work which provided the basic framework for both geologic mapping of Quaternary units and stratigraphic analysis of trench exposures in the

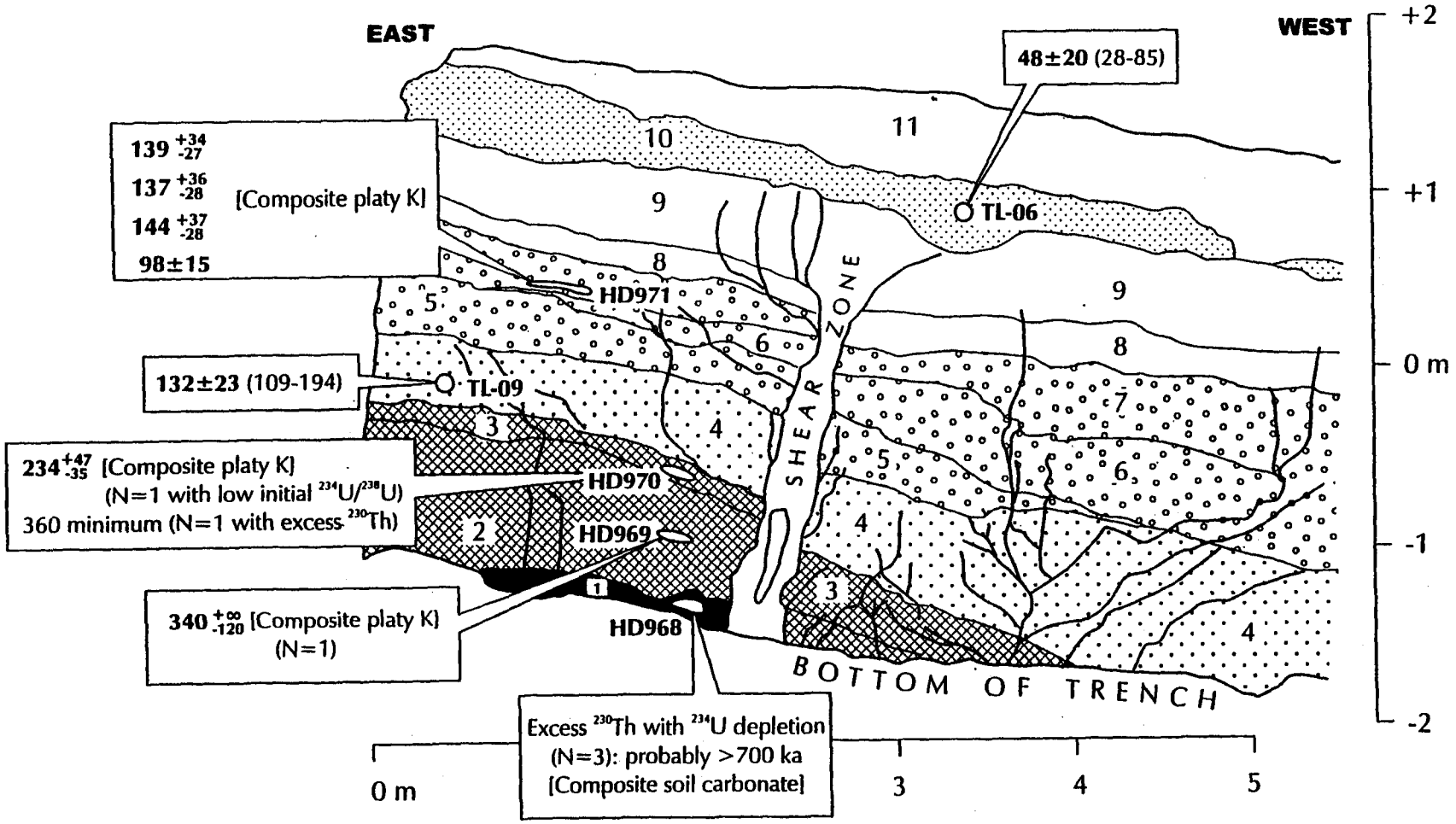

Figure 6: The Bow ridge fault is exposed on this generalized geological log of the south wall of the inner box of Midway Valley Trench 14D. Geochronological data is mainly from U-series ages, although two TL samples were taken in Unit 10 (compacted, clay-rich, reddened B horizon) and Unit 4 (a silty loam rich unit).

Yucca Mountain area. In the mid-1980's E. Taylor first studied the soils and mapped Quaternary deposits in parts of Fortymile Wash and Midway Valley using units adapted from the Quaternary mapping of the Nevada Test Site region by Swadley and his coworkers at the U.S. Geological Survey. In the early 1990's, J. Wesling , B. Swan, and co-workers from Geomatrix refined and renamed this stratigraphy and mapped it in detail throughout Midway Valley as part of a geologic-neotectonic-geomorphic study of the site near the North Portal under consideration for the surface waste-handling facilities of the potential repository. The Geomatrix study included excavation by backhoe of a number of soil pits on all major alluvial units. Starting in 1992, S. Lundstrom further refined Quaternary mapping in Midway Valley and along Fortymile Wash as the first stage in his detailed mapping and analysis of alluvial, colluvial and eolian Quaternary deposits in the Yucca Mountain area. In Midway Valley he also completed detailed descriptions and laboratory analyses of the soils and stratigraphy exposed in the soil pits in Midway Valley.

> Soeder--History of the drilling program and tunneling operations (including the ESF) conducted for site characterization and scientific testing at Yucca Mountain (see Soeder, this volume).

Depart the Nevada Test Site through the Lathrop Wells Gate. We need to be through the gate by 6:30

Day 1, Stop 1

The Viability Assessment of the Yucca Mountain Site

J. Timothy Sullivan and Richard Craun

Abstract

Congress directed the Department of Energy (DOE) to produce a Viability Assessment (VA) to provide information to allow an assessment of the viability of developing a repository at Yucca Mountain. The VA constitutes a logical convergence point to provide information to the Administration and Congress to support future decisions on Program activities.

The VA uses a design focused on elements that are critical to determining the feasibility and performance of the repository. The VA also includes a total system performance assessment (TSPA) to evaluate the expected behavior of the potential repository. The TSPA evaluates the possible range of performance, considering uncertainty in key factors such as ground-water flow, thermal effects on the host rock, and corrosion of the waste package. A TSPA peer review is being conducted to strengthen the basis for licensing arguments in the future.

The VA presents cost and schedule information for the repository system, the completion of site characterization, construction, operation, and closure of a repository at Yucca Mountain. The final component of the VA is the license application plan, which describes DOE's integrated approach for completing the necessary site studies, design activities and performance assessment work to support submittal of the License application to the Nuclear Regulatory Commission in 2002.

Together, these VA products will provide policy makers with a better understanding of the repository design and its performance in the volcanic rocks at Yucca Mountain, a better appreciation of the remaining work needed to prepare a license application, and a more precise estimate of the cost of a repository.

Introduction

The U. S. Department of Energy has been characterizing Yucca Mountain on the western boundary of the Nevada Test Site since the late 1970s to determine if it is suitable for development of a repository for high-level radioactive waste. This fall DOE will reach an important milestone in its progress toward the suitability determination—the Viability Assessment (VA). Required by the Energy and Water Appropriations Act of 1997, the VA includes four main elements:

- a description of a preliminary repository design,
- an assessment of the performance of that design in the geologic setting at Yucca Mountain,
- a plan and a cost estimate for the work required to complete a License Application, and
- an estimate of the costs to construct and operate a repository at Yucca Mountain.

The VA draws on what the DOE has learned in over 20 years of scientific and design work at Yucca Mountain. Guided by the Site Characterization Plan that was released in 1988, DOE has gained a comprehensive understanding of the geology and hydrology of the site based on data collected from more than 100 boreholes and 5 miles of tunnels at Yucca Mountain. The key factors that led to the identification of Yucca Mountain as a potential site—favorable host rocks and an unsaturated zone setting—are now well understood. The proposed repository (fig.

1) will be developed in dense welded tuffs of the Topopah Springs Formation, a Miocene ash-flow tuff deposited 13 million years ago as part of a sequence of tuffs about 5000 ft thick erupted from the Timber Mountain caldera complex north of Yucca Mountain. At Yucca Mountain the groundwater table is between 1500 and more than 2000 ft below the ground surface. The proposed repository will be located about midway between the ground surface and the water table ensuring that future water table rise, estimated not to exceed 400 ft, will not flood the repository and that surface erosion cannot expose the waste. Based on the results of extensive testing in boreholes and in the underground DOE has gained sufficient confidence in its understanding of the patterns and amounts of water flow in the unsaturated zone at Yucca Mountain to make reliable assessments of the long-term repository performance.

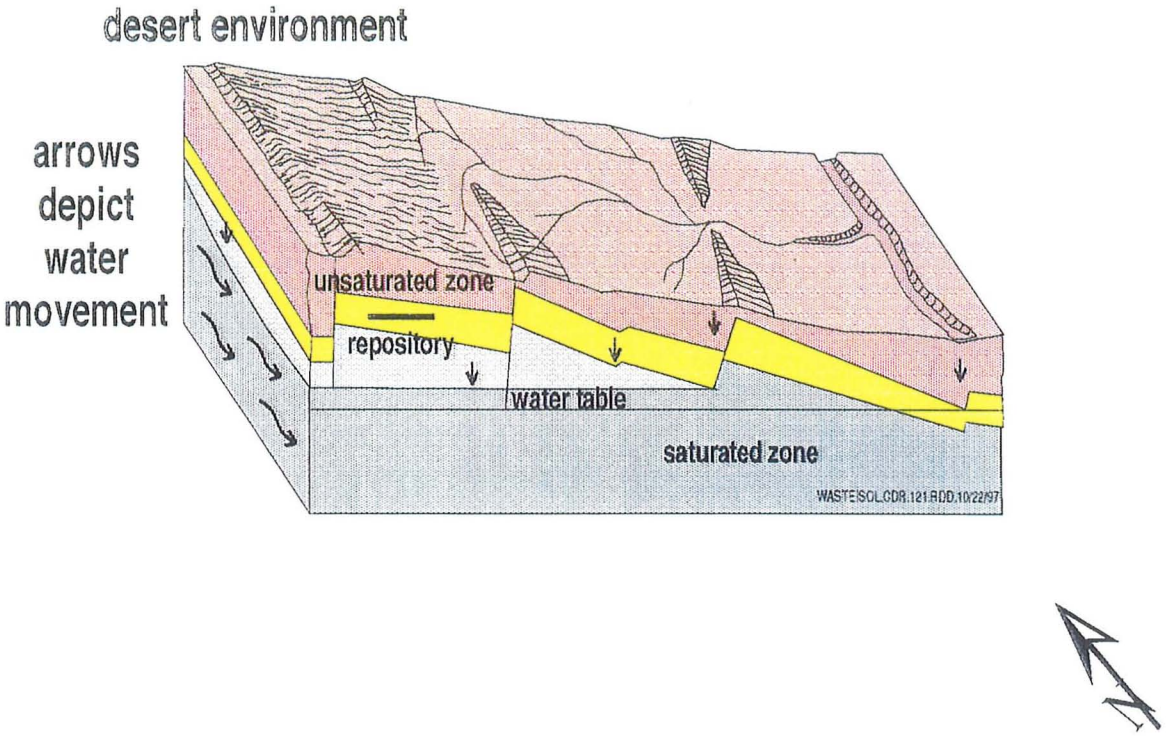

Figure 1 – Schematic cross-section of Yucca Mountain

The Reference Design for a Repository at Yucca

The reference design concept for the underground repository is a series of parallel, nearly horizontal precast concrete-lined emplacement drifts totaling about 100 miles and occupying an underground area of about 2 miles by 1 mile (figure 2). The 5 m diameter emplacement drifts, excavated by tunnel boring machine, will be spaced 28 m apart with waste package spacing within the drift configured to produce a high repository thermal load (85 MTU per acre). This arrangement minimizes the repository construction costs, reduces the area required for development of the repository, and results in temperatures above boiling in the surrounding rock mass for the first few thousand years after closure, thus driving water away from the waste packages and limiting corrosion during this period. DOE's understanding of the thermal effects on water flow is expected to continue to improve as data from the drift-scale heater test, started this year, become available.

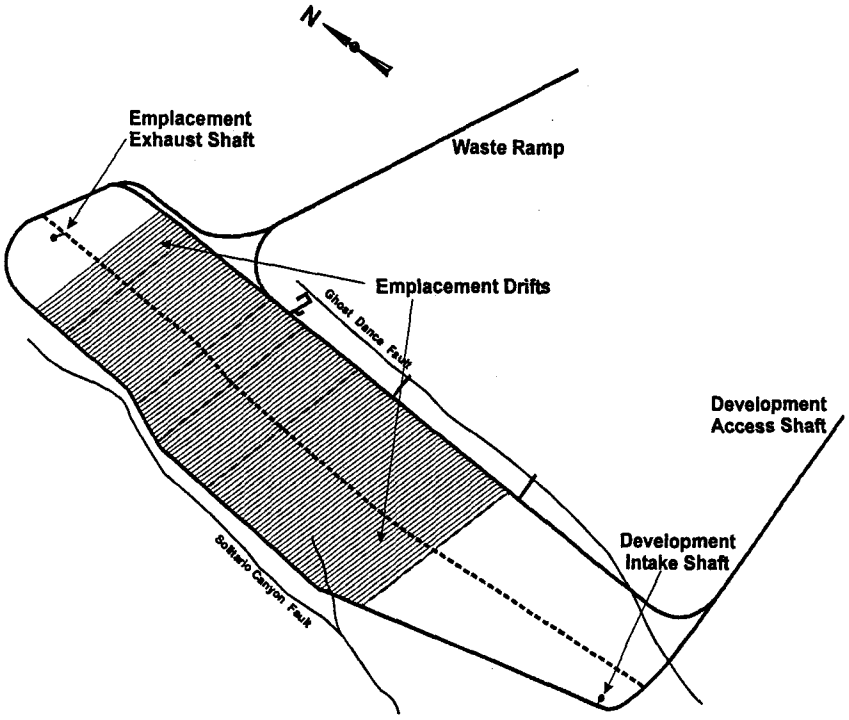

Figure 2 – Repository subsurface layout for reference design. Emplacement drifts are each about one kilometer long.

The reference design concept includes robust waste packages, with a 2 cm thick nickel alloy inner barrier to provide corrosion resistance and a 10 cm thick outer barrier of carbon steel to provide structural strength, enough radiation shielding (figures 3a and 3b) and protection of the inner barrier. The waste package outer diameter is 2 m with a length of 6 m. These reference features govern the design of the twelve different types required to accommodate the different waste forms that will be disposed of at Yucca Mountain. The waste package size and internals are designed to ensure that maximum waste package internal temperature does not exceed 350 deg C. The large waste package size is an efficient cost-effective design, but it does not provide radiation protection for workers. Shielded transporters will carry the waste packages underground (1 to 2 per day during operations). The waste packages are emplaced into the drifts with a remote handling system which features a gantry positioning system. Waste packages will rest on a steel pedestal in the drift, facilitating retrieval if necessary.

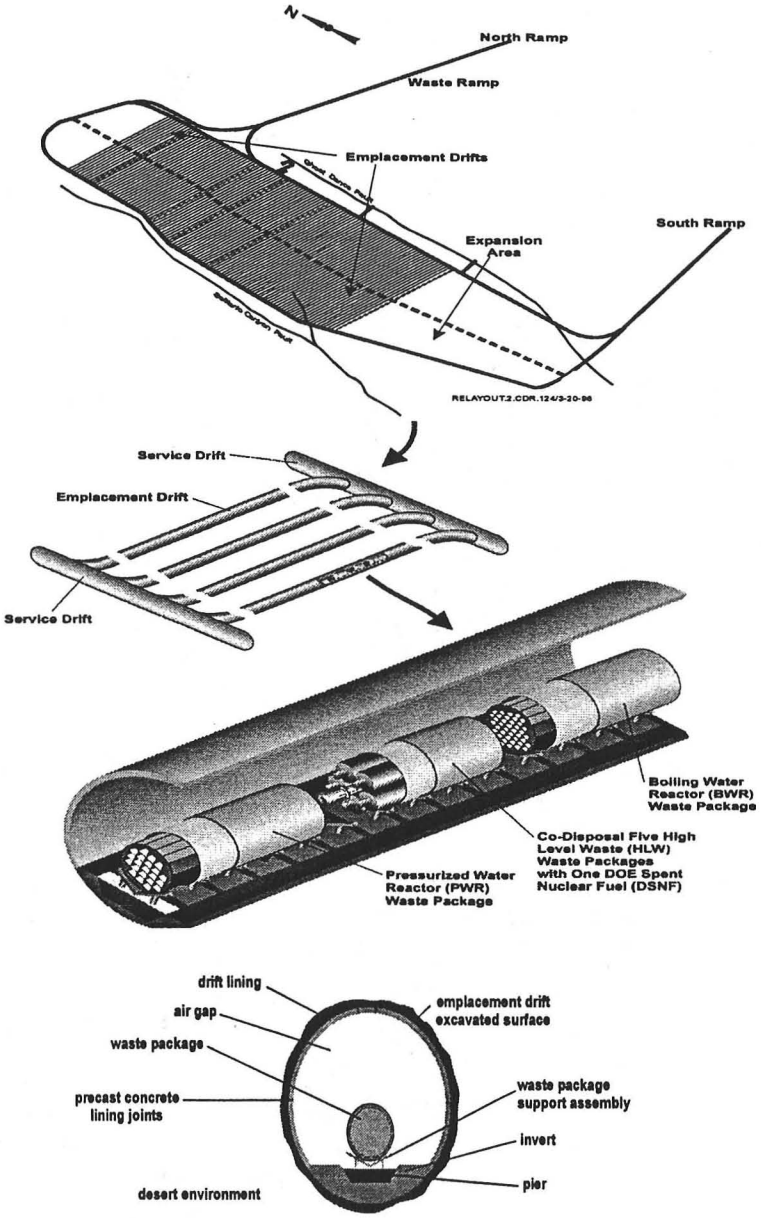

Figures 3a. The top portion is the repository subsurface layout. The middle portion is the emplacement drift with waste packages. The bottom portion is the cross sectional view of an emplacement drift (diameter is 5.5 m).

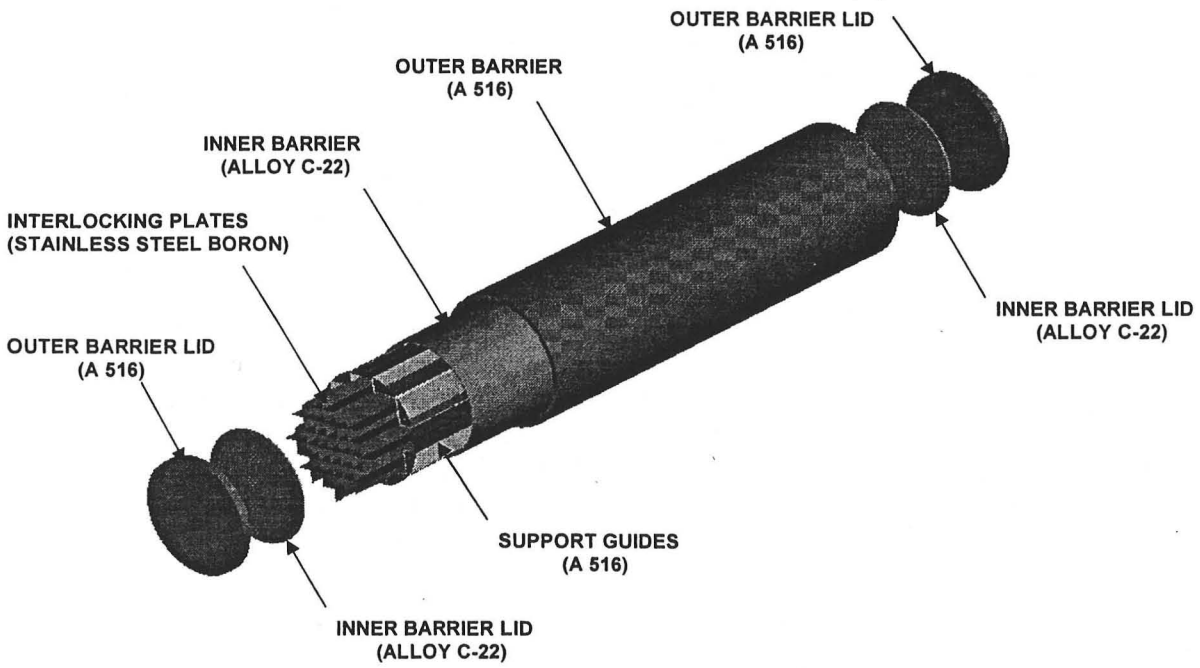

Figure 3b – A typical waste package; 2 meters in diameter and 6 meters long

The surface facilities are designed to accept canistered or uncanistered fuel by rail or road. The design accommodates spent nuclear fuel and high level waste received in disposable or nondisposable canisters as well as noncanistered spent nuclear fuel. The facility initially will handle about 300 tons of fuel per year. The reference concept calls for development of the surface facilities at the north portal and emplacement of the waste through the north ramp and main drift that have already been developed. Men, materials, and muck will move through the south portal. For worker safety separate ventilation systems are provided for excavation and emplacement operations which are conducted simultaneously throughout the operations period. Two exhaust shafts are required. One exhaust main will be excavated below the repository drifts.

Performance Assessment

Assessing the risk to public health and safety requires an integrated understanding of all of the components of the natural and engineered systems at Yucca Mountain. To accomplish this process models have been developed from scientific and engineering data to describe in detail the system components. These stand-alone models then are summarized or abstracted for use in the Total System Performance Assessment simulations (fig. 4). Natural system process models describe future climate, precipitation and infiltration through the soil zone, unsaturated zone water flow through the rocks above the repository, flow and radionuclide transport through the rocks below the repository to the water table, and saturated zone flow and transport below the

groundwater table to the accessible environment (assumed to be 20 km or 12.4 miles south in Amargosa Valley for the VA). Engineered barrier system models, conditioned by thermal hydrology models that describe conditions in and near the drift during the thermal pulse, describe the degradation of the waste package and radionuclide release by the waste forms within.

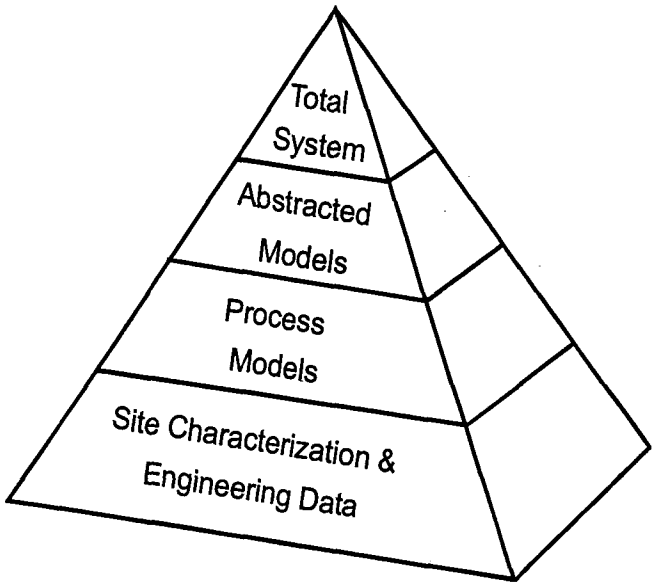

Figure 4 – The Performance Assessment Pyramid illustrating how site characterization and engineering data form the foundation for detailed process models that are abstracted for use in Total System Performance Assessment.

For the Total System Performance Assessment—Viability Assessment (TSPA-VA), a base case has been developed using single values (most likely values) for the parameters derived from the process models. For probabilistic results and sensitivity studies, the key parameters from the process models are used a probability distribution functions (PDFs). The PDFs for the key parameters have been developed from the process models and from the results of expert elicitations sponsored by the DOE. These elicitations focused on the key process models identified from the results of earlier performance assessments. Technical experts from outside the project and from within evaluated the existing information and process models then provided their assessments of the mean values and associated uncertainties in key parameters. Aggregated results have been used in the TSPA-VA.

The base case dose curves (figure 5) are provided for three time periods -- 10,000, years, 100,000 years, and a million years. The results for 10,000 years indicate that annual peak doses at 20 km are less than 0.1 mrem/yr. The low dose rate for this period indicates that the robust waste package that includes a corrosion resistant material, works well in concert with the natural system that limits water flow into the drifts where it can affect waste packages. For 100, 000 years doses increase to about 5 mrem/yr as more waste packages corrode and waste forms degrade allowing more radionuclides to enter the groundwater system. Finally, for 1,000,000 years doses are seen to rise to about 300 mrem/yr, synchronous with a significant change in future climate. For comparison the average background radiation dose from all sources for

persons in the United States is about 360 mrem/yr. No compliance standard is currently in place for Yucca Mountain. The EPA is revising the existing release standard and is expected to issue a new dose-based standard. In anticipation of this DOE has used a performance measure of 25 mrem/yr at 20 km for 10,000 years to guide the repository design.

While these results are promising, DOE is also evaluating additional Engineered Barrier System design options in the VA that could improve system performance for longer time periods. The options include a combinations of backfill (dry granular material placed in the drifts prior to closure that would further protect the waste packages), drip shields (metal half-cylinders placed over the waste packages), and ceramic coatings placed on the waste packages or drip shields. If ceramics can be effectively bonded to the waste packages or the drip shields they could offer corrosion protection for very long time periods.

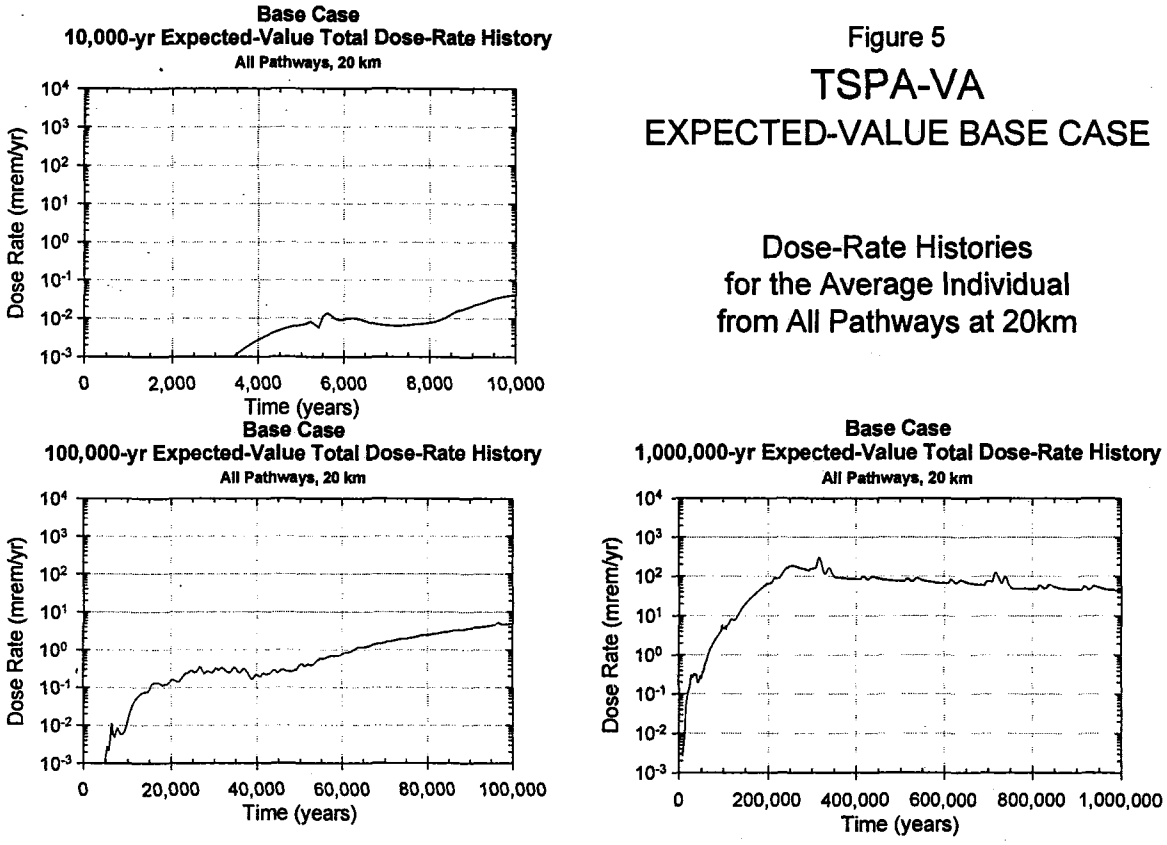

Figure 5

TSPA-VA

EXPECTED-VALUE BASE CASE

Dose-Rate Histories
for the Average Individual
from All Pathways at 20km

TSPA-VA also includes the results of extensive sensitivity studies. These probabilistic simulations focus on isolating individual key parameters and determining their effects on the overall results. In this way the importance of the current uncertainties in the natural system and engineered barrier system models can be better understood. These sensitivity studies serve to prioritize future work needed to better understand the behavior of the system. Key parameters identified from the sensitivity studies are the fraction of waste packages contacted by water seeping into the drifts, the mean corrosion rate for the waste package corrosion resistant inner barrier, and the saturated zone dilution factor.

Sensitivity studies are also used to evaluate the effects of disruptive events on the repository system. Some key results relate to earthquakes and volcanoes. DOE is nearing completion of a comprehensive evaluation of the hazards posed by earthquakes based on evaluations of the history of earthquakes in the region and detailed studies of the faults at Yucca Mountain. The results are used for the design of the surface facilities and the postclosure assessment of repository performance. The principal effect of earthquakes would be to produce or increase the rate of rockfalls in the drift. TSPA—VA sensitivity study results indicate that no significant increase in risk results from earthquakes. DOE has completed a comprehensive evaluation of the hazards posed by volcanic events in or near the repository based on detailed studies of volcanoes in the region. Again, TSPA-VA sensitivity studies indicate no significant increase in risk results from volcanic events.

License Application

If the Yucca Mountain site is found suitable and is recommended by the President to Congress and approved by Congress, DOE must then submit a license application (LA) to the Nuclear Regulatory Commission for review. The current schedule calls for that submittal in March 2002 (figure 6). This LA plan describes the technical work remaining to be done prior to that submittal. To do this the plan describes the elements of the postclosure safety case that DOE will make in the LA. This consists of five elements—expected repository performance, design margin or defense in depth, disruptive events, insights from natural analogs, and a performance confirmation plan. To define the work required, the LA Plan builds on the TSPA-VA sensitivity study results. These results, together with the work required to develop the preclosure safety case, form the basis for the License Application Plan. The core of the work is further development of the process models for the natural and engineered systems to reduce uncertainties and ensure defensibility of the models. The results are then abstracted for use in the TSPA-LA. The reference design reported in the VA is an evolution of earlier design concepts and improves the balance between the natural and engineered barriers at Yucca Mountain, but it is not yet the final design for the LA. DOE will continue its evaluation of other design concepts over the next year before focusing the program on the LA design next summer. Design work to demonstrate safe operations of the surface facilities during the preclosure phase is also included in the LA work plans.

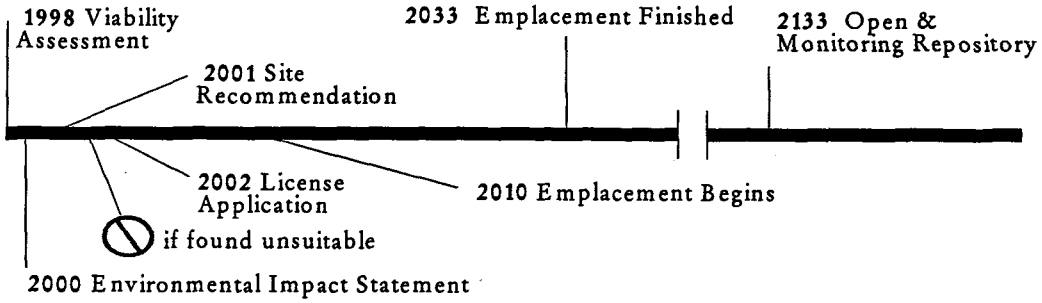

Figure 6 – Repository Timeline

The major work activities required to support the license application are identified in a summary schedule in the LA Plan that is related to the work scope descriptions and costs to provide an integrated picture of the work plans.

Cost Estimate for Construction and Operation

The final element of the VA is an estimate of the cost in 1998 dollars to complete design, construct and operate a repository at Yucca Mountain using the reference design. The total estimated cost to complete the design, support NRC license review, construct, operate, monitor, decommission and close the repository is estimated to be $18.7 billion constant value 1998 dollars. The principal cost elements are: surface facilities construction, $5.4 billion; fabrication and loading of waste packages, $4.1 billion; construction of subsurface facilities, $5.0 billion; completion of a performance confirmation program, $2.1 billion; and regulatory, infrastructure and management support, $2.1 billion.

The cost estimate was developed in accordance with the following operations schedule:

March 2002 to February 2005 (Licensing phase)	$0.8 billion
March 2005 to February 2010 (Pre-emplacement construction phase)	$2.9 billion
March 2010 to September 2033 (Emplacement Phase)	$11.1 billion
October 2033 to September 2110 (Monitoring Phase)	$3.5 billion
March 2110 to September 2116 (Closure and Decommissioning Phase)	$0.4 billion

DOE engaged an independent outside cost estimating consultant to thoroughly review the basis for the VA cost estimate. They found the cost estimate to be a reasonable and prudent representation of the costs based on the reference design.

DOE recognizes that the VA cost estimate, while responsive to the mandate of Congress, does not address all aspects of a total life cycle cost for the program. The total System Life Cycle

Cost Estimate, being prepare as a VA companion document, provides a total cost picture for use in financial planning, policy making, as well as assessing the adequacy of the fees paid by commercial utilities for the storage of their spent nuclear fuel.

Summary

In the VA, DOE presents a reference design for a repository at Yucca Mountain and an integrated assessment of the expected performance of the repository for long future time periods. This assessment is based on the science and engineering work that has been done at Yucca Mountain for the last 20 years. Significant improvements have been made in representing these results in the TSPA-VA that should build confidence in the program. As a management tool the VA is effective in focusing the program on remaining technical issues and it has led to the development of a sound plan to develop the license application by 2002.

Day 1, Stop 1

Nucleation and Interactions of Faults at Yucca Mountain, Nevada

Potter, C.J., Sweetkind, D.S., and Day, W.C.
Geological Society of America Abstracts with Programs, 1997, v. 29, no. 6, p. A-199.

At the site of the potential underground nuclear waste repository at Yucca Mountain, Nevada, structural studies at scales of 1:120 through 1:24,000 have yielded a systematic understanding of interactions among faults and joints whose lengths span three orders of magnitude. The hierarchy of structures includes: north-striking block-bounding faults spaced one to four km apart, commonly with hundreds of meters of normal-sense Tertiary displacement; northwest-striking relay faults that transfer displacement between block-bounding faults; smaller intrablock faults (commonly with 1 to 20 m of displacement); and a network of joints and tectonic fractures that, where best-developed, divides the rock mass at the cubic-meter scale. These structures are developed in Miocene pyroclastic rocks dominated by thick welded ash-flow tuffs and thinner nonwelded tuffs of the 12.8 to 12.7-Ma Paintbrush Group. Our studies have documented the relative influences of local stratigraphic control *vs.* regional tectonic control for the genesis of this spectrum of structures. The smallest intrablock faults were controlled by local stratigraphy, and block-bounding faults were controlled by the regional Miocene tectonic stress field. Structures intermediate in scale between these two end members were influenced by both factors.

At the mesoscopic scale, the internal stratigraphy of the Paintbrush Group strongly controlled the development of early-formed networks of cooling joints that form the fundamental fabric element subsequently exploited by younger fault patterns (fig. 1). Intrablock faults inherited their near-vertical dips and discontinuous natures from cooling joints along which they nucleated. In highly jointed stratigraphic zones, intrablock fault zones widen, and minor tectonic activation of myriad cooling joints accounts for a significant component of the intrablock strain. Displacement along the joint network may also accommodate strain between discontinuous intrablock faults. Among intrablock faults that are 0.5 km or greater in length, there is a transition from those whose geometry is fundamentally controlled by cooling joints (e.g., Sundance Fault), and those whose geometry appears controlled by block-bounding fault displacements (e.g., Ghost Dance Fault and block-margin faults in the hanging-wall of the Bow Ridge Fault). The former tend to be zones of discontinuous faulting whereas the latter are defined by fairly continuous map traces. Splays along these continuous traces, locally forming narrow grabens analogous to tension gashes, probably exploited pre-existing cooling joints. Relay faults are a fundamental part of the block-bounding fault systems, although their specific location may be influenced by pre-existing cooling joints. The stratigraphic control so important to intrablock fault growth did not affect the propagation and geometry of block-bounding faults, which are purely a reflection of regional tectonic influences.

Figure 1. Site area geologic map

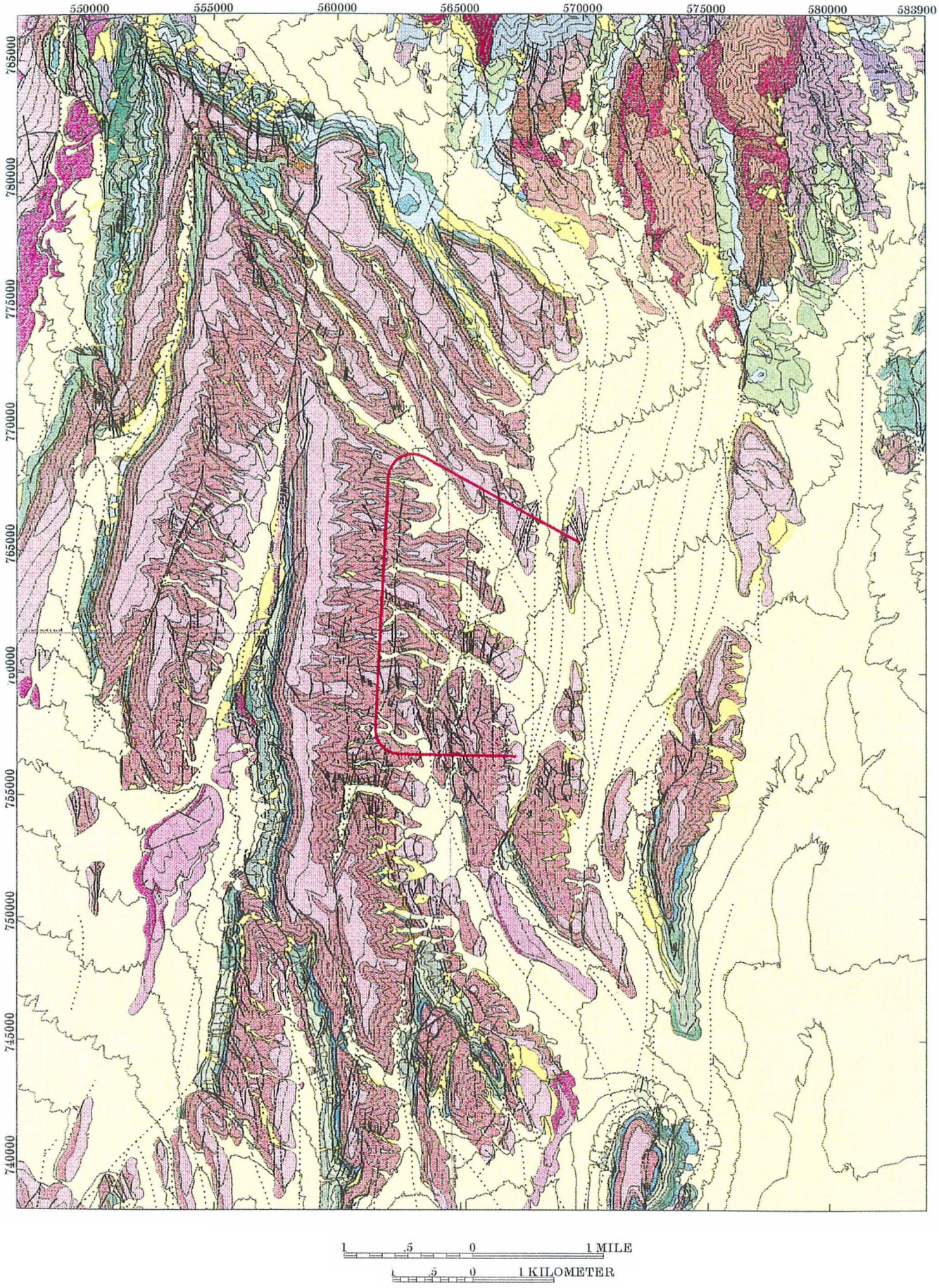
550000
555000
560000
565000
570000
575000
580000
583900
785000
780000
775000
770000
765000
760000
755000
750000
745000
740000
1 .5 0 1 MILE
1 .5 0 1 KILOMETER

EXPLANATION: GEOLOGIC MAP OF THE NYE COUNTY AREA

Day 1, Stop 2

A Long-term Paleoseismic Record of the Paintbrush Canyon Fault Interpreted from Faulted Sand-Ramp Deposits at Busted Butte, Nye County, Nevada

Christopher M. Menges, John W. Whitney, Jeff A. Coe, John R. Wesling and Andrew Thomas

Introduction

The Paintbrush Canyon fault is a 26- to 33-km-long, normal to left-normal-oblique fault on the eastern margin of Yucca Mountain that contains abundant evidence for Quaternary activity (Simonds and others, 1995). This fault is the dominant block-bounding fault on the east side of the mountain in terms of both length and bedrock displacement. The fault primarily strikes north to northeast (N. 5-45° E., averaging N. 10° E.) (Scott and Bonk, 1984; Simonds and others, 1995). Fault dips in bedrock vary from 45° W. to 85° W. and average 70° W. Estimates of down-to-the-west vertical separations of middle Miocene volcanic units based on geologic mapping, borehole data, and structural cross-sections increase southward from 210 m at the north end of the fault to as much 500 to 550 m on two adjacent splays of the fault at the southeastern corner of Midway Valley (Dickerson and Spengler, 1994; Scott and Bonk, 1984). The fault is nearly continuously exposed in bedrock to the north of Yucca Wash, but the surface trace is mostly buried by a thin veneer of unfaulted alluvial, colluvial, and eolian deposits at the western bases of the discontinuous bedrock ridges of Alice Ridge, Fran Ridge, and Busted Butte (fig. 1; Dickerson and Spengler, 1994; Dickerson and Drake, 1998; Simonds and others, 1995). The southern extent of the fault is unclear; it may either terminate beneath the sand ramps at the southern end of Busted Butte, or more likely continue to the southwest beneath unfaulted alluvium to either connect with the fault scarps of the Stagecoach Road fault at southern Yucca Mountain (fig. 1; Simonds and others, 1995) or possibly merge with a large bedrock fault at the southeastern corner of the mountain (C. Potter and D. Sweetkind, U.S. Geological Survey, written commun., 1998).

Figure 1. Location map of major faults and trenches at Yucca Mountain, including the natural exposures at Busted Butte (BB1 to BB4).

Paleoseismic investigations conducted at three sites (A1 at Alice Ridge, MWV-T4 in southeastern Midway Valley, and BB-W1 to BB-W4 at Busted Butte; fig. 1) demonstrate multiple Quaternary surface displacements on the central and southern sections of the Paintbrush Canyon fault. At the latter site, thick deposits of eolian sand are banked steeply along both flanks of Busted Butte, a prominent isolated bedrock knoll on the southeastern edge of Yucca Mountain (Fig. 1). These sand ramps are dissected by gullies as much as 25 m deep that spectacularly expose the surface trace of the Paintbrush Canyon fault. The displacement of discrete strata, stonelines, and buried soils in the sand ramp exposures provide an unusually long and well constrained paleoseismic record of prehistoric surface-rupturing earthquakes on this fault, a record which spans essentially the complete middle to late Pleistocene time interval (post 700 ka) (see following section on stratigraphy and soils).

LOCATION MAP OF MAJOR FAULTS AND TRENCHES AT YUCCA MOUNTAIN

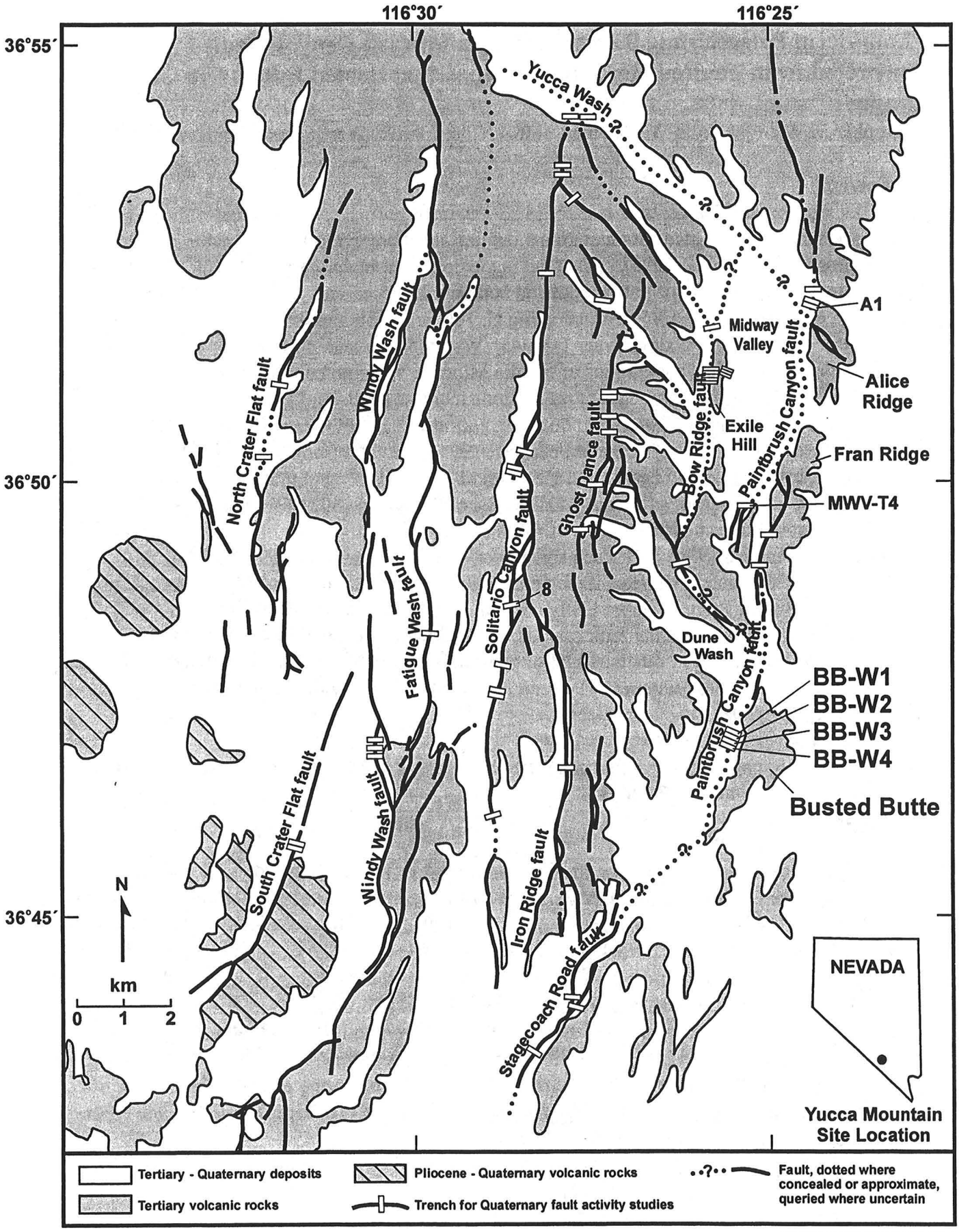

GEOXSEC3.CDR.123/10-1-98

Specifically, four gully walls with approximately 30° slopes were cleaned in August 1992 to enhance the natural exposures of the main and subsidiary fault traces, as well as adjacent displaced strata and soils. There is no fault scarp or other topographic expression of the fault where it crosses the broad interfluve surfaces between the gullies. All or parts of three exposures (walls 1, 2, and 4) were logged in detail (see below; figures 2, 3, 4); however, the following discussion focuses on the logs and interpretations from walls 1 and 4, with an emphasis on the latter, because they contain the most complete stratigraphic record of faulting.

Figure 2. Simplified log of a natural exposure of lithologic units, soils and the Paintbrush Canyon fault in sand ramp deposits at Busted Butte wall 4. The box outlines the area of figure 3. The position, labels, and age of geochronologic samples (selected set for sites with multiple determinations) are shown except in area of box (refer to figure 3)

Figure 3. Detail of log of the upper part of the natural exposure of lithologic units, soils and the Paintbrush Canyon fault in sand ramp deposits at Busted Butte wall 4. See figure 2 for location within the full exposure. The position, labels and age of geochronologic samples (selected set for sites with multiple determinations) are shown, except for HD1455, which was not used in interpretations because of especially poor age resolution and large analytical uncertainties.

Figure 4. Simplified log of a natural exposure of lithologic units, soils and the Paintbrush Canyon fault in sand ramp deposits at Busted Butte wall 1.

This type of displacement record provides critical data for seismic hazard analyses which are an important component of site characterization for the potential high-level radioactive waste repository at Yucca Mountain (U.S. Department of Energy, 1988). Seismic source characterization of site faults in particular must rely on paleoseismic investigations because of the general low level of historical seismicity on the Yucca Mountain fault (Brune and others, 1992).

Methods

All of walls 1 and 4 (the northernmost and southernmost exposures, respectively) and the lower part of wall 2 were carefully cleaned and locally excavated where necessary by hand prior to flagging of lithologic contacts, soil horizons, and structures. Logs were prepared for walls 1 and 4 using the close-range photogrammetric technique of Fairer and others (1989) and Coe and others (1991) in order to facilitate accurate digital rendering of the 20- to 25-m high sloping gully walls in a vertical projection. Individual sand units and soils in each logged wall were described in detail and correlated among walls (table 1). The relations among soils, lithologic units, buried scarps, and structures were used to interpret the stratigraphic position, size and age of surface faulting events, and these in turn were used to derive paleoseismic parameters such as recurrence intervals and slip rates (Schwartz, 1988; McCalpin, 1996). Offsets of units and soils across the fault were measured where possible both in the field and on the logs.

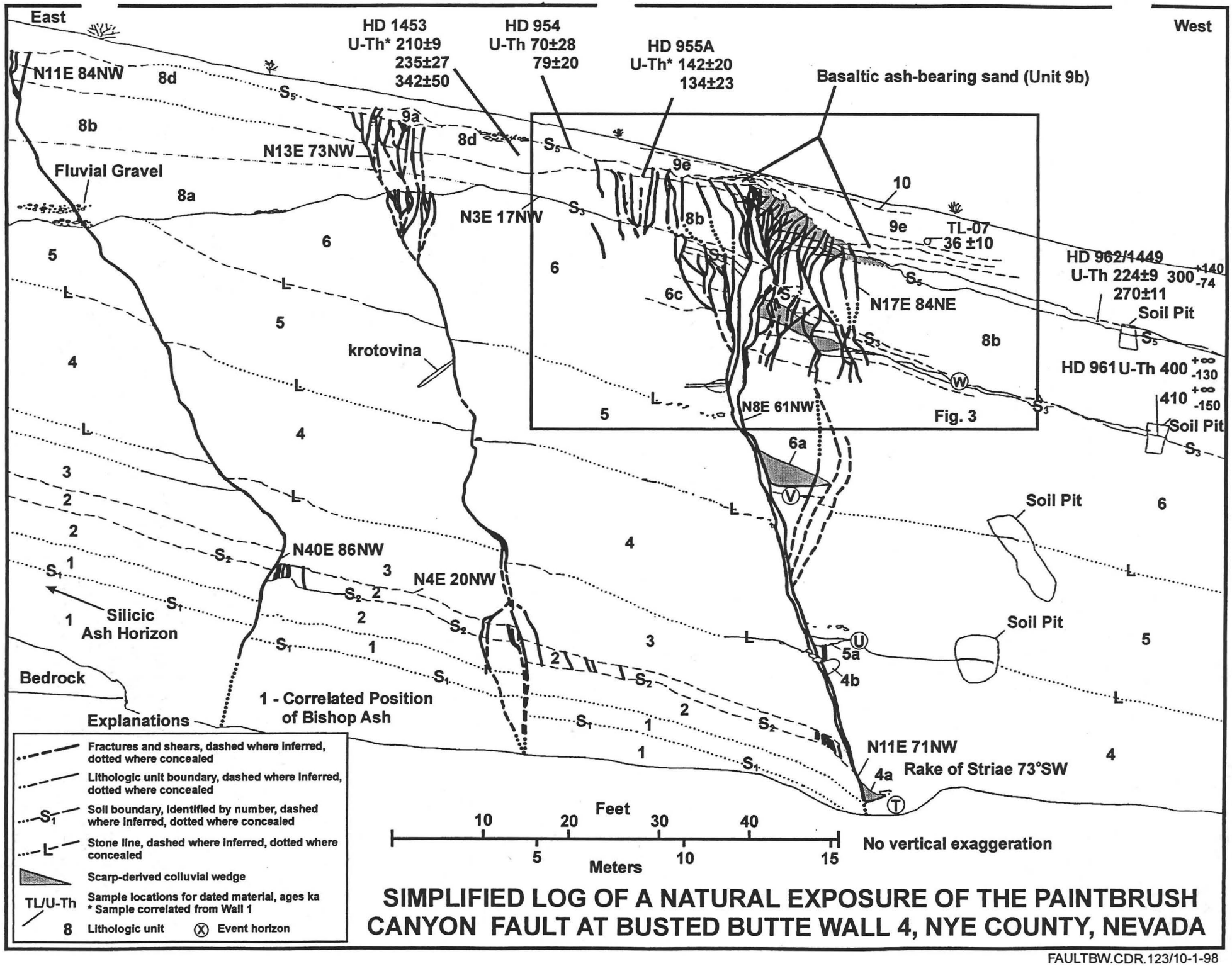

SIMPLIFIED LOG OF A NATURAL EXPOSURE OF THE PAINTBRUSH CANYON FAULT AT BUSTED BUTTE WALL 4, NYE COUNTY, NEVADA

FAULTBW.CDR.123/10-1-98

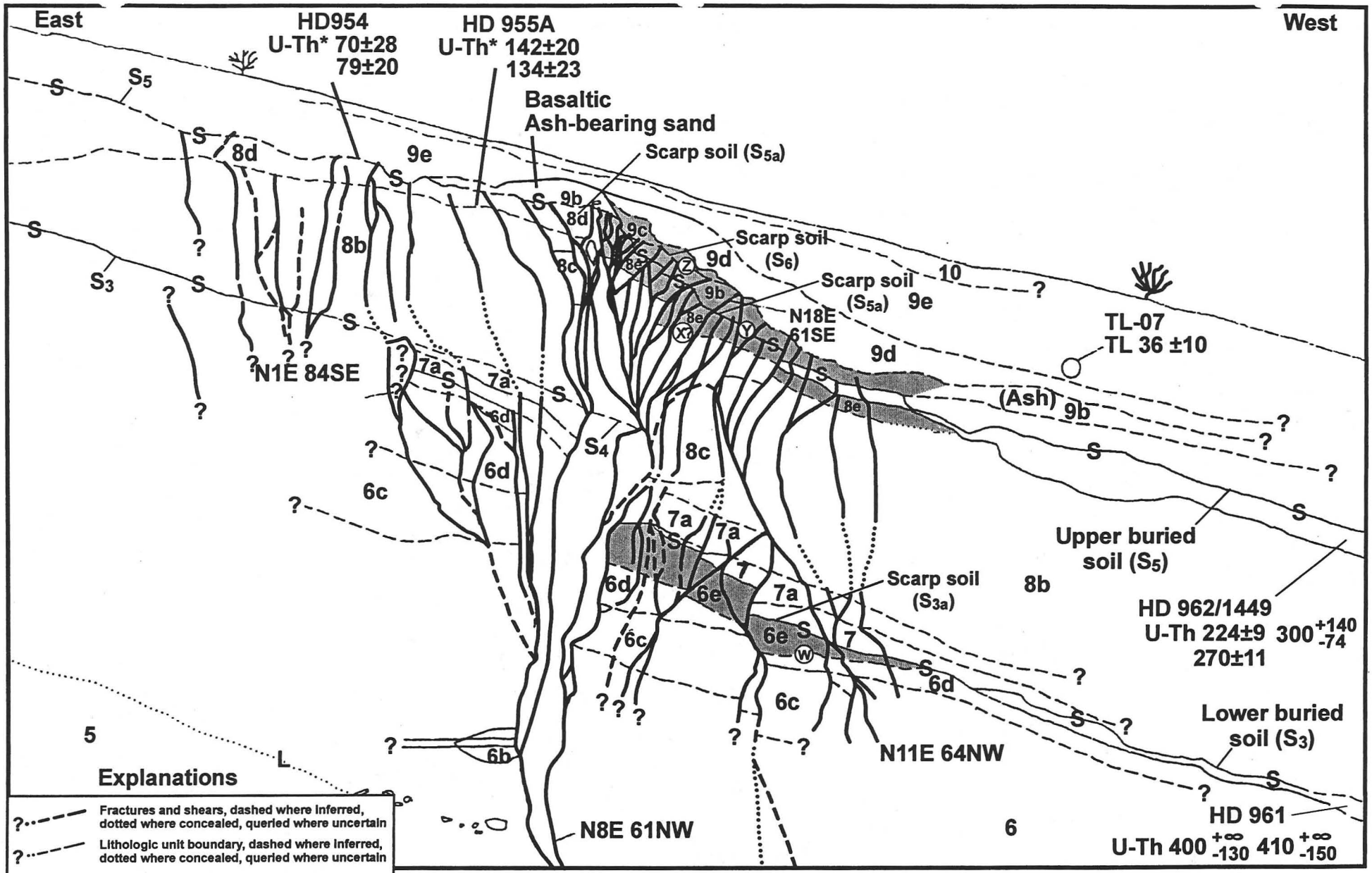

SIMPLIFIED LOG OF NATURAL EXPOSURE OF PAINTBRUSH CANYON FAULT UPPER PART, BUSTED BUTTE WALL 4

FAULTBW.CDR.123/10-1-98

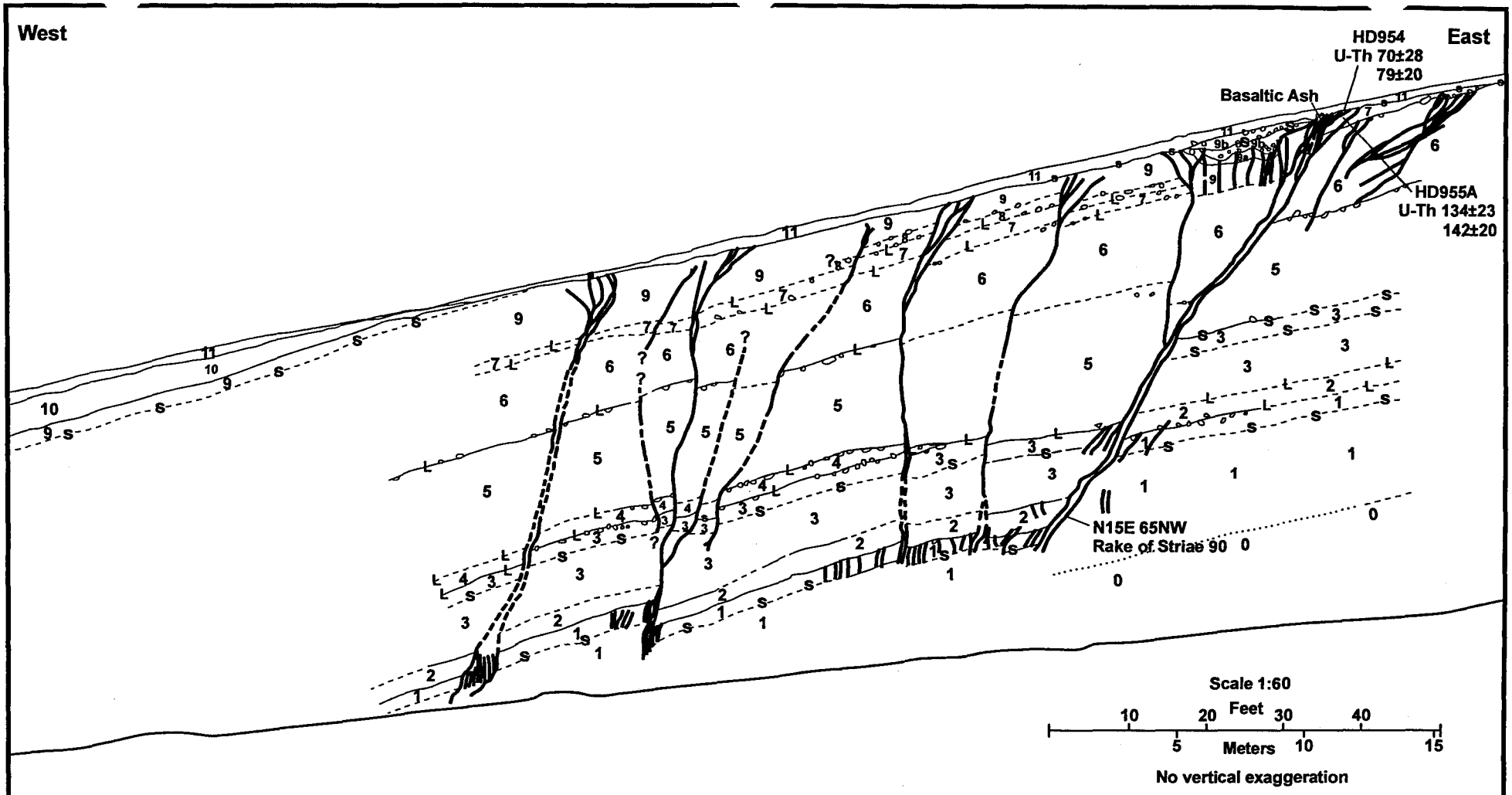

? Fractures and shears, dashed where inferred, queried where uncertain

Lithologic unit boundary, dashed where inferred, dotted where concealed

S Soil boundary, dashed where inferred

L Stone line, dashed where inferred

TL/U-Th Sample locations for dated material, ages ka

8 Lithologic unit

SIMPLIFIED LOG OF A NATURAL EXPOSURE OF THE PAINTBRUSH CANYON FAULT AT BUSTED BUTTE WALL 1, NYE COUNTY, NEVADA

Table 1. Lithostratigraphic correlations of depositional units in walls 1 and 4 at Busted Butte. [All units are shown in trench logs of figures 2, 3, and 4.}

Wall 4 Units	Wall 1 Units
1	0
2	1
3	2, 3
3a	within 3
4	4
4a	within 4
4b	within 4
5	5
5a	within 5
6	6
6a	within 6
6b	within 6
6c	within 6
6d	within 6
6e	within 7, 8, 9
7	within 7, 8, 9
7a	within 7, 8, 9
8a	within 10
8b	within 10
8c	within 10
8d	within 10
8e	9a
9a	9b
9b	within 11
9c	within 11
9d	within 11
9e	within 11
10	within 11

Age control for faulted and unfaulted deposits and soils was obtained by two methods. Minimum ages of soils and lithologic units in wall 1, 3 and 4 were derived by U-Th disequilibrium (U-series) dating of 10 sample sets of secondary pedogenic carbonate or silica laminae, soil matrix carbonate, and (or) rhizoliths (carbonate-replaced root casts) (table 2; J.B. Paces and others, U.S. Geological Survey, written commun., 1995; Muhs, U.S. Geological Survey, written commun., 1989). The majority (8) of the U-series samples were analyzed with older alpha-spectrometry technology, although three samples were analyzed with the more robust and reliable mass spectrometry method. Analyses completed after 1992 in conjunction with the exposure mapping on walls 1 and 4 are emphasized more than earlier U-series dating of secondary carbonate from the unlogged wall 3. In addition, one sample of fine-grained polymineralic sediment from wall 4 was dated by thermoluminescence (TL) analysis (table 1; J.B. Paces and others, U.S. Geological Survey, written commun., 1995).

Stratigraphy and Soils

Wall 4 contains a westward-dipping sequence of 10 unconsolidated lithologic units with seven buried soils that represents the single most complete stratigraphic succession at the Busted Butte site (fig. 2). The thickness of the exposed section is 22 m. Bedrock is locally exposed at the bottom of the gully in the footwall block. Bishop ash (about 760 ka; van den Bogaard and Schirnick, 1995) is preserved near the base of eolian sand-ramp deposits at the south end of Busted Butte (site 50, Izett and others, 1988), and similar silicic ash is intercalated with sand layers at the base of wall 4 (unit 1, fig. 2). Thus, the sand ramps in this area chronicle approximately the last 700 to 600 k.y. of displacement history on the Paintbrush Canyon fault. The lower part of the sequence consists of thick massive well sorted sand layers (units 1 through 5, fig. 2) which are differentiated primarily on the basis of bounding discontinuous stone lines. Lithologic units in the upper part of the wall (units 6 through 10; figs. 2, 3) tend to be thinner and display greater lateral variations in thickness, relative to the lower sand deposits. The predominantly sandy units in the upper wall also contain more coarse-grained gravelly layers that typically mantle the slopes of two distinct buried fault scarps (see below).

Weak calcic soils (stage I-II, after Birkeland, 1984 and Machette, 1985,) typically consisting of nodular carbonate and (or) discontinuous coatings on the underside of gravel clasts (S1 and S2, fig.2), are locally associated with stone lines in the lowermost part of wall 4. Two moderately to well-developed buried soils with carbonate stage II-IV morphologies and locally abundant rhizoliths are prominent features in the upper part of wall 4 (S3 and S5, figs. 2, 3). Although both of these major soils are disrupted by prominent buried fault scarps, soil formation continued after development of the scarps, producing a zone of silica-carbonate laminae (S3a and S5a, fig. 3) which mantles the scarp slope. At least one thin, poorly-developed carbonate soil has formed locally on units that bury the fault scarps as well (S4 on unit 7a and S6 on unit 9b, fig. 3). On the other walls the two prominent upper buried soils (S3 and S5) are erosionally truncated at or westward (downslope) from the fault beneath weak pavements and thin soils developed on the erosional upper surface of the sand ramps (for example, fig. 4). This type of erosional truncation apparently did not occur on wall 4, perhaps in part because here the fault intersects the sand ramp at a site of net deposition located downslope from areas of erosional stripping.

Table 2. Summary of geochronologic samples and radiometric age determinations from walls 1, 3 and 4 at Busted Butte.

[Ages for walls 1 and 4 are cited from Paces and others, U.S. Geological Survey, written commun., 1995, which supersede preliminary ages reported in Paces and others (1994) and Menges and others (1994). Stratigraphic units reported include local lithologic units and soils, followed by correlations to regional geochronologic units (in parentheses). Specifically, local units are correlated with the Qe sand-ramp unit in the surficial mapping of Yucca Mountain (Lundstrom and others, U.S. Geological Survey, written commun., 1998). The Qe unit spans a broad Holocene to middle Pleistocene time interval approximately equivalent to alluvial units Q5 to Q1 (mostly late to middle Pleistocene units Q3 and Q4). All TL and U-series age estimates are reported with 2 σ errors. Most measurements of U-series samples were conducted with an alpha spectrometer (as) although three samples were analyzed with a mass spectrometer (ms). Table modified from E. M. Taylor, U.S. Geological Survey , written commun., 1998]

Sample Number	Material Dated	Lithologic Units and Soils	Age Estimate (ka)	Dating Technique	Purpose and Interpreted Context of Age	Reference[1]
Wall 1						
HD 959	Upper K horizon, hanging wall	9 / top (Qe)	20 ± 6	U-series (as)	Composite soil sample	1, 2
HD 954	Upper K horizon, footwall	7+8 / top (Qe)	70 ± 28 77 ± 19 79 ± 20	U-series (as)	Composite soil sample	1, 2
HD 955A	Upper K horizon, rhizolith, footwall	7+8 / mid (Qe)	134 ± 23 137 ± 27 142 ± 20	U-series (as)	Composite sample of rhizoliths	1, 2
HD 955B	Rhizolith, main fault zone	9 / mid (Qe)	187 ± 8	U-series (as)	Age of secondary carbonate that replaces root	1
Wall 4						
TL-07	Sand, above upper K horizon, hanging wall	9e / bot (Qe)	36 ± 10	TL	Time when eolian sand last exposed to sunlight	1, 2
HD 1455	Uppermost calcic horizon, (soil S6), hanging wall	9c / top (Qe)	9.7 ± 0.8 43 ± 8 173 ± 11	U-series (ms)	Age of secondary carbonate and silica, in platy rootlets and composite soil	1
HD 1455	Upper K horizon (see above)	9c / top (Qe)	127 ± 19	U-series (as)	Composite soil sample	1

Sample Number	Material Dated	Lithologic Units and Soils	Age Estimate (ka)	Dating Technique	Purpose and Interpreted Context of Age	Reference[1]
HD 1453	Rhizoliths, in and below soil S5, footwall	8d / top (Qe)	63.7 ± 1.2 210 ± 9 212 ± 25 235 ± 27 342 ± 50 454 +76/-51 590 +∞/-130	U-series (ms)	Ages of carbonate/opaline silica replacement of root casts	1
HD 1449	Upper K horizon (soil S5), hanging wall	8b / top (Qe)	224 ± 9 270 ± 11	U-series (ms)	Age of secondary carbonate/opaline silica	1
HD 1449	Upper K horizon (see above)	8b / top (Qe)	272 +35/-28	U-series (as)	Composite soil sample	1
HD 962	Upper K horizon (soil S5), hanging wall	8b / top (Qe)	300 +140/-74 340 +82/-53	U-series (as)	Composite soil sample	1, 2
HD 961	Lower K horizon (soil S3), hanging wall	6 / top (Qe)	196 +36/-28 400 +∞/-130 410 +∞/-150 750 +∞/-150	U-series (as)	Composite soil sample	1, 2
<u>Wall 3</u>						
HD 57	Upper K horizon, upper part, hanging wall	(Qe)	180 ± 20	U-series (as)	Age of secondary carbonate	3
HD 58 HD 58R	Upper K horizon, lowest part, hanging wall	(Qe)	116 ± 10 179 ± 17	U-series (as)	Age of secondary carbonate	3, 4
HD 59-1-A HD 59-1-B	Rhizoliths immediately below upper K horizon, hanging wall	(Qe)	318 ± 23 209 ± 7	U-series (as)	Age of secondary carbonate that replace root	3
HD 76	Second K horizon below surface, lower part, hanging wall	(Qe)	182 ± 11 174 ± 10	U-series (as)	Age of secondary carbonate	3, 4
HD 77-1-A HD 77-1-B	Rhizoliths immediately below lower K horizon, hanging wall	(Qe)	>350 200 ± 7	U-series (as)	Age of secondary carbonate	3

1 References for samples and geochronologic data are: 1- Paces and others, U.S. Geological Survey, written commun., 1995; 2- Paces and others, 1994; 3 - Muhs, U.S. Geological Survey, written commun., 1989; 4 - Muhs and others, 1990.

Structure

The main trace of the fault zone is well defined by a 0.2- to 5-m-wide zone of carbonate-coated shears and fractures that commonly increase in complexity upsection (figs. 2, 3, 4). The average orientation of the main fault zone in these exposures is N.15° E., 70° W. Striations of probable tectonic origin on carbonate-coated shears (N. 11° E.; 71° W.) in the sand-ramp fault zone of wall 4 exhibit left-oblique slip with a rake of 73°SW (fig. 2), and slickenlines with left-oblique slip with a rake of 47° are observed in nearby similarly oriented bedrock exposures of the fault (Whitney and Muhs, 1991; Simonds and others, 1995). The former orientation is used to correct for net tectonic displacements because it represents the most direct and unambiguous link to Quaternary slip on the fault. Vertical slickenlines were observed on carbonate coatings in the fault near the bottom of wall 1 (fig. 4), and thus no net tectonic corrections are required for dip-slip displacements on this exposure.

The hanging-wall block in the upper part of most exposures is deformed by a complex network of synthetic and antithetic minor faults and fractures. Secondary hanging-wall deformation approaches 25 m in width in the northernmost exposure (wall 1; fig 4) and includes a small antithetic graben adjacent to the main fault near the top of the wall. In wall 4, two secondary synthetic fault strands displace sand-ramp units in the footwall block to the east of the main fault trace (fig. 2).

Paleoseismic Interpretations

Event Identification. Structural and stratigraphic relationships used in event identification are summarized below for wall 4 because this wall provides the most complete and interpretable record of fault displacements. Successively smaller displacements of younger horizons, fault-generated colluvial wedges, and several buried scarps are interpreted to represent six to seven individual ruptures. Minimum and maximum estimates of dip-slip displacements per event across all faults vary from 0 (no displacement) to 246 cm, with preferred estimates in the range of 42 to 160 cm (table 3). Preferred estimates of net displacements per event vary from 44 to 167 cm. All seven of the buried soils and three additional distinct stone lines are offset along the main fault trace (figs. 2, 3).

Table 3. Identification criteria, reliability, separation and displacement per event estimates, and age constraints for surface-rupturing events interpreted in wall 4 at Busted Butte.

The uppermost buried soil (S5) appears displaced by at least two surface-rupturing events (the most recent (Z) and penultimate (Y) events) that in part have produced colluvial slope deposits (units 9c and 9b, respectively; fig. 3; table 3). These units drape downslope across the upper composite fault scarp developed above unit 8e. The most recent event (Z) deforms and thus postdates a colluvial gravel unit (9b) with a thin calcic soil (S6) which buries the initial fault scarp and related soil (S5a). The scarp and units associated with event Z in turn are buried by several unfaulted gravel or sand deposits that locally are plugged with secondary carbonate (for example units 9c, 9d, and 9e, fig. 3). The penultimate event is interpreted from a set of shears and fractures that displace the scarp and related soil (S5a) but terminate at the base of unit 9b. A possible third event (event X, table 3) may have produced a small initial paleoscarp (represented by the top of unit 8e) that developed following offset of the original buried soil (S5). This paleoscarp was reruptured subsequently by the two younger events to form the composite upper buried scarp. Event X is queried because it is possible, although difficult, to produce the composite upper scarp from only two events (Y and Z). A third event is suggested, but not required, to account for the observed displacements at this stratigraphic level. The cumulative vertical displacements of the two or three most recent fault events is approximately 1.2 m, as measured by the total offset of unit 7a along all of the strands of the fault zone below the upper composite scarp (Fig. 3).

The next lower buried soil (S3) developed on unit 6 (figs. 2, 3; table 3) is displaced by one earlier surface rupture (event W). This event occurred during soil development and caused a dip-slip displacement along the main fault trace of about 1.3 m that is associated with a lower buried fault scarp developed at the top of a colluvial wedge (unit 6e, fig. 3). The total dip-slip displacement across the main fault strand of the original surface above and below the lower scarp is 2.2 to 2.5 m; this measurement includes the cumulative displacement of the three to four events at and above this stratigraphic horizon. An additional 25 cm displacement occurred during event W on one of the eastern fault strands as well.

Below the two upper buried soils, two events (events V and T) are recorded by carbonate-impregnated colluvial wedges in the mid-to-lower slope of the sand ramp (units 6a and 4a, fig. 2; table 3). A third event (event U) is indicated in the lower part of the exposure by terminations of fractures against a small gravelly channel deposit adjacent to the fault zone (unit 5a, fig. 2; table 3), and by decreasing differential displacements of units 4 and 5.

Minimum constraints on the cumulative dip-slip displacement of the buried stone line on top of unit 3 (fig. 2) are estimated as 4.3 to 6.7 m, with a preferred value of 5.1 m. Net-slip adjustments increase these displacements to 4.5 to 7.0, with a preferred value of 5.3 m. These values are calculated by adding the cumulative offset of the top of unit 4, as measured on the log, to the total displacement of the rupture event (event T, table 3) recorded in a stratigraphically lower colluvial wedge within unit 4 (unit 4a, fig. 2). This procedure is required because the downthrown equivalent of the unit 3 stone line is not exposed on the hanging wall. The two

Table 3. Identification criteria, reliability, separation and displacement per event estimates, and age constraints for surface-rupturing events interpreted at wall 4 at Busted Butte.

[Faults and stratigraphic positions of events are shown on figures 2 and3. Refer to text for additional discussion. cm: centimeters; ka: thousands of years ago]

Event	Event Horizon[1]	Dip Separation, Main Fault[2] (cm)		Dip Separation, All Faults[3] (cm)		Net Tectonic Displacement[4] (cm)		Reliability[5]	Evidence	Comments	Age Criteria[6]
		Range	Pref	Range	Pref	Range	Pref				
Z	Top of unit 9b	0 - 69	42	0 - 69	42	0 - 72	44	H	Fractures that displace, and terminate at the top of, unit 9b (ashy sand) on all faults.	Event post-dates deposition of sand deposit with basaltic ash (unit 9b) on previously existing upper fault scarp, but predates units 9c, 9d, and 9e that bury scarp.	30 - 90 (≥40-50)
Y	Top of unit 8d	15 - 54	27	15 - 54	27	16 - 56	28	H	Fractures that terminate at the base of unit 9b. Top of unit 8d is displaced more than top of unit 9b.	Event occurred during upper scarp soil development (soil S5a on units 8b-8d) and prior to the deposition of unit 9b with basaltic ash.	80 - 300, probably 80 - 150 (≈110)
X?	Top of unit 8d	33 - 66	45	33 - 66	45	35 - 69	47	P	Thickening of unit 8d on hanging wall of main fault. Differential displacement of the base and top of unit 8d.	Possible event occurred during deposition of unit 8d and between development of upper scarp soil S5a on unit 8d and soil S5 on unit 8.	300 - 150 (≈225)
W	Top of unit 6d	84 - 146	135	84 - 196	160	88 - 205	167	H	Top of unit 6 is displaced more than the top of unit 7a on main fault. Fractures terminate at top of unit 6 on secondary fault. Probable colluvial wedge (unit 6e) on main fault.	Event occurred during or after development of soil S3 on units 6, 6c, and 6d, but prior to development of soil S5 on unit 8b. Displacement also on middle secondary fault.	400 - 300 (≈350)
V	Top of unit 5	4 - 162	111	4 - 212	136	4 - 222	142	H-M	Base of unit 6 is displaced more than top of unit 6. Probable colluvial wedge (unit 6a) in unit 6 on main fault.	Event occurred during deposition of unit 6 and prior to development of soil S3 on unit 6. Displacement also on middle secondary fault.	400 - 700
U	Top of unit 4	0 - 216	60	40 - 246	100	42 - 257	105	M	Base of unit 5 is displaced more than base of unit 6 on main fault. Several fractures terminate at base of unit 5a.	Event occurred during deposition of unit 5. Displacement also on easternmost secondary fault.	400 - 700

Event	Event Horizon[1]	Dip Separation, Main Fault[2] (cm)		Dip Separation, All Faults[3] (cm)		Net Tectonic Displacement[4] (cm)		Reliability[5]	Evidence	Comments	Age Criteria[6]
		Range	Pref	Range	Pref	Range	Pref				
T	Top of unit 3	72 - 192	90	72 - 192	90	75 - 201	94	M	Base of unit 4 is displaced more than base of unit 5 on main fault. L Probable colluvial wedge (unit 4a).	Event occurred during deposition of unit 4.	400 - 700

Table 3. Identification criteria, reliability, separation and displacement per event estimates, and age constraints for surface-rupturing events interpreted at wall 4 at Busted Butte–cont.

1. Event horizons are described, and shown on logs, at the stratigraphic horizons where the event is interpreted to occur, commonly in this exposure based on the horizon where differentioal displacements are observed. Events T, V, and X occurred above the designated horizons as indicated by colluvial wedges (units 4a, 6a, and overthickened 8a) that occur within the overlying unit (see fig. 2).

2.Estimated dip separation per event measured from log, and checked where possible in field, along the main (westernmost) fault stand on figure 2. Both minimum-maximum ranges related to measurement uncertainties are given, with preferred value in parentheses.

3. Estimated dip separation per event measured from log, and checked where possible in field, along all faults (main plus secondary strands) on figure 2. Both minimum-maximum ranges related to measurement uncertainties are given, with preferred value in parentheses.

4. Net tectonic displacements calculated by applying to the dip separation a left-oblique rake of 73°, which is derived from the orientation of striations on carbonate coatings along the fault plane exposed in a pit at the base of the exposure. Both minimum-maximum ranges related to measurement uncertainties are given, with preferred value in parentheses.

5. Reliability of event identification: H, high (clear expression with diagnostic criteria); M, moderate (strongly suggestive, but nondiagnostic criteria); P, poor (suggestive, but ambiguous evidence).

6. Age constraints on faulting, generally consisting of lower and upper bracketing ages related to dated units or soils that are interpreted to predate or post-date the event. Maximum and minimum age constraints are given, with preferred ages in parentheses. Most of the geochronologic control are U-series or TL age determinations listed in table 2. The 700 ka lower age constraints for events V through T results from the presence of felsic ash correlated with the Bishop Tuff eruption (760 ka) that is present in soil S1 and unit 1 at the base of the exposure; an exposure of a similar more concentrated ash unit identified as the Bishop Ash is present at the base of the sand-ramp section exposed in a gully wall at the southern end of Busted Butte (site 50, Izett and others, 1988).

eastern secondary faults on wall 4 add another 0.9 m of cumulative dip-slip displacement at the stratigraphic levels of units 5 and 6, which, combined with offsets observed on the main strand, produces a minimum estimate of 5.5 to 8.0 m (preferred value of 6.3m) for the post-700 ka net cumulative displacement on units 1and 2 at the base of the exposure.

The number and amounts of the younger set of displacements cannot be deciphered clearly on the other walls because there is a significant loss of stratigraphic record at the fault zone resulting from erosional truncation of soils and units beneath the upper surface of the sand ramps. This problem is especially acute on the footwall block of these exposures. Wall 3 and the upper part of wall 2 were not logged because of severe erosion of units at upper stratigraphic levels near the fault. On wall 1 the last two or three events associated with graben deformation (events Z to X) on the main fault zone can be correlated confidently with the fault chronology of wall 4. Three older events (events W to U) at wall 1 have been correlated provisionally as well, but these correlations are less confident because a significant stratigraphic section underlying the graben was stripped from the area now exposed in wall 1. This indicates a period of erosion that predates graben formation. Erosion during and postdating graben development is confined primarily to the footwall block.

Event Timing Constraints. Age constraints for this long paleoseismic record are based on the combined U-series and TL dates from walls 1 and 4 (tables 2, 3). Correlations of dates between walls primarily are based on the context of samples relative to stratigraphic units, soils, and local fault chronology on each exposure. An approximate maximum age of 650-700 ka for the lowermost buried soil on wall 4 is derived from its stratigraphic position above unit 1, which is correlated with an exposure of a basal sand ramp layer containing the Bishop Ash at the southern end of Busted Butte (site 50, Izett and others, 1988). This correlation is supported by a concentration of felsic ash resembling the nearby Bishop Ash outcrop within a sandy layer of unit 1 on wall 4. The lithology and soils of units 2 through 5 in the lower and middle sections of the wall were not suitable for dating, and thus the only age constraints on the older events (T, U, and V) are that they all postdate 650-700 ka (ash-bearing unit 1) and predate approximately 400 ka (age of the lower buried soil S3, see below).

U-series analyses of pedogenic carbonate laminae collected on wall 4 (Paces and others, U.S. Geological Survey, written commun., 1995) suggest poorly constrained ages mostly from matrix or laminar carbonate of approximately 400 ka for the soil (S3) predating formation of the lower buried scarp (unit 6, figs. 2, 3), and 270 to 300 ka for the soil (S5) disrupted across the upper fault scarp (top of unit 8, figs. 2, 3). Event W occurred sometime between the formation of soils S3 and S5. A suite of rhizoliths in a soil (S5a) formed on the crest of a correlative upper buried scarp to the north on wall 1 yielded U-series ages of about 140 ka, although some of these rhizoliths could be associated with the main soil S5 as well. These rhizolith ages are somewhat younger than the cluster of rhizolith ages of 210 to 340 ka from a lithologically and stratigraphically similar unit (unit 8b) in wall 4. Some of this wide variation in the rhizolith ages may reflect inclusion of reworked older rhizoliths washing out from an eroding fault scarp.

The last two to three events postdate the upper soil (S5) and the units containing these rhizoliths. That is, event X occurred sometime after the formation of soil S5 at 300 ka and probably before at least part of soil S5a development between 300 and 150 ka, based on the

rhizolith ages from both walls. Carbonate laminae with U-series ages of 70 to 80 ka along the fault zone on wall 1 is correlated with the soil (S6) that formed on a unit (9b) burying the upper scarp on wall 4 (figs. 2, 3). The time interval between soils S5a and S6 approximately brackets the penultimate event (event Y) between approximately 300 and 80 ka, and probably between 150 and 80 ka (tables 2, 3), allowing for uncertainties in using minimum ages from rhizoliths and soils to constrain event timing. Soil S6 is displaced by only the most recent rupture (event Z). Unfaulted sand deposits with a TL age of 36 ±10 (unit 9e; fig. 4-D) buries the fault scarp and postdates all events. This establishes a crude bracket for the most recent event of 30 to 90 ka (tables 2, 3, 4). Fractures related to the most recent rupture are coated extensively with carbonate; thus, this faulting probably occurred early in this time bracket (probably ≥40-50 ka). A sand layer (unit 9b, fig. 3) with sparse basaltic ash overlies both the carbonate laminae and upper fault-scarp soil (S5a) and was deposited between the most recent and the penultimate faulting events. This reworked basaltic ash is correlated provisionally with primary tephra from the Lathrop Wells cone with an assigned age of 75±10 ka (B. Crowe, Los Alamos National Laboratory, oral commun., 1995), which establishes an additional maximum age for the faulted unit 9b.

Recurrence Intervals and Fault Slip Rates. These timing relations indicate average recurrence intervals ranging from 40 to 270 thousand years m (k.y.) for the complete sequence of recognizable events; preferred values are 50 to 120 k.y. (table 4). Individual recurrence intervals for the three most recent events with the best timing constraints are 10 to 275 k.y., with preferred intervals of 35 to 100 k.y. Maximum and minimum slip rates of 0.001-0.015 millimeters/year (mm/yr) are computed, based on the net tectonic displacements of three marker horizons at different stratigraphic levels on wall 4 (soil S5 on top of unit 8a; soil S3 on top of unit 6; top of unit 3; table 4). The preferred values are 0.004 to 0.009 mm/yr, with 0.007 mm/yr as a best estimate for the entire middle to upper part of the wall 4 sequence. Long-term average slip rates computed from the lowermost soil (S1) which span the entire post-700 ka paleoseismic record are in the range of 0.008 to 0.01 mm/yr (table 4). The broad range of values in recurrence and slip rate parameters reflect the large uncertainties in age control (both analytical errors and context uncertainties between events and samples), combined with large displacement measurement uncertainties incorporated in slip rate calculations.

Table 4. Summary of paleoseismic parameters for middle to late Quaternary activity on the Paintbrush Canyon fault at Busted Butte.
[cm, centimeters; ka, thousands of years ago; k.y., thousands of years; mm/yr, millimeter per year]

Parameter	Minimum	Maximum	Preferred
Number of events			
Wall 4 only	6	7	7
All walls (1, 2, 4)	7	9	9
Displacements per event (all walls)			
Dip slip	0 cm	246 cm	160 cm
Net tectonic	0 cm	257 cm	167 cm
Age - most recent event	30 ka	90 ka	≥40-50 ka
- penultimate event	80 ka	300 ka	80-150 ka (≈110 ka)
Recurrence intervals			
Average[1]	40 k.y.	270 k.y.	50-120 k.y.
Individual[2]	10 k.y.	275 k.y.	35-100 k.y.
Slip rates			
Three marker horizons[3]	0.001 mm/yr	0.015 mm/yr	0.004-0.009 mm/yr (0.007 mm/yr)
Long term average[4] (Post 700 ka)	0.008 mm/yr	0.01 mm/yr	0.009 mm/yr

1 Average recurrence intervals calculated using the 6-7 events identified in wall 4 which postdate 700 ka (approximate age of ash-bearing unit 1 and soil S1. Large variation in age range results from dating uncertainties combined with sample context problems arising from ambiguity in relating faulting events to dated units.

2 Individual recurrence intervals given only for three most recent events (Z, Y, X) with best age control. Large variation in age range results from dating uncertainties combined with sample context problems arising from ambiguity in relating faulting events to dated units.

3 Range of slip rates calculated using three specific marker horizons on middle and upper part of wall 4 (soil S5 on top, unit 8a; soil S3 on top, unit 6; top, unit 3). Large variation in values reflects both dating uncertainties (analytical and sample context error) and measurement uncertainties of net tectonic displacement.

4 Long-term average slip rate computed from the cumulative offset of the post 700 ka ash-bearing unit 1 and soil S1. Variation in values primarily reflects both dating uncertainties (mainly sample context error) and measurement uncertainties of net tectonic displacement.

References Cited

Birkeland, P.W., 1984, Soils and geomorphology: Oxford University Press, 372 p.

Brune, J.N., Nicks, W., and Aburto, A., 1992, Microearthquakes at Yucca Mountain, Nevada: Bulletin of the Seismological Society of America, v. 82, p. 164-174.

Coe, J.A., Taylor, E.M., and Schilling, S.P., 1991, Close-range geophotogrammetric mapping of trench walls using multi-model stereo restitution software: American Society of Photogrammetry, Engineering, and Remote Sensing, Technical Papers, v. 5, p. 30-43.

Dickerson, R.P., and Drake, Ronald M. II, 1998, Geologic map of the Paintbrush Canyon area, Yucca Mountain, Nevada: U.S. Geological Survey Open File Report 97-783, 25 p., with 2 plates, 1:6,000 scale.

Dickerson, R.P., and Spengler, R.W., 1994, Structural character of the northern segment of the Paintbrush Canyon fault, Yucca Mountain, Nevada: International High-Level Radioactive Waste Management Conference, 5th, Las Vegas, Nevada, April 1994, Proceedings: v. 4, p. 2367-2372.

Fairer, G.M., Whitney, J.W., and Coe, J.A., 1989, a close-range photogrammetric technique for mapping neotectonic features in trenches: Bulletin of Association of Engineering Geologists, v. 26, p. 521-530.

Izett, G.A., Obradovich, J.D., and Mehnert, H.H., 1988, The Bishop Ash bed (Middle Pleistocene) and some older (Pliocene and Pleistocene) chemically and mineralogically similar ash beds in California, Nevada, and Utah: U.S. Geological Survey Bulletin, 1675, 37 p.

Machette, M.N., 1985, Calcic soils of the southwestern United States, *in* Weide, D.L., ed., Soils and Quaternary geology of the southwestern United States: Geological Society of America Special Paper 203, p. 1-21.

McCalpin, J.P., 1996, Paleoseismology: Academic Press, New York, New York, 588 p.

Menges, C.M., Wesling, J.R, Whitney, J.W., Swan, F.H., Coe, J.A., Thomas, A.P., and Oswald, J.A., 1994, Preliminary results of paleoseismic investigations of Quaternary faults on eastern Yucca Mountain, Nye County, Nevada: International High-Level Radioactive Waste Management Conference, 5th, Las Vegas, Nevada, April 1994, Proceedings: v. 4, p. 2373-2390.

Muhs, D.R., Whitney, J.W., Shroba, R.R., Taylor, E.M., and Bush, C.A., 1990, Uranium-series dating of secondary carbonates near Yucca Mountain, Nevada: Application to tectonic, paleoclimatic, and paleohydrologic problems: International High-Level Radioactive Waste Management Conference, 1st, Las Vegas, Nevada, April 1990, Proceedings: v. 2, p. 924-929.

Paces, J.B., Menges, C.M., Widmann, Beth, Wesling, J.R., Bush, C.A., Futa, K., Millard, H.T., Maat, P.B., and Whitney, J.W., 1994, U-series disequilibrium and thermoluminescence ages of paleosols associated with Quaternary faults, east side of Yucca Mountain: International High-Level Radioactive Waste Management Conference, 5th, Las Vegas, Nevada, April 1994, Proceedings: v. 4, p. 2391-2401.

Schwartz, D.P., 1988, Geologic characterization of seismic sources: Moving into the 1990's, *in*, von Thun, ed., Earthquake engineering and soil dynamics, v. 2, Recent advances in ground-motion evaluation: American Society of Civil Engineers Geotechnical Special Publication 20, p. 1-42.

Scott, R.B., 1990, Tectonic setting of Yucca Mountain, southwest Nevada, *in* Wernicke, B.P., ed., Basin and Range extensional tectonics near the latitude of Las Vegas, Nevada: Geological Society of America Memoir 176, p. 251-282.

Scott, R.B., and Bonk, Jerry, 1984, Preliminary geologic map of Yucca Mountain, Nye County, Nevada, with geologic sections: U.S. Geological Survey Open-File Report 84-494, scale 1:12,000, 9 p.

Simonds, F.W., Whitney, J.W., Fox, K.F., Ramelli, A.R., Yount, J.C., Carr, M.D., Menges, C. M., Dickerson, R.P. and Scott, R.B., 1995, Fault map of the Yucca Mountain area, Nye County, Nevada: U.S. Geological Survey Miscellaneous Investigations Series Map I-2520, scale 1:24,000.

U.S. Department of Energy, 1988, Site characterization plan, Yucca Mountain site, Nevada, research and development area, Nevada: U.S. Department of Energy Report DOE/RW-0199, 8 vol., variously paged.

van-den-Bogaard, P., and Schirnick, C., 1995, $^{40}Ar/^{39}Ar$ laser probe ages of Bishop Tuff quartz phenocrysts substantiate long-lived silicic magma chamber at Long Valley, United States: Geology, v. 23, p. 759-762.

Whitney, J.W., and Muhs, D.R., 1991, Quaternary movement on the Paintbrush Canyon-Stagecoach Road fault system, Yucca Mountain, Nevada: Geological Society of America Abstract with Programs, v. 23, no. 5, p. A119.

Day 1, Stop 3

Modern Flooding and Runoff of the Amargosa River, Nevada–California, Emphasizing Contributions of Fortymile Wash

Patrick A. Glancy and David A. Beck

The Amargosa River drains about 5,500 mi2 (Grasso, 1996, table 1) of arid rugged terrain from southwestern Nevada to southeastern California (fig. 1). Total basin relief is about 8,000 ft, ranging from about 300 ft below sea level at the Badwater Basin salt pan of Death Valley to about 7,700 ft at the top of Pahute Mesa. The Amargosa River is unusual because it seldom flows. Runoff is infrequent because much of the river basin receives less than 6 in. of precipitation per year (Hardman, 1965), and one part, the Death Valley terminal segment, averages only 1.5 in. (Hunt, 1975, p. 7). Short reaches of the river system fed by springs are exceptions to the long reaches that normally remain parched for months, or even years, at a time. When the normally dry segments flow, it is usually in response to severe rainstorms, or less common meteorological events such as rainfall melting high-altitude snowpacks. Because flow is so infrequent, any flow often is considered locally to be a flood.

Historically, little interest in gaging and documenting flow of the large and complex Amrgosa River drainage system has been shown because the river does not provide an acceptable and dependable water-supply resource. The lack of quantitative flow records following discovery of the river in the mid-1800's by immigrant travelers results in a deficient understanding of the drainage system's flow characteristics. Settlement of the river basin has generally remained sparse since discovery; human occupation has spasmodically flourished in localized areas because of mining, military activities, nuclear-weapons testing on the Nevada Test Site (NTS), tourism, and marginally successful agricultural pursuits that utilize chiefly ground water rather than surface water. Although sparsely settled, the river basin is visited by substantial numbers of people travelling between Reno and Las Vegas and those drawn largely by the tourist attractions of Death Valley, a National Park of increasing popularity at the terminus of the river system.

Flow characteristics of the Amargosa River and particularly those of one of its major upstream tributaries, Fortymile Wash (fig. 1), have become more important during the last two decades. The focus of increased attention is the result of plans for possible long- term storage of highly radioactive nuclear wastes in the Fortymile Wash subbasin at Yucca Mountain. A safety concern is whether nuclear-waste products can be entrained by Fortymile Wash flow, transported downstream, and subsequently incorporated within flow of the Amargosa River.Site-characterization investigations have been ongoing for almost two decades to determine the suitability of the Yucca Mountain area for potential storage of high-level nuclear wastes. These investigations are now (1998) reaching completion. This report summarizes results of nearly three decades of streamflow measurements in the Amargosa River Basin that were made for various purposes, including the site- characterization efforts of the Yucca Mountain Project. The report does not include all streamflow data collected as part of the Yucca Mountain Project, but focuses on data that depict general runoff characteristics of Fortymile Wash and the contributions of that tributary and the upper Amargosa River Basin to flows that reached the river basin terminus in Death Valley during the latter part of the twentieth century.
Quantitatively, flow characteristics of the Amargosa River were defined prior to late 1983,

mainly by the only long-term streamflow-gaging record for the basin at Tecopa, California (site I, fig. 1). This gage was operated by the U.S. Geological Survey in cooperation with the California Department of Water Resources. The streamflow record for this gage (September 1961–August 1983) integrated all upstream runoff derived from about 3,100 mi2, about 55 percent of the total river basin area.

Table 1. Ten largest storm runoff periods recorded for the Amargosa River at Tecopa, California (site I, figure 1), 1962-83, ranked in chronological order[1]. [Abbreviations: acre-ft, acre-feet (rounded); ft3/s, cubic feet per second]

Storm runoff period				Ranking by magnitude	Peak discharge	
Start date	End date	Duration (days)	Volume (acre-ft)		Date	Discharge (ft3/s)
Dec. 8, 1965	Dec. 24, 1965	16	3,310	5	Dec. 11, 1965	2,420
Jan. 17, 1969	Feb. 4, 1969	18	1,470	10	Jan. 25, 1969	1,700
Feb. 24, 1969	March 8, 1969	12	3,880	2	Feb. 26, 1969	5,000
Sept. 9, 1976	Sept. 19, 1976	10	3,720	3	Sept. 11, 1976	725
Sept. 23, 1976	Sept. 30, 1976	7	1,720	8	Sept. 26, 1976	1,060
Sept. 30, 1976	Oct. 10, 1976	10	2,280	7	Oct. 2, 1976	2,600
Aug. 16, 1977	Aug. 25, 1977	9	3,370	4	Aug. 17, 1977	1,680
Feb. 12, 1980	March 1, 1980	18	1,680	9	Feb. 17, 1980	686
Feb. 23, 1983	March 16, 1983	21	3,270	6	March 3, 1983	1,260
Aug. 15, 1983	Sept. 9, 1983	25	6,320	1	Aug. 18, 1983	10,600

[1]Modified from Grasso (1996, p. 19)

Figure 1. Location of Amargosa River area and selected hydrologic features.

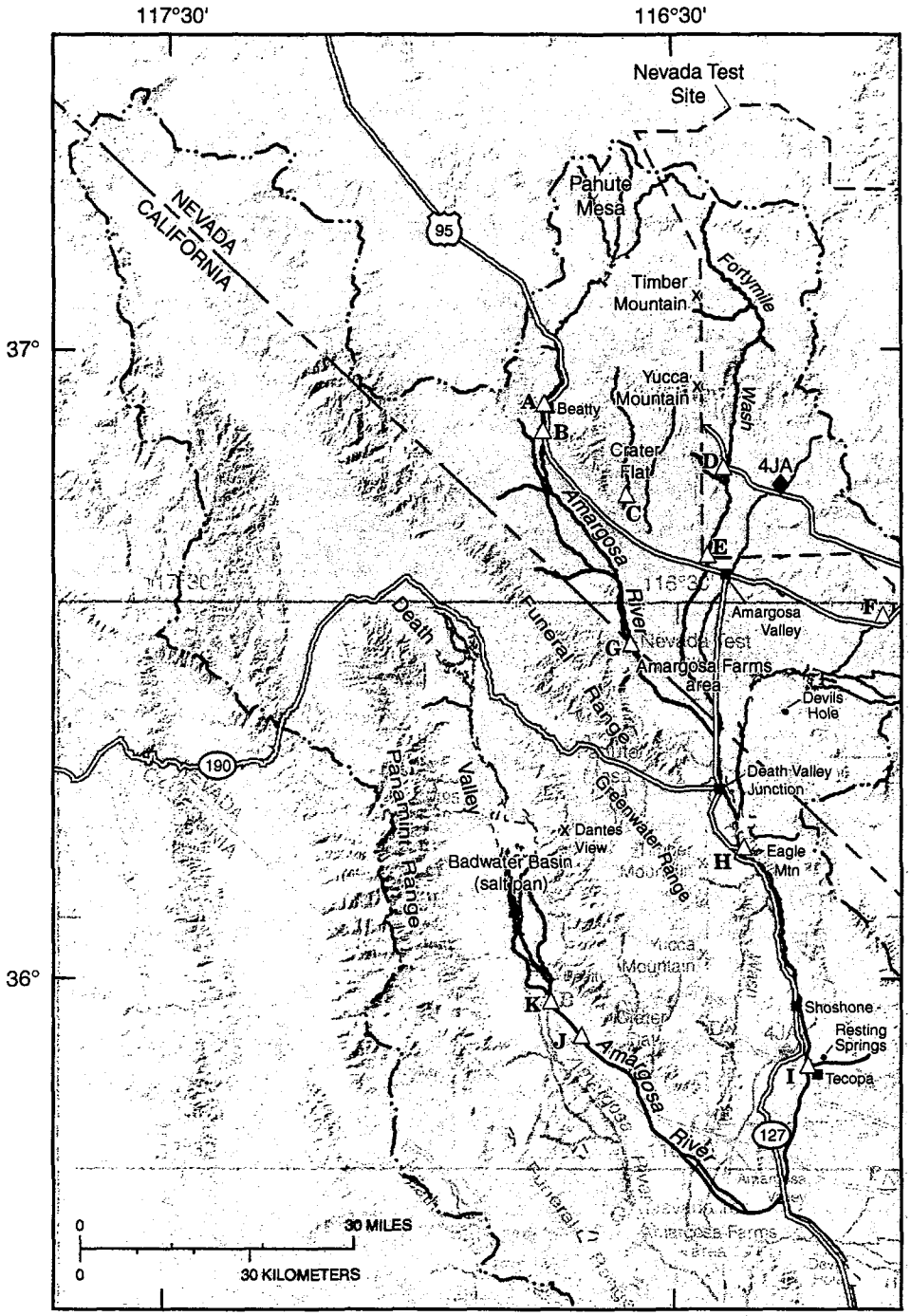

Base modified from U.S. Geological Survey digital data, 1:100,000, 1979-93. Universal Transverse Mercator projection, Zone 11

EXPLANATION

—·—·— **Boundary of Amargosa River Basin**

4JA◆ Precipitation gage

A△ **Surface-water site**

- **A** Amargosa River at Beatty
- **B** Amargosa River near Beatty
- **C** Unnamed Crater Flat drainage
- **D** Fortymile Wash just downstream from Yucca Mountain road crossing
- **E** Fortymile Wash near Amargosa Valley
- **F** Unnamed Amargosa River tributary from Mercury (east of map area)
- **G** Amargosa River at State line
- **H** Amargosa River at Eagle Mtn.
- **I** Amargosa River at Tecopa
- **J** Amargosa River at Westside Road
- **K** Amargosa River near Badwater Basin (salt pan), approximately located

Figure 1. Location of Amargosa River area and selected hydrologic features.

The U.S. Geological Survey briefly operated a recording streamflow gage near Beatty, Nevada, during 1963–68 (near site B, fig. 1). Periodic and miscellaneous streamflow measurements have been made throughout the Nevada part of the river basin since 1962 in cooperation with the Nevada Department of Transportation, and also basinwide since 1983 in cooperation with the U.S. Department of Energy.

Fortymile Wash (fig. 1) is nearly 400 mi2 in basin area and about 5,500 ft in overall relief (7,700–2,200 ft). It flows ephemerally as a result of intense rainfall and melting snowpack, like the overall Amargosa River as described above. Fortymile Wash runoff infiltrates the stream channel at high rates downstream past Yucca Mountain to distal reaches of its alluvial fan (Osterkamp and others, 1994, table 2 and p. 503, 504). As a result of progressive downstream channel losses and flow attenuation, channel capacity decreases along the approximately 15-mi reach from the northern, upstream part of Yucca Mountain to U.S. Highway 95 near Amargosa Valley. Downstream flow attenuation and infiltration cause large-scale sediment deposition enroute that transforms the deeply entrenched channel flood plain near Yucca Mountain into a broadly braided flood plain downstream at U.S. Highway 95 near Amargosa Valley. Downstream from Highway 95, the weakly defined distributary channels continue another 14 mi or more to their diffuse junction with the wide and braided Amargosa River in the Amargosa Farms area. The poorly defined drainage channels of both the Amargosa River and Fortymile Wash, approaching and flowing through the Amargosa Farms reach, give rise to a fundamental question of drainage integrity—do modern flows of the Amargosa River or Fortymile Wash, or their combined flows, really negotiate passage through the Amargosa Farms area and ultimately reach Death Valley? If so, with what magnitudes and frequencies? The answers to these questions are important to public safety with regard to potential fluvial transport of radionuclides through the Amargosa Farms area and downstream past the riparian settlements of Death Valley Junction, Shoshone, and Tecopa, and especially to the more populous tourist attraction of Death Valley.

Prior to 1983, Fortymile Wash was ungaged, but peak flow was measured twice near Amargosa Valley (E, fig. 1) following major floods in 1969. Streamflow gages were installed near and downstream from Yucca Mountain (D and E, fig. 1) in 1983 and have since recorded several runoffs. Additional streamflow gages were installed during the late 1980's and early 1990's along the Amargosa River from Beatty to Tecopa (fig. 1) and in upstream reaches and tributaries of Fortymile Wash (not shown in fig. 1) by the U.S. Geological Survey, in cooperation with the U.S. Department of Energy. Most were deactivated during the mid 1990's because of funding cuts. Although some streamflows were recorded by these gages, the overall periods of flow records are short. The only gages still active (late 1998) are those near Yucca Mountain (D and E, fig. 1).

Table 2. Post-1983 storm-runoff peaks of the Amargosa River at Tecopa, California (site I, figure 1) [Abbreviations: ft3/s, cubic feet per second]

Date	Peak discharge (ft3/s)	Remarks
August 1984	Unknown	Severe runoff described (Desert Breeze, 1984, p. 1) but no date given; possibly during Aug. 14-19, a period of intense convective storms throughout southern Nevada.
July 16, 1990	1,200	Heavy flow from Resting Springs area (east of Tecopa) but preceded peak flow from Death Valley Junction area to north (Tom Pickett, Inyo Co., oral commun., July 26, 1990). Field reconnaissance by authors on Aug. 2, 1990, disclosed major source area in hills near Devils Hole. Only minor flow in Amargosa River at State line.
		Peak river flow at Eagle Mountain (H, fig. 1) of 1,390 ft3/s (Kane and others, 1994, p. 35). Glancy estimated peak flow of Amargosa River on Aug. 3, 1990, at Westside Road crossing in Death Valley (J, fig. 1) from this runoff at 500-600 ft3/s.
August 14-15, 1990	430	Field reconnaissance by Glancy on Aug. 17, 1990, disclosed major source to have been the Greenwater Range, west of Death Valley Junction. Flow evidence in river channel at both Tecopa and Eagle Mountain confirm that this runoff was of lower magnitude than that of July 16, 1990.
February 8, 1992	430	Numerous pulses of runoff during February and March 1992, caused by recurrent, widespread rain storms in southern Nevada. Cumulative flow formed a sizeable lake on the Badwater Basin salt pan of Death Valley during Feb.–Mar. 1992 (Glancy, personal observations; fig. 2). Runoffs also discussed in text and reported by Emett and others (1994, p. 534).
March 11, 1995	170	Discussed in text. Qualitatively described by Beck and Glancy (1995).
February 22-23, 1998	250	Discussed in text.

The following summary of modern Amargosa River flows, and relations of the flows to up-basin tributaries, mainly those of Fortymile Wash, is based on the fragmentary streamflow records and miscellaneous measurements described above. The flows are discussed chronologically.

Grasso (1996, table 1) analyzed the roughly 20-year streamflow record of the Amargosa River documented by the Tecopa streamflow gage (I, fig. 1). He grouped the 10 largest runoffs at that site from the 1962–83 water years in decreasing order of flow volume (table 1). These 10 flows are discussed chronologically below.

No upstream data are available to assess source areas for the December 11, 1965, flood.

The flood on or about January 25, 1969, was the result of a regional rainstorm that may have been amplified by high-altitude snowmelt. Fortymile Wash flowed at about 1,500 ft3/s near U.S. Highway 95 (E, fig. 1) on January 25, 1969, but whether this flow reached and contributed to the tenth highest flow volume recorded by the Tecopa gage (peak flow of 1,700 ft3/s) is unknown.

The flood of February 24, 1969, although only of "first-runner-up" magnitude at the Tecopa gage (table 1), is believed by us to have been, overall, the most severe flood in the Amargosa River Basin during recent time. Although the only recording streamflow gage in the Amargosa drainage was the one near midbasin at Tecopa (site I, fig. 1), measurements of peak flows were made by indirect methods (after flow recession) at several other sites as well (U.S. Geological Survey, 1970, p. 173) for the flood of late February 1969:

Site	**Peak-flow rate (cubic feet per second)**
Amargosa River near Beatty (B, fig. 1)	16,000
Unnamed Crater Flat drainage (C, fig. 1)	3,000
Fortymile Wash near Amargosa Valley (E, fig. 1)	3,300
Amargosa River at Tecopa (I, fig. 1)	5,000

The February 1969 peak flow in Fortymile Wash, just downstream from the Yucca Mountain road crossing (D, fig. 1), was estimated much later by Squires and Young (1984, p. 12) at about 20,000 ft3/s on the basis of channel geometry and residual evidence discovered during their 1981 flood prediction study. Although seemingly large, the order of magnitude they estimated was later (1991) independently supported by the recollections of Charles E. Finch, an NTS security guard who witnessed the February 1969 flow from the high south terrace about 3-1/2 mi downstream from the Yucca Mountain road crossing.

Finch described the February 1969 flow to Glancy on March 13, 1991. He characterized the flow as "wall-to-wall" water across the broad (800-900 ft wide, as scaled from plate 1 of Squires and Young, 1984) flood plain at the bottom of the deeply incised channel. He estimated the average depth of flow at about 4 ft, and described the flow as highly turbid with white, frothing waves over the fluid surface. His assessment of average flow depth was based on the absence of any protrusions of boulders, islands, and vegetation above the surface. At an average depth of 4 ft, the cross-sectional flow area would be on the order of 3,200–3,600 ft2. Assuming a peak flow of 20,000 ft3/s, the resultant average velocity of about 5-1/2–6-1/4 ft/s, depending on cross-sectional area, does not exceed the realm of believability. For comparison, average runoff velocities near the Yucca Mountain road crossing during March 1995 (peak flow of 3,500 ft3/s) and February 1998 (peak flow of 200 ft3/s) were 7–8 ft/s and 3 ft/s, respectively. The marked downstream attenuation of flow peaks (from 20,000 ft3/s to 3,300 ft3/s) in February 1969 from the Yucca Mountain road crossing (site D, fig. 1) to Highway 95 (site E, fig. 1), a distance of about 13 mi, seems large. Details in the basic data are insufficient to confirm, refute, or modify the peak-flow estimates; thus, we report them as originally stated.

Effects of this large regional flood of 1969 were noted by Charles B. Hunt (1975, p. 15) in his description of "Death Valley's Most Recent Lake." He estimated that 80 mi2 (51,200

acres) of the Badwater Basin salt pan were flooded to depths of as much as 3 ft, and thereby calculated a resultant lake volume of about 50,000 acre-ft. He further estimated peak discharge of the Amargosa River near its terminus (approximately at K, fig. 1), near the south end of the salt pan, at about 750 ft3/s (Hunt, 1975, fig. 12, p. 23).

We believe that the Amargosa River flowed continuously from most headwaters to the Death Valley salt pan during this large modern flood. This conclusion is supported by data from 1990's floods described below.

No streamflow data were collected at Fortymile Wash for correlation with the peak- flow data recorded at Tecopa in September 1976, October 1976, August 1977, or February 1980 (table 1). Annual peak flows for 1976, 1977, and 1980 for the Amargosa River near Beatty (B, fig. 1), and an unnamed Amargosa River tributary from Mercury at U.S. Highway 95 (F, fig. 1), were minimal (0–100 ft3/s) and dates of those peaks did not match those recorded at Tecopa. Therefore, no flows from those upbasin sites contributed to the peaks recorded at Tecopa.

Fortymile Wash flowed on March 3, 1983, as a result of a regional rainstorm that may have melted some snowpack at the higher basin altitudes (Pabst and others, 1993). Flow peaked at 570 ft3/s near the Yucca Mountain road crossing (D, fig. 1), and at about 400 ft3/s downstream near U.S. Highway 95 (E, fig. 1). Peak flow of the Amargosa River near Beatty (B, fig. 1) on that date was 120 ft3/s. Mean-daily discharge rose abruptly at the Tecopa gage (I, fig. 1) from 63 ft3/s on March 2 to 448 ft3/s on March 3. Although this rapid increase of flow at Tecopa is circumstantial evidence of possible input from Fortymile Wash and the Amargosa River near Beatty, the widespread and cumulative nature of runoff from this storm may have triggered the increased flow at Tecopa without input from these upstream tributaries. Therefore, whether any of the March 3, 1983, flow of Fortymile Wash reached and contributed to the sixth highest flow recorded by the downstream Tecopa gage (table 1) is unknown.

The largest flood of record, both by volume and peak-flow rate, at the Tecopa gage in August 1983, is somewhat enigmatic. Grasso (1996, p. 18) describes the prime mover of this flood as ". . . an intense, slow-moving storm that came into the area from the south after 3 days of unusually wet weather that was triggered by large amounts of atmospheric moisture from tropical storms to the south and southeast," and credits this knowledge to the National Climatic Center (1983). Grasso graphically correlates the Tecopa-gage flood hydrograph (1996, fig. 10) with a histogram of precipitation at NTS gage 4JA, the upper Amargosa weather station recording the greatest rainfall. Gage 4JA is about 5 mi east- southeast of the reach of Fortymile Wash near the site of proposed waste storage at Yucca Mountain (fig. 1). Author Glancy was present at Fortymile Wash, near station 4JA, during most of the storm; he witnessed extensive runoff in many small drainages of the area and noted that, in spite of substantial runoff in small streams, Fortymile Wash did not flow. Thus, record-breaking Amargosa River flow at Tecopa was not fed by, nor did it originate from, Fortymile Wash.

No peak-flow data for the August 1983 storm have been located for the crest-stage gage on the Amargosa River near Beatty (B, fig. 1); also, no reports of river runoff in Beatty have been discovered. Thus, the flow at Tecopa probably did not originate around or upstream from Beatty. Likewise, no reports of Amargosa River flow were received from the Amargosa Farms area. The lack of evidence of flow from these upper basin areas indicates that the bulk of the record flow at Tecopa (10,600 ft3/s) must have originated somewhere downstream from the Amargosa Farms area. Grasso's map (1996, fig. 11) of overall regional rainfall does not clarify the mystery of the origin of Tecopa gage runoff. The complexity of Amargosa River runoff, even

during severe, geographically widespread storms, is demonstrated by these few data.
The severity of the August 18, 1983, flooding of the Amargosa River at Tecopa destroyed the streamflow gage, and thereby terminated the continuous 20-year record of streamflow. The demise of the Tecopa gage occurred at a critical time with regard to the development of essential knowledge on the hydrologic behavior and flood potential of the Amargosa River deemed necessary to site-characterization studies at Yucca Mountain. Streamflow records at Tecopa were fragmentary after August 1983 until continuous records of flow were re-established through gage reconstruction and reactivation in 1992 (Emett and others, 1994, p. 148). However, some important peak-flow data were collected following periods of known flooding during 1983-92. These data are summarized in table 2. All major floods at Tecopa since August 1983 are believed to have been thus documented, if only minimally, with the exception of those for July–September 1984.
The Amargosa River flowed at Tecopa at least once during the summer of 1984, in response to up-basin storm runoff (Desert Breeze, 1984, p. 1). Sources of this flow, which further exacerbated severe highway damage at the Tecopa gage site initiated by the August 1983 flood, are largely unknown, but numerous severe, localized thunderstorms repeatedly scourged southern Nevada during July–September 1984.
Fortymile Wash flowed three times in the summer of 1984 in response to convective rainstorms during a prolonged and unusually intensive monsoonal storm season. Magnitudes of the flows, listed in chronological order, are as follows (Pabst and others, 1993, p. 11, 22, and 23):

	Peak-flow rate (cubic feet per second)	
Date in 1984	**Near Yucca Mt. road crossing (D, fig. 1)**	**Near U.S. Highway 95 (E, fig. 1)**
July 21-22	1,860	1,430
July 22	about 150	about 100
August 19	about 850	about 380

Whether any of these flows reached the former site of the Tecopa gage is unknown.
Convective storms were severe and moderately numorous throughout southern Nevada during July and August of 1990 (Glancy, unpublished field notes). As a result, the Amargosa River at Tecopa flowed twice (table 2). Neither runoff was augmented by contributions from Fortymile Wash, which remained dry (Kane and others, 1994).
Late winter and early spring of 1992 was an exceptionally wet time in southern Nevada. The lower Amargosa River flowed repeatedly, but moderately, during February and March. The resultant cumulative flows emplaced a sizeable lake on the Badwater Basin salt pan that was repeatedly observed during its evolution by Glancy from the unique perspective afforded at Dantes View on the eastern rim of Death Valley (fig. 2). Again, lower Fortymile Wash remained dry and noncontributing (Emett and others, 1994, p. 142 and 145).

Figure 2. Progressive growth of lake Badwater Basin salt pan, Death Valley, during February-March of 1992, as observed by author Glancy in a west-northwest direction from Dantes View.

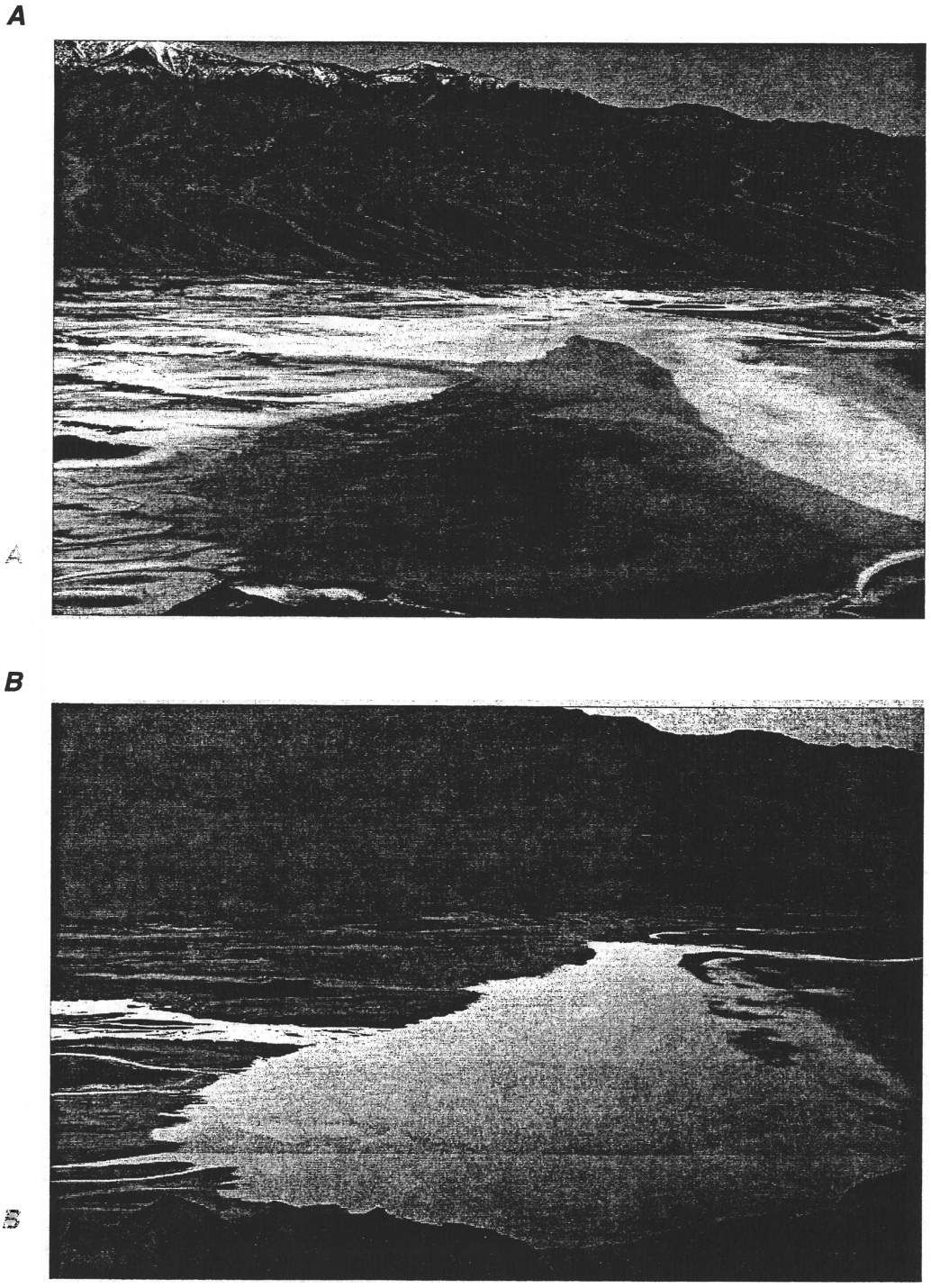

Figure 2. Progressive growth of lake on Badwater Basin salt pan, Death Valley, during February-March of 1992, as observed by author Glancy in a west-northwest direction from Dantes View: ***A***, February 25, after Amargosa River runoff of February 12-13. ***B***, March 12, after Amargosa River runoffs of March 2-4 and 7-10. Contributing Amargosa River runoffs are quantified by Emett and others (1994, p. 148).

Fortymile Wash did not flow again, near or downstream from Yucca Mountain, for almost 11 years following the runoff of August 19, 1984. It next flowed for 10-12 hours on March 11, 1995, in upper-basin reaches as the result of a regional rainstorm, probably amplified by rainfall-induced, high-altitude snowmelt on the highlands of Timber Mountain and Pahute Mesa (Beck and Glancy, 1995). The Amargosa River upstream from Amrgosa Farms also flowed on the same day, similarly for 10-12 hours. Flow peaked at Tecopa on March 12. This runoff was important to site-characterization studies for proposed nuclear waste storage at Yucca Mountain because it represented the first documented condition wherein Fortymile Wash and the Amargosa River flowed simultaneously throughout their mainstem-channel reaches to Death Valley. A summary of the peak flows on March 11-12, 1995, at key sites follows:

Site		Peak-flow rate (cubic feet per second)
Amargosa River	at Beatty (A, fig. 1)	1,000
	at State line (G, fig. 1)	27
	at Tecopa (I, fig. 1)	170
Fortymile Wash	at Yucca Mountain road crossing (D, fig. 1)	3,500
	near Amargosa Valley (E, fig. 1)	1,500

A similarly triggered runoff, but of lower magnitudes and intensities, occurred on February 22–23, 1998. Again, Fortymile Wash and the Amargosa River flowed simultaneously throughout their mainstem-channel reaches to Death Valley. Precipitation during the preceding week caused continuous flow of the Amargosa River during that week from Eagle Mountain (H, fig. 1) to Death Valley. A summary of peak flows at key sites for the February 22–23 runoff follows:

Site		Peak-flow rate (cubic feet per second)
Amargosa River	at Beatty (A, fig. 1)	90
	at State line (G, fig. 1)	30
	at Tecopa (I, fig. 1)	250
Fortymile Wash	at Yucca Mountina road crossing (D, fig. 1)	200
	near Amargosa Valley (E, fig. 1)	340

Characteristics of the 1995 and 1998 rain storms were different. The March 1995 storm was largely relegated to high-altitude, upstream areas, whereas the February 1998 storm was more widely distributed over both uplands and valleys throughout the basin.
The foregoing data and discussions verify the capability of the Amargosa River and its tributary,

Fortymile Wash, to flow throughout their mainstem reaches to the river terminus in Death Valley. Streamflow data collected in February 1998, shown above, verify that moderate runoff from the Yucca Mountain area can flow to Death Valley. The array of data presented in this brief summary indicates that, although throughflows are relatively infrequent, they are not rare or unusual. Lower Fortymile Wash flowed six times during 15 years from March 1983 through February 1998, and at least eight times during the 29 years from 1969 to 1998. Streamflow data for Fortymile Wash and Amargosa River collected during runoffs of 1995 and 1998 indicate that most, and possibly all, of the six, pre-1995 flows probably continued downstream to Death Valley.

Site-characterization studies for proposed nuclear-waste storage have focused attention on the need to better understand the Amargosa River system. The studies stimulated and supported streamflow gaging throughout the basin, which improved our understanding of this complex drainage system. However, much of this gaging has since been discontinued. Knowledge of Amargosa River drainage characteristics would be further enhanced by additional streamflow monitoring.

References Cited

Beck, D.A., and Glancy, P.A., 1995, Overview of runoff of March 11, 1995, in Fortymile Wash and Amargosa River, southern Nevada: U.S. Geological Survey Fact Sheet FS- 210-95, 4 p.

Desert Breeze, 1984, "Weather, weather, and more weather!": Tecopa, Calif., v. 19, no. 1, September 1984, p. 1.

Emett, D.C., Hutchinson, D.D., Jonson, N.A., and O'Hair, K.L., 1994, Water resources data, Nevada, water year 1993: U.S. Geological Survey Water-Data Report NV-93-1, 596 p.

Grasso, D.N., 1996, Hydrology of modern and late Holocene lakes, Death Valley, California: U.S. Geological Survey Water-Resources Investigations Report 95-4237, 54 p.

Hardman, George, 1965, Nevada precipitation map: University of Nevada Agricultural Experiment Station Bulletin 183, 57 p.

Hunt, C.B., 1975, Death Valley—Geology, ecology, archaeology: Berkeley, University of California Press, 234 p.

Kane, T.G., III, Bauer, D.J., and Martinez, C.M., 1994, Streamflow and selected precipitation data for Yucca Mountain region, Southern Nevada and eastern California, water years 1986–90: U.S. Geological Survey Open-File Report 94-312, 118 p.

National Climatic Center, 1983, Weekly weather and map bulletin: Ashville, N.C., National Oceanic and Atmospheric Administration, v. 70, no. 34, August 23, 1983.

Osterkamp, W.R., Lane, L.J., and Savard, C.S., 1994, Recharge estimates using a geomorphic/distributed-parameter simulation approach, Amargosa River Basin: Water Resources Bulletin, v. 30, no. 3, p. 493-507.

Pabst, M.E., Beck, D.A., Glancy, P.A., and Johnson, J.A., 1993, Streamflow and selected precipitation data for Yucca Mountain and vicinity, Nye County, Nevada, water years 1983-85: U.S. Geological Survey Open-File Report 93-438, 66 p.

Squires, R.R., and Young, R.L., 1984, Flood potential of Fortymile Wash and its principal southwestern tributaries, Nevada Test Site, southern Nevada: U.S. Geological Survey Water-Resources Investigations Report 83-4001, 33 p.

U.S. Geological Survey, 1970, Surface water records for Nevada, water year 1969: Carson City, Nev., U.S. Geological Survey Water-Data Report, 215 p.

Day 1, Stop 3

Late Quaternary history of Fortymile Wash in the area near the H-road crossing

Lundstrom, S.C., Paces, J.B., Mahan, S.A.

Introduction

Fortymile Wash (FW) has the largest and highest drainage basin of any tributary of the upper Amargosa River, and heads on the upland areas of Eastern Pahute Mesa (Fig. 1) within the late Miocene southern Nevada volcanic field (Frizzell and Shulters, 1990). The ephemeral channels of FW join those of the Amargosa River within the Amargosa Desert and continue 100 km southward before turning north into Death Valley. The watershed of FW consists of an upper northern basin that includes the east half of the Timber Mountain caldera and a lower part dominated by a large alluvial fan extending into the central Amargosa Desert, and flanked on the west by the block faulted ridge of Yucca Mountain (Fig. 1). The throughgoing drainage of Fortymile Canyon through the south rim of the caldera into the Amargosa Desert basin was established between 7.5 and 2.8 Ma (Lundstrom and Warren, 1994). In more societally relevant terms, the uppermost part of the FW watershed overlaps the part of the Nevada Test Site that has undergone most underground nuclear testing, and the lower part provides surface drainage from most of Yucca Mountain, a potential nuclear waste repository. The climate of the watershed ranges from semi-arid in the upper parts to arid in the lower, with slightly bimodal but largely winter dominated annual precipitation of 15 cm at Yucca Mountain ranging up to 35 cm on forested Rainier Mesa. The historical record of FW shows it to be extremely ephemeral with observed flow near Yucca Mountain only 6 times for generally less than 1-2 days of duration over the past 15 years (Glancy and Beck, this guidebook). However the fan of FW is one of the largest in the southern Basin and Range province. At this stop, we view evidence for significant aggradation and incision during the late Quaternary history of FW.

Figure 1. Drainage basin and alluvial fan of Fortymile Wash within the physiographic setting of the upper Amargosa River drainage basin (thick dashed line), showing major wash channels (thick solid lines). Uplands in light, with dark grey on areas above 2000 m. Dome Mountain (DM) basalt clast source with pattern overlay. Generalized delineation of FW fan into late Pleistocene (diagonal down to right) Holocene (diagonal down to left [red]), past discharge area (pattern) intermixed area (cross hatched). Other alluviated areas are undivided and uncolored. Geographic features are Crater Flat (CF), Death Valley (DV), Devils Hole (DH), Eastern Pahute Mesa (EPM), Eleana Range (ER), Funeral Mountains (FM), Jackass Flats (JF), Lathrop Wells (LW), Timber Mountain (TM), Yucca Mountain (YM). Main highways in thin dashed line.

Stratigraphy and geochronology

The surface of the southern and central part of the FW fan (south of US highway 95) is a smooth southward slope composed of both Holocene (units Qfy) and Pleistocene alluvium (units Qf3 and Qf4) at similar grades (Figs. 1,2). In contrast, the northern part of the fan (unit Qf3) is

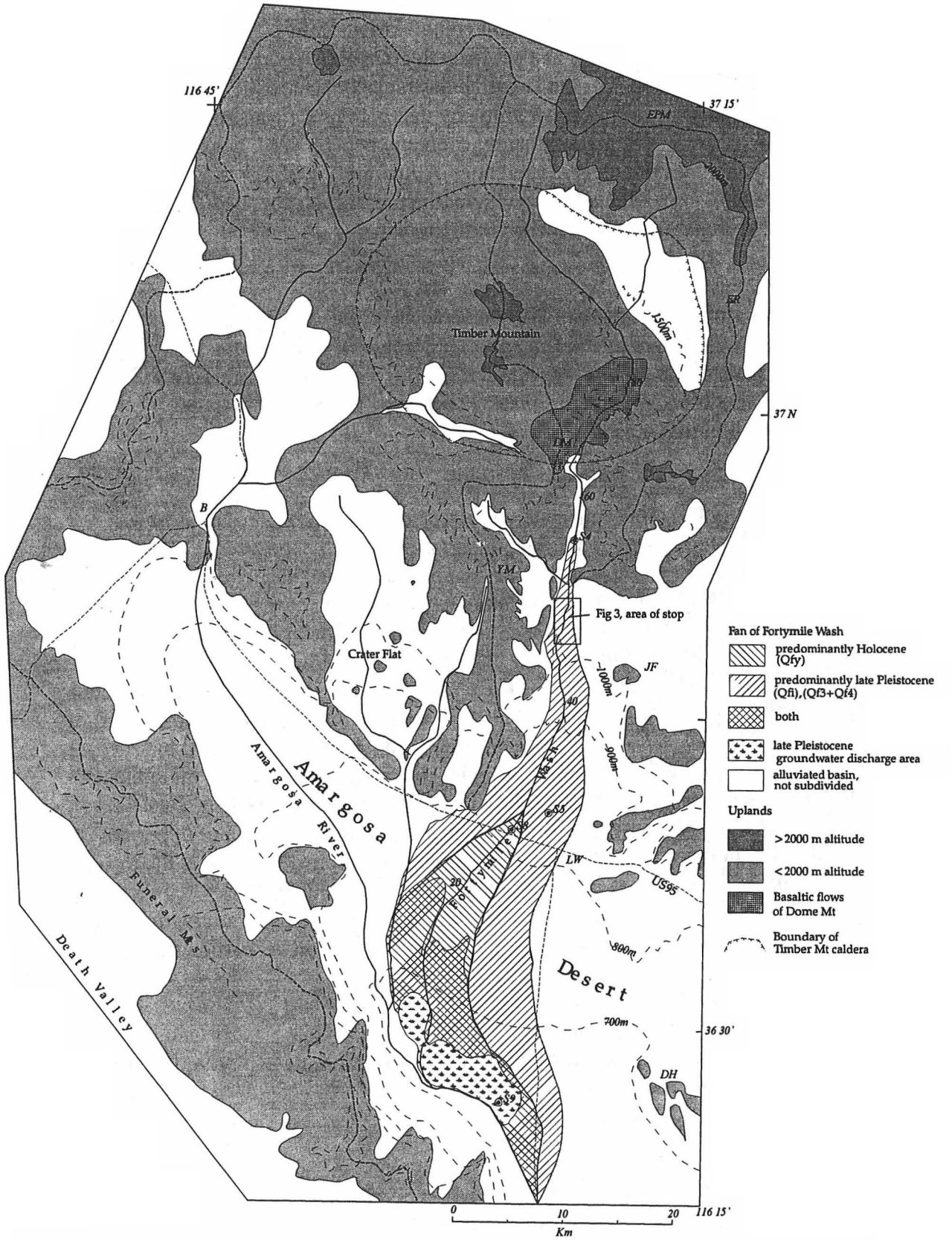

Fig. 1. Drainage basin and alluvial fan of Fortymile Wash within the physiographic setting of the upper Amargosa River drainage basin (thick dashed line), showing major wash channels (thick solid lines). Uplands in light with dark grey on areas above 2000 m. Dome Mountain (DM) basalt clast source with pattern overlay. Generalized delineation of FW fan into late Pleistocene (diagonal down to right) Holocene (diagonal down to left [red]), past discharge area (pattern) intermixed area (cross hatched). Other alluviated areas are undivided and uncolored. Geographic features are Crater Flat (CF), Death Valley (DV), Devils Hole (DH), Eastern Pahute Mesa (EPM), Eleana Range (ER), Funeral Mountains (FM), Jackass Flats (JF), Lathrop Wells (LW), Timber Mountain (TM), Yucca Mountain (YM). Main highways in thin dashed line.

incised increasingly northward from an intersection point 2 km north of US 95 . North of this point, the main fan surface forms a terrace at a grade up to 20 m above units of younger inset alluvium of FW (Fig. 2). This stop near the H-road crossing is located in the area of maximum incision, where there are good exposures of stratigraphy that both predate and postdate the incision. Gravelly alluvium of FW is predominantly cobble to pebble sized, has a coarse sand matrix , and commonly includes trough cross bedding. Alluvium of FW is readily distinguished at the surface and in section from tributary alluvium by the presence of rounded cobbles and boulders of basalt and rhyolite derived from Fortymile Canyon.

Figure 2. Longitudinal profiles along lower Fortymile Wash of (a.) modern wash, late Pleistocene fan surface (Qf3) above intersection point, interpolated top of groundwater saturated zone, and area of late Pleistocene groundwater discharge; (b.) height above modern wash of surface of late Pleistocene fan (Qf3) and inset later Pleistocene terrace (Qf4); and (c.) percentage of gravel clasts that are basaltic for each unit.

The surficial soil of unit Qf3 is characterized by cemented carbonate and silica morphology (stage III, Taylor, 1986) and a smooth surface in which depositional bar and swale morphology has been largely obliterated by subsequent pedogenic and surficial processes. An eolian mantle of predominantly fine sand occurs above the K horizon of the surface soil. The eolian sand is mixed through infiltration and pedoturbation with alluvial gravel and ranges in thickness from <20 cm in the north to >1 m over much of the southern and central part of the fan. At the northern end of the fan , clay and silt enriched Bt and Av horizons are associated with a well packed and darkly varnished desert pavement, whereas over the southern and main part of the fan, the Av and Bt horizons have either been been buried or sufficiently diluted by subsequent eolian addition that the associated surficial pebble pavement is much more loosely packed. 230Th dates on innermost carbonateclast coats from the K horizon of the surficial soil of Qf3 range from 42 - 81 ka, and provide minimum ages on gravel deposition of uppermost unit Qf3. The oldest dates on innermost clast coats at each site range from 53 $\pm$ 2 ka at the top of the N85 section (s1, Fig.3; Fig. 4) in view of this stop, 74 $\pm$ 3 ka at s2 (Fig. 3), 42 $\pm$ 0.5 ka at s3 (Fig. 3), to 81 $\pm$ 5 ka at s5 (Fig. 1). On the basis of results on underlying stratigraphy discussed below, all of these dates are plausible close minima (within 10 k.y.) on deposition of gravel parent material at each of these sites.

Figure 3. Map of geology and sites discussed in area of H-road crossing of Fortymile Wash

---

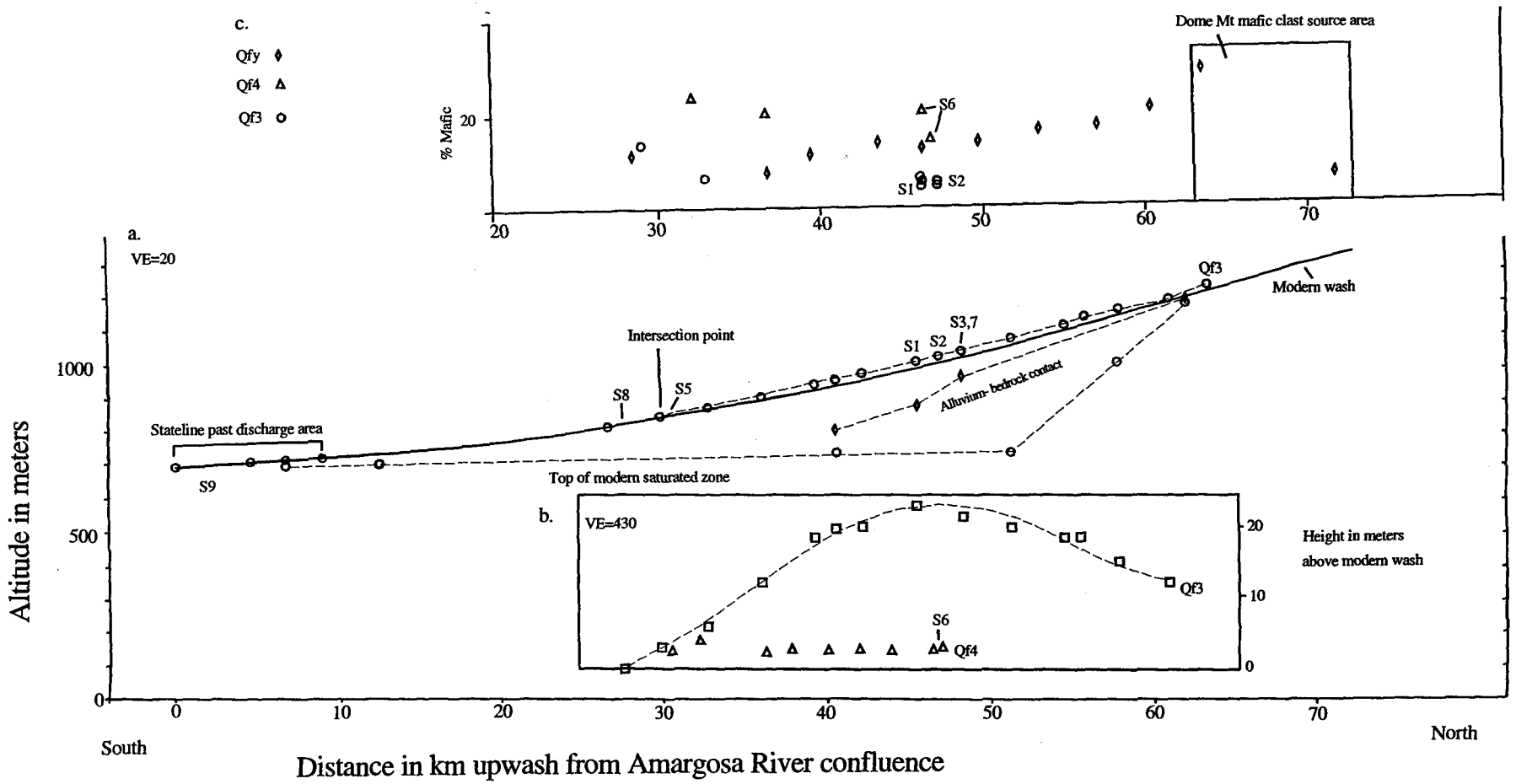

Fig. 2. Longitudinal profiles along lower Fortymile Wash of (a.) modern wash, late Pleistocene fan surface (Qf3) above intersection point, interpolated top of groundwater saturated zone, and area of late Pleistocene groundwater discharge; (b.) height above modern wash of surface of late Pleistocene fan (Qf3) and inset later Pleistocene terrace (Qf4); and (c.) percentage of gravel clasts that are basaltic for each unit.

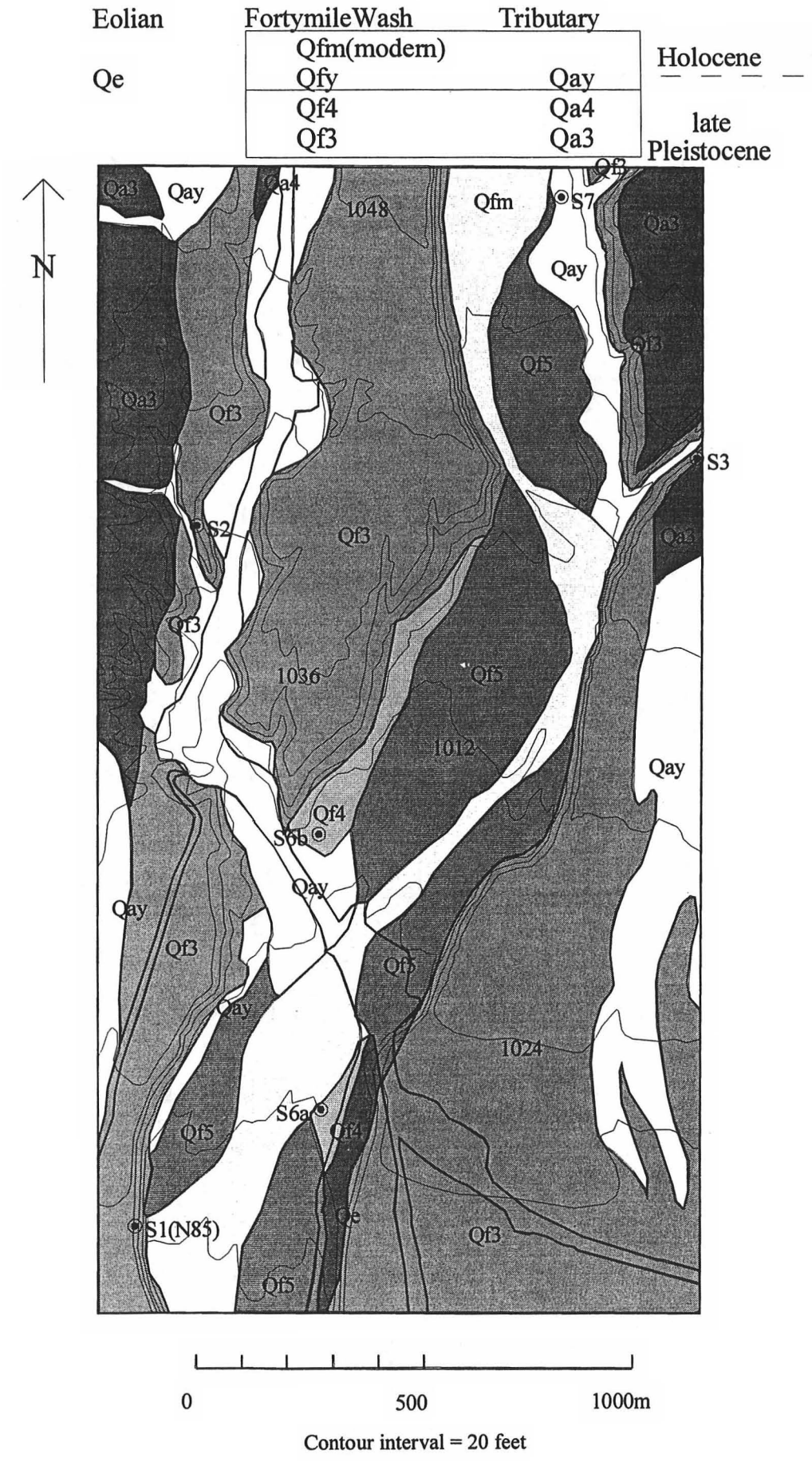

Fig. 3. Map of geology and sites discussed in area of H-road crossing of Fortymile Wash

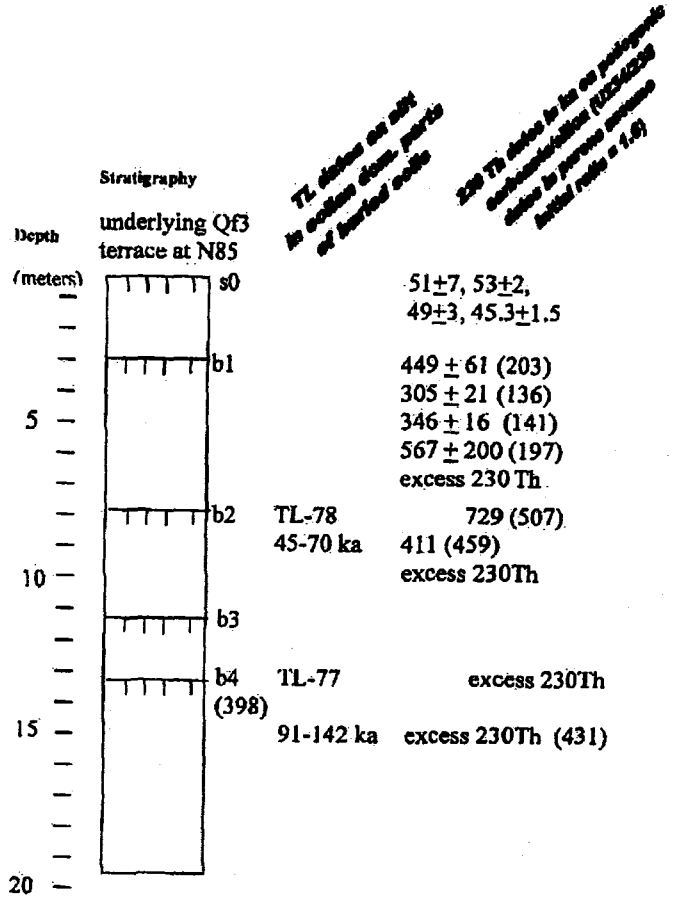

Figure 4. Stratigraphy and geochronology below Qf3 surface at s1 N85 section. Surface soil s0, and buried soils b1, b2, b3, and b4, consist of partially eroded (by laterally persistent unconformity), fine sand rich slightly red brown eolian cap 30-90 cma thick in which gravel clasts flat, and which grade downward into stage II-III carbonate cemented Bkb horizon developed within fluvial cobble-pebble gravel, subrounded, clast supported, common cross beds, and discontinuous interbedded sand lens. This fluvial gravel of Fortymile Wash (FW) comprises the depositional units in which the surficial and buried soils formed after each unit was deposited in this aggregational sequence.

Thermoluminescence (TL) dates on silt within fine sand-dominated horizons interpreted to be eolian provide maximum dates on overlying alluvial gravel. The N85 section (Fig. 4; s1, Fig.3) that we see on the west side of the FW incision, consists of a continuous natural exposure about 400 m long and 3-20 m high along modern FW beneath the Qf3 terrace surface in the area of maximum fan incision. Over the length of this exposure, gravelly FW alluvium is intercalated with laterally persistent horizons that are predominantly fine sand. We interpret these horizons as the eolian dominated upper parts of buried soils on the basis of (1) redder tones than in interbedded fluvial sand lens, (2) the occurrence of gravel clasts floating in the sand matrix which is more consistent with eolian inflation in a soil (McFadden and others) than with fluvial deposition, (3) an associated concentration of carbonate/silica cementation in the gravel underlying the sand as is seen in moderately developed surface soils, and (4) lateral continuity . All of these characteristics occur in surficial soils of the area (Taylor, 1986). The eolian interpretation is significant to consideration of the reliability of TL dates on these horizons because eolian sediment is most effectively zeroed and is the most favorable type of sediment for TL dating (Berger, 1988; Millard and Maat, 1994). At the N85 section, the TL dates on b2 and b4 are robust (Fig. 5): glow curves are well shaped with coincident peaks at 300C, natural TL levels are well below saturation levels determined by artificial radiation, and partial and total bleach yield similar results . Acceptance of these results along with 230 Th dates on the surface

soil constrain 13 m of local net aggradation and formation of 3-4 soils between 140 and 50 ka, including 6 m of aggradation during 65-50 ka. The implied rapid soil formation does not conflict with this age control because the buried soils consist mainly of eolian sand addition which probably closely follows large fluvial depositional events that supply fine sediment to lower energy facies of fan alluvium.

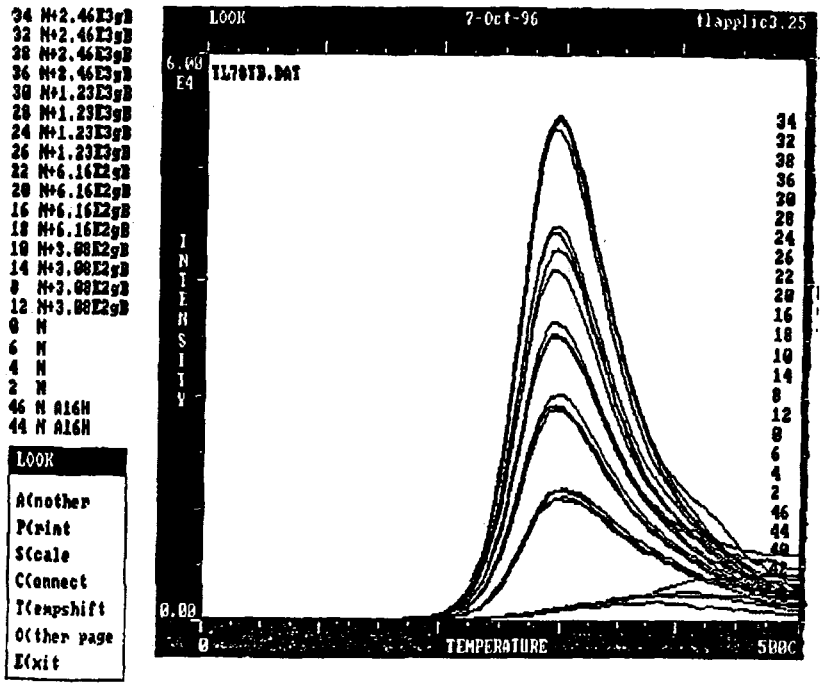

Fig. 5. normalized thermoluminescence glowcurve data of natural and irradiated sample TL-78. As keyed in upper left corner, lowest cluster is sunlight bleached sample, next higher cluster is TL of natural sample, and higher clusters are artifically irradiated samples.

However, in contrast with concordance with U-series results on surficial soil, the TL dates on b2 and b4 are in conflict with U-series results on buried soils (Fig.4). Also in contrast with results from surface soils, U-series results on buried soils, especially at the s1-N85 section yield problematic results, including excess Th, large analytical error, and higher calculated initial Uranium ratios than for the range of most pedogenic carbonates in the area. The latter could result from partial dissolution of carbonate in a buried soil and resulting Uranium mobility (loss) and lack of a closed system. Once a surface soil is buried, it is removed from the surficial setting where high evaporation occurs, and is subject to the additonal flux of groundwater associated with channel infiltration during deposition of the overlying alluvium. Because the TL dates are analytically well-behaved and the U-series dates on the buried soils only are not, Lundstrom favors the TL dates as constraining in this section at least 13 m of early late Pleistocene (130-50 ka) aggradation of alluvium with at least 2 and possibly 4 buried soils. In this interpretation, the buried soils are not likely to represent significant intervals of time, but rather brief episodes of eolian addition to freshly deposited alluvial gravel, with the eolian material derived from deflation of fine sand-rich facies of freshly deposited alluvium. However, author J.B. Paces favors an interpretation that the U-series dates on the problematic buried soils can still provide approximate ages if U234/238 ratios only are used, with an assumed initial ratio

of 1.6, which is that found to be typical of pedogenic carbonate in the area. The dates calculated this way are shown in parentheses in Fig. 4 next to the more usual 230 Th dates. In this alternative interpretation, the TL dates on the buried soils are discounted and the U234/238 dates on the buried soils are used to indicate that the net aggradation in the section spans more than the past 500 ky.

Following the period of aggradation, about 20 m of fanhead incision occurred by 24-36 ka, which is the age range of 7 U-series dates (with analytical uncertainty from 0.8 to 3 ky and in one case 6 k.y) on the innermost pedogenic coating on gravel clasts in the surface soil at 2 sites (s6a, s6b, Figure 3) on unit Qf4, the oldest inset terrace. Qf4 is inset about 18 m below unit Qf3 in the area of maximal incision and occurs discontinuously about 2-3 m above the modern wash for about 15 km to the south (Fig.2). The soil on unit Qf4 includes a well cemented K horizon (Taylor, 1986) and a darkly varnished, tightly packed desert pavement underlain by silt-rich Av and red-brown Bt horizons.

Less than 2-3m of net incision occurred since 24 ka, and adjoining but contrasting, younger noncemented Holocene alluvium Qay is overlain by fine sand dominated eolian material yielding TL dates of 7 ka and 8 ka (site s7 , Fig. 3) in concordance with stratigraphic position. Soil development on this unit is weak (Taylor, 1986) with thin carbonate/silica coats on clast undersides.

Hydrologic and geomorphic response to climatic change

Comparison of the above record to other regional paleoenvironmental records, including those of lake histories (Smith, 1979, Smith and Bischoff, 1997, Bradbury, 1997, Lowenstein, 1997), packrat middens (Spaulding, 1985, 1990, 1994; Wigand, 1997), and groundwater systems (Winograd and others, 1992; Szabo and others, 1994), including groundwater discharge areas (Quade and others, 1995, Paces and others, 1996, 1997), allows an evaluation of the response of FW to climatic change (Fig. 6). The most continuous and inclusive of available proxy records of climate history for the past 100 ka in this area is that of a core from Owens Lake (Smith and Bischoff, 1997) located about 150 km west of the study area. Evaluation of the varying types of diatoms, pollen, mineralogy and other related properties for the past 200 ka (Bradbury, 1997) indicate that the early part of the late Pleistocene, from about 120 ka to 50 ka, was highly variable but generally wetter than present, and included a greater occurrence of saline lake conditions requiring greater relative warmth than the latter part of the late Pleistocene. In contrast, the period from 50-15 ka was dominated by freshwater conditions and greater effective moisture that overlapped glaciation in the Sierra Nevada.

Fig. 6. Surface processes and geomorphic response to climate change in the Fortymile Wash/Yucca Mountain area

---

We interpret the >13m of aggradation that occurred in the fanhead area of FW during 100-50 ka as a depositional response to intense rainfall events that generated runoff on hillslopes, gully erosion and significant sediment yield from substantial areas of hillslopes contributing flow to lower FW. Historic analogues for such events occurred in July and August 1984 (Coe and others, 1997) and on March 11, 1995 (Beck and Glancy, 1995) - these events included

Fig. 6 Surface processes and geomorphic response to climate change, Fortymile Wash

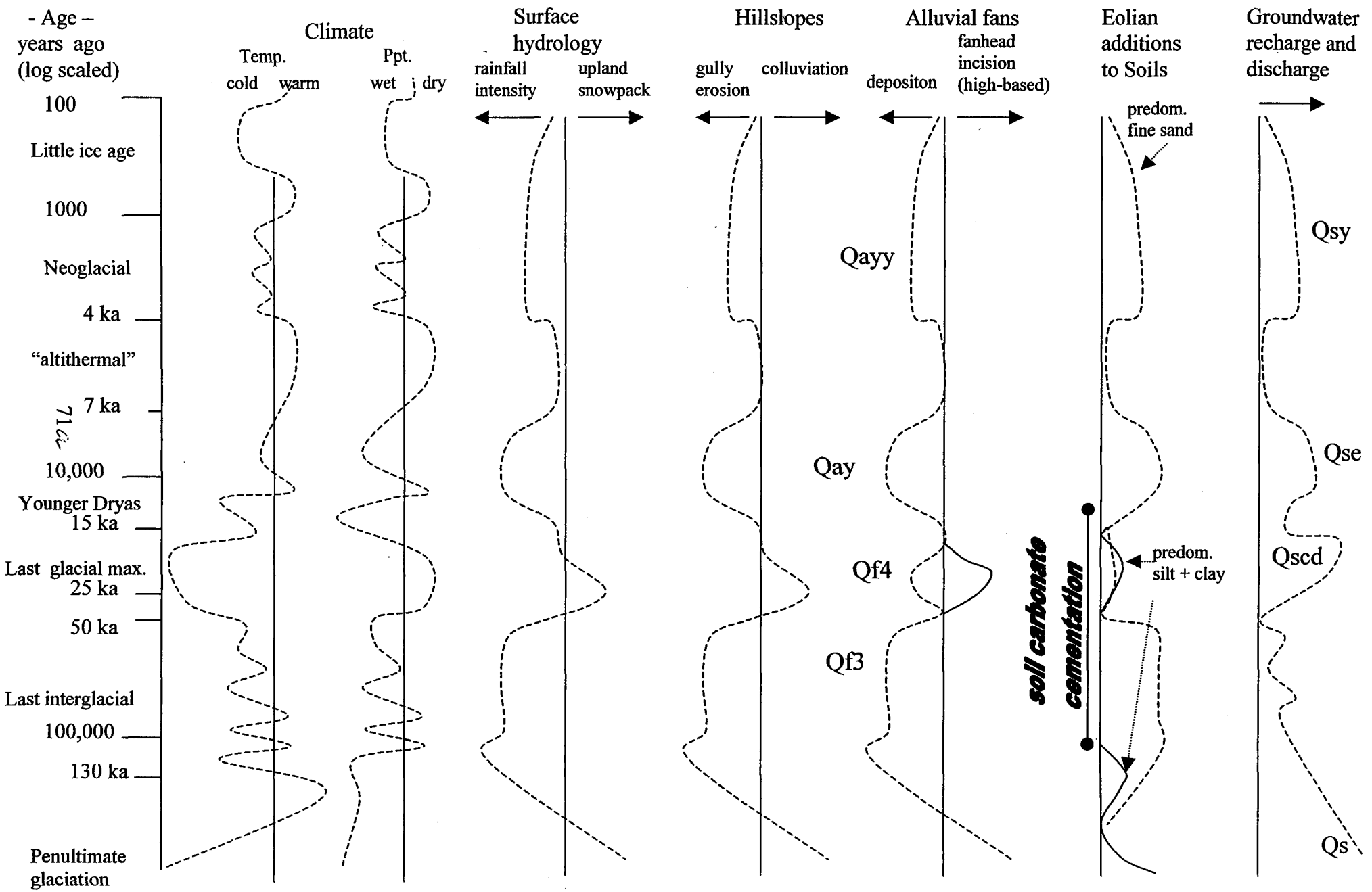

substantial convective activity to produce the relatively intense rainfall, and were associated with relatively warm temperatures. Because significant infiltration to alluvial channels occurs during such flows (Savard, 1998, Osterkamp and others, 1994), peak discharge and competence generally decrease downstream during these occasional flow events and deposition of gravelly alluvium is a natural consequence. Though it is plausible that some aggradation was due to destabilization of hillslopes from change in vegetation (Bull, 1991), it is unlikely that the prolonged (100-50 ka) >13m of aggradation in the area of the now incised fanhead was mainly due to vegetation change alone - intense rainfall events were necessary, perhaps related to relatively warm, moist, possibly monsoonal atmospheric circulation.

In contrast to the preceding period of aggradation, the following period of fanhead incision required generation of flows competent to incise bouldery alluvium up to 20 m, but with a significantly reduced sediment supply. We suggest that a probable mechanism to generate such runoff during the relatively cool latter part of the late Pleistocene (Bradbury, 1997) might have been concentrated seasonal melt of substantial winter snowpacks. The upper part of the FW basin (that above the 1000 m contour) includes substantial areas (30%) above 1750 m and up to 2250 m that are now variably but generally covered by pinyon juniper-woodland, and receive much (most) precipitation as winter snowfall, though seasonal snowmelt is not concentrated enough to generate flows on FW. The period from 50 to25 ka within which our geochronologic data constrains most of the observed fanhead incision on FW includes episodes from 35,000 to 22,000 years 14C yr B.P. when white fir occurred at elevations lower than it did during most of marine stage 3 time (Wigand, 1997). White fir is a montane species adapted to heavy winter snowpack. Its record of occurrence at altitudes below 1800 m at similar latitudes in the Great Basin, indicates that it was likely in the upper basin of FW . The wettest conditions recorded in Fortymile Canyon come from two strata from the FMC-7 midden, dated at >52,000 and 47,200 $\pm$ 3000 14 C yrs B.P. (Spaulding, 1994) Relatively short episodes of net fanhead incision on FW may similarly correlate with relatively cold and moist climatic events that produced mud horizons within the Lower Salt of Searles Lake (Smith, 1979). There is no evidence for glaciation in the upper watershed of FW and the 2250 m altitude of the highest uplands is well below the late Pleistocene glaciation threshold of 3600 m interpolated over this area (Porter and others, 1983).

Packrat midden records within the last glacial maximum (Spaulding, 1985, 1990) indicate maximum relative temperature depressions, and precipitation that was probably less than 1.5x modern precipitation. Our stratigraphy and age control indicate that most of the present level of incision occurred before 24 ka and there is no record or evidence requiring incision or aggradation during 25 ka to 15 ka, though it is possible that minor incision during this period could be buried by subsequent Holocene aggradation.

Aggradation during the global deglacial transition from latest Pleistocene (post 15 ka) into the early Holocene (pre 7 ka) occurs during a period that various paleoenvironmental records, especially packrat middens (Spaulding, 1985,1990, 1994) indicate to be wetter than present, wetter than the preceding glacial maximum, and significantly warmer than the preceding 30,000 years. As hypothesized for the period 100-50 ka, aggradation is attributed to intense rainfall to generate runoff, gully erosion and gravelly sediment yield from hillslopes, perhaps related to convective storms of warm relatively moist climates such as increased monsoonal or meridional atmospheric circulation would provide to the area. An additional or alternative mechanism would be convective recycling of higher than present soil moisture accumulated

during wet winter or spring seasons.

There is no compelling record in this area for major geomorphic activity during the mid Holocene (7-5 ka). This is consistent with the few records for the Mojave during this time (i.e. Spaulding, 1991), and with most other Holocene records for the Great Basin as compiled by Grayson (1993) that are supportive of Antev's concept of a relatively warm, dry altithermal. In contrast to the common assumption that warmer and drier implies greater eolian geomorphic activity, we consider eolian deposition in this area, especially eolian sand dominated addition to soil profiles to relate to sediment supply during alluviation during warm but relatively wet and stormy periods.

Somewhat wetter than present climates are known for the past 5000 years from midden records (Spaulding, 1990, 1994), and from pollen and peat records (Mehringer and Warren, 1976, Wigand, 1997). Late Holocene alluvial units known in Midway Valley, Coyote Wash, (Glancy, 1994) and elsewhere around Yucca Mountain, as well as paleoflood records throughout the SW (Ely, 1993) may relate to such conditions.

The hypothesized geomorphic response to climate change is supported by clast compositions of dated alluvial units on FW (Figure 2c) The basaltic gravel component of Holocene alluvium of FW is supplied by a shield volcano over which the course of FW was superposed and incised (Frizell and Shulters, 1990, Lundstrom and Warren, 1994). The generally monotonic decrease of the basalt component downstream from the source area is related to dilution from felsic volcanic uplands tributary to FW below upper Fortymile canyon, consistent with hillslope erosion and sediment supply during Holocene aggradation. A similar but greater dilution of basaltic alluvium is apparent from the few clast counts in the earlier aggradational sequence (100-50 ka). In contrast, the basaltic component of alluvium of the late Pleistocene terrace inset and related to fanhead incision is substantially higher than the aggradational units and moreover, increases in a downwash direction. This suggests that during fanhead incision, hillslope sediment supply from felsic volcanic uplands downstream from upper Fortymile Canyon was low relative to supply of basaltic clasts from reworking and incision of basalt rich alluvium and colluvium within upper Fortymile Canyon.

Geologic mapping and results of studies to the west of Yucca Mountain (Faulds and others map, 1995, Peterson and others, 1995) are also consistent with the above hypothesis for climatic controls on aggradation and incision. There alluvial units are mapped and have age control similarly indicating alluviation prior to 50-70 ka and after 14 ka, but there is no evidence of more than a few meters of intervening incision. The watersheds for drainages on this side are smaller than that of FW, and in contrast to upper FW, do not include significant areas above altitudes of 1750 m, so there was little area for higher altitude snowpacks to seasonally accumulate, consistent with the lack of evidence for significant incision between periods of alluviation.

Channel infiltration and deposition of alluvium are magnified where younger alluvium spreads out as a fan over an older surface below the intersection point because distributary flow results in a given discharge occurring over a greater total wetted perimeter of the cross section area. Aggradation is thus magnified in this area of distributary flow. A locally higher aggradation rate in this reach would decrease channel gradient and favor increased deposition, thus providing a positive feedback on aggradation that would tend to move the intersection point upwash with time. These very strong positive feedbacks on aggradation on an arid fan system

must be overcome to produce fanhead incision.

The late Quaternary history of FW documented here differs substantially from assumed chronologies based on *correlation* to U-trend ages (Rosholt, 1985) used to calibrate rates of soil development (Taylor, 1986, Harden and others, 1991, Reheis and others, 1995), and rock varnish chemistry (Harrington and Whitney, 1987; Whitney and Harrington, 1993) on alluvial units of FW .

Conclusions

The huge alluvial fan of FW of the Amargosa River drainage includes a substantial late Quaternary record of aggradation from 100-50 ka during variable but generally warm and wetter conditions than historic climate, followed by up to 20 m of fanhead incision by about 36-24 ka during significantly cooler and effectively wetter conditions than occurred in the preceding 50 ky or the following 20 ky. Aggradation on the lower part of the fan below the intersection point resumed during the deglacial climatic transition with warming and wetter than present conditions, perhaps with a more frequent monsoonal component than present.

References Cited

Beck, D.A., and Glancy, P.A., 1995, Overview of runoff of March 11, 1995, in Fortymile Wash and Amargosa River, southern Nevada: U.S. Geological Survey Fact Sheet FS-210-95

Benson, L., and Klieforth, H., 1989, Stable isotopes in precipitation and groundwater in the Yucca Mountain Region, southern Nevada: Paleoclimatic implications: American Geophysical Union Geophysical Monograph 55, p. 41-59

Berger, G.W., 1988, Dating Quaternary events by luminescence: Geological Society of America Special Paper 227, p. 13-50

Bradbury, J.P., 1997, A diatom record of climate and hydrology for the past 200 ka from Owens Lake, California with comparison to other Great Basin records: Quaternary Science Reviews, v. 16, p. 203-219

Bull W.B., 1991, Geomorphic Responses to Climatic Change, Oxford University Press, New York, 304 p.

Claassen, H.C., 1985. Sources and mechanisms of recharge for ground water in the west-central Amargosa Desert, Nevada: a geochemical interpretation: U.S. Geological Survey Professional Paper 712-F.

Coe, J., P. Glancy, and J.W. Whitney, 1997, Volumetric analysis and hydrologic characterization of a modern debris flow near Yucca Mountain, Nevada: Geomorphology, v. 20, p. 11-28.

Ely, L.L., 1993, A 5000-year record of extreme floods and climate change in the southwestern United States: Science, v. 262, p. 410-412

Faulds, J.E., Bell, J.W., Feuerbach, D.L., and Ramelli, A.R., 1994, Geologic Map of the Crater Flat Area, Nevada: Nevada Bureau of Mines and Geology Map 101, scale 1:24,000

Frizell, V.A., and Shulters, J., 1990, Geologic map of the Nevada Test Site: U.S. Geological Survey Map I-2046

Glancy, P.A., and Beck, D.A., this guidebook, Modern flooding and runoff of the Amargosa River, Nevada—California, emphasizing contributions of th Fortymile Wash.

Grayson, D.K., 1993, The Desert's Past: a Natural History of the Great Basin, Smithsonian Institution, 356 p.

Harden, J.W., Taylor, E.M., Hill, C, Mark, R.K., McFadden, L.D., Reheis, M.C., Sowers, J.M., and Wells, S.G., 1991, Rates of soil development from four soil chronosequences in the southern Great Basin: Quaternary Research, v. 35, p. 383-399

Harrington, C.D., and Whitney, J.W., 1987, Scanning electron microscope method for rock-varnish dating: Geology, v. 15, p. 967-70

Ludwig, K.R., K.R. Simmons, B.J. Szabo, I.J. Winograd, J.M Landwehr, A.C. Riggs, and R.J. Hoffman, 1992. Mass-spectrometric ^{230}Th, ^{234}U, ^{238}U dating of the Devils Hole calcite vein: Science, v. 248, p. 284

Lowenstein, T.K., 1997, Death Valley salt core: 200,000 year paleoclimate record from sedimentary structures, saline mineralogy, fluid inclusions in halite, and ostracodes (Abs) IN Great Basin Aquatic System History Symposium, University of Utah and Smithsonian Institution

Lundstrom, S.C., J.R. Wesling, and E.M. Taylor, in press. Preliminary surficial deposits map of the northeast 1/4 of the Busted Butte 7.5' quadrangle, Nye County, Nevada: U.S. Geological Survey Open File Report 94-341.

Lundstrom, S.C., J.W. Whitney, J.B. Paces, S.A. Mahan, and K.R. Ludwig, in press. Preliminary map of the surficial deposits of the southern half of the Busted Butte 7.5" quadrangle, Nye County, Nevada. U.S. Geological Survey Open File Report 95-311.

Lundstrom, S.C., McDaniel, S.M., Guertal W.R., Nash, M.H., Wesling, J.R., Cidziel, J., Cox, S, and Coe, J.A, 1995: Characteristics and development of alluvial soils of the Yucca Mountain area, southern Nevada: U.S. Geological Survey Milestone Report 3GCH510M

Lundstrom, S.C. and R.G. Warren, 1994. Late Cenozoic evolution of Fortymile Wash: major change in drainage pattern in the Yucca Mountain, Nevada region during late Miocene volcanism: *in* American Nuclear Society, LaGrange Park, IL, Proceedings of the Fifth Annual International Conference on High Level Radioactive Waste Management, volume 4, p. 2121-2130.

Mehringer, P.J., Jr., and Warren, C.N., 1976, Marsh, dune, and archaeological chronology, Ash Meadows, Amargosa Desert, Nevada, IN Elston, R., ed., Holocene environmental change in the Great Basin, Nevada Archeological Survey Research Paper n. 6, p. 120-150

Millard, H.T., and Maat, P.B., 1994, Thermoluminesence dating procedures in use at the U.S. Geological Survey, Denver, Colorado: U.S. Geological Survey Open-File Report 94-249.

Osterkamp, W.R., Lane, L.J., and Savard, C.S., 1994, Recharge estimates using a geomorphic/distributed-parameter simulation approach, Amargosa River Basin: Water Resources Bulletin, v. 30, n. 3, p. 493-507

Paces, J.B., Mahan, S.A., Ludwig, K.R., Kwak, L.M., Neymark, L.A., Simmons, K.R., Nealey, L.D., Marshall, B.D., Walker,A., 1995, Progress report on dating Quaternary surficial deposits, 1995 Milestone Report 3GCH510M

Peterson, F.F., Bell, J.W., Dorn, R.I., Ramelli, A.R., and Ku, T.L., 1995, Late Quaternary geomorphology and soils in Crater Flat, Yucca Mountain area, southern Nevada: Geological Society of America Bulletin, v. 107, p. 379-395

Porter,S.C., Pierce, K.L., and Hamilton, T.D., 1983, Late Wisconsin mountain glaciation in the western United States, IN Wright, H.E., Jr., and Porter, S.C., eds., Late Quaternary environments of the United States, v.1, University of Minnesota Press, p. 71-111.

Quade J., M.D. Mifflin, W.L. Pratt, W. McCoy, and L. Burckle, 1995. Fossil spring deposits in

the southern Great Basin and their implications for changes in water-table levels near Yucca Mountain, Nevada during Quaternary time: Geological Society of America Bulletin, v. 107, p. 213-230.

Reheis, M.C., Goodmacher, J.C., Harden, J.C., McFadden, L.D., Rockwell, T.K., Shroba, R.R., Sowers, J.M., Taylor, E.M., 1995, Quaternary soils and dust deposition in southern Nevada and California: Geological Society of America Bulletin, v. 107, p. 1003-1022.

Rosholt, J. N., C.A. Bush, W.J. Carr, D.L. Hoover, W.C. Swadley, and J.R. Dooley, Jr., 1985. Uranium-trend dating of Quaternary deposits in the Nevada Test Site area, Nevada and California: U.S. Geological Survey Open File Report 85-540.

Savard, C.S., 1998, Estimated ground-water recharge from streamflow in Fortymile Wash near Yucca Mountain, Nevada: U.S. Geological Survey Water Resources Investigations Report 97-4273, 30 p.

Smith, G.I., 1979, Subsurface Stratigraphy and Geochemistry of late Quaternary Evaporites, Searles Lake, California: U.S. Geological Survey Professional Paper 1043, 130 p.

Smith, G.I., and Bischoff, J.L., eds., 1997, An 800,000-year paleoclimatic record form Core OL-92, Owens Lake, southeast California: Geological Society of America Special Paper 317

Spaulding, W.G. 1985, Vegetation and climates of the last 45,000 years in the vicinity of the Nevada Test Site, south central Nevada: U.S. Geological Survey Professional Paper 1329.

Spaulding, W.G. 1990. Vegetational and climatic development of the last glacial maximum to the present: in Betancourt, J.L., T.R. VanDevender, and P.S. Martin, eds., Packrat middens: the last 40,000 years of biotic change, Chapter 9, University of Arizona Press, Tucson.

Spaulding, W.G. 1994, Paleohydrologic investigations in the vicinity of Yucca Mountain: Late Quaternary paleobotanical and palynological records: Dames and Moore report.

Szabo, B.J., Kolesar, P.T., Riggs, A.C., Winograd, I.J., and Ludwig, K.R., 1994, Paleoclimatic inferences from a 120,000-yr calcite record of water-table fluctuation in Browns Room of Devils Hole, Nevada: Quaternary Research, v. 41, p. 59-64

Taylor, E.M., 1986. Impact of time and climate on Quaternary soils in the Yucca Mountain area of the Nevada Test Site: MS Thesis, University of Colorado, Department of Geological Sciences, Boulder Colorado.

Whitney, J.W., and Harrington, C.D., 1993, Relict colluvial boulder deposits as paleoclimatic indicators in the Yucca Mountain region, southern Nevada: Geological Society of America Bulletin, v. 105, p. 1008-1018

Wigand, P.E., 1997, Late Quaternary climates, Great Basin vegetation and aquatic system history (Abs) IN Great Basin Aquatic System History Symposium, University of Utah and Smithsonian Institution

Winograd, I.J., T.B.Copeland, J.M. Landwehr, A.C. Riggs, K.R. Ludwig, K.R. Simmons, B.J. Szabo, P.T. Kolesar, and K.M. Revesz, 1992. Continuous 500,000-year climate record from vein calcite in Devils Hole, Nevada: Science, v. 258, p. 255-284.

Day 1, Stop 4

The July 1984 debris flows at Jake Ridge - an example of hazardous mass movement and hillslope erosion near Yucca Mountain

Jeffrey A. Coe, Patrick A. Glancy, and John W. Whitney

Author's Note: Most of the following text and some figures were extracted from Coe, J.A., Glancy, P.A., and Whitney, J.W., 1997, Volumetric analysis and hydrologic characterization of a modern debris flow near Yucca Mountain, Nevada: Geomorphology, v. 20, p. 11-28.

Introduction

On July 21 or 22, 1984, debris flows triggered by rainfall occurred on the south hillslope of Jake Ridge (fig. 1), a flat-topped ridge located about 6 km east of the crest of Yucca Mountain. These debris flows eroded unconsolidated colluvium from the upper hillslope, deepened and widened existing hillslope channels, and deposited debris up to about 1.2 m deep on a dirt road at the base of the hillslope (figs. 2 and 3). In this paper, we briefly summarize the triggering storms, sediment budget, a possible initiation mechanism, and the calculated recurrence interval of the triggering storms.

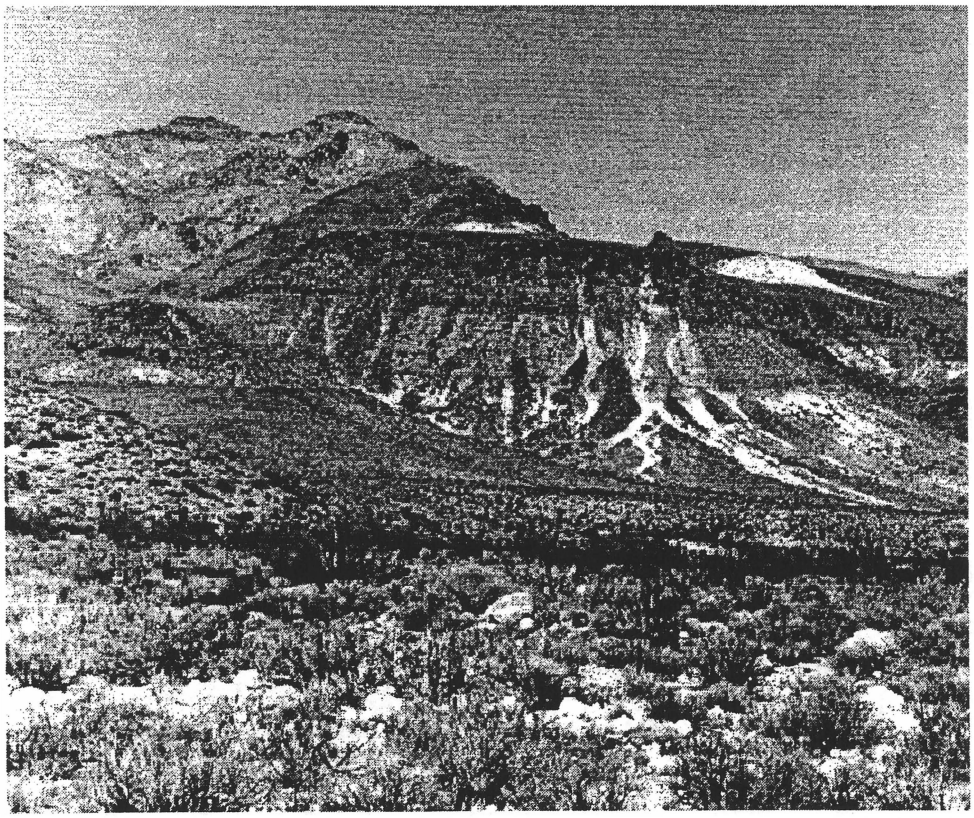

Figure 1. Jake Ridge with debris flows scars on the south hillslope. The elevation at southern lip of Jake Ridge, right above the south hillslope, is about 1260 m. Total topographic relief of the south hillslope is about 130 m. Photograph taken October, 1989.

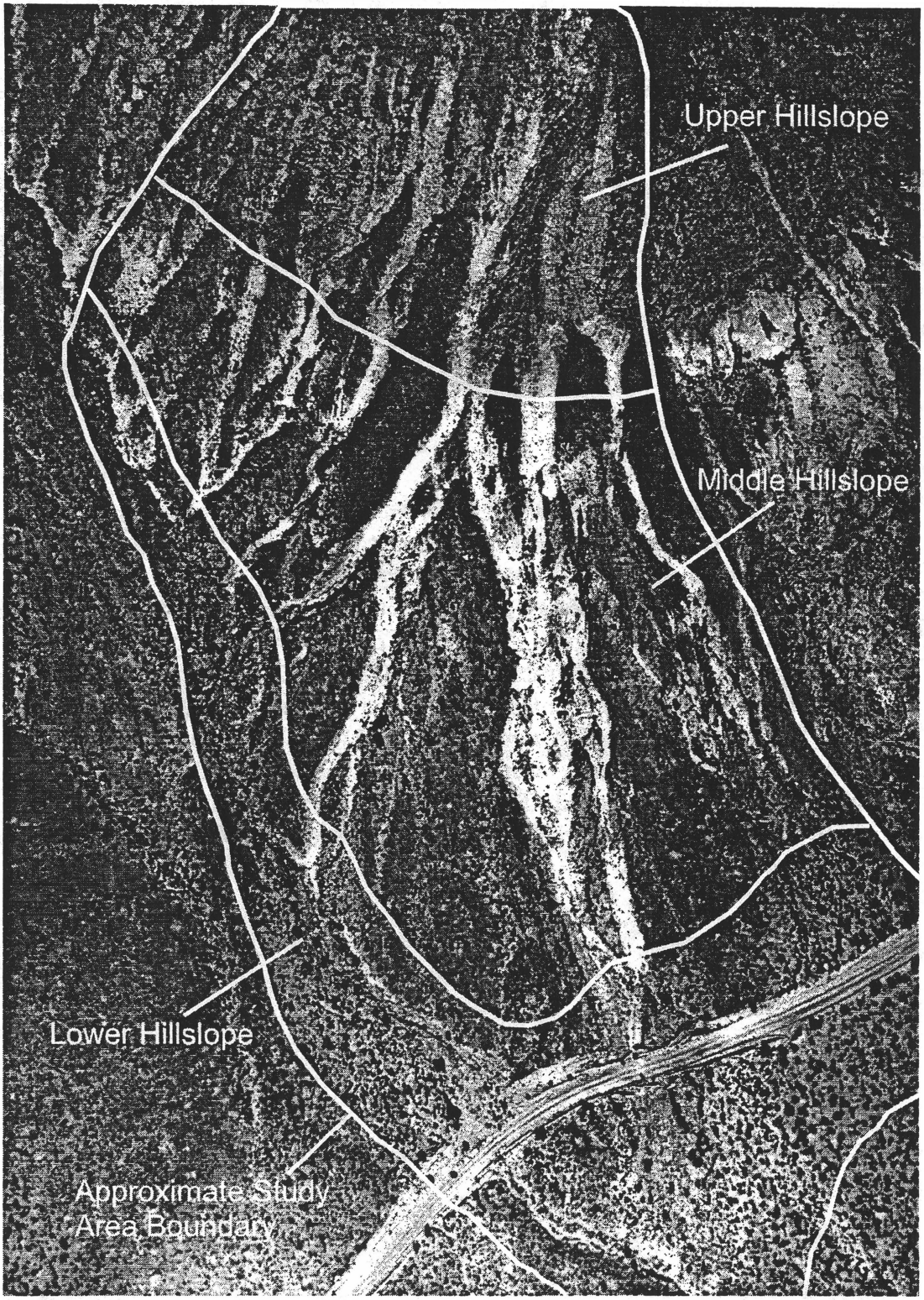

Figure 2. Portion of Septermber 30, 1991 aerial photograph of Jake Ridge. Approzimate boundary of the sediment budget study area with hillslope zones outlined. The road at the base of the hillslope is about 5 m wide.

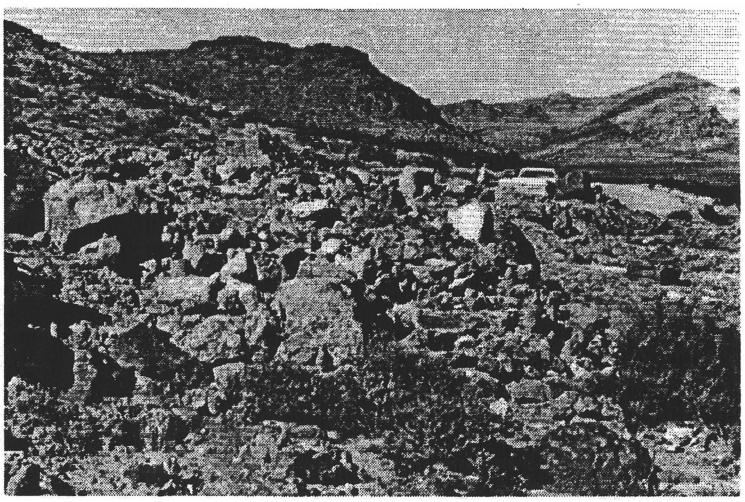

Figure 3. Debris flow depositional lobe on the road on August 16, 1984. View is to the north. Boulders range up to about 1 m in diameter. See pickup truck for scale. Photograph by Pat Glancy See pickup truck for scale. Photograph by Pat Glancy

The Storms

The storms that caused the debris flows were severe, localized, convective storms that occurred during the early part of the monsoonal storm period in summer. Minimal precipitation in early-middle July suggests that local hillslope colluvium was dry or nearly dry prior to the July 21 storm. Two rain gages, one at the east base of Yucca Mountain, about 5.4 km southwest of Jake Ridge (gage YA), and the other (gage YR) near the crest of Yucca Mountain 7.5 km southwest of Jake Ridge, recorded rainfall from storms on July 21 and 22 (fig. 4). Twenty-four hour accumulation totals of 64 mm and 20 mm were recorded at gage YA on July 21 and 22, respectively. Gage YR recorded totals of 69 mm on the July 21 and 17 mm on July 22. Maximum hourly rates of rainfall intensities were 73 mm/hr at gage YA on the twenty-first, and 15 mm/hr at gage YA on the twenty-second. The most intense period of rainfall was recorded during a 2-hr period on the evening of July 21 when the gages recorded 60 and 58 mm of rainfall.

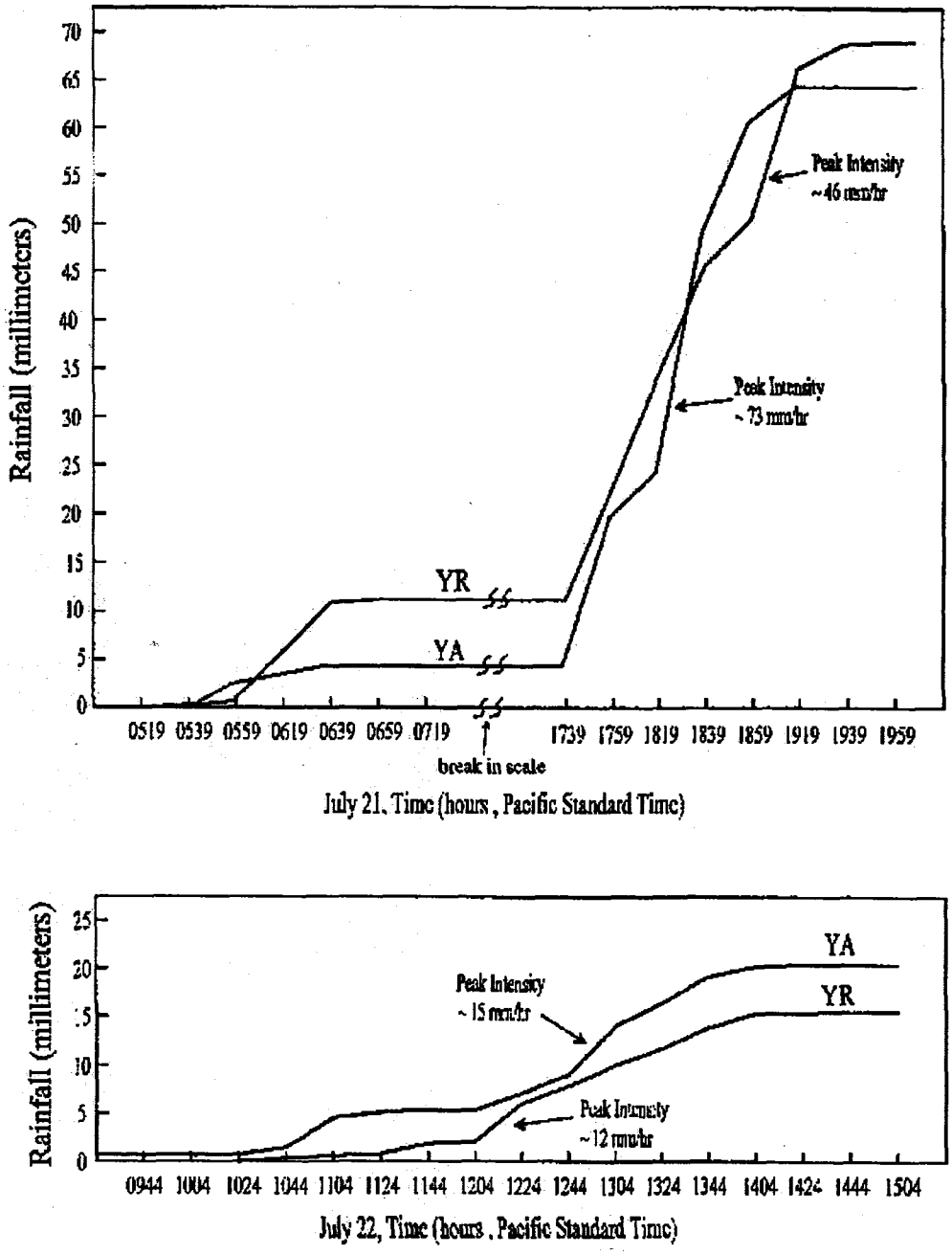

Figure 4. Cumulative rainfall records for July 21 and 22, 1984, for storm events at gages YA and YR, respectively located about 5.4 and 7.5 km southwest of Jake Ridge. YA and YR are no longer in operation. They were tipping bucket rain gages operated by Sandia National Laboratories. YA was at the east base of Yucca Mountain, elevation about 1143 m. YR was at the crest of Yucca Mountain, elevation about 1469 m.

Geologic Setting

Jake Ridge is capped by the Topopah Spring Tuff of the Paintbrush Group (fig. 5, Sawyer and others 1994;Scott and Bonk, 1984), a moderately transmissive aquifer (Winograd and Thordarson, 1975), but in contrast to Yucca Mountain, is also underlain by tuffaceous beds of the Calico Hills Formation (Sawyer and others, 1994; Christiansen and Lipman, 1965), a relatively nonabsorptive aquifer. The south-facing hillslope at Jake Ridge is mantled by less than 2 m of bouldery colluvium and has a slope gradient that ranges from about 32° just below the caprock to less than 4° at the base of the slope. The hillslope drains to a minor and relatively short tributary of Fortymile Wash. The top surface of Jake Ridge, a dip-slope on resistant caprock, grades slightly (about 4°) to the southeast and is covered by a mantle of cobbly colluvium less than 30 cm thick (fig. 6). Post-storm observations on the top of Jake Ridge revealed no evidence of intense runoff over the thinly mantled surface.

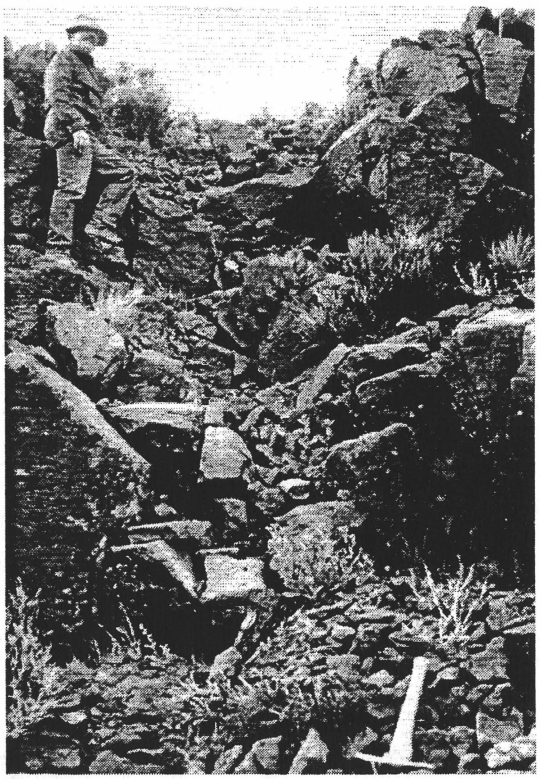

Figure 5. Topopah Spring Tuff caprock. Rainfall percolating through the thin colluvial mantle on the ridgetop may have exited through the fractures in this unit, leading to the initiation of the debris flows. See pick for scale. Photograph taken March 21, 1992.

Figure 6. Thin cobble mantle on the top of Jake Ridge just above the south hillslope. View is to the southeast. Fortymile Wash is visible in the middle of the photograph. Photograph taken March 21, 1992.

Sediment Budget

To examine topographic changes caused by the debris flows, we used digital elevation models (DEMs) with 2.0 m grid-node spacing, measured from pre-storm and post-storm aerial stereo-photographs of 1:8000 and 1:3000 scales, respectively. To calculate volumetric changes, as well as map hillslope erosion and downslope distribution of debris caused by the debris flows, an elevation-difference DEM (fig. 7) was created by subtracting the 1982 DEM from the 1991 DEM. The standard deviation of each elevation in the difference DEM was about 0.14 m. Volumetric calculations indicate that about 7,040 m^3 of debris was redistributed on the hillslope study area during the two-day storm period (table 1). About 4,580 m^3 (65 %) of the eroded sediment was deposited on the hillslope (within the study area) and the remaining 35 % was deposited in a short tributary to Fortymile Wash and in the wash itself (outside the study area). The debris lobe on the road at the base of the main hillslope channel (figs. 2, 3, and 7) was the primary area of deposition within the study area. Results from sieve and pipet particle-size analysis of a sample of matrix taken from near the center of this debris lobe yielded sand, silt, and clay splits of 56%, 37 %, and 7%, respectively. The maximum and mean depths of erosion in the study area were about 1.8 m and 5 cm, respectively. The mean depths of erosion on the upper and middle hillslope were 27 and 4 cm, respectively. The mean depth of deposition on the lower hillslope was 16 cm.

About 2,460 m^3 of sediment was removed from the 49,132 m^3 study area and deposited in Fortymile Wash and its tributary. Field observations indicate that non-channelized areas of the south hillslope are generally mantled by 0-2 m of colluvium. If a mean value of 1 m is assumed for the amount of unconsolidated colluvium cover, approximately 49,000 m^3 of debris would have existed on the south-facing hillslope prior to the July 1984 storms. Therefore, about 5 % of the available colluvium was removed from the hillslope during the two-day storm.

Table 1. Volumetric results for each hillslope zone shown in ure 2. Percentages are of the total area for each zone.

Zone	Area (m^2)	Negative Volume (m^3)	Area with negative cell volumes (m^2)	Positive Volume (m^3)	Area with positive cell volumes (m^2)	Area with cell volumes = 0 (m^2)	Volume Sum (m^3)
Upper Slope	11748	-3520 ±55	9532 (81%)	+310 ±15	1184 (16%)	332 (3%)	-3210 ±61
Middle Slope	25688	-2970 ±67	14200 (55%)	+1890 ±58	10908 (43%)	580 (2%)	-1080 ±90
Lower Slope	11696	-550 ±32	3228 (28%)	+2380 ±50	8012 (68%)	456 (4%)	+1830 ±61
Study Area	49132	-7040 ±92	26960 (55%)	+4580 ±81	20804 (42%)	1368 (3%)	-2460 ±124

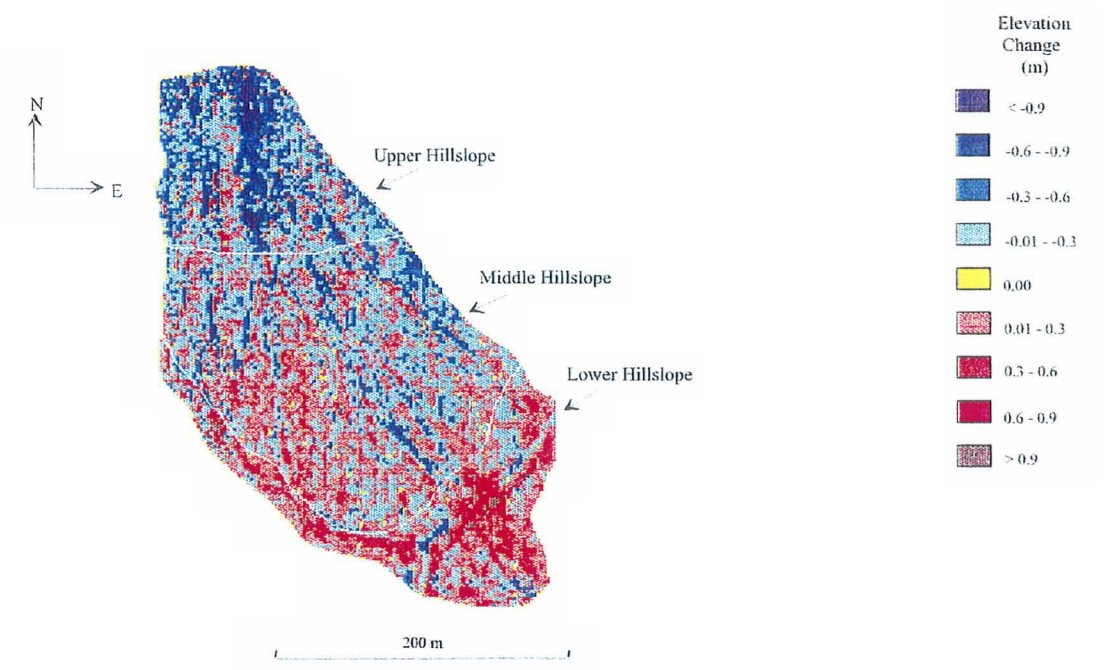

Figure 7. Plan view elevation-difference map of the Jake Ridge hillslope created by subtracting the pre-storm (1982) DEM from the post-storm (1991) DEM. Red and blue areas experienced positive and negative elevation change, respectively. Yellow areas showed no elevation change. Northeast-southwest trending deposits in the southeast corner of the map are the sides of a dirt road (see . 2) that are visible because of road grading between 1982 and 1991.

Initiation Mechanisms

We propose a 'fire hose' initiation mechanism (e.g., Johnson and Rodine, 1984) for the generation of the debris flows. This fire-hose mechanism would have started with rainfall percolating through the cobble mantle on the hilltop (fig. 6) and into the underlying fractured Topopah Spring caprock (fig. 5). This water would then have migrated south, along the dip of the caprock, toward the south hillslope, where it exited the fractures at the cliff face. Several light-colored triangular stripped areas that increase in size downslope from fractures in and just below the cliff face (figs. 1 and 2) support this hypothesis. These features suggest that debris movement was initiated by streams of water flowing from the caprock, like from a fire hose. These streams of water, impacting saturated colluvium on the upper hillslope, would have caused a mixture of debris and water to flow downhill. The flows of this mixture were probably extremely erosive on the upper hillslope, and became charged with additional debris as they continued downslope. On the middle hillslope, some of the flows were eroding and others were depositing, as evidenced by stripped (fig. 8) and incised channels (fig. 9) and lateral levees (fig. 10). As the flows continued to pick up debris, they changed into non-erosive debris flows.

When the flows reached the lower hillslope, they spread laterally and stopped. Some erosion and deposition was also probably accomplished by the flow of water before and after the main debris flow events.

Figure 8. Stripped channel on middle hillslope. See pick for scale. Photograph taken March 21, 1992.

Figure 9. Channel incision on the middle hillslope Photograph taken March 21, 1992.

Figure 10. Levee on the middle hillslope. Photograph taken October, 1989.

Recurrence Interval

A magnitude of about 29 mm for a 2-hr storm with a probable 100-year recurrence interval was calculated using methods prescribed in the Precipitation-Frequency Atlas of the western United States (Miller et al., 1973). Thus, the 2-hr totals of 60 and 58 mm recorded by gages on the evening of July 21, are about twice those expected with a 1 % probability of occurrence in any given year. A probable maximum precipitation amount calculated for a 2-hr duration storm in the arid southwestern U.S. is about 307 mm (Hansen et al., 1977); or about five times greater than that recorded by the Yucca Mountain rain gages on July 21.

The average intensity of the 2-hr storm on July 21 was about 30 mm/hr. The expected intensity for a 2-hr storm with a 100-year return period at the Cane Springs, Nevada precipitation station, located about 30 km southeast at the same elevation as Jake Ridge, ranges from about 14 - 19 mm/hr (French, 1983). The expected intensity for a 2-hr storm with a 500-year return period at this same station ranges from about 18 - 25 mm/hr. Thus, the intensity of the July 21 storm was greater than that expected for a storm with a 500-year return period at the Cane Spring station.

References Cited

Campbell, R.H., 1975, Soil slips, debris flows, and rainstorms in the Santa Monica Mountains and vicinity, southern California. U.S. Geological Survey Professional Paper 851, 51 pp.

Christiansen, R.L., and Lipman, P.W., 1965, Geologic map of the Topopah Spring Northwest quadrangle, Nye County, Nevada. U.S. Geological Survey Geologic Quadrangle Map GQ-444, scale 1:24000.

Ellen, S.D., and Fleming, R.W., 1987, Mobilization of debris flows from soil slips, San Francisco Bay region, Californi, *in.* Costa, J.E, and Wieczorek, G., eds.,

Flows/avalanches--process, recognition, and mitigation. Geological Society of America, Reviews in Engineering Geology, 7: pp. 31-40.

French, R.H., 1983, A preliminary analysis of precipitation in southern Nevada. Desert Research Institute, University of Nevada System Report DOE/NV/10162-10, 39 pp.

Hansen, M.E., Schwartz, F.K., and Riedel, J.T., 1977, Probable maximum precipitation estimates, Colorado River and Great Basin drainages. U.S. Department of Commerce and U.S. Department of the Army Hydrometeorological Report 49, 161 pp.

Johnson, A.M. and Rodine, J.R., 1984, Debris flows, *in* Brunsden, D. and Prior, D.B., eds., Slope instability. Wiley, Chichester, pp. 257-361.

Miller, J.F., Frederick, R.H., and Tracey, R.J., 1973, Precipitation-frequency atlas of the western United States, NOAA Atlas 2, Volume VII-Nevada. U.S. Department of Commerce, National Oceanic and Atmospheric Administration, National Weather Service, Silver Spring, Maryland, 43 pp.

Sawyer, D.A., Fleck, R.J., Lanphere, M.A., Warren, R.G., Broxton, D.E., and Hudson, M.R., 1994, Episodic caldera volcanism in the Miocene southwestern Nevada volcanic field: revised stratigraphic framework 40Ar/39Ar gechronology, and implications for magmatism and extension: Geological Society of America Bulletin, v. 106, p.1304-1328.

Scott, R.B. and Bonk, Jerry, 1984, Preliminary geologic map of Yucca Mountain, Nye County, Nevada with geologic sections. U.S. Geological Survey Open-File Report 84-494.

Winograd, I.J., and Thordarson, William, 1975, Hydrogeologic and hydrochemical framework, south-central Great Basin, Nevada-California, with special reference to the Nevada Test Site. U.S. Geological Survey Professional Paper 712-C, 126 pp.

Day 1, Stop 4

Coyote Wash

Patrick A. Glancy

Coyote Wash, an approximately 0.3-mi^2 ephemeral drainage on the eastern flank of Yucca Mountain, was, during the early- to mid-1980's, the proposed location for a vertical exploratory shaft. The purpose of the shaft was to allow evaluation of the subsurface hydrogeological environment pertinent to construction of an underground repository for high-level radioactive waste (fig. 1). The proposed shaft site was within the narrow canyon floodplain, a short distance downstream from the junction of the North and South Forks, the principal tributaries of Coyote Wash. Cumulatively, the tributary drainage areas of 0.094 mi^2 and 0.105 mi^2, respectively, comprise approximately two-thirds of the total basin area. Drainage area of 0.095 mi^2 downstream from the proposed shaft site accounts for the remaining one-third of the total basin area. Total basin relief is about 860 ft, and average basin slope is about 13 percent, or 7.5 degrees.

A geomorphic reconnaissance of the proposed shaft site and surrounding environs, during early 1983, disclosed land-surface evidence of a flood history that probably included debris flows as classified by Costa and Jarrett (1981). This cursory assessment of flood history and resultant cumulative evidence indicated the potential for future flood hazards at the proposed location of the exploratory shaft. The apparent hazard potential prompted a more detailed flood-hazard study of the proposed shaft site that included both hydraulic engineering and geomorphic (paleoflood) investigative approaches.

The geomorphic investigative component was initially facilitated by the excavation of two trenches into the unconsolidated valley fill of North Fork Coyote Wash a short distance upstream from the proposed shaft location (fig. 1). The trenches provided vertical walls that exposed valley-fill sediments for subsequent interpretive analyses. A cross-channel trench fully penetrated and vertically exposed unconsolidated sediments down to the underlying bedrock surface. A T-shaped trench, about 5 ft deep, excavated a short distance downstream, between the cross-channel trench and the proposed shaft site, exposed stratigraphy of valley sediments beneath a hummocky land surface that was suspicioned to be the product of debris-flow deposition.

Figure 1. Coyote Wash drainage

Stratigraphic analyses of the sediments exposed in the trenches revealed multiple flood deposits, including several debris-flow deposits containing boulders as large as 2– 3 ft in diameter. The deposits also revealed a stage-I pedogenic carbonate zone, about 3 ft thick, that conforms to the land-surface profile and mantles most of the younger (upper) nonindurated deposits just below land surface. The pedogenic carbonate indicates some degree of antiquity for the underlying deposits, but ages are at best speculative because the rate of carbonate accumulation in the vicinity of Yucca Mountain is, as yet, uncertain. The lack of a well-defined B-horizon within the upper soil, above the zone of carbonate accumulation, indicates a relatively young age for the near-surface deposits; thus, a tentative age range of several thousand years was

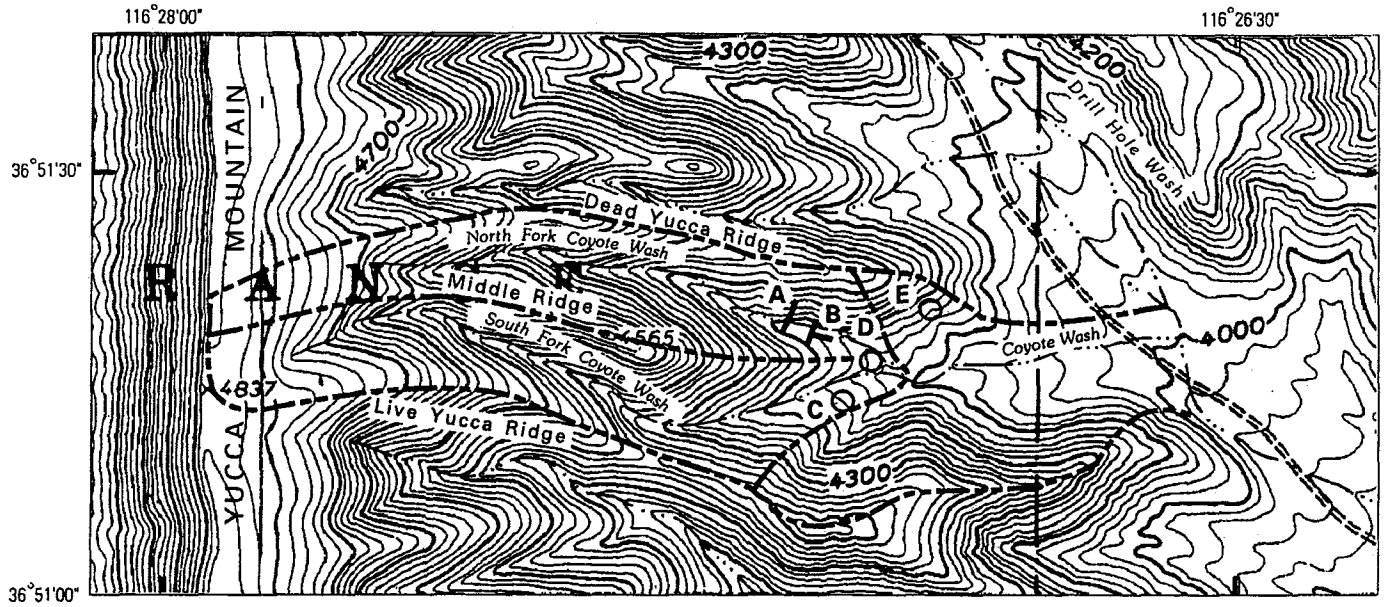

Base from U.S. Geological Survey
1:24,000 Busted Butte, NV Quadrangle, 1961

0 0.5 1 MILE
0 1 2 KILOMETERS

CONTOUR INTERVAL 20 FEET
NATIONAL GEODETIC VERTICAL DATUM OF 1929

EXPLANATION

- **A** CROSS-CHANNEL TRENCH
- **B** T-SHAPED TRENCH
- **C** WELL USW G-4
- **D** ORIGINAL PROPOSED-EXPLORATORY-SHAFT LOCATION
- **E** RELOCATED PROPOSED-EXPLORATORY-SHAFT LOCATION

NOTE: MAP LOCATIONS ARE APPROXIMATE

Figure 1. Coyote Wash Drainage

assigned to the uppermost deposits that contain the pedogenic carbonate. Basal deposits overlying bedrock were commonly lightly to highly indurated, indicating a substantially older age than the upper nonindurated sediments. The upper nonindurated deposits unconformably overlie the variably indurated deposits of slightly less overall volume and lateral extent. The variably indurated deposits were tentatively assigned a late Pleistocene or early Holocene (?) age on the basis of their indurated character and color, which contrasts with the nonindurated, overlying deposits (Glancy, 1994).

Thermoluminescence (TL) dates of fine-grained components in three of the deposits were determined after an interpretive report of the trench analyses was published (Glancy, 1994). TL dates are derived by select analyses of only the finest sediments (silt size and finer). The depositional history of these fines with respect to the deposits is critically important to a proper interpretation of ages of deposits. If the fines were originally part of debris flows, they may incorporate an older relict age; if they were added to the deposits by eolian processes after debris-flow deposition, they will date younger than the true age of the deposits. Dates obtained for select stratigraphic units of the trenches range approximately as follows (Shannon Mahan and Scott Lundstrom, U.S. Geological Survey, written commun., 1998): variably indurated, older deposits near the bottom of the cross-channel trench, 25,000 to 32,000 years; nonindurated deposits near the top of the cross-channel trench, but within the zone of stage-I pedogenic carbonate accumulation, 2,850 to 3,550 years; and nonindurated deposits of the T-shaped trench, near mid-depth, and within the zone of stage-I pedogenic carbonate accumulation, 4,000 to 4,810 years.

The stratigraphically intermixed deposits of both Newtonian and debris-flow fluids portray a complex flood and depositional history. Abundant unconformities between different strata attest that the trench exposures probably portray an incomplete stratigraphic sequence of flood deposits. Although the upstream drainage area is quite small (less than 0.094 mi^2), the catchment is adequate to generate severe floods when storms are sufficiently prolonged and intense. Lack of a complete stratigraphic record and uncertainty of ages of the various deposits preclude the formulation of a reliable record of flood frequency. Magnitudes of individual floods are equally elusive. However, the depositional evidence confirms repeated flooding, with at least some severe and hazardous floods on the basis of the abundant debris-flow evidence. Evidence from the past is a worthy harbinger of the potential for future hazards.

Restoration of the terrain by trench backfilling now (1998) prevents onsite examination of the stratigraphic evidence; however, the evidence can be tentatively viewed and reviewed in photographs and trench diagrams contained in the interpretive report (Glancy, 1994).

Extreme magnitudes of possible future flooding were estimated using empirically derived calculations (table 1). One of the numerical techniques (Costa, 1983) is based on paleoflood evidence in the channel of North Fork Coyote Wash. Although the resultant magnitudes of potential extreme floods range from 900 to 2,600 ft^3/s, the conservative requirements associated with safety of nuclear-waste storage favor the larger estimates for design acceptance. The proposed shaft location at the junction of North and South Forks Coyote Wash would require that peak floods of similar magnitudes (similar drainage areas and geomorphic settings) should be expected to cumulatively impact the proposed shaft site. A peak "design" flood of 2,600 ft^3/s was recommended for North Fork Coyote Wash, doubled (5,200 ft^3/s) to accommodate a similar flow magnitude and timing from South Fork Coyote Wash, and appropriately rounded to 5,000 ft^3/s to reflect an acceptable confidence level inherent in the empirical nature of the estimates.

Table 1. Estimates of maximum peak-flow rates for North Fork Coyote Wash derived using various methods (from Glancy, 1994) [ft^3/s, cubic feet per second]

Method	Calculated flow rate (ft^3/s)
Costa's (1983) boulder technique	2,400 or more
Matthai's (1969) runoff-area envelope curve	2,600
Aldridge's runoff-area envelope curve[1]	1,000
Costa's (1987) runoff-area envelope curve	900
Crippen amd Bue's (1977) runoff-area envelope curve	1,000
U.S. Bureau of Reclamation probable maximum foold for North Fork Coyote Wash (Bullard, 1986)[2]	2,500

[1]B.N. Aldridge (U.S. Geological Survey, written commun., 1985)
[2]Bullard's clean-water flow of 1,600 ft^3/s was increased by 55-percent volume to accommodate anticipated entrained sediment load

Results of this investigative strategy were used to relocate the proposed shaft out of the anticipated floodplain (fig. 1). Additional trenching of nearby drainages was planned to evaluate the "normalcy" of Coyote Wash flood history compared to that of nearby Yucca Mountain drainages, but plans did not materialize because of funding reductions.

Plans for the proposed exploratory shaft ultimately ended when hydrogeologic investigations shifted to the "tunnel concept" currently (1998) in progress.

References Cited

Bullard, K.L., 1986, Probable maximum flood study for Nevada Nuclear Waste Storage Investigation Project: Bureau of Reclamation, Department of the Interior, 11 p., 61 pls.

Costa, J.E., 1983, Paleohydraulic reconstruction of flash-flood peaks from boulder deposits in the Colorado Front Range: Geological Society of America Bulletin, v. 94, no. 8, p., 986-1004.

——1987, A comparison of the largest rainfall-runoff floods in the United States with those of the People's Republic of China and the world: Journal of Hydrology, v. 96, no. 1-4, p. 101-115.

Costa, J.E., and Jarrett, R.D., 1981 Debris flows in small mountain stream channels of Colorado and their hydrologic implications: Bulletin of the Association of Engineering Geologists, v. XVIII, no. 3, p. 309-322.

Crippen, J.R., and Bue, C.D., 1977, Maximum floodflows in the conterminous United States: U.S. Geological Survey Water-Supply Paper 1887, 52 p.

Glancy, P.A., 1994, Evidence of prehistoric flooding and the potential for future extreme

flooding at Coyote Wash, Yucca Mountain, Nye County, Nevada: U.S. Geological Survey Open-File Report 92-458, 31 p.

Matthai, H.F., 1969, Floods of June 1965 in South Platte River Basin, Colorado: U.S. Geological Survey Water-Supply Paper 1850-B, 64 p.

Day 1, Stop 5

Stratigraphic And Geomorphic Evidence Against Middle to Late Quaternary Activity on The Ghost Dance Fault at Yucca Mountain, Nye County, Nevada

Emily M. Taylor, Christopher M. Menges, and John W. Whitney

Introduction

Site characterization for a potential high-level nuclear waste repository at Yucca Mountain, Nevada, includes studies of seismic hazards such as ground shaking and surface rupturing associated with active faults in and adjacent to the site. Most faults with documented Quaternary activity are large block-bounding faults located in areas surrounding the potential repository block of Yucca Mountain (fig. 1; Piety, 1995; Menges and others, 1994; Simonds and others, 1995) and thus are associated primarily with vibratory ground motion hazards. A number of faults are mapped at the surface and subsurface in the volcanic rocks of the central block area (Scott and Bonk, 1984; Frizzell and Shulters, 1990; Spengler and others, 1993; Day and others, 1998). Future surface displacements on these faults could pose an additional seismic hazard that is particularly important to the safety and performance of both the potential repository and waste-handling facilities. Evaluation of fault-displacement potential within the repository block is therefore a critical part of the site characterization process (U.S. Department of Energy, 1988).

Figure 1. Location of major faults and trenches at Yucca Mountain.

This report summarizes the geologic and geomorphic characteristics of the Ghost Dance fault (GDF), the largest and most important north-trending fault currently mapped within the potential repository block (fig. 1; Scott and Bonk, 1984; Scott, 1990; Day and others, 1998).

Investigation Methods

Seven trenches were excavated across the GDF where it is covered by Quaternary deposits (figs. 1 and 2). These trenches are designated (from south to north) Whale Back Ridge trench (WBRT), trenches 5 and 5a at the base of Antler Ridge, trenches 4, 4a, and 4b in Split Wash, and trench 2 in Drill Hole Wash. The Ghost Dance fault is exposed in the bedrock in the WBRT, and in trenches 5, 5a, and 4a. One or both walls of the trenches were mapped and surveyed in detail to determine whether Quaternary deposits were disturbed by the underlying faults.

Figure 2. Location of the Ghost Dance and Sundance faults, and trenches in Quaternary deposits that intersect the bedrock fault projections. Fault traces are modified from Day and others (1998) and Scott and Bonk (1984).

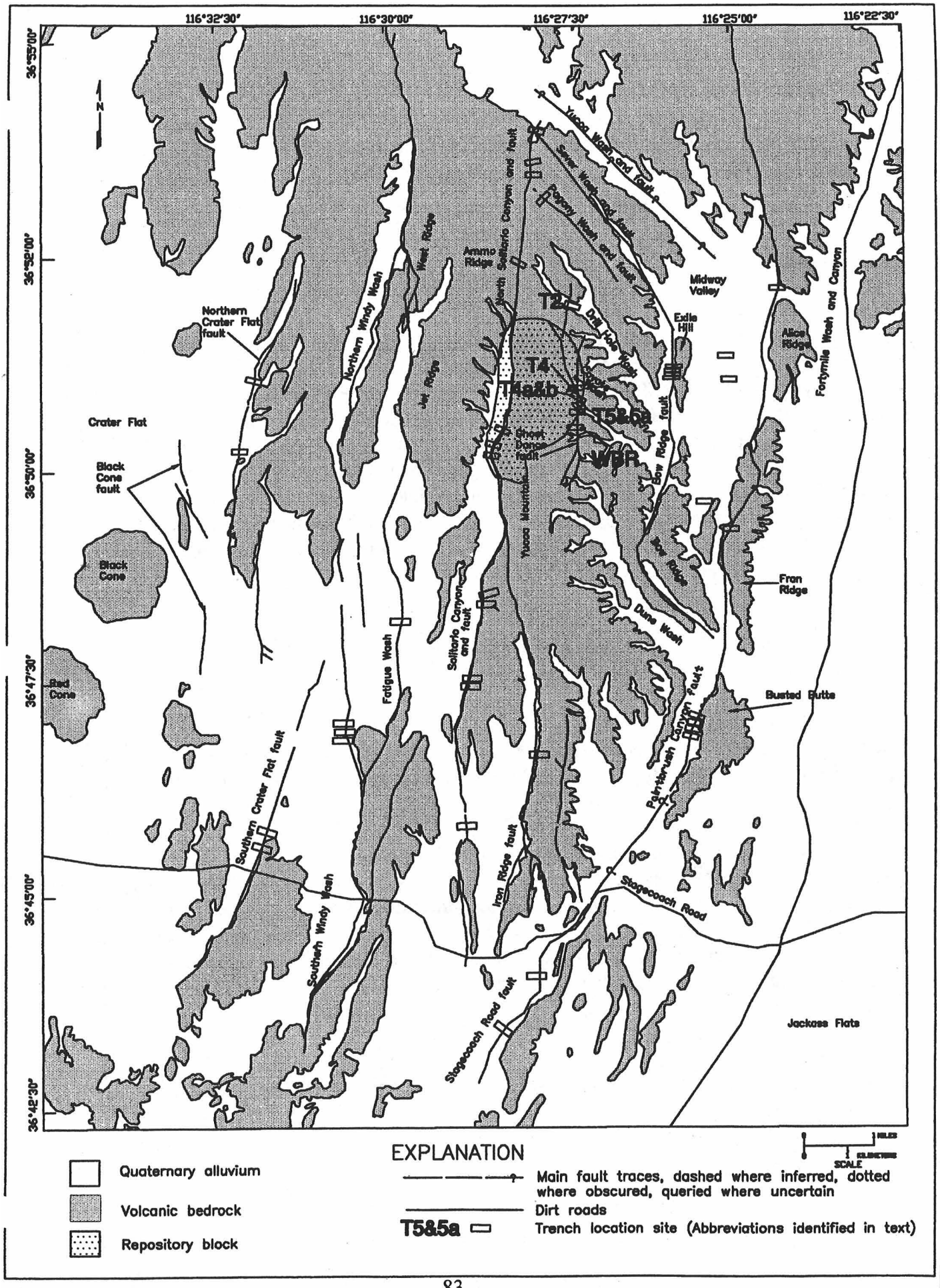

Figure 1. Location of major faults and trenches at Yucca Mountain

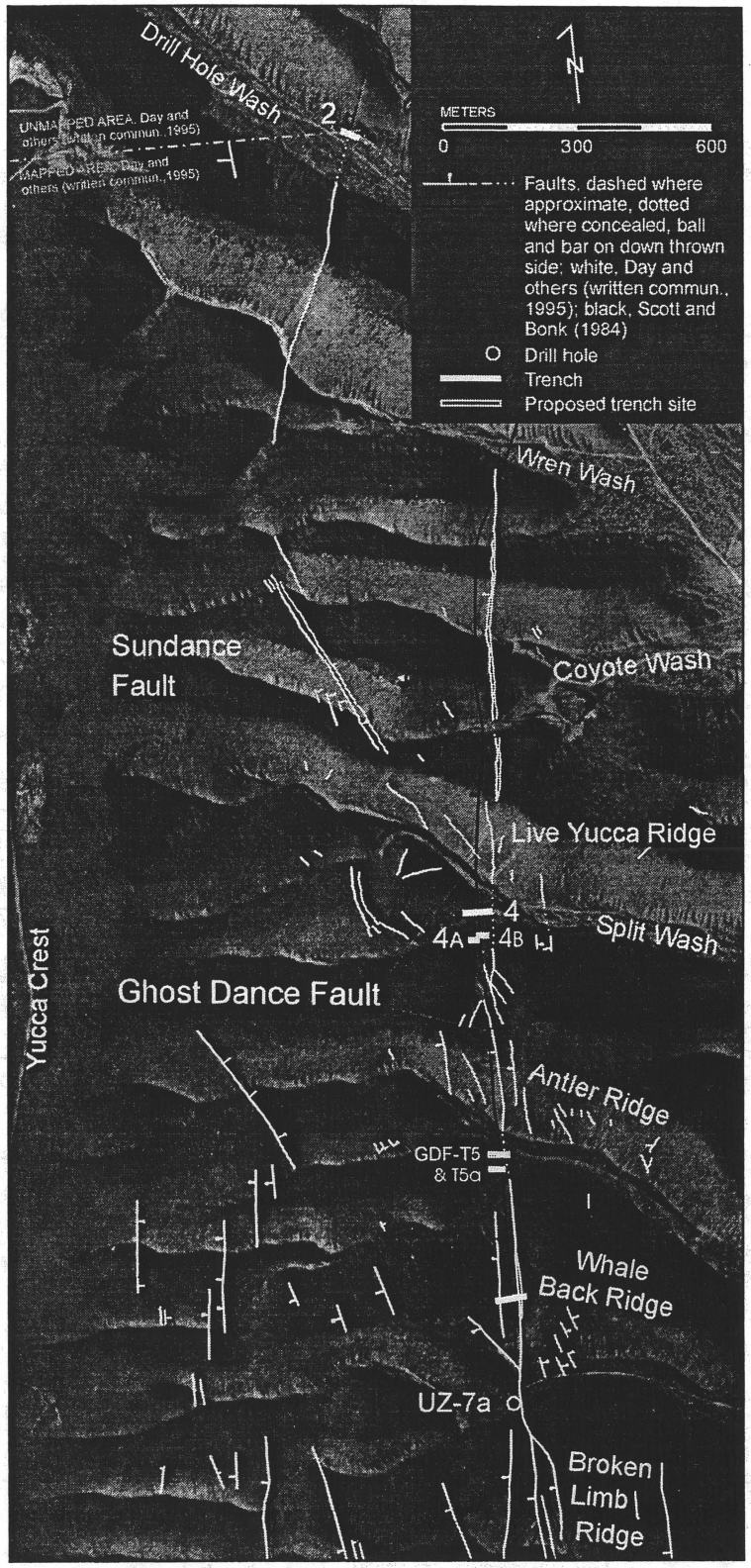

Figure 2. Location of the Ghost Dance and Sundance faults, and trenches in Quaternary deposits that intersect the bedrock fault projections. Fault traces are modified from Day and others (U.S. Geological Survey, written commun., 1995) and Scott and Bonk (1984).

Table 1. Uranium-series dates on secondary opaline silica and calcium carbonate from deposits exposed in trenches that intersect the Ghost Dance fault. No samples were collected in trench 4. Samples were analyzed from dense opaline silica laminae, when available.

Trench	U-series sample number	Material sampled	Age x 10^3 ±2 sigma
Whale Back Ridge, South Wall	110494-GDF1, HD1721	Basal laminae, 1-2 cm thick, Unit 2, 2Kqm--opaline silica sampled	42.7±0.6 53.4±0.5 81±2, 83±2
	110494-GDF2, HD1722	Basal laminae, 3 cm thick, Unit 2, Kqm--opaline silica sampled	17±6 9.6±0.1
	110494-GDF3, HD1723	Laminae, Unit 2, Kqm--opaline silica sampled	21.8±0.09 84.8±1.8 90.9±1.0
	092595-CDF-1, HD2128-A1 and A2	"Biogenic soil carbonate", silica-rich laminae	33.3±0.12 64.2±0.3
	092595-CDF-2, HD2129-B1	"Biogenic soil carbonate", silica-rich laminae	42.0±0.2
	092595-CDF-2B, HD2130-B1 and B2	"Biogenic soil carbonate", silica-rich laminae	37.9±0.5 45.9±0.2
	092595-CDF-3, HD2131-B2	"Biogenic soil carbonate", silica-rich laminae	64.5±0.3
	110494-GDF4, HD1724	Rind on the underside of a clast in the fault breccia--opaline silica sampled	269+∞/-270, 392+70/-48 Excess Th 392±29, 418+∞/-420
	110494-GDF5, HD1725	Disseminated carbonate matrix within fault zone--opaline silica sampled	No data
Trench 4a, North Wall	033095-GDF3-1, HD1829	Slope-parallel densely cemented fluvial gravel--opaline silica sampled	45.2±0.5 49.6±1.0
	033095-GDF3-3, HD1831	Slope-parallel laminae in the bedrock--opaline silica sampled	22.2±0.9 23.0±1.0 37.2±1.9
	033095-GDF3-2, HD1830	Dense fracture fill in the bedrock--opaline silica sampled	253±13 265±12 132±7
Trench 2, South Wall	110494-GDF2-1, HD1717	Clast rind, Unit 2, 2Kb (Q3)--opaline silica sampled	95±12 88±12
		Matrix carbonate, Unit 2, 2Kb (Q3)--opaline silica	26±13 33±10
	110494-GDF2-2, HD1718	Rhizolith, Unit 2, 2Kb (Q3)	66.9±1.5, 67.0±1.5 67.5±1.1
	110494-GDF2-3, HD1719	Carbonate rich rootlet mass, Unit 2, 2Kb (Q3)--opaline silica sampled	19.6±1.6
		Laminae in carbonate rich rootlet mass--opaline silica sampled	24.6±1
	110494-GDF2-4, HD1720	Rhizolith, Unit 2, 2Kb (Q3)--opaline silica sampled	71±3 73±3

Several other indirect methods were also used to provide supportive information regarding Quaternary displacements on the GDF. These methods include: (a) comparative analysis of the geomorphic expression of these faults, relative to the northern Solitario Canyon fault (NSCF); (b) exposure dating of the fault-line escarpment along the GDF (see Gosse and others, this volume); (c) descriptive analysis of fault characteristics in outcrop; and (d) analogue studies of total bedrock displacements on the GDF and Sundance fault (SF), a small northwest-trending fault adjacent to the GDF (Day and others, 1998), compared to other block-bounding and intrablock faults at Yucca Mountain.

Results

The GDF is a north-trending fault with cumulative vertical displacement down-to-the west that decreases northward from up to 27 m at Whale Back Ridge near the south end to less than 6 m on Live Yucca Ridge (Day and others, 1998). Dips are vertical to steeply westward. The GDF at the surface consists of a complex zone of both subparallel and branching strands with a maximum width of 150 m at Whale Back Ridge narrowing northward to a 2-4 m-wide zone north of Live Yucca Ridge. This fault lies entirely within the block bounded by the Solitario Canyon fault on the west and the Bow Ridge fault on the east.

There is little direct geomorphic expression of the GDF in canyon walls. Topographic profiles across ridgecrest escarpments display broadly concave to linear forms suggestive of post-displacement erosion, but lacking steps or scarps indicative of late Quaternary fault disruptions. Preliminary cosmogenic ^{10}Be and ^{26}Al analyses on bedrock along the profile transects suggest that the escarpment surfaces have been stable for at least 750 ka and perhaps as long as 1.0 to 1.1 M.A. (Gosse and others, 1996). These geomorphic characteristics of the GDF contrast with the strong physiographic expression of the NSCF trace, marked by linear gullies on sideslopes and graben-like swales or scarps on ridgecrests, which has had probable Quaternary activity.

Seven trenches excavated across the Ghost Dance fault expose unfaulted Quaternary-age depositional units. In the WBRT, a thin (40-50 cm thick) sequence of undisturbed late Pleistocene to early Holocene colluvium and eolian fines overlie the Tiva Canyon Tuff bedrock which has been disrupted by two splays of the GDF and associated small faults and fractures (Stop 4; fig. 3). The inner rinds of dense carbonate and silica coating bedrock breccia fragments in the cemented main fault zone yield U-series ages as old as 390-420 ka. In places the upper bedrock surface in the trench is draped by dense secondary carbonate and silica (Kqm; fig. 3) having a minimum U-series age estimate of middle Pleistocene ($\geq$ 90 ka, table 1). Locally the overlying colluvium is separated from the zone of dense carbonate and opaline silica by a laminar carbonate layer (K; fig. 3). There is no offset of either the slope-wash colluvium or the laminar carbonate layer (2K) across the main trace of the GDF; however there is one discontinuous fracture in the dense carbonate-silica cemented layer (Kqm) at the bedrock interface in the center of the trench which does not continue upwards into the overlying carbonate laminae. The origin of the fracture in carbonate is unclear, but even if tectonic, the feature is more likely related to shaking from earthquakes on other Quaternary faults in the area than to activity on the GDF itself.

Figure 3. Simplified logs of the north and south walls of the Whale Back Ridge trench across the Ghost Dance fault zone, Yucca Mountain.

In three trenches, 14 samples of opaline silica and 4 samples of pedogenic carbonate were collected for uranium-series (U-series) dating (1). These age estimates provide minimum time for the formation of specific soil characteristics in the unfaulted deposits.

Trench 4 in Split Wash exposes only alluvium, which buries the projected traces of the GDF and SF exposed in nearby bedrock. There is no evidence (i.e, vertical fractures, rotated clasts, offset bedding, vertical laminae) that the middle Pleistocene to late Holocene alluvium is deformed.

In trench 4a which intersects Tiva Canyon Tuff in the fractured footwall of the GDF, undisturbed Quaternary alluvium, colluvium, and eolian fines comprise a late Pleistocene to early Holocene deposit that buries an older middle Pleistocene unit (Fig. 4?). Two U-series ages between 45 and 50 ka provide a maximum age for the surface soil and a minimum age for the buried unit (table 1). Samples of opaline silica laminae mixed with dense secondary carbonate in the fractured bedrock provide a minimum age estimate between 22 and 265 ka which may date infilling of tectonic fractures, stripping of the surface deposits and onset of near-surface carbonate infiltration, and (or) replacement of carbonate by opaline silica.

Figure 4 Simplified log of north wall of trench 4a.

Trench 2 intersects a parallel en echelon fault to the northwest of the GDF in Drill Hole Wash. Two unfaulted or unfractured alluvial units are separated by an erosional unconformity. The surface soil in unit 1 is as young as late Pleistocene to late Holocene in age and buries a well developed soil on unit 2 with a probable middle to late Pleistocene age. U-series age estimates suggest minimum ages of 20 ka and 95 ka for units 1 and 2, respectively (table 1).

Conclusions

There was no stratigraphic or geomorphic evidence for surface displacements on the GDF in at least late to middle Quaternary time. Only a single fracture of uncertain tectonic or nontectonic origin has been observed in dense carbonate and opaline silica which drapes bedrock in the WBRT.

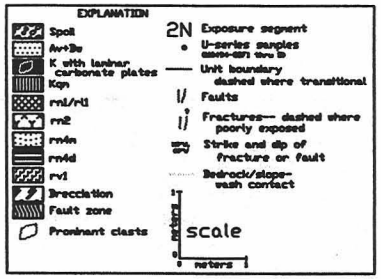

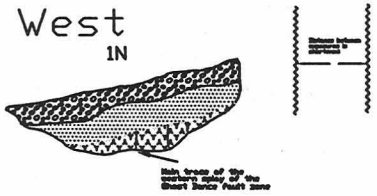

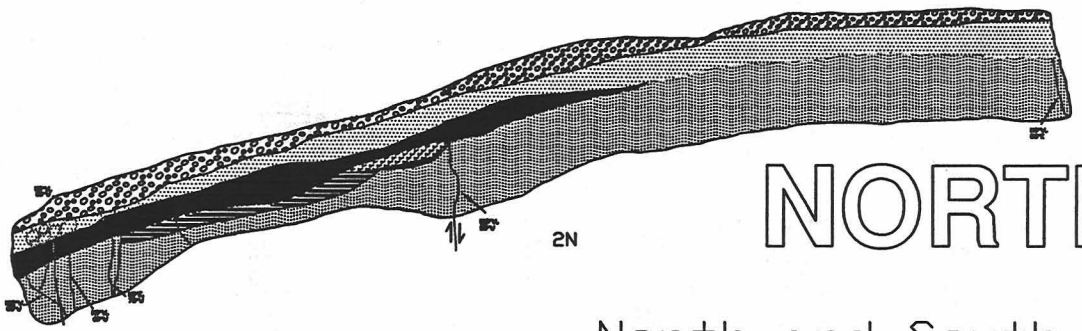

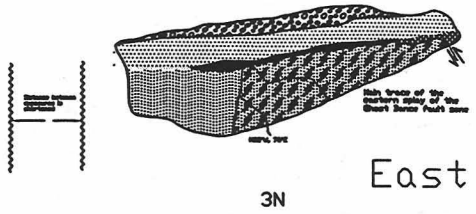

NORTH WALL

North and South Walls of the Whale Back Ridge trench, Ghost Dance fault zone, Yucca Mountain

E.M. Taylor, C.S. de Fontaine, D.C. Buesch,

B.O. Mundo, C.M. Menges and Michele Murray

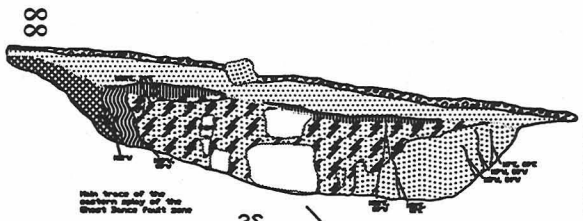

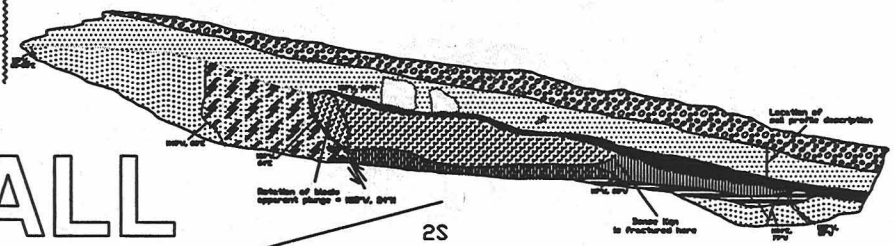

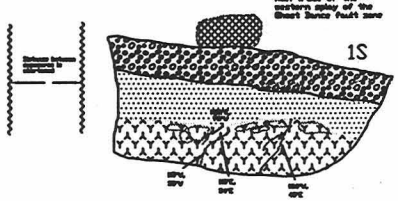

East

West

SOUTH WALL

Logs on next page

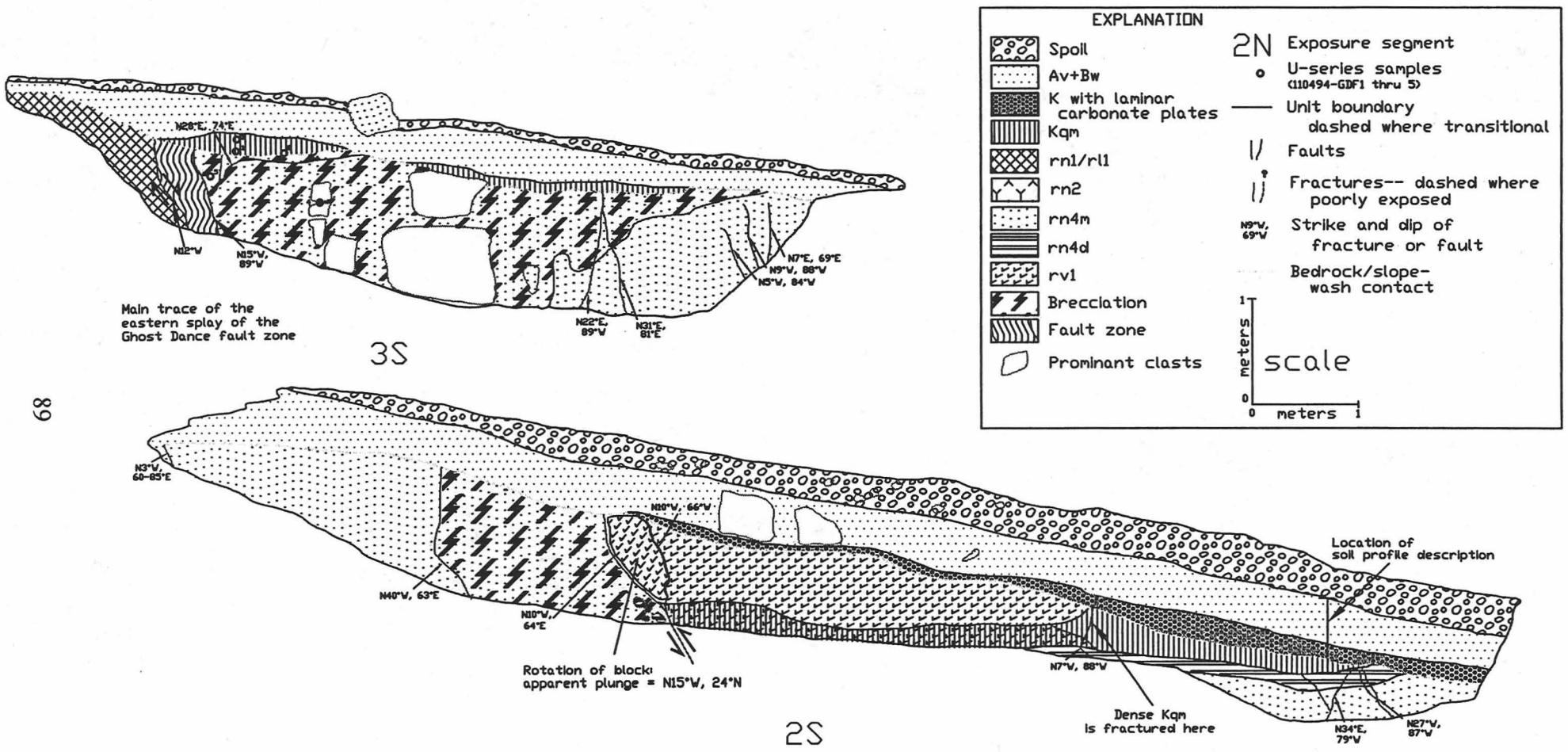
EXPLANATION
Spoil
Av+Bw
K with laminar carbonate plates
Kqm
rn1/rl1
rn2
rn4m
rn4d
rv1
Brecciation
Fault zone
Prominant clasts
2N Exposure segment
U-series samples (110494-GDF1 thru 5)
Unit boundary dashed where transitional
Faults
Fractures-- dashed where poorly exposed
N9°W, 69°W Strike and dip of fracture or fault
Bedrock/slope-wash contact
meters
scale
0
1
N28°E, 74°E
N12°W
N15°W, 89°W
N7°E, 69°E
N9°W, 88°W
N5°W, 84°W
N22°E, 89°W
N31°E, 81°E
Main trace of the eastern splay of the Ghost Dance fault zone
3S
N3°W, 60-85°E
N10°W, 66°W
N40°W, 63°E
N10°W, 64°E
Rotation of block apparent plunge = N15°W, 24°N
Location of soil profile description
N7°W, 88°W
Dense Kqm is fractured here
N34°E, 79°W
N27°W, 87°W
2S

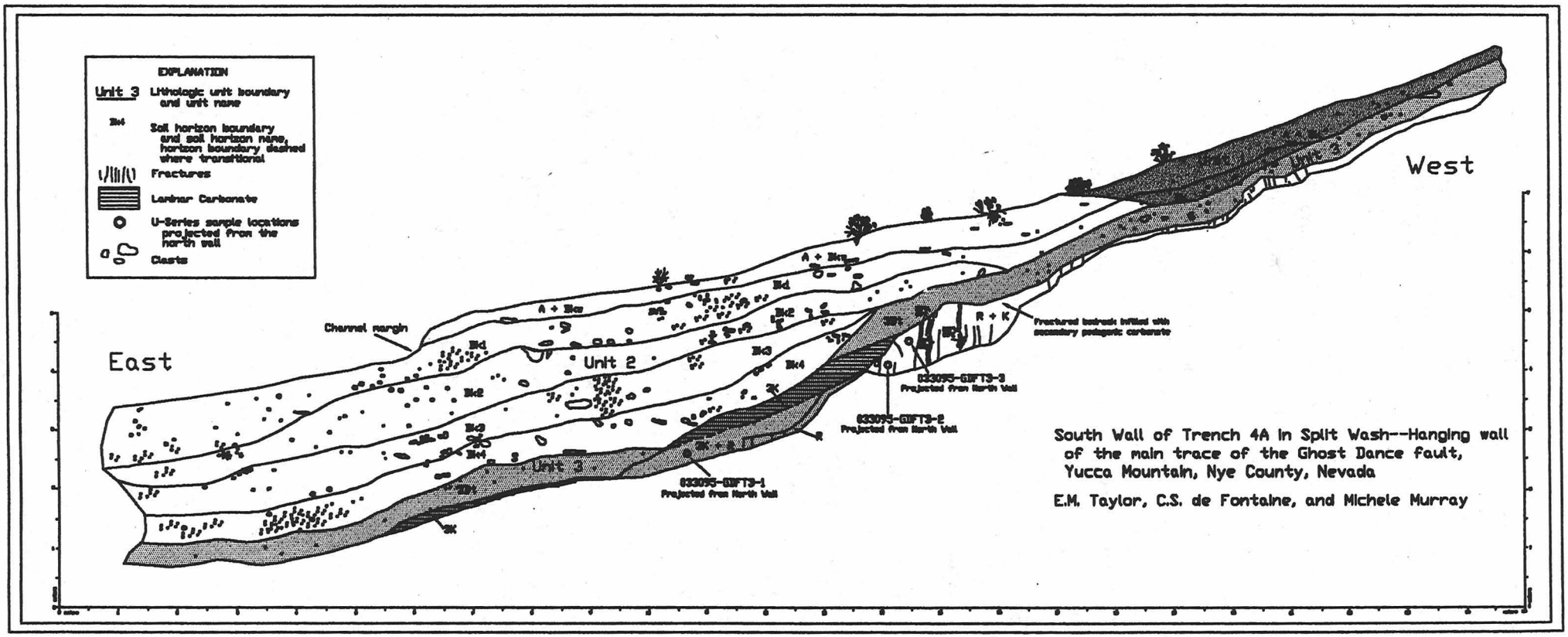
EXPLANATION
Unit 3 Lithologic unit boundary and unit name
Bk4 Soil horizon boundary and soil horizon name, horizon boundary dashed where transitional
Fractures
Laminar Carbonate
U-Series sample locations projected from the north wall
Clasts
West
East
Channel margin
Unit 2
Unit 3
A + Bkq
Bkd
Bk1
Bk2
Bk3
Bk4
Bkm
2K
R + K
Fractured bedrock infilled with secondary pedogenic carbonate
023095-GIFT3-3
Projected from North Wall
023095-GIFT3-2
Projected from North Wall
023095-GIFT3-1
Projected from North Wall
South Wall of Trench 4A in Split Wash--Hanging wall of the main trace of the Ghost Dance fault, Yucca Mountain, Nye County, Nevada
E.M. Taylor, C.S. de Fontaine, and Michele Murray

References Cited

Day, W.C., Potter, C.J., Sweetkind, D., Dickerson, R.P., and San Juan, C.A., 1998, Bedrock geologic map of the Central Block area, Yucca Mountain, Nye County, Nevada: U.S. Geological Survey Miscellaneous Investigations Map I-1601, scale 1:6,000, with text, 15 p.

Frizzell, V.A., Jr., and Shulters, Jacqueline, 1990, Geologic map of the Nevada Test Site, Nevada: U.S. Geological Survey Miscellaneous Investigations Map I-2046, scale 1:100,000.

Gosse, J.C., Harrington, C.D., and Whitney, J.W., 1996, Applications of in situ cosmogenic nuclides in the geologic site characterization of Yucca Mountain, Nevada: Materials Research Society Symposium, v. 412, p. 799-806.

Menges, C.M., Wesling, J.R., Whitney, J.W., Swan, F.H., Coe, J.A., Thomas, A.P., and Oswald, J.A., 1994, Preliminary results of paleoseismic investigation of Quaternary on eastern Yucca Mountain, Nye County, Nevada in Radioactive Waste Management Conference, 5th, Las Vegas, Nevada, April 1994, Proceedings: La Grange Park, Illinois, American Nuclear Society and American Society of Civil Engineers, v. 4, p. 2373-2390.

Piety, L.A., 1995, Compilation of known and suspected Quaternary faults within 100 km of Yucca Mountain: U.S. Geological Survey Open-File Report 94-112, 2 plates, scale 1:250,000.

Scott, R.B., 1990, Tectonic setting of Yucca Mountain, southwest Nevada, in Wernicke, B.P., ed., Basin and Range extensional tectonics near the latitude of Las Vegas, Nevada: Geological Society of America Memoir 176, p. 251-282

Scott, R.B., and Bonk, J., 1984, Preliminary geologic map of Yucca Mountain, Nye County, Nevada, with geologic section: U.S. Geological Survey Open-File Report 84-494, scale 1:12,000.

Simonds, F.W., Whitney, J.W., Fox, K.F, Ramelli, A.R., Yount, J.C., Carr, M.D., Menges, C.M., Dickerson, R., and Scott, R.B., 1995, Map showing fault activity of the Yucca Mountain area, Nye County, Nevada: U.S. Geological Survey Miscellaneous Investigations Series Map I-2520, scale 1:24,000.

Spengler, R.W., Braun, C.A., Linden, R.M., Martin, L.G., Ross-Brown, D.M., and Blackburn, R.L., 1993, Structural character of the Ghost Dance fault, Yucca Mountain, Nevada: Proceedings of the Fourth International Conference, High-Level Radioactive Waste Management, p. 653-659.

U.S. Department of Energy, 1988, Site characterization plan: DOE/RW-0199, Office of Civilian Radioactive Waste Management, Washington, D.C.

Day 1, Stop 6

Origin of secondary carbonate and opaline silica exposed in trench 14 on the Bow Ridge Fault, Yucca Mountain, Nevada

Emily M. Taylor and Heather Huckins Gang

Introduction

Trenches were excavated in the Yucca Mountain region as part of the Yucca Mountain Site Characterization Project. Trench 14, which was excavated across the Bow Ridge Fault on the west side of Exile Hill, exposes nearly vertical veins containing calcium carbonate, opaline silica, and fine-grained sediments. Although the original purpose of the excavation of trench 14 was to evaluate the nature and frequency of Quaternary movement on the Bow Ridge Fault, concern arose as to whether the calcium carbonate-enriched deposits at and adjacent to the fault zone were deposited by springs. Spring deposits of Quaternary age would indicate that water, in the recent geologic past, had reached the surface from below.

From east to west, trench 14 exposes (1) fractured volcanic tuffs; (2) a main fault zone marked by discrete nearly vertical veins within brecciated bedrock; and (3) colluvium and slope-wash alluvium. The brecciated bedrock has been locally recemented by secondary calcium carbonate and opaline silica, especially within the main fault. The fault zone is filled by a prominent mass of banded calcium carbonate and opaline silica veins, that is about 2.5 meters wide on the north wall and splays into a zone about 4 meters wide, consisting of five main veins, on the south wall. The well-cemented slope-wash alluvium adjacent to the main fault is sandy and contains a large component of angular rock fragments. Coarser colluvial deposits, which are present adjacent to the bedrock scarp located at the base of the slope-wash alluvium, pinch out west of the main fault. Soil formed in the slope-wash alluvium has a well-developed K horizon that is cemented by secondary calcium carbonate and opaline silica. The slope-wash alluvium and veins are unconformably overlain by a finer grained depositional unit consisting of slope wash and eolian sand and silt.

Physical, chemical, mineralogic, biologic, petrographic, and isotopic data were collected to determine the origin of the calcium carbonate and opaline silica in the veins and slope-wash alluvium. These data were used to determine general properties that are characteristic of pedogenic deposits. The colluvial deposit is laterally persistent, the concentration of secondary calcium carbonate decreases with depth below a maximum concentration, and discrete soil horizons are present. The initial deposition of calcium carbonate occurs on the underside of clasts, and the clasts within the deposit have been displaced by the precipitation of the secondary calcium carbonate and are no longer in clast-to-clast contact. The calcium carbonate in the veins and in the slope-wash alluvium contains ooids, primarily opal-CT, and sepiolite; it is well stratified and has a microcrystalline crystallitic b-fabric. Opaline silica concentrations in the veins and slope-wash alluvium are typical of pedogenic duripans, not silcretes. Oxygen, lead, strontium and uranium, isotopic data indicate that the calcium carbonate in trench 14 were precipitated from meteoric water rather than ground water. Carbon isotopic data indicate that the meteoric water had equilibrated with root-zone carbon dioxide. No ostracodes, which are characteristic of spring deposits, have been found. Therefore, the calcium carbonate and opaline silica present in the veins and in the slope-wash alluvium in trench 14 are most likely products of

pedogenic processes. The calcium carbonate is primarily from wind blown dust that moves in solution and has been precipitated from downward percolating meteoric water, rather than originating from ground water.

Conspicuously well-laminated calcium carbonate and opaline silica have been deposited along the fault plane in trench 14. Because the unconsolidated sandy slope-wash alluvium could not support an open fracture very long, these laminae probably record episodes of opening and incremental filling of fractures that developed along the Bow Ridge Fault. However, each lamina probably does not record a single fracturing event. The fault zone and fractures contain a tentatively dated black ash that is chemically indistinguishable from ashes derived from the Crater Flat cinder cones and thought to be 1.1 and 1.3 millions of years old, and the Lathrop Wells Cone dated from 70,000 to 80,000 years old. The ash-filled fractures are crosscut in places by fractures that contain fine-grained sediments and secondary calcium carbonate, and they are the only fractures that extend through the platy K soil horizon. The ash is probably coeval with one of the most recent fracturing events recorded in the trench. The ash-filled fractures also indicate that tectonic events produced open fractures that were subsequently filled by pedogenic translocation of calcium carbonate, opaline silica, and fine-grained sediment, rather than these deposits resulting from action of ground water.

Two general azimuth orientations are observed in the fractures in trench 14. About 85 percent of the bedrock fractures are oriented northwest; the remainder in the bedrock and all the fractures in the slope-wash alluvium are oriented northeast.

Quaternary deposits exposed in trench 14

In trench 14, locally derived, sandy slope-wash alluvium is downfaulted against volcanic bedrock of Miocene age along a near-vertical fault zone (Taylor and Huckins, 1995). This unit was originally described by Swadley and others (1984) as a fluvial sand sheet (Q2s). The current stratigraphy would correlate this deposit to Q3. The slope-wash alluvium contains from 5 to 25 percent gravel. The nearest and, therefore, most likely source of the boulders is the bedrock slope of Exile Hill, east of trench 14. Alternatively, the boulders may have been transported northward to their present position during building of the northern salient of the fan at the mouth of Drill Hole Wash, 1.5 km to the southwest. A soil profile within the slope-wash alluvium was described, sampled, and analyzed in detail (fig. 1, tables 1, 2 and 3). The ages of the Quaternary deposits vary according to the dating technique involved, however the exposed alluvial/colluvial deposit is probably correlative to a sandy facies of stratigraphic mapping unit Q3 thought to be 90-130 ka. Recent U-series analyses of secondary carbonate sampled from trench 14 are consistent with these estimates.

Figure 1. Log of Trench 14

Table 1. Field description of a characteristic soil exposed in the slope-wash alluvium in trench 14.

Table 2. Selected grain-size data, bulk density, and calcium carbonate content from a characteristic soil exposed in the slope-wash alluvium in trench 14.

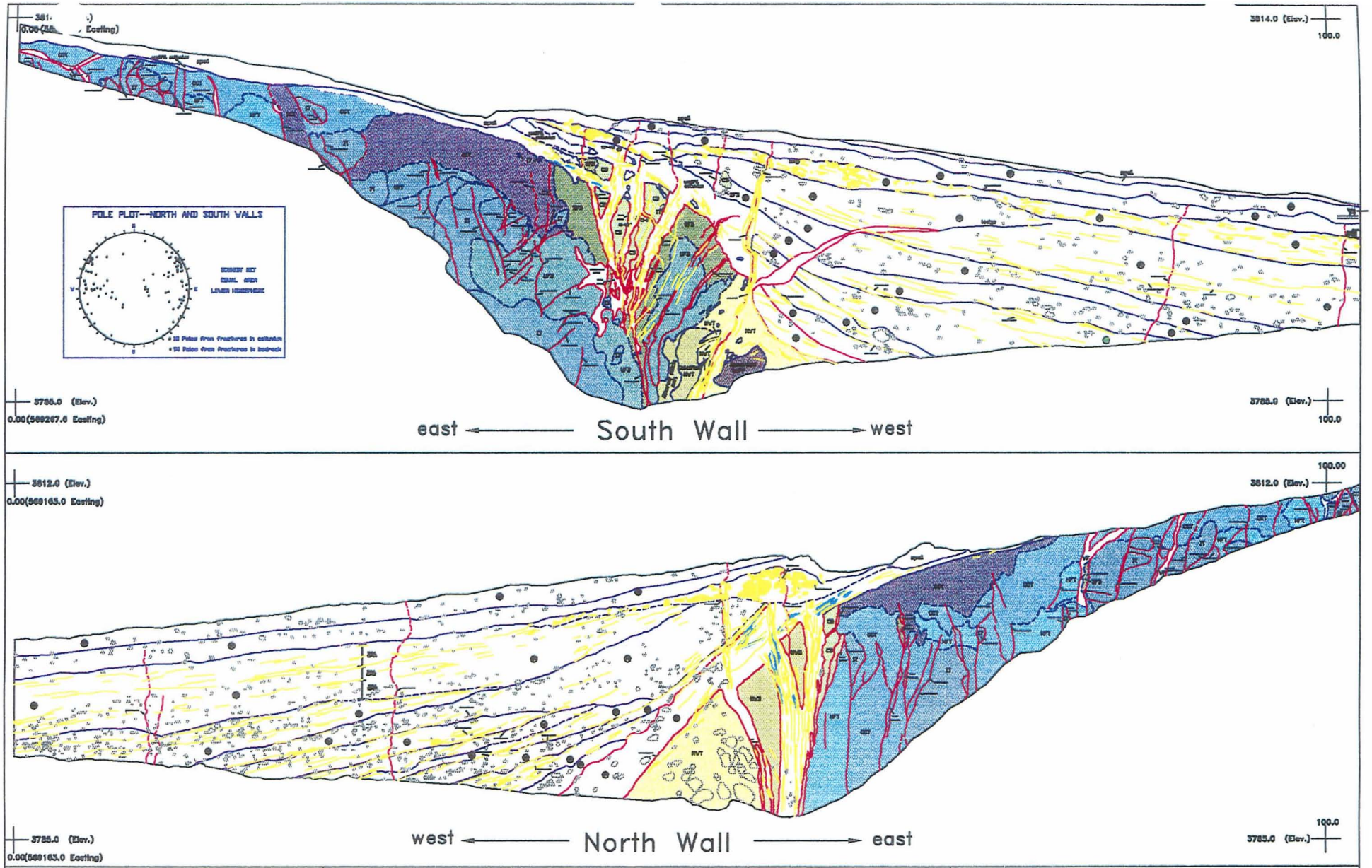

Compiled by photogrammetric methods from close-range photographs taken July, 1989 and March, 1992

Survey control by Raytheon Services, Nevada

Photography by Johnson Controls

Orthographic Projection – Three dimensional data projected onto vertical planes striking 272° (south wall) and 92° (north wall)

Plane Origins (Nevada State Plane Coordinate System)
South wall – 569267.6 Easting and 755448.4 Northing
North Wall – 569163.0 Easting and 755457.5 Northing

Scale 1:30

10 Feet

3 Meters

GEOLOGIC SECTION SHOWING THE BEDROCK AND DEPOSITIONAL UNITS EXPOSED ON THE SOUTH AND NORTH WALLS OF TRENCH 14 ON THE BOW RIDGE FAULT AT EXILE HILL, NYE COUNTY, NEVADA

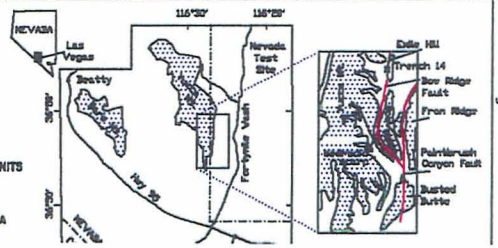

EXPLANATION

LITHOLOGIC UNIT BOUNDARIES—Solid line where contact is clear, dashed were inferred

SELECTED CLASTS

LITHOLOGIC UNIT DESIGNATION

CELLULAR VOIDS—Including undifferentiated cellular; N and S designate north and south walls

CALCIUM CARBONATE STRINGERS

CALCIUM CARBONATE PLATELETS

OPALINE SILICA STRINGERS

FRACTURES AND FAULTS—dashed were inferred or concealed

FRACTURE, FAULT, AND DIKE/SILL ORIENTATIONS—strike and dip direction are measured in degrees

URANIUM-SERIES sample

URANIUM-THORIUM sample— approximate location

FAULT ZONE—BRECCIA AND VEIN FILLING

TERTIARY VOLCANIC ROCKS

- HVT—Highly fractured welded tuff
- Reworked tuff
- IT—Slightly-fractured Inlet Tuff Canyon Member of the Paintbrush Tuff
- HVT—Highly-fractured Tiva Canyon Tuff
- CCT—Carbonate-cemented and fractured Tiva Canyon Tuff
- DCT—Densely carbonate-cemented and fractured Tiva Canyon Tuff

Table 1. Field description of a characteristic soil exposed in the slope-wash alluvium in trench 14

[Units and soil horizons are shown on plates 5 and 6 and figure 5. Horizon boundaries (hzn bnd)--as, abrupt smooth; aw, abrupt wavy; cw, clear wavy; and dashes, no data. Textual classes (based on grain size analyses)--SL, sandy loam; LS, loamy sand. Structure--(1) Grade--2, moderate; 3, strong; m, massive; m-sg, massive to single; (2) Strength--m, medium; co, coarse; vco, very coarse; and (3) Kind--sbk, subangular blocky; pr, prismatic; pl, platy; abk, angular blocky. Dry consistence--so, soft; sh, slightly hard; h, hard; eh, extremely hard. Wet consistence--so, nonsticky; ss, slightly sticky; s, sticky; po, nonplastic; ps, slightly plastic. CaCQ matrix--e, slightly effervescent; es, strongly effervescent; ev, violently effervescent. cm, centimeters; %, percent; <, less than; dashes (--), no data]

SOIL HORIZON	DEPTH (cm) TOP	BASE	HZN BND	COLOR [1] DRY	MOIST	TEXTURE	STRUCTURE	CONSISTENCE DRY	WET	$CaCO_3$ [2] MATRIX	STAGE	% GRAVEL VOLUME	SiO_2 [3] STAGE
							UNIT 1 [4]						
Av	0	9	as	10YR 6/3	10YR 4/3	SL	3 co sbk	so	ss,ps	0	0	10	0
Btk	9	20	aw	10YR 6/3	10YR 4/3	SL	2 co sbk	so	ss+,ps	es	I	25	0
							UNIT 2 [5]						
2Btj	20	50	cw	10YR 5.5/4	10YR 3.5/4	SL	2-3 m-co pr, 2 co sbk	h	s,ps	e-es	I	5	0
2B+K	50	61	as	10YR 6/3.5	10YR 6/3.5	SL	2 m sbk	sh	ss,ps	es, ev in K	5-20	0	
							UNIT 3 [6]						
3Kmq1	61	77	aw	10YR 8/0	10YR 8/2	LS	3 vco pl	eh	so,po	ev	IV	5	4
3Kmq2	77	119	aw	10YR 8/2	10YR 8/3	LS	3 vco pl, m	eh	so,po	ev	IV, 50 % ooids	10	4 (<5 mm) 10YR 7/3(dry), 7/4(moist)
3Kq	119	138	as	10YR 8/0	10YR 8/2	SL	m	eh	so,po	ev	III	5	3, 4 in places
3Bkq1	138	202	aw	10YR 8/2	10YR 5/3	LS	2 co abk, m-sg	so	so,po	ev	II dense, III lenses, ooid lenses	25	2, 3-4 in places
3Bkq2	202	247	--	10YR 7.5/2	10YR 5/3	LS	m-sg	so	so,po	ev	II, III lenses, ooid lenses	10	2-3

[1] $CaCO_3$ stages from Gile and others (1966).
[2] SiO_2 stages from table 1.
[3] Colors are from the Munsell soil color charts (1954).
[4] Parent material is slope-wash alluvium and fine-grained eolian sand and silt.
[5] Parent material is slope-wash alluvim with 5 percent K plates derived from Unit 3.
[6] Parent material is fine-grained slope-wash alluvium

Table 2. Selected grain-size data, bulk density, and calcium carbonate content from a characteristic soil exposed in the slope-wash alluvium in trench 14

[Units and soil horizons are shown on plates 5 and 6 and figure 5. Values for sand, silt, and clay are based on sieve and pipette analyses. Particle-size limits--sand 2-0.05 millimeters; silt, 0.05-0.002 millimeter; clay, less than 0.002 mm. Textural classes--vco, very coarse; co, coarse; med, medium; fi, fine; vfi, very fine. cm, centimeter; gm/cm^3, grams per centimeter cubed; NA, not applicable]

SOIL HORIZON	DEPTH (cm) top	base	PERCENT SAND vco	co	med	fi	PERCENT SILT vfi	co	PERCENT CLAY m + fi	vfi	co + m	fi	TOTAL (percent) SAND	SILT	CLAY	DENSITY (gm/cm^3)	$CaCO_3$ (percent)
									UNIT 1								
Av	0	9	2.45	2.94	6.09	42.45	18.85	5.77	8.84	5.41	4.51	2.71	72.77	20.01	7.21	1.63	0.46
Btk	9	20	2.34	2.45	4.90	33.71	19.99	9.56	9.56	4.78	8.64	4.05	63.40	23.91	12.69	1.69	1.22
									UNIT 2								
2Btj	20	50	1.54	1.96	5.45	38.08	17.74	8.40	11.80	5.54	6.79	2.68	64.77	25.75	9.48	1.67	0.34
2B+K (B)	50	61	1.75	2.07	5.85	39.99	17.65	8.08	11.32	4.49	5.92	2.87	67.32	23.89	8.80	1.65	2.37
(K)	50	61	28.13	15.71	11.34	16.92	6.72	3.85	4.92	3.42	4.49	4.49	78.82	12.20	8.98	1.34	33.05
									UNIT 3								
3Kmq1	61	77	13.21	10.41	11.57	32.69	9.92	4.11	6.99	3.29	3.91	3.91	77.80	14.38	7.81	1.62	40.12
3Kmq2	77	119	13.76	12.03	14.51	32.67	9.67	4.18	5.23	3.14	0.63	4.18	82.63	12.56	4.82	1.66	45.92
3Kq	119	138	12.46	11.78	14.96	28.10	9.14	4.35	7.09	3.66	2.74	5.72	76.45	15.09	8.46	1.46	56.14
3Bkq1	138	202	4.66	4.24	9.44	44.87	16.01	5.85	5.85	2.42	3.63	3.03	79.22	14.12	6.66	1.73	26.81
3Bkq2	202	247	6.37	4.86	7.94	49.02	14.14	3.64	5.47	2.55	4.01	2.00	82.32	11.67	6.01	1.55	23.56
									CALCIUM CARBONATE FRACTURE FILL FROM BEDROCK								
NA	NA	NA	26.88	16.55	11.59	12.77	7.73	4.26	8.25	2.92	1.33	7.72	75.52	15.43	9.05	NA	69.41
									MATERIAL FROM VEIN III CONTAINING BASALTIC ASH (D15S [1])								
NA	NA	NA	2.60	3.99	11.89	60.40	11.15	2.20	1.32	2.20	1.90	2.34	90.03	5.72	4.25	NA	23.69

[1] Location on the south wall of trench 14, plate 4.

Table 3. Dominant physical characteristics and percentges of calcium carbonate in the deposits exposed in trench 14.

Three distinct lithologic units are present in the slope-wash alluvium at the surface of the trench where the modern soil is developed--units 1, 2, and 3. The slope-wash alluvium has been divided into nine soil horizons based on the morphology of secondary carbonate and opaline silica (table 1), and the amount of secondary clay (table 2). Soil formed in the slope-wash alluvium is characterized by a well-developed K horizon (stage III and IV) that is cemented by secondary carbonate and opaline silica. The sandy slope-wash alluvium (unit 3) and the veins are unconformably overlain by two fine-grained depositional units consisting of slope wash and eolian sand and silt (units 1 and 2).

In the following discussions of the units, colors refer to the <2-mm particle-size fraction, unless otherwise stated. Soil textures refer to the <2-mm fraction in which secondary carbonate, opaline silica (where present), and organics have been removed.

Unit 1

Unit 1 is a pale brown (10YR 6/3), gravelly silty sand, with a soft consistence. It contains moderately sorted, subangular to subrounded sand, and less than 30 percent angular to subrounded pebble-cobble gravel. Unit 1 appears to be mostly eolian, based on the uniform sorting, particle size distribution, and lack of coarse gravel (table 2 and 3). Secondary carbonate forms thin coatings on the underside of pebbles. The basal contact is wavy. This unit is correlated, on the basis of its stratigraphic position and its physical and chemical properties, with similar deposits in the Yucca Mountain region which are dated or inferred to be latest Pleistocene to early Holocene (Taylor, 1986). Within unit 1, there are two discrete soil horizons--Av and Btk (tables 1, 2 and 3)

Unit 2

Unit 2 is a light yellowish brown to yellowish brown (10YR 5-6/4), compact, silty sand, and contains from 5 to 20 percent angular to subangular pebble-cobble gravel. The sand is moderately sorted, and subangular to subrounded. Near the base of unit 2, indurated plates from unit 3, which are cemented by secondary carbonate and opaline silica, have been reworked into the fine-grained matrix. Unit 2 is late Pleistocene in age. Unit 2 pinches out downslope. Within unit 2 there are two discrete soil horizons--2Btj and 2B+K.

Unit 3

Unit 3 is a white to light gray (10YR 7-8/0-2), moderately well- to well-sorted sand to silty sand, pebble-cobble gravel, and contains rare boulders. The consistence is from soft to extremely hard where the unit is indurated by secondary carbonate and opaline silica. The sandy matrix is weakly to well cemented. Carbonate along fracture surfaces is common.

Unit 3 can be correlated on the basis of physical and chemical characteristics to a sand sheet unit, unit Q2s, described by Hoover and others (1981). Ash of the Bishop Tuff is present in several places at or near the base of unit Q2e, an eolian unit from which the sand sheets were derived. The presence of this ash places a constraint of <740 ka on the age of Q2s and unit 3.

Table 3. Dominant physical characteristics and percentages of calcium carbonate in the deposits exposed in trench 14D

[Units and soil horizons are shown on figure 14. Textual classes (based on grain size analyses)--SL, sandy loam; LS, loamy sand; S, sand. Structure--(1) Grade--1, weak; 2, moderate; 3, strong; (2) Strength--n, thin or very fine; f, fine; m, medium; co, coarse; vco, very coarse; and (3) Kind--sbk, subangular blocky; pr, prismatic; pl, platy; abk, angular blocky. Dry consistence--lo, loose; so, soft; sh, slightly hard; h, hard; eh, extremely hard. Clay films--(1) Frequency--1, few; (2) thickness--mk, moderately thick; k, thick; (3) location--pf, ped face. %, percent; <, less than; >, greater than; cm, centimeter; m, meter; dashes (--), no data]

Soil Hzn	Thickness Cm	Color Dry	Color Moist	Percent Sand	Percent Silt	Percent Clay	Texture	Structure	Dry Con	Clay Films	$CaCo_3$ Stage	$CaCo_3$ Percent	Gravel Percent	Parent Material	Miscellaneous
										UNIT 1D					
Av	4-12	10YR 6.5/2	10YR 4/3	--	--	--	SL	2 m-co sbk	sh	0	0	0	<5	eolian	best preserved E side of fault, disturbed in fracture zone
										UNIT 2D					
Ab	5-17	10YR 6/3	10YR 4/3	--	--	--	SL	3 n pl	so-sh	0	0	0	<10	eolian	dominantly roots, thickens downslope on west
2Bk	5-17	10YR 6.5/3	10YR 5/4	66.5	23.0	9.9	SL	f sbk	so	0	I-II	1.42	60	slope-wash alluvium	weakly cemented, dominantly gravel clasts 6-10 cm, thins and disappears downslope
										UNIT 3D					
3Bkq	25-40	10YR 6/4 7.5YR-10YR 8/0 (carb)	10YR 4/4	77.7	17.0	5.0	LS	2-3 vco pl vco sbk	eh	0	I	1.90	<10	slope-wash alluvium	few Mn stains on ped faces, Stage 3 silica cementation?
										UNIT 4D					
4Btk (W side of fault)	30-40	7.5YR 5.5/4	7.5YR 5/5	84.6	11.4	4.0	LS-S	f-m abk-sbk	h-eh	1 mk pf	I-II	0.30	70-80 wedge	colluvial mod well sorted,	Mn stains on gravel & ped face, poorly bedded, thins & disappears W in approx 4 m
										UNIT 5D					
5Btk1 (E side of fault)	18-38	7.5YR 6/6	7.5YR 5/6	59.8	27.7	12.5	SL	f pr f-m sbk 1 pl (top of hz)	h-eh	mk-k pf	I pinches out toward fault	0.73	50-60	colluvium/ debris flow	very common Mn stains
5Btk2 (E side of fault)	20-25	7.5YR-10YR6-7/4	7.5YR 5/4	71.4	21.2	7.4	SL	1 pr f-co sbk	eh	mk pf I in matrix	II-II+	0.56	50-60	colluvium/ debris flow	very common Mn staining on gravel and matrix
5Btk3 (E side of fault)	15-43	7.5YR 6.5/4	7.5YR 4/4	77.9	17.2	4.0	LS	m-co abk-sbk 1 pl (in places)	h-eh	0	II stringers of III	1.40	50-60	colluvium/ debris flow	common Mn staining, poorly sorted, dominantly gravel clasts >6 cm

Soil Hzn	Thickness Cm	Color Dry	Moist	Percent Sand	Silt	Clay	Texture	Structure	Dry Con	Clay Films	$CaCo_3$ Stage	Percent	Gravel Percent	Parent Material	Miscellaneous
										UNIT 6D					
6Btk (W side of fault)	30-35	7.5YR-10YR 7/4	7.5YR 5/4	83.3	11.2	5.5	LS	f pr f-m abk	h-eh	0	I-II co pf	0.72	<5	slope-wash alluvium	few Mn stains on ped faces
										UNIT 7D					
7K	>50	7.5YR 7/4 10YR 8/0 (carb)	--	87.0	9.8	3.3	S	m co sbk	lo-eh	0	III stringers up to 10 cm wide; I, III adj. to fault	6.30	<10	slope-wash alluvium	poorly sorted, poorly bedded

Unit 3 yields ages of 88±5 ka (D.R. Muhs, U.S. Geological Survey, written commun., 1989). The uppermost part of unit 3 (3Kmq1) has a U-series age of 88±5 ka, indicating a long and continuous period of horizon formation since deposition. Over time, continuous translocation of carbonate and its reprecipitation at depth tend to plug horizons, forcing them to grow upward; as a result, the progressively younger ages toward the surface of the maximally developed K horizon of unit 3 indicate a long and continuous period of soil formation. An opaline silica band, which is in the maximally developed K horizon above the main fault zone and which continues into the slope-wash alluvium is dated at >350, >440, >400, and >550 ka or is older than the sensitivity of the U-series technique. Within unit 3, there are five discrete soil horizons--3Kmq1, 3Kmq2, 3Kq, 3Bkq1 and 3Bkq2

Colluvium

The depositional stratigraphy can be subdivided on the north wall of trench 14 into 12 colluvial units, and on the south wall into 10 colluvial units. These units can be correlated across the wall, however two units described on the north wall are not present on the south wall (table 4). Colluvial units are white to light yellowish brown (10YR 8/0-10YR 6/4), soft to hard where cemented by carbonate and opaline silica, poorly sorted, and poorly bedded sand to silty sand pebble-cobble gravel. There is more massive secondary carbonate on the south wall, than on the north wall. The porous nonwelded tuff is not as close to the surface on the south wall, less infiltration occurs into the bedrock, and carbonate that does infiltrate is not masked by the white nonwelded tuff. The gravel content grades from about 5 to 80 percent as depth increase. The matrix is a weakly to well-cemented sand to loamy sand.

Table 4. Colluvial and alluvial unit discriptions for the north and south walls of Trench 14.

The dip of the depositional packages decreases, or flattens, toward the surface of the exposure, suggesting a nontectonic origin for the colluvial units. The fabric, defined by bedding and subparallel stringers and laminae of carbonate and opaline silica, dips 30-60° SW in the basal colluvium and 8-10° SW in the upper colluvium. A few of the colluvial units and fissure fillings have been dated by uranium-series analyses.

Colluvial units 1N and 1S are composed primarily of nonwelded tuff in a fine-grain matrix, with a few clasts of intact Tiva Canyon Tuff. Within this unit there are common Mn oxide stains. Colluvial units 2N-12N and 2S-10S are composed of locally derived sandy slope-wash and angular to subrounded gravel. Units 10N (8S), 11N (9S), and 12N (10S) are comparable to unit 3, unit 2, and unit 1, respectively, in Taylor and Huckins (1995).

Origin of Secondary Calcium Carbonate and Opaline Silica

The abundance of secondary carbonate and opaline silica in the slope-wash alluvium and veins has drawn the attention of many people who have seen the exposures in trench 14. Concern arose as to whether these materials were deposited from infiltrating meteoric water or from upwelling ground water or perched water. Translocation of carbonate and opaline silica by infiltrating meteoric water result from pedogenic processes that are described more fully below.

Table 4. Colluvial and alluvial unit discriptions for the north and south walls of trench 14. Generally the dip of the bedding and and he coarseness of the gravel increases with depth. There is more secondary carbonate cement on the south than the north wall, probably because the more porous NWT is not as close to the surface and less infiltration occurs on the south wall. The massive carbonate makes it difficult to distinguish the depositional packages on the south wall. Colluvial wedges 1N and 1S are composed primarily of NWT in a fine-grain matrix, with a few clasts of IT. Within this unit there are common Mn stains. Units 10N (8S), 11N (9S), and 12N (10S) are comparable to Unit 3, Unit 2 and Unit 1 respectively in Taylor and Huckins (1993). Texture of the less than 2 mm fraction is loamy sand.

South Wall of Trench 14

Colluvial or alluvial wedge (basal contact) Correlative unit on the north wall	Matrix color--dry (d) and moist (m)	Gravel percent, size, and angularity	Compaction/ consolidation, clast/matrix supported	Sorting, bedding orientation, and imbrication	Calcium carbonate--dissiminated (diss), effervescence violently (ev)	Opaline silica
1S (diffuse to bedrock) 1N	10YR 8/0 (d) 10YR 6/3 (m)	50%, ≤10 cm, subrounded-rounded	Well cemented, matrix supported	Mod-well sorted, nonbedded, avg dip 29° SW	Dominated by carbonate matrix forming plates up to 15 cm, diss, ev	Common stringers
2S (abrupt) 2N	10YR 8/2 (d) 10YR 6.5/4 (m)	70%, ≤20 cm, few clasts ≤45 cm, subangular-subrounded	Well cemented, matrix supported	Mod-well sorted, nonbedded, avg dip 33° SW, well imbricated	Lenses of ooids, ev	Common stringers
3S (clear) 3N	10YR 8/2 (d) 10YR 7/3 (m)	20%, ≤15 cm, subangular-subrounded, parts are gravel free	Well cemented, matrix supported	Mod-well sorted, nonbedded, avg dip 27° SW	Lenses of ooids, very few stringers	Few stringers 1-2 cm
4S (clear) 4N	10YR 8/3 (d) 10YR 5/3 (m)	50%, ≤5 cm, few clasts ≤15 cm, subangular-angular	Well cemented, matrix supported	Mod-well sorted, nonbedded, avg dip 22° SW, well imbricated	Common thin stringers, lenses of ooids	--
5S (clear) 7N	10YR 8/2 (d) 10YR 5/3 (m)	20%, ≤7 cm, angular-subrounded	Well cemented, matrix supported	Mod-well sorted, nonbedded avg dip 22° SW	Dominated by stringers	--
6S (gradual) 8N	10YR 8/2 (d) 10YR 5.5/3 (m)	40%, ≤7 cm, few ≤30 cm, subangular- subrounded	Mod cemented, matrix supported	Mod-well sorted, nonbedded, avg dip 13° SW	Very few stringers, some contain ooids	--
7S (clear) 9N	10YR 7.5/2 (d) 10YR 6/3 (m)	50-60%, ≤5 cm, few clasts ≥10 cm, subangular-subrounded	Weakly cemented, matrix supported	Mod-well sorted, nonbedded, avg dip 8° SW	Dominated by stringers, up to 40% of unit	--

Colluvial or alluvial wedge (basal contact) Correlative unit on the north wall	Matrix color--dry (d) and moist (m)	Gravel percent, size, and angularity	Compaction/ consolidation, clast/matrix supported	Sorting, bedding orientation, and imbrication	Calcium carbonate--dissiminated (diss), effervescence violently (ev)	Opaline silica
8S (clear) 10N	10YR 8/0-2 (d) 10YR 2-3 (m)	5-10%, ≤5 cm, subangular- subrounded	Well cemented, matrix supported	Mod-well sorted, nonbedded	Dominated by carbonate plates, Stage IV, ≤50% ooid lenses	Stage IV
9S (abrupt) 11N	10YR 6/4 (d) 10YR 4/4 (m)	5%, ≤5 cm, subangular-subrounded	Wealky cemented-well cemented in carbonate plates, matrix supported	Well sorted, nonbedded	Fines includes reworded carbonate plates from 7S--Stage IV	--
10S (abrupt) 12N	10YR 6/3 (d) 10YR 4/3 (m)	10-25%, ≤5 cm, subangular- subrounded	Noncemented, matrix supported	Well sorted, nonbedded	Stage I on gravel clast	--
North Wall of Trench 14						
1N (diffuse to bedrock) 1S	10YR 8/0 (d,m)	80%, ≤25 cm, subangular-subrounded	Well cemented, matrix supported	Poorly sorted, nonbedded, avg dip 58° SW	common ooids and stringers, ev	Stringers 1-2 cm wide
2N (abrupt) 2S	7.5-10YR 8/2 (d) 7.5-10YR 5/3 (m)	80%, ≤22 cm, subangular	Well cemented, matrix supported	Poorly sorted, nonbedded, avg dip 34° SW	Stage I-II on gravel, common carbonate root casts on the surface of clasts, ev, diss	--
3N (clear) 3S	10YR 8/2 (d) 10YR 6/4 (m)	20%, ≤10 cm, subrounded	Well cemented, matrix supported	Mod-well sorted, nonbedded, avg dip 30° SW	Locally common ooids, springers up to 2 cm wide	--
4N (gradual) 4S	10YR 8/2 (d) 10YR 6/3.5 (m)	70-80%, ≤12 cm, subrounded	Well cemented-uncemented in places, matrix supported, locally clast supported	Mod sorted, nonbedded, avg dip 27° SW	Stage I on clasts, ev, diss	--
5N (gradual) not exposed on the south wall	10YR 7.5/2 (d) 10YR 5/3 (m)	50%, ≤7 cm, subrounded	Moderately well cemented, matrix supported	Mod-well sorted, nonbedded, avg dip 24° SW	Stage I on clast, ev, diss	--
6N (diffuse) not exposed on the south wall	10YR 7.5/2 (d) 10YR 5/3 (m)	70%, ≤10 cm, subrounded	Well cemented, matrix supported	Mod-well sorted, nonbedded, avg dip 20° SW	Stage I on clasts, ev, diss	--

Colluvial or alluvial wedge (basal contact) Correlative unit on the north wall	Matrix color--dry (d) and moist (m)	Gravel percent, size, and angularity	Compaction/ consolidation, clast/matrix supported	Sorting, bedding orientation, and imbrication	Calcium carbonate--dissiminated (diss), effervescence violently (ev)	Opaline silica
7N (gradual) 5S	10YR 8/2 (d and m)	20%, ≤5 cm, subrounded	Mod cemented, locally well cemented, matrix supported	Mod sorted, poorly bedded, avg dip 19° SW	Unit is dominated by carbonate stringers	Very thin laminae associated with carbonate stringers and base of ooid lenses
8N (gradual) 6S	10YR 8/2 (d) 10YR 6/3 (m)	30-50%, ≤25 cm, subrounded- subangular	Well cemented, matrix supported	Poorly sorted, non bedded, avg dip 11° SW	Few thin stringers ≤1 cm, diss, ooids in lenses	--
9N (clear) 7S	10YR 7/2 (d) 10YR 6/3 (m)	40%, ≤5 cm, subangular	Well cemented, matrix supported	Well sorted, little or no bedding, avg dip 8° SW	Common stringers	--
10N (clear) 8S	10YR 8/0-2 (d) 10YR 2-3 (m)	5-10%, ≤5 cm, subangular- subrounded	Well cemented, matrix supported	Mod-well sorted, nonbedded	Dominated by carbonate plates, Stage IV, ≤50% ooid lenses	Stage IV
11N (clear) 9S	10YR 6/4 (d) 10YR 4/4 (m)	5%, ≤5 cm, subangular-subrounded	Wealky cemented-well cemented in carbonate plates, matrix supported	Well sorted, nonbedded	Fines includes reworded carbonate plates from 7S--Stage IV	--
12N (abrupt) 10S	10YR 6/3 (d) 10YR 4/3 (m)	10-25%, ≤5 cm, subangular- subrounded	Noncemented, matrix supported	Well sorted, nonbedded	Stage I on gravel clast	--

Criteria for distinguishing pedogenic and non-pedogenic carbonate and opaline silica are summarized in table 5.

Table 5. General criteria for distinguishing nonpedogenic from pedogenic calcium carbonate and opaline silica.

Laminated carbonate and opaline silica deposits are common in sediments of Quaternary age throughout the arid and semiarid parts of the southwestern United States. The processes that form these deposits also form carbonate- and opaline silica-enriched soil horizons. Carbonate is leached from the surface and upper horizons of soils by downward-percolating meteoric water and subsequently precipitates in lower soil horizons at a depth controlled by soil moisture and texture (McFadden and Tinsley, 1985). Over thousands of years, calcium carbonate-rich horizons form from the continual translocation of Ca^{++} and the subsequent precipitation of carbonate. Soils in these sediments have variations in the concentration and morphology of these secondary constituents because of the combined effects of (1) the age of the soil; (2) the concentration and seasonal distribution of Ca^{++} and readily soluble silica in precipitation; (3) the initial carbonate and silica content of a deposit; and (4) the rate of influx of calcium- and silica-bearing eolian dust.

At Yucca Mountain, the soil parent material is chiefly silicic volcanic rock, containing little or no carbonate and only small concentrations of calcium. In this area, the calcium accumulated in soils is derived primarily from the influx of eolian dust (Gile and others, 1966, 1981; Bachman and Machette, 1977). Calcium is dissolved from the dust at and near the surface by percolating meteoric water. A small contribution to the carbonate may be derived from *in-situ* leaching of calcium from the parent material. Carbon dioxide is contributed by, or equilibrated with, CO_2 that is derived from the atmosphere through root respiration. The calcium and CO_2 are subsequently combined and precipitated as secondary carbonate at depth.

Secondary carbonate is concentrated at the bedrock-alluvium contact in trench 14 by increased runoff from the less-permeable bedrock that is upslope. The concentration of secondary carbonate decreases with distance from the bedrock-alluvium contact. Most of the runoff percolates into the near-vertical fractures (forming veins) in the Bow Ridge Fault zone bedrock, and into the slope-wash alluvium at the bedrock contact. The available moisture decreases downslope away from the bedrock-alluvium contact.

Pedogenic silica cementation is common in the soils in the Yucca Mountain region (Taylor, 1986). The morphology of opaline silica varies with age. Stages of development are listed in table 1. Opaline silica is common in soils that are developed in parent material containing readily soluble silica-rich glass, as is characteristic of pyroclastic rocks in the Yucca Mountain region. Eolian influx of readily soluble silica-rich dust also is a source of silica.

In general, two terms are used for soil layers cemented with opaline silica: (1) Duripan--specifically applied to pedogenic accumulations (Soil Survey Staff, 1975) and (2) silcrete--for more generic geologic accumulations (Summerfield, 1982, 1983; Nettleton and Peterson, 1983). Both terms are applied to an indurated product of surficial and near-surface silicification, formed by the cementation or replacement of bedrock, unconsolidated sediments, or soil. Duripans and silcretes are produced by low-temperature physiochemical processes and are not produced by

Table 5. General criteria for distinguishing nonpedogenic from pedogenic calcium carbonate and opaline silica

[%, percent; >, greater than; <, less than; <<, much less than; 1°, primarily]

Factor	Nonpedogenic	Pedogenic	Observed in trench 14
Geomorphology, spatial arrangements	Isolated points at or near springs, downslope of fractures or faults in bedrock or surficial deposits [1]	Follow topography and geomorphic surfaces, laterally persistent [2]	Laterally persistent in slope-wash alluvium
Location of the initial $CaCO_3$ and opaline SiO_2 deposition in a gravelly deposit [3,4]	Random orientation, gravel remains in contact (clast supported); bedding features may be preserved	Deposition on the underside of clasts; gravel does not remain in clast contact (matrix supported); bedding features lost or poorly preserved in advanced stages	Initial deposition on the underside of gravel, matrix supported; bedding features lost or poorly preserved
Physical characteristics of maximally developed $CaCO_3$	Discrete stratiform; mounded, or draped strata; commonly displaying vegetative molds and vugs [1]	Continuous laminar layers underlain by bedrock or a plugged horizon [2,3]	Continuous laminar layers that have formed plates [5]
Change in concentration of $CaCO_3$ and opaline SiO_2 with depth [1,2,4]	No systematic change, uniform deposition	Decreases with depth below a near-surface maximum	Decreases with depth below a near-surface maximum [6]
General distinguishing petrographic and mineralogic characteristics	High temp--no ooids [7]; 1° opal-C [8] Low temp--few ooids [7]; 1° opal-A [8] Both are poorly stratified [7] and have common sulfide, sulfate, and manganese minerals [7]	Ooids common [7]; usually opal-CT [8]; well stratified [7]; common smectitic and illitic clay minerals [9]	Ooids common; primarily opal-CT; well stratified; common smectitic and illitic clay minerals [7]
Ca:Mg ratio of clay minerals [2]	No systematic depletion of Mg^{++} over time when compared to $CaCO_3$ precipitation	Progressive depletion of Mg^{++} in comparison to the accumulation of secondary $CaCO_3$; formation of Mg-rich clays	Formation of Mg-rich clays including sepiolite and palygorskite [7]
$CaCO_3$ crystallinity and percent	Coarse sparry calcite crystals, microsparite, and sparite; crystals >99.5% pure [1]	Microcrystalline (micrite), crystallitic b-fabric [10]; commonly clay, $MgCO_3$, and opaline SiO_2 present; <<99.5% pure [11]	Microcrystalline, crystallitic b-fabric with clay and opaline SiO_2; <70% pure
Opaline SiO_2% and crystallinity [8,11]	Silcrete, >85% SiO_2, amorphous SiO_2 to coarsely crystalline quartz	Duripan, <<85% opaline SiO_2, amorphous	Duripan, <85% amorphous opaline SiO_2 [7]

Factor	Nonpedogenic	Pedogenic	Observed in trench 14
$\delta^{13}C$ vs $\delta^{18}O$ in $CaCO_3$ [12]; $\delta^{13}C$ is vegetation dependent and $\delta^{18}O$ is dependent on mineralization temperature of $CaCO_3$ and fluid source	Expected range within concentrations reported for spring deposited $CaCO_3$	Expected range within concentrations reported for pedogenic $CaCO_3$ [13]	Range within concentrations reported for pedogenic $CaCO_3$ [12,13]
δD vs $\delta^{18}O$ in $CaCO_3$ [12,14,15]	Shift in $\delta^{18}O$ concentrations away from the concentrations for meteoric water	No shift in $\delta^{18}O$ concentrations away from the concentrations for meteoric water	Concentrations are equal to those of meteoric water [12]
Pb [^{204}Pb, ^{206}Pb, ^{208}Pb] isotopes [16]; reflects the iso-topic composition of the rocks with which the water that precipitated the $CaCO_3$ was in contact	Dominated by isotopic concentrations different from that of the soil parent material or, in the veins, the adjacent bedrock	Dominated by isotopic concentrations of the soil parent material, or the veins, the adjacent bedrock	Pb isotopic composition very similar to bedrock from which the slope-wash alluvium is derived and through which the veins penetrate [16]
Sr isotopes [17]; geochemical analog to Ca^{++}; indicates the isotopic composition of the rocks with which the water that precipitated the $CaCO_3$ was in contact	Expected $^{87}Sr/^{86}Sr$ concentrations within the range of independently obtained samples from ground water, spring water, spring deposits, limestone or volcanic tuffs, or both	Expected $^{87}Sr/^{86}Sr$ concentrations within the range of independently obtained samples from soils developed on stable alluvial surfaces or from eolian samples	$^{87}Sr/^{86}Sr$ concentrations in the slope-wash alluvium and veins are similar to independently obtained soil and eolian samples [17]
U-series [^{238}U, ^{234}U, and ^{230}Th] isotopes [19] indicates the isotopic composition of the rocks with which the water that precipitated the $CaCO_3$ was in contact	Dominated by isotopic concentrations similar to samples independently obtained from ground water and spring water [18]	Dominated by isotopic concentrations from samples independently obtained from soil and eolian samples [19]	U-series concentrations in the slope-wash alluvium and veins are similar to independently collected soil and eolian samples [18]

Factor	Nonpedogenic	Pedogenic	Observed in trench 14
Ostracodes--a calcareous micro-fossil that requires a a saturated and oxygenated environment. Species are dependent on water temperature and chemistry [20]	Almost always in spring deposits	Not present, or if present in a soil environment, are part of the eolian component, and external surfaces must have evidence of wind abrasion	No ostracodes were present [20]

[1] Winograd and Doty, 1980
[2] Bachman and Machette, 1977
[3] Gile and others, 1966
[4] Taylor, 1986
[5] Table 1
[6] Table 2
[7] Vaniman and others, 1988
[8] Jones and Signit, 1971
[9] Birkeland, 1984
[10] Bullock and others, 1985
[11] Summerfield, 1982; 1983
[12] J.S. Whelan, U.S. Geological Survey, written commun., 1989
[13] Quade and others, 1989
[14] Benson and McKinley, 1985
[15] Benson and Klieforth, 1989
[16] R.E. Zartman, U.S. Geological Survey, written commun., 1989
[17] Stuckless and others, 1992
[18] Stuckless and others, 1991
[19] Rosholt and others, 1985
[20] R.M. Forester, U.S. Geological Survey, oral commun., 1990

metamorphic, volcanic, or plutonic processes associated with deep burial or by diagenetic processes associated with more moderate burial. Silcretes are almost exclusively present in saturated ground-water environments. No minimum silica content is defined for a duripan, whereas a silcrete has an arbitrary lower limit of 85 percent silica by weight (Summerfield, 1982, 1983).

No silcretes are present in the Yucca Mountain region (Taylor, 1986), but duripans are common. They vary in cementation by secondary opaline silica and commonly contain accessory cements, mainly carbonate.

Conspicuously well-laminated carbonate and opaline silica have been deposited along several fault planes within the Bow Ridge Fault zone at trench 14. Because the unconsolidated sandy slope-wash alluvium could not support open fractures very long, the laminae probably record episodes of opening and incremental filling of fractures developed along the fault. Similarly, the ash-filled fractures indicate that open fractures were formed and then subsequently filled through the action of surficial processes.

Finally, the modern water table ranges from 300 to 670 m below the surface in the Yucca Mountain region. There is no evidence from the area immediately adjacent to Yucca Mountain to indicate that rises in the water table have occurred during the last 500 ka (Winograd and Doty, 1980). Spring deposits do exist, however, west of Yucca Mountain at the south end of Crater Flat, and in the Amargosa area.

Summary

Trench 14 was excavated across the Bow Ridge Fault on the west side of Exile Hill to study the nature and frequency of Quaternary movement on the fault. Quaternary depositional units between the ages of 480,000±90,000 years and latest Pleistocene to early Holocene are in fault contact with brecciated volcanic tuff of Tertiary age. The main fault is characterized by vertical veins that intersect both the Quaternary deposits and the Tertiary bedrock. These veins contain primarily fine-grained sediments, secondary calcium carbonate and opaline silica, and a black ash. There is also a minor component of local rock fragments. The exposure provided very little information for the interpretation of Quaternary faulting on the Bow Ridge Fault. However, concern arose as to the origin of the secondary calcium carbonate and opaline silica in the vertical veins exposed in the fault zone. The veins physically resemble those found in spring deposits formed by ascending water. Physical, chemical, mineralogical, biologic, petrographic, and isotopic data collected indicate the calcium carbonate and opaline silica in the veins and slope-wash alluvium are characteristic of an environment with descending water--a pedogenic environment.

Two general azimuth orientations on fractures are observed in trench 14. About 85 percent of the bedrock fractures are oriented northwest, and the remainder of bedrock fractures and all of the fractures in the slope-wash alluvium are oriented northeast.

References Cited

Bachman, G.O., and Machette, M.N., 1977, Calcic soils and calcretes in the southwestern United States: U.S. Geological Survey Open-File Report 77-794, 163 p.

Benson, L.V., and McKinley, P.W., 1985, Chemical composition of ground water in the Yucca Mountain area, Nevada, 1971-84: U.S. Geological Survey Open-File Report 85-484, 10 p.

Benson, L.V., and Klieforth, Harold, 1989, Stable isotopes in precipitation and ground water in the Yucca Mountain region, southern Nevada--Paleoclimatic implications, in Peterson, D.H., ed., Aspects of climate variability in the Pacific and western Americas: American Geophysical Union Geophysical Monograph 55, p. 41-59.

Birkeland, P.W., 1984, Soils and geomorphology: New York, Oxford University Press, 372 p.

Bullock, P., Fedoroff, N., Jongerius, A., Stoops, G., and Tursina, T., 1985, Handbook for soil thin section description: Wolverhampton, England, Waine Research, 152 p.

Gile, L.H., Peterson, F.F., and Grossman, R.B., 1966, Morphological and genetic sequences of carbonate accumulations in desert soils: Soil Science, v. 101, no. 5, p. 347-360.

Hoover, D.L., Swadley, W C, and Gordon, A.J., 1981, Correlation characteristics of surficial deposits with a description of surficial stratigraphy in the Nevada Test Site region: U.S. Geological Survey Open-file Report 81-512, 27 p.

Jones, J.B., and Signit, E.R., 1971, The nature of opal, I. Nomenclature and constituent phases: Geological Society of Australia Journal, v. 18, p. 57-68.

McFadden, L.D., and Tinsley, J.C., 1985, Rate and depth of pedogenic-carbonate accumulation in soils--Formulation and testing of a compartment model, in Weide, D.L., ed., Soils and Quaternary geology of the southwestern United States: Geological Society of America Special Paper, 203, p. 23-41.

Nettleton, W.D., and Peterson, F.F., 1983, Aridisols, in Wilding, L.P., Smeck, N.E., and Hall, G.F., eds., Pedogenesis and soil taxonomy--v. II, The soil orders: New York, Elsevier, p. 165-214.

Quade, Jay, and Cerling, T.E., 1990, Stable isotopic evidence for a pedogenic origin of carbonates in trench 14 near Yucca Mountain, Nevada: Science, v. 250, p. 1549-1552.

Quade, Jay, Cerling, T.E., and Bowman, J.R., 1989, Systematic variations in the carbon and oxygen isotopic composition of pedogenic carbonate along elevation transects in the southern Great Basin, United States: Geological Society of America Bulletin, v. 101, p. 464-475.

Stuckless, J.S., Peterman, Z.E., Forester, R.L., Whelan, J.F., Vaniman, D.T., Marshall, B.D., and Taylor, E.M., 1992, Characterization of fault-filling deposits in the vicinity of Yucca Mountain, Nevada: Waste Management 92, Tucson, 1992, Proceedings, p. 929-935.

Stuckless, J.S., Peterman, Z.E., and Muhs, D.R., 1991, U and Sr isotopes in ground water and calcite, Yucca Mountain, Nevada: Evidence against upwelling water: Science, v. 254, p. 551-554.

Summerfield, M.A., 1982, Distribution, nature and probable genesis of silcrete in arid and semi-arid southern Africa, in Yaalon, D.H., ed., Aridic soils and geomorphic processes: Catena Supplement 1, p. 37-65. [Jerusalem], Proceedings of the International Conference of the International Society of Soil Science.

——1983, Silcrete as a paleoclimatic indicator--Evidence from southern Africa: Palaeogeography, Palaeoclimatology, Palaeoecology, v. 41, no. 1-2, p. 65-79.

Swadley, W C, Hoover, D.L., and Rosholt, J.N., 1984, Preliminary report on late Cenozoic faulting and stratigraphy in the vicinity of Yucca Mountain, Nye County, Nevada: U.S. Geological Survey Open-File Report 84-788, 42 p.

Taylor, E.M., 1986, Impact of time and climate on Quaternary soils in the Yucca Mountain area of the Nevada Test Site: Boulder, University of Colorado, Master's thesis, 217 p.

Taylor, E.M. and Huckins, H.E., 1995, Lithology, fault displacement, and origin of

secondary calcium carbonate and opaline silica at trenches 14 and 14D on the Bow Ridge fault at Exile Hill, Nye County, Nevada: U.S. Geological Survey Open-File Report 93-477, 38 p.

Vaniman, D.T., Bish, D.L., and Chipera, S., 1988, A preliminary comparison of mineral deposits in faults near Yucca Mountain, Nevada, with possible analogs: Los Alamos, New Mexico, Los Alamos National Laboratory Report LA-11289-MS, 54 p

Winograd, I.J., and Doty, G.C., 1980, Paleohydrology of the southern Great Basin, with special reference to water table fluctuations beneath the Nevada Test Site during the late(?) Pleistocene: U.S. Geological Survey Open-File Report 80-569, 91 p.

Day 1, Stop 6

Quaternary Deposits and Soils in Trench 14d: Implications for the Paleoseismicity of the Bow Ridge Fault near Exile Hill, Yucca Mountain, Nye County, Nevada

Christopher M. Menges and Emily M. Taylor

Introduction

Evaluations of seismic hazards such as vibratory ground motion and surface fault displacements are an important element of site characterization for the potential high-level nuclear waste repository at Yucca Mountain (U.S. Department of Energy, 1988). Given the general low level of historical seismicity in the Yucca Mountain area (Brune and others, 1992), seismic source characterizations of site faults with documented Quaternary activity are derived from geologic investigations of surface-rupturing prehistoric earthquakes. These paleoearthquakes are inferred primarily from the displacement of Quaternary deposits and soils in natural fault exposures or artificial trenches excavated across the fault trace (Menges and others, 1994, 1997, 1998). Detailed mapping and descriptions of Quaternary deposits and soils and estimation of their ages provide the basic stratigraphic constraints for these paleoseismic investigations (McCalpin, 1996).

This paper summarizes the stratigraphy and geochronology of colluvial deposits and soils exposed in trench 14D. These data were used to interpret the paleoseismic history of the Bow Ridge fault at the western base of Exile Hill near the northeastern corner of Yucca Mountain (figs. 1, 2; Menges and others, 1997). The Bow Ridge fault is a 6- to 10-kilometer-long normal to normal-oblique fault that strikes north to northeast (N. 5°-20° E.) (Scott and Bonk, 1984; Simonds and others, 1995; Day and others, 1998). The fault dips subvertical to steeply westward in outcrop and trench exposures, but structural cross-sections, borehole data, and subsurface exposures of the fault in the walls of the Exploratory Studies Facility tunnel beneath trench 14D indicate steep westward dips of 60°-65° at depths of 40 to 70 meters (m) (Scott and Bonk, 1984; Buesch and others, 1994; Simonds and others, 1995; Day and others, 1998). These subsurface data also indicate 125 ± 9 m of down to the west vertical separation on the top of a subunit within volcanic rocks of the Tiva Canyon Tuff (Scott and Bonk, 1984; Buesch and others, 1994). There are no fault scarps or other direct surface expression of the Bow Ridge fault in the Quaternary colluvial or alluvial deposits at the base of the bedrock ridge of Exile Hill. Here trench exposures reveal that the buried fault zone displaces Pleistocene deposits beneath a thin veneer (≤1 m thick) of undisturbed Holocene and latest Pleistocene sediments (see below; Menges and others, 1994, 1997; Taylor and Huckins, 1994).

Figure 1. Map showing faults, generalized bedrock outcrop, and trench locations in the Yucca Mountain area.

Figure 2. Geologic map showing bedrock and surficial deposits in area of trenches on the Bow Ridge fault near Exile Hill.

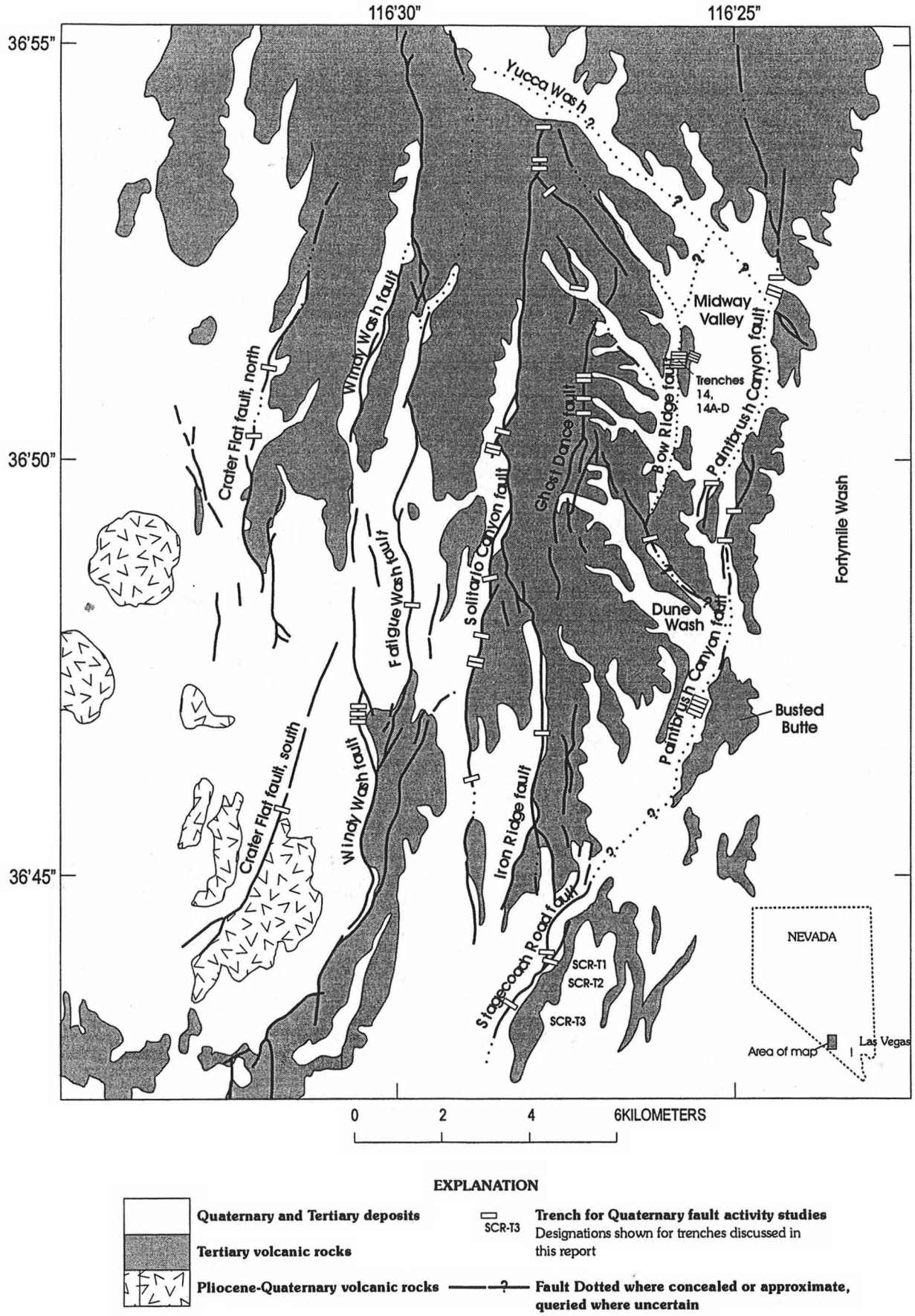

Figure 1. Map showing faults, generalized bedrock outcrop, and trench locations in the Yucca Mountain area.

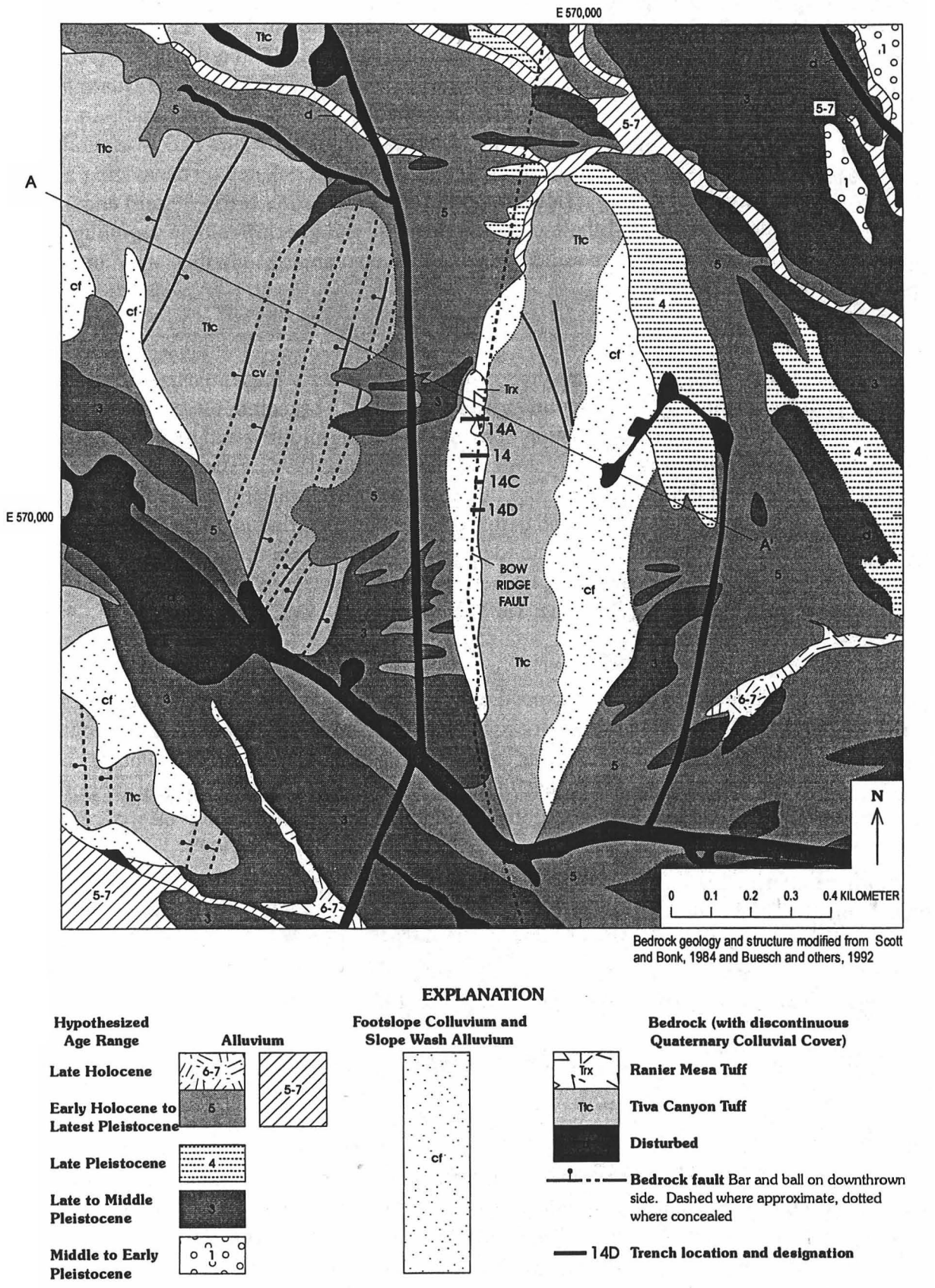

Figure 2. Geologic map showing bedrock and surficial deposits in area of trenches on the Bow Ridge fault near Exile Hill.

Trench 14D is one of five trenches excavated across the surface trace of the Bow Ridge fault at this site (figs. 1, 2). The original Trench 14 first was opened in 1982, and this trench was deepened and four new trenches (14A to 14D) were excavated in 1985 in order to resolve controversy on the origin of secondary carbonate and silica and to better define the Quaternary displacement history of the Bow Ridge fault (Taylor and Huckins, 1994; this volume). In 1992, the trench with the best exposures of the fault in Quaternary deposits, trench 14D, was modified by extending one end eastward 40 m in an attempt to intersect bedrock and by excavating a box network of auxiliary trenches 7 m on a side around the main fault zone at the western end. Detailed mapping, descriptions of lithologic units and soils, and geochronologic sampling from the north and south branches of the modified trench 14D are summarized in this paper and in Menges and others (1997).

Methods

Detailed maps, or logs, have been prepared in trench 14D for the southern wall of the southern branch and the northern and southern walls of the north branch in the box extension (for example, see figs. 3, 4), using a combination of manual gridding-plotting and total station theodolite techniques (Hatheway and Leighton, 1979; McCalpin, 1996). These trench logs are supplemented by detailed field descriptions of lithologic units and soil profiles (tables 1 and 2). Relations among lithologic units, soils, and deformational features (that is, fissures, shears, fractures, and unit displacements) are used to identify and characterize the size and timing of surface-faulting events, and paleoseismic parameters such as recurrence intervals and fault slip rates are derived from these data (Schwartz, 1988; Nelson, 1992; McCalpin, 1996).

Figure 3. Simplified interpretive log of exposures of the Bow Ridge fault in part of trench 14D, north branch, south wall. Note central fault zone is well defined by multiple carbonate-coated shears and fissure fills. Two to three faulting events (Z to X?) have been identified on the basis of incremental downsection increases in the amount of vertical displacements at marker horizons, upward truncation of shears and fractures along the fault, and presence of colluvial wedges.

Figure 4. Simplified interpretive log of exposures of the Bow Ridge fault in part of trench 14D, south branch, south wall. The most recent event (Z) is well expressed in this exposure by displaced units and a prominent scarp-derived colluvial wedge (unit 13a).

Table 1. Summary characteristics of lithologic units in trench 14D.

Table 2. Summary of soil profile descriptions for trench 14D.

Age control for faulted and unfaulted deposits and soils are provided by several techniques. The ages of soils and lithologic units in the trench were directly dated using either (a) U-Th disequilibrium (U-series) dating of four sample sets of secondary pedogenic carbonate and silica laminae or soil matrix carbonate, or (b) thermoluminescence (TL) analysis of two samples of fine-grained polymineralic sediment (table 3; J.B. Paces and others, U.S. Geological Survey, written commun., 1995).

Trench 14D, North Branch, South Wall

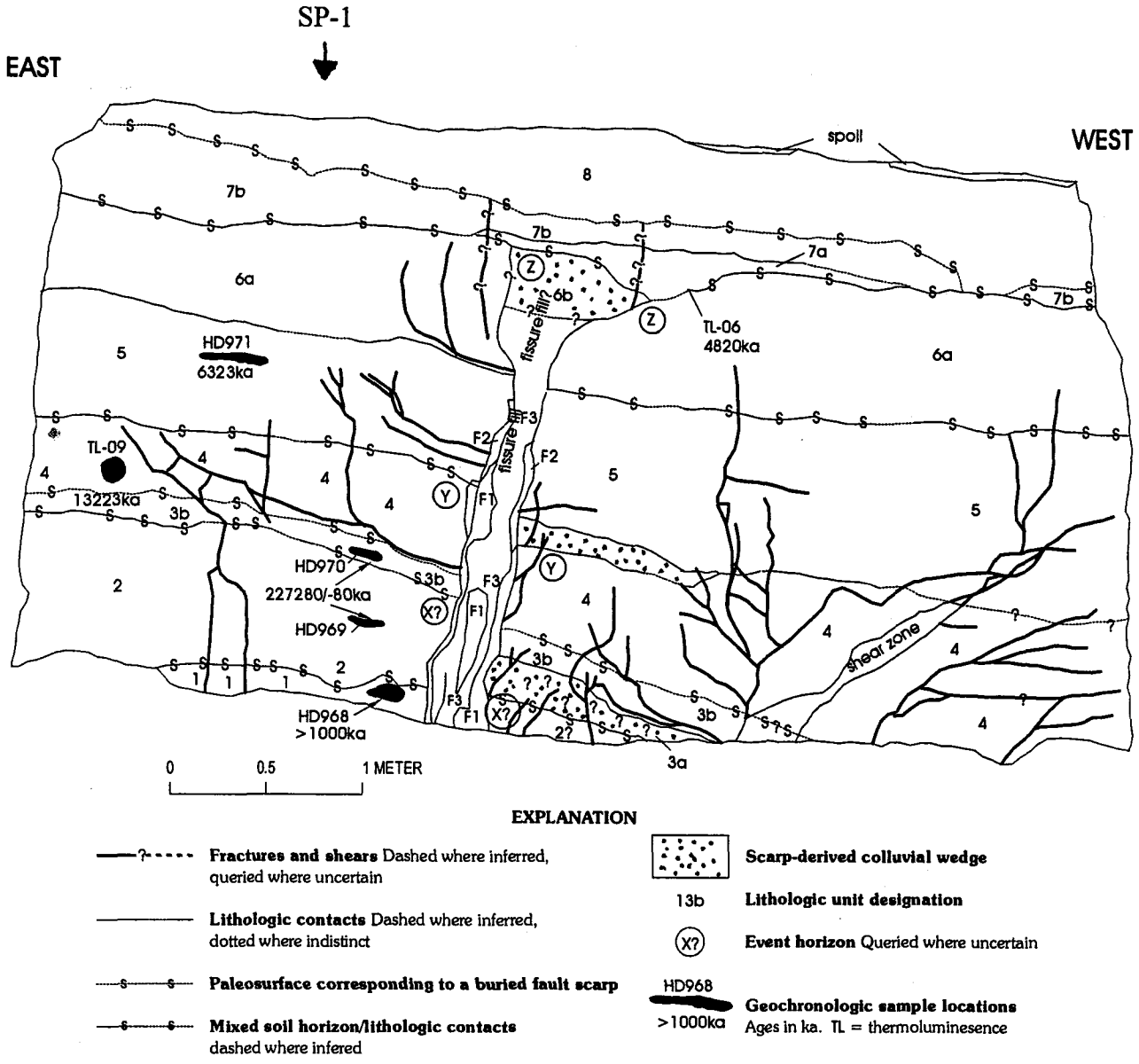

Figure 3. Simplified interpretive log of exposures of the Bow Ridge fault in part of trench 14D, north branch, south wall. Note central fault zone is well defined by multiple carbonate-coated shears and fissure fills. Two to three faulting events (Z to X?) have been identified on the basis of incremental downsection increases in the amount of vertical displacements at marker horizons, upward truncation of shears and fractures along the fault, and presence of

Trench 14D, South Branch, South Wall (Western Part)

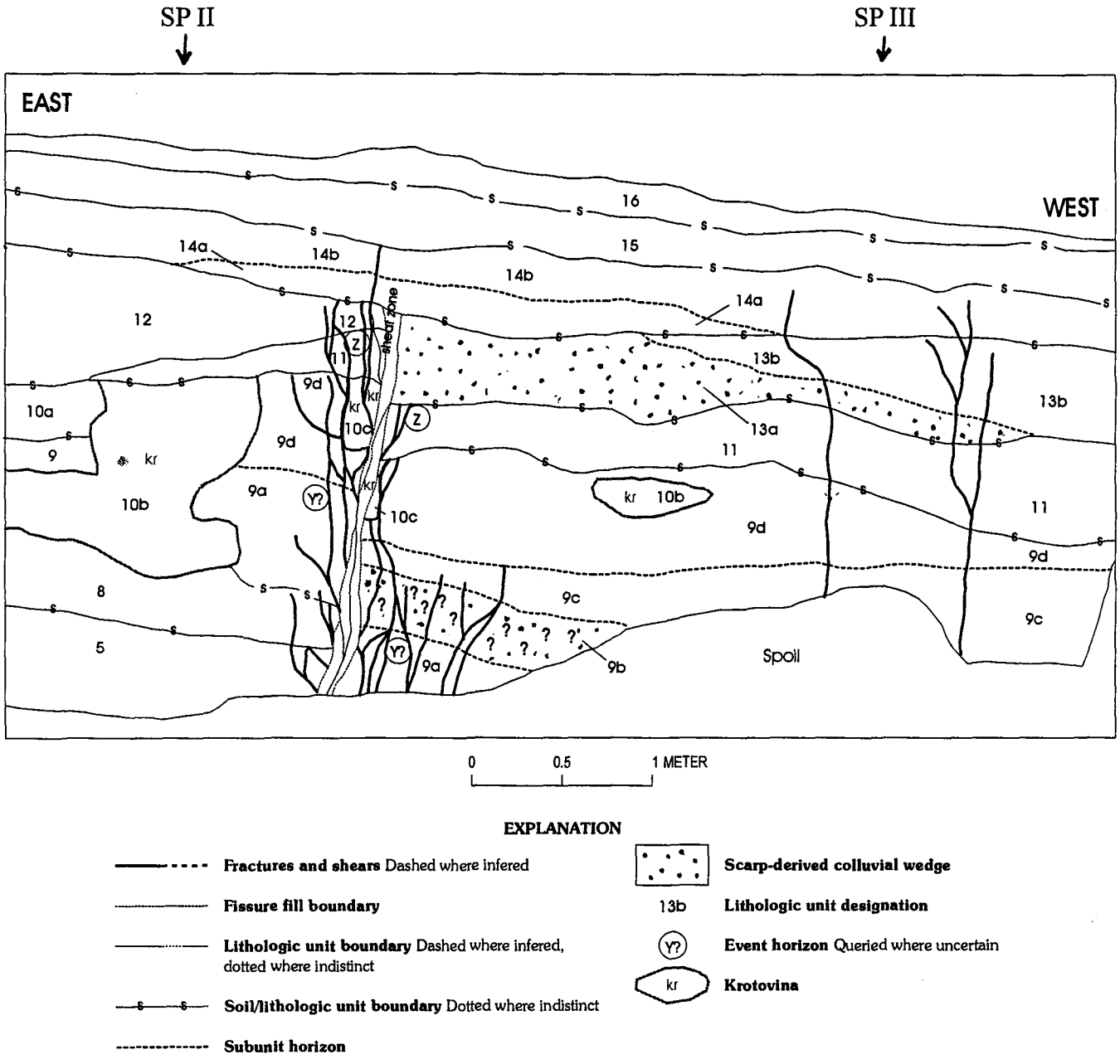

Figure 4. Simplified interpretive log of exposures of the Bow Ridge fault in part of trench 14D, south branch, south wall. The most recent event (Z) is well expressed in this exposure by displaced units and a prominent scarp-derived colluvial wedge (unit 13a).

Table 3. Summary of geochronologic samples and radiometric age determinations from north branch, trench 14D.
[Ages cited from Paces and others, U.S. Geological Survey, written commun., 1995, which supersede preliminary ages reported in Paces and others (1994) and Menges and others (1994). Stratigraphic units reported include local trench lithologic units and groups, followed by correlations to regional geochronologic units (see text, table 4). All TL and U-series age estimates are reported with 2 σ errors. Measurements of all U-series samples were conducted with an alpha spectrometer.]

Sample Number	Material Dated	Lithologic Units	Age Estimate (ka)	Dating Technique	Purpose and Interpreted Context of Age
TL-06	Colluvium, north wall	7, Group D (Q4)	48 ± 20	TL	Time when material was last exposed to sunlight
HD 971	Colluvium, south wall	5d, Group B (Q3)	98 ± 15, 137 +36/-28 139 +34/-27 144 +37/-28	U-series	Composite soil sample (upper carbonate soil)
TL-09	Colluvium, south wall	4, Group B (Q3)	132 ± 23	TL	Time when material was last exposed to sunlight
HD 970	Colluvium, south wall	3b, Group B (Q3)	234 +47/-35	U-series	Composite soil sample (lower carbonate soil)
HD 969	Colluvium, south wall	2, Group B (Q3)	340 +∞/-120	U-series	Composite soil sample (lower carbonate soil)
HD 968	Colluvium, south wall	1, Group A (≥Q1)	> 700	U-series	Composite soil sample (basal petrocalcic soil in trench)

Trench Stratigraphy and Soils

Trench 14D contains a vertical sequence of lower Pleistocene to Holocene lithologic units deposited along the western margin of Exile Hill (figs. 3, 4; table 1). Bedrock consisting of the middle Miocene Tiva Canyon Tuff (Buesch and others, 1994; Day and others, 1998) is exposed only in the eastern section of trench 14D, 15 m to the east of the main fault zone. This bedrock is buried by 1.5 to 2 m of surficial deposits. The Quaternary section in the trench comprises a westward-thickening package of surficial deposits of mixed colluvial, alluvial, and eolian origins that have been subdivided into 8 to 15 lithologic units (table 1). Most of the units are fine- to medium-grained silty sand to sandy silt with varying proportions of pebble-cobble gravel interbeds. These sediments typically are unconsolidated to moderately cemented, very poorly sorted, and massive to poorly bedded. The deposits include locally derived colluvium, eolian silt and sand, poorly channelized fluvial gravels, and localized debris flows. Many of the pebbly fine-grained colluvial and eolian units have been reworked locally by slope wash.

Deposits in the western end of the trench contain a complex set of weakly to well

developed soils (figs. 3, 4; table 2). The sequence includes a vertically stacked to partially overlapping series of two to five buried paleosols below a thin surface soil. The buried soils are 0.3 to 2 m thick and consist of cemented zones and stringers of secondary carbonate and silica (Bkq to Kq horizons with Stage II to IV carbonate morphology) and (or) argillic horizons with Bt or Btk morphology. The surface soil is relatively thin (≤0.5 m) and consists of at most a Bw or weak Bt horizon above a Bk horizon with discontinuous Stage I carbonate coatings on the undersides of clasts. To the east in trench 14D, these soils merge in the upslope direction into a single composite relict soil. Laboratory data for soils in the west part of the south branch of trench 14D are described in Taylor and Huckins (1994).

The Quaternary deposits described above have been divided into lithologic units based on variations in stratigraphic features such as lithology, texture, color, bedding characteristics, and the presence of buried soils. A separately numbered local sequence was developed for the northern branch and southern branches of trench 14D because of uncertainties in defining and correlating specific units from one trench exposure to another, particularly those units in the lower part of the trenches. Table 4 presents proposed correlations of individual units between the two lithostratigraphic sequences in trench 14D. Individual units at each site have also been grouped on the basis of general similarities in lithology, stratigraphic positions, and soil-stratigraphic characteristics in the following discussions. This table also contains general age assignments based on both trench-specific geochronologic data and general correlations between deposits in the trenches and units in the chronosequence developed for the Midway Valley area of Yucca Mountain (see summary at stop 6, day 1, this volume).

Group A in the south branch directly overlies bedrock and associated colluvium (unit 1, S) and is characterized by silty sand with scattered gravel clasts that are impregnated predominantly with Stage III carbonate and silica. These units may correlate with the basal unit (unit 1) in the north branch which contains a poorly exposed petrocalcic soil with a U-series age exhibiting excess ^{230}Th and depleted ^{234}U; thus this soil is at least 400-600 ka and probably exceeds 700 ka (fig. 3; sample HD968, table 3).

Group B is a 1- to 3-m-thick sequence of silty sand layers with locally interbedded sandy gravel that overlies the older group of deposits in both branches of the trench. A thick complex petrocalcic soil with Stage II to IV carbonate morphology is developed within this sequence. The lower carbonate laminar zone yields poorly constrained composite U-series ages from two samples of 340 + ∞/-120 ka and 234 +47/-35 (fig. 3; samples HD969 and HD970, respectively, table 3). These dates represent minimum pedogenic ages for carbonate accumulation postdating deposition of the units (units 2 and 3, N). A depositional age of 132 ± 23 ka (fig. 3; sample TL-09, table 3) was determined for a TL sample collected from the overlying silty sand unit (unit 4, N). Carbonate-silica laminae from the base of the upper carbonate zone of the petrocalcic soil provides four U-series ages that are concentrated between 135 and 145 ka (fig. 3; 98 ± 15 ka, 137 +36/-28 ka, 139 +34/-27 ka, 144 +37/-28 ka, sample HD971, table 3). These dates represent close minimum ages for calcic horizon development at the top of the depositional package (unit 5, N).

Group C overlies the petrocalcic soil and is characterized by a distinctive reddish brown clay-rich silty sand, ≤1 m in thickness, with colors, texture, and structure indicative of an argillic horizon (unit 11, S; unit 6, N; figs. 3, 4).

Table 4. Lithostratigraphic correlations and estimated ages of lithologic sequences in north and south branches of trench 14D.
[General ages assigned based on soil stratigraphy and numerical age ranges derived from geochronologic control described in text. Stratigraphic groups are defined in text and individual units are described in tables 1 and 2. Age symbols are H, Holocene; lsP, latest Pleistocene; lP, late Pleistocene; mP, middle Pleistocene; eP, early Pleistocene; lM, late Miocene; ka, thousand years ago; leaders (___), no data]

Lithologic unit Numbers		Stratigraphic group	Estimated age (ka)
Trench 14D, south	Trench 14D, north		
1 (Bedrock and colluvium)	___	___	lM to eP
2-4	1	A	eP (≥1,000)
5	2, 3	B	mP (150-400)
6-8	___	B	mP (150-400)
9	4-5	B	m-lP (100-150)
10	___	B	m-lP (100-150)
11	6	C	lP (50-120)
12-13	___	C	lP (50-120)
14	7	D	lP (30-70)
15-16	8	E	lsP-H (0-20)

Group D includes thin layers of silty sand ≤0.4 m in total thickness (unit 7, N and unit 14, S) that were deposited on the underlying units of group C (figs. 3, 4). Group D is present only in the western part of trench 14D where it buries the main fault zone. Local vesicular silty textures and the lack of stratigraphic suggest that in places the unit may contain a buried Av horizon formed primarily on eolian or reworked eolian deposits. Distinguishing characteristics of these units include a pale orangish-brown color, large subangular blocky structure, and formation of a

duripan soil horizon characterized by moderate to strong cementation by secondary silica with little or no visible carbonate. A late Pleistocene depositional age of 48 ± 20 ka is provided by a TL sample (fig. 3; sample TL-06, table 3) collected from the base of the group in the north branch of the trench.

The uppermost deposits in the sequence, group E, consist of gravelly silty sand to sandy gravel layers (unit 8, N; units 15 and 16, S; figs. 3, 4). The group is associated with a weakly developed soil consisting of Av, Bw/Bt, and Bk horizons with, at most, Stage I carbonate morphology characterized by thin discontinuous coatings on the underside of clasts. This type of soil is typical of deposits with middle Holocene to latest Pleistocene ages in the Yucca Mountain area (Wesling and others, 1992; Lundstrom and others, 1993, 1994).

Structure

The main strand of the Bow Ridge fault in trench 14D is characterized in the lower part of the trench walls by a very distinct, irregular 20- to 40-centimeter (cm)-wide shear zone. Multiple veins and laminae of secondary carbonate and silica coat the walls of this shear zone. Three sets of fissures have developed along the main fault in the north branch of the trench. These fissures are filled with several deposits of sand, silt, and gravel with at least two distinct stages of cementation by carbonate and silica. The main fault in both trenches strikes N 5° to 15°E and dips 80°-85°SE, indicative of slight over steepening of the fault in the direction of the downdropped block. The fault trace is best expressed in both trenches where it displaces units and carbonate-silica laminae in the petrocalcic soil of groups A and B. The fault zone can be traced upwards with greater difficulty through the argillic horizons of group C units in trench 14D by either weakly-expressed filled fissures or by tectonic alignment of clasts along the fault zone. The fault trace terminates abruptly beneath undisturbed deposits of group D and E in the upper meter of trench 14D (figs. 3, 4), although group D units are locally fractured without displacement above the fault.

Numerous small secondary fractures with little or no offset occur within a 2- to 3-m wide zone of deformation on both sides of the main fault. These fractures typically are very thin (≤1 cm in width) and are delineated by thin coatings of carbonate or silica where they have formed in the petrocalcic soil of group B units. There is no evidence in either trench of eastward backtilting or antithetic graben formation in the hanging wall of the fault.

Paleoseismic Interpretations

Two to three surface-faulting events are recognized in trench 14D (table 5). Identification of these events is based on criteria such as (a) incremental up-section decreases in the displacement amounts of successive marker horizons, (b) development of multiple fissure fills that terminate at discrete horizons, (c) local upward terminations of fractures and shear zones at specific horizons, (d) disruption of a unit by shearing or fracturing, (e) the position of possible buried scarp-derived colluvial wedges on the downthrown block (Swan and others, 1980; Nelson, 1992), and (f) cross-cutting relations among more than one set of shears or fractures. Specifically, in the north branch of the trench, a possible old event (X) may have occurred at the top of unit 2 in group B; the penultimate event (Y) is interpreted with greater confidence at the top of unit 4, also in group B deposits (table 5; fig. 3). The most recent event is well expressed in both branches of the trench, where it may be traced to the top of units 6 (N) and 11 (S) in group C (Fig. 3, 4; table 5). Stratigraphically higher deposits in group D and E are not displaced

by the fault in either branch, although a fracture of uncertain origin does continue upward through group D above the buried fault trace.

Table 5. Characteristics, criteria, reliability of identification, and preferred age estimates for interpreted surface-faulting events on the Bow Ridge fault in trench 14D.
[Refer to text for discussion. Event horizons also are shown in figures 3 and 4; leaders (__), not applicable]

Fault event	Criteria[1]	Reliability[2]	Event horizon (top of unit)	Colluvial wedge (unit)	Fissure (fill unit)	Preferred Age (ka)[3]
			south branch, south wall			
Z	D, S, W	H	11	13a, 14a(?)	___	(see north branch)
Y	D	P	9a	9b(?)	___	(see north branch)
			north branch, south wall			
Z	D, U, F	H	6	7a(?)	F3, F2	≥40-60
Y	D, U, W	M	4	5a, 5b(?)	F1	140 ± 30
X	D, F(?), W	P	2	3a	F1(?)	350 ± 100

1. Criteria for identifying events: D, incremental downsection increase in measurable displacement at horizon; U, upward termination of two or more fractures of shears at horizon; S, disruption of unit by shearing; F, fault fissure filled with debris at and below horizon; W, colluvial wedge inferred as scarp derived; C, cross-cutting relationships between fractures/shears and soil features.

2. Reliability of event identification: H, high (clear expression with diagnostic criteria); M, moderate (strongly suggestive, but nondiagnostic criteria); P, poor (suggestive, but ambiguous evidence).

3. Preferred estimate of age range for event, based on minimum and maximum age brackets for each event provided by dated units summarized in table 3, as described in text.

The amount of vertical displacements per event is small, in the range of 1 to 46 cm, with preferred values of 12 to 40 cm (table 6). Corrections for oblique left slip, determined from possible slickenline striations with plunges of 65° and 35° on carbonate coatings in the fault, increase these values by factors of 1.1 to 1.7, yielding preferred net slip amounts of 13 to 70 cm.

A composite fault chronology has been developed from the age control in the northern branch of trench 14D (see above; fig. 3; tables 3, 5). The possible oldest event (X) predates the carbonate accumulation of the lower calcic soil (dated at ≈340-234 ka), probably by a relatively short amount, and thus the event is assigned a poorly resolved age of approximately 350 ± 100 ka. The penultimate event (Y) displaces unit 4 (TL age of 135 ka), but is buried by the overlying

upper calcic soil at the top of unit 5 with the oldest U-series dates ranging between 134 to 145; these relationships suggest a poorly constrained preferred age for the event of 140 ± 30 ka. The most recent event is certainly younger than 140-98 ka because it ruptures unit 4 and the overlying calcic soil (see above); the event probably closely predates 40-60 ka, because it is buried by the lower part of unit 7 (group D) with a TL age of 48 ± 20 ka (table 6), which is interpreted as colluvium deposited within a tectonic depression on the rupture.

Table 6. Summary of paleoseismic parameters for middle to late Quaternary activity on the Bow Ridge fault at the trench 14D site.
[cm, centimeters; ka, thousand years ago; ky, thousand years; mm/yr, millimeter per year]

Parameter	Minimum	Maximum	Preferred
Number of events	2	3	2
Displacements per event			
Dip-slip	1 cm	46 cm	12-40 cm
Net	1 cm	80 cm	13-44 cm
Age--most recent event	30 ka	90 ka	40-60 ka
Recurrence intervals[1]	75 ky	215 ky	100-140 ky
Slip rates[2]	0.002 mm/yr	0.007 mm/yr	0.003 mm/yr

1. Average recurrence intervals calculated for last three events Z to X. Large variation in age range results from dating uncertainties combined with sample context problem arising from ambiguity in relating faulting events to dated units.

2. Slip rates should be treated with caution because they are derived from units that have experienced, at most, two faulting events. They may also include the effects of the elapsed time since the most recent event.

Recurrence intervals are difficult to calculate because of the small number of events relative to available age control. Average recurrence intervals between the last three events range from 75 to 215 ka with a preferred value of 145 ka (table 6). Individual recurrence intervals between events Z and Y and events Y and X vary between 40 and 350 ky, with preferred values of 90 to 210 ka based on additional geologic and pedogenic constraints.

Fault slip rates are computed from the amount of cumulative net-slip displacements of two dated units in the trench which have experienced at most two events. These reference datum are unit 4 with a TL age of 132 ± 23 in the north branch, and the petrocalcic soil in unit 9d with an age range of ≥135 to 145 (~137) ka in the south branch. Preferred cumulative net displacements are 35 cm (2 events) and 44 cm (1 event) for these two marker units, respectively. Average slip rates thus calculated vary between 0.002 mm/yr and 0.007 mm/yr; the preferred value at this location on the Bow Ridge fault is 0.003 mm/yr (table 6). These slip rates should be treated cautiously because the calculations are based on a small number of events and the rates are strongly influenced by the elapsed time since the most recent event. Nevertheless, these slip

rates are very low even with the large uncertainties.

References Cited

Birkeland, P.W., 1984, Soils and geomorphology: Oxford University Press, 372 p.

Brune, J.N., Nicks, W., and Aburto, A., 1992, Microearthquakes at Yucca Mountain, Nevada: Bulletin of the Seismological Society of America, v. 82, p. 164-174.

Buesch, D.C., Dickerson, R.P., Drake, R.M., and Spengler, R.W., 1994, Integrated geology and preliminary cross section along the north ramp of the exploratory studies facility, Yucca Mountain: International High-Level Radioactive Waste Management Conference, 5th, Las Vegas, Nevada, April 1994, Proceedings: v. 4, p. 1055-1065.

Day, W.C., Potter, C.J., Sweetkind, D., Dickerson, R.P., and San Juan, C.A., 1998, Bedrock geologic map of the Central Block area, Yucca Mountain, Nye County, Nevada: U.S. Geological Survey Miscellaneous Investigations Map I-1601, scale 1:6,000, with text, 15 p.

Hatheway, A.W., and Leighton, F.B., 1979, Trenching as an exploratory method, *in* Hatheway, A.W., and McClure, C.R., Jr., eds., Geology in the siting of nuclear power plants, Geological Society of America Reviews of Engineering Geology, v. 4, p. 169-195.

Lundstrom, S.C., Wesling, J.R., Swan, F.H., Taylor, E.M., and Whitney, J.W., 1993, Quaternary allostratigraphy of surficial deposit map units at Yucca Mountain, Nevada: A progress report: Geological Society of America, Abstracts with Programs, v. 25, no. 5, p. Al 12.

Lundstrom, S.C., Wesling, J.R., Taylor, E.M., and Paces, J.B., 1994, Preliminary surficial deposits map of the northeast 1/4 of the Busted Butte 7.5'quadrangle, Nye County, Nevada: U.S. Geological Survey Open-File Report 94-34 1, scale 1: 12,000.

McCalpin, J.P., 1996, Paleoseismology: Academic Press, New York, New York, 588 p.

Menges, C.M., Wesling, J.R, Whitney, J.W., Swan, F.H., Coe, J.A., Thomas, A.P., and Oswald, J.A., 1994, Preliminary results of paleoseismic investigations of Quaternary faults on eastern Yucca Mountain, Nye County, Nevada: International High-Level Radioactive Waste Management Conference, 5th, Las Vegas, Nevada, April 1994, Proceedings: v. 4, p. 2373-2390.

Menges, C.M., Taylor, E.M., Vadurro, G., Oswald, J.A., Cress, R., Murray, M., Lundstrom, S.C., Paces, J.B., and Mahan, S.A., 1997, Logs and paleoseismic interpretations from trenches 14C and 14D on the Bow Ridge fault, northeastern Yucca Mountain, Nye County, Nevada: U.S. Geological Survey Miscellaneous Field Studies Map MF-2311, 4 pls, with text, 33 p.

Menges, C.M., Oswald, J.A., Coe, J.A., Lundstrom, S.C., Paces, J.B., Mahan, S.A., Widmann, Beth, and Murray, Michelle, 1998, Paleoseismic investigations of Stagecoach Road fault, southeastern Yucca Mountain, Nye County, Nevada: U.S. Geological Survey Open-File Report 96-417, 71 p, with 3 pls.

Munsell Color Company, Inc., 1992, Munsell soil color charts, revised edition: Baltimore, MD.

Nelson, A., 1992, Lithofacies analysis of colluvial sediments--An aid to interpreting the recent history of Quaternary normal faults in the Basin and Range province, western United States: Journal of Sedimentary Petrology, v. 62, no. 4, p. 607-621.

Paces, J.B., Menges, C.M., Widmann, Beth, Wesling, J.R., Bush, C.A., Futa, K., Millard, H.T., Maat, P.B., and Whitney, J.W., 1994, U-series disequilibrium and thermoluminescence ages of paleosols associated with Quaternary faults, east side of Yucca Mountain:

International High-Level Radioactive Waste Management Conference, 5th, Las Vegas, Nevada, April 1994, Proceedings: v. 4, p. 2391-2401.

Schwartz, D.P., 1988, Geologic characterization of seismic sources: Moving into the 1990's, *in*, von Thun, ed., Earthquake engineering and soil dynamics, v. 2, Recent advances in ground-motion evaluation: American Society of Civil Engineers Geotechnical Special Publication 20, p. 1-42.

Scott, R.B., and Bonk, Jerry, 1984, Preliminary geologic map of Yucca Mountain, Nye County, Nevada, with geologic sections: U.S. Geological Survey Open-File Report 84-494, scale 1:12,000, 9 p.

Simonds, F.W., Whitney, J.W., Fox, K.F., Ramelli, A.R., Yount, J.C., Carr, M.D., Menges, C. M., Dickerson, R.P. and Scott, R.B., 1995, Fault map of the Yucca Mountain area, Nye County, Nevada: U.S. Geological Survey Miscellaneous Investigations Series Map I-2520, scale 1:24,000.

Swan, F.W., Schwartz, D.P., and Cluff, L.S., 1980, Recurrence of moderate to large magnitude earthquakes produced by surface faulting on the Wasatch fault zone, Utah: Bulletin of the Seismological Society of America, v. 70, p. 1431-1462.

Taylor, E.M., and Huckins, H.E., 1994, Lithology, fault displacement, and origin of secondary calcium carbonate and opaline silica at Trenches 14 and 14D on the Bow Ridge fault at Exile Hill, Nye County, Nevada: U.S. Geological Survey Open-File Report 93-477.

Taylor, E.M., and Huckins, H.E., 1998, Lithology, fault displacement, and origin of secondary calcium carbonate and opaline silica at Trenches 14 and 14D on the Bow Ridge fault at Exile Hill, Nye County, Nevada, this volume.

U.S. Department of Energy, 1988, Site characterization plan, Yucca Mountain site, Nevada, research and development area, Nevada: U.S. Department of Energy Report DOE/RW-0199, 8 vol., variously paged.

Wesling, J.R., Bullard, T.F., Swan, F.H., Perman, R.C., Angel, M.M., and Gibson, J.D., 1992, Preliminary mapping of surficial geology of Midway Valley, Yucca Mountain, Nye County, Nevada: Sandia National Laboratory Report SAND91-0607, 56 p 5 pls.

Table 1. Summary characteristics of lithologic units in trench 14D

[%, percent ; cm, centimeters; exp., exposed; ≥, same as or older than; <, less than; n/a, not applicable; dashes (--), no data; >, greater than]

Lithologic unit[1]	Group	Position[2]	Associated soil unit[3]	General lithology[4]	Clast[5] size %	Matrix[6]	Cementation[7]	Thickness	Shape	Deformation[8]	Correlative unit[9]
1 (S-2,3,4)	A	FW	S1	snd pbl cbl gvl	pbl-f cbl 10-30%	f-c snd	CO_3 mod-stg	20 cm exp. in trench	tabular	F	≥Q1
2 (S-5)	B	FW & HW	S5-2	snd pbl cbl gvl with slt	pbl-c cbl 10-15%	f-m snd with slt	CO_3 stg	50-60 cm	tabular	F	Q3 upper
3 (S-5)	B	FW & HW	S5-2	pbl slt snd	c pbl-f cbl 5-10%	f-c snd with slt	CO_3 stg	8-35 cm	tabular	F	Q3
4 (S-9)	B	FW & HW	S5-2	pbl snd slt with ash?	f-c pbl <5%	slt with f-c snd	CO_3/SiO_2 mod-stg	40-60 cm	tabular	F	Q3
5 (S-9)	B	FW & HW	S5-2	pbl cbl slt snd	f-c cbl <5-15%	slt-snd	CO_3/SiO_2 mod-stg	80-155 cm	tabular	F	Q3
6 (S-11)	C	FW & HW	S6	pbl cbl snd	c pbl-f cbl <5% locally 20%	cly-f snd	CO_3 non-stg	50-65 cm	tabular	F	Q3-Q4
7a (S-14)	D	FW & HW	S7	pbl slt snd	pbl-f cbl 5-10%	f-c snd with slt/f ash(<1%)	SiO_2 with minor CO_3 stg	0-25 cm	tabular lenticular	U, EW_z	Q4
7b (S-14)	D	FW & HW	S7	snd pbl cbl gvl	pbl-c cbl 10-50%	vf-m snd with slt	CO_3/SiO_2 wk/stg	25-35 cm	tabular	U	Q4

Table 1. Summary characteristics of lithologic units in trench 14D--Continued

Lithologic unit[1]	Group	Position[2]	Associated soil unit[3]	General lithology[4]	Clast[5] size %	Matrix[6]	Cementation[7]	Thickness	Shape	Deformation[8]	Correlative unit[9]
8 (S-15,16)	E	FW & HW	S8	cly slt snd-pbl slt snd	pbl-f cbl 0-10%	pbl snd-slt	CO_3/fines wk	21-50 cm	tabular	U	Q5
				North branch Fault zone fissure fill descriptions:							
				north wall							
F1	B	n/a	S5-2	pbl slt snd	pbl <5%	vf-c snd with slt	CO_3/SiO_2 stg-ind	<15 cm	fissure	FF lam	Q3?
				south wall							
F2	D	n/a	S6	pbl slt snd	f pbl <5%	f-m snd with slt	CO_3/SiO_2 stg-ind	<5 cm	fissure	FF	Q3?
F3	D	n/a	S6	pbl cbl slt snd	pbl-f cbl 5-30%	f-m snd with slt	CO_3/SiO_2 wk-stg	7-25 cm	fissure	FF	Q4?
				South branch south wall							
1 (N-none)	A	FW	S1	tuff/coll	pbl-bld 40-80%	CO_3 slt snd	CO_3/SiO_2 ind	base not exp.	n/a	F	--
2 (N-1)	A	FW	S2-3	pbl cbl slt snd	pbl-f cbl 5-15%	f-m snd with slt minor c snd	CO_3/SiO_2 ind	0-40 cm	lenticular	F	≥Q1
3 (N-1)	A	FW	S2-3	slt snd-pbl cbl slt snd	pbl-f cbl 5-15%	f-m snd with slt minor c snd	CO_3/SiO_2 well-ind	0-50 cm	tabular lenticular	F	≥Q1?

Table 1. Summary characteristics of lithologic units in trench 14D--Continued

Lithologic unit[1]	Group	Position[2]	Associated soil unit[3]	General lithology[4]	Clast[5] size %	Matrix[6]	Cementation[7]	Thickness	Shape	Deformation[8]	Correlative unit[9]
4 (N-1)	A	FW	S9-4	snd slt gvl-pbl snd	pbl-c cbl 15-60%	vf-m snd with slt minor c snd	CO_3/SiO_2 wk-top mod-bttm	0-55 cm	tabular lenticular	F	≥Q1?
5 (N-2,3)	B	FW	S9-4	pbl cbl slt snd	cbl 3-10%	f-m snd with slt minor c snd	CO_3/SiO_2 wk-ind	0-95 cm	tabular lenticular	F	Q3
6 (N-none)	B	FW	S9-4	pbl cbl sub-bld slt snd-snd slt gvl	pbl-sub-bld 30-40%	f-m snd with slt c snd	CO_3 wk-local mod	0-60 cm	tabular lenticular	F	Q3
7 (N-none)	B	FW	S9-4	pbl cbl snd slt	pbl-c cbl 3-30%	slt-m snd with minor c snd	CO_3 with minor SiO_2 mod-stg-top wk-bttm	0-90 cm	tabular lenticular	F	Q3
8 (N-none)	B	FW	S9-4	snd slt pbl cbl gvl	pbl-c cbl 10-40%	f-m snd with slt minor c snd	CO_3/SiO_2 wk-mod local stg	0-50 cm	tabular lenticular	F	Q3
9 (N-4,5)	B	FW & HW	S9-4	pbl slt snd	pbl <5%	f-m snd with slt minor c snd	CO_3/SiO_2 stg-top wk-bttm	0-110 cm	tabular	F	Q3
10 (N-none)	B	FW & HW	S9-4	pbl cbl snd-snd slt pbl cbl gvl	pbl-f cbl <10% locally 40%	f-c snd with minor slt	CO_3 wk-mod	0-30 cm	boot shaped lenticular	F	Q3
11 (N-6)	C	FW & HW	S11	pbl cbl slt snd	pbl-f cbl <5%	slt-f snd with minor c snd/ vf	CO_3 wk	30-35 cm	tabular lenticular	F	Q3-Q4

Table 1. Summary characteristics of lithologic units in trench 14D--Continued

Lithologic unit[1]	Group	Position[2]	Associated soil unit[3]	General lithology[4]	Clast[5] size %	Matrix[6]	Cementation[7]	Thickness	Shape	Deformation[8]	Correlative unit[9]
						basaltic ash					
12 (N-none)	C	FW & HW	S12	snd gvl	pbl-c cbl 20-40%	f-m snd with slt minor c snd	CO_3 non-wk	0-80 cm	irregular lenticular	F	Q3-Q4
13 (N-none)	C	HW	S13	snd slt pbl cbl gvl	pbl-f cbl 40-50%	f-m snd with slt minor c snd	CO_3 with minor SiO_2 wk	35-50 cm	tabular	EW_y	Q3-Q4
14 (N-7)	D	FW & HW	S14	pbl cbl snd slt-pbl cbl slt snd	pbl-f cbl <10%	slt with f snd minor m-c snd	opaline SiO_2/CO_3 mod	24-40 cm	tabular	U	Q4
15 (N-8)	E	FW & HW	S15	pbl cbl slt snd	pbl-c cbl 10-60%	slt-f snd minor m-c snd	CO_3 wk	25 cm	tabular	U	Q5
16 (N-8)	E	FW & HW	S16	pbl slt snd	pbl-f cbl <10%	slt-f snd with m snd minor c snd	fine non-wk	4-12 cm	tabular	U	Q5

[1]Lithologic unit, with correlative unit in other branch of trench in parentheses (see table 4). N - north branch; S - south branch.

[2]Position: FW= footwall; HW= hanging wall; FW & HW= unit in both footwall and hanging wall blocks.

[3]Soil unit in table 3 associated with unit.

[4]General lithology: pbl= pebble; cbl= cobble; bld= boulder; snd= sand; slt= silt.

[5]Upper line denotes range of clast sizes. Lower line denotes percentage of clasts in lithologic units.

[6]Matrix size: f ,vf= fine, very fine; m= medium; c ,vc= coarse, very coarse; snd= sand; slt= silt.

[7]Cementation: CO_3= carbonate; Si= silica; wk= weak; mod= moderate; stg= strong; ind= indurated; non= uncemented; bttm= bottom.

[8]Deformation: F= faulted; U= unfaulted; EW.= event $wedge_{event\ ndesignation}$.

[9]Correlative Quaternary surficial deposit in regional chronosequence of Wesling and others (1992) and Lundstrom and others (1993, 1994) (see text).

Table 2. Summary of soil profile descriptions for trench 14D

[See log for location of profiles; cm, centimeters; CO_3, carbonate; HCl, cold dilute hydrochloric acid; %, percent; n/a, not applicable; n.o., not observed; <, less than; >, greater than; *, soil property found locally]

Horizon	Depth (cm)	Associated unit	Color[1] Wet	Color[1] Dry	Percent gravel	Texture[2]	Structure[3]	Consistence Dry[4]	Consistence Wet[5]	CO_3 Stage[6]	Efferves-cence (HCl)[7]	Cemen-tation[8]	Horizon boun-dary[9]	Roots[10]	Pores[11]	Rhizo-liths[12]	Clay films[13]
SP I: north branch south wall (0.5 m east of main fault zone)																	
Av	0	S8	10YR 4/4-4/3	10YR 7/4-7/3	10-20%	slt s	1 m-c sbk	sh	so-ss po	N/a	vse-e	cw fines disc	g w	1 f-co	1-2 vf v local	n.o.	n.o.
Bw	6	S8	10YR 4/4-4/3	10YR 7/3-6/4	<10%	slt l	1 m-c sbk	so-sh	so-ss po-ps	n/a	e	cw fines cont	a-g w	1 f-m	1-2 f i	n.o.	n.o.
Bk	17	S8	10YR 4/4	10YR 7/3	30-40%	gvl slt l	1 m-c sbk	sh	so-ss po	I local	e	cw CO_3 cont	a s	1 vf	2-3 vf-f v-t	n.o.	n.o.
2Bkq1b1	27	S7	7.5YR 5/4	7.5YR 8/2-8/4	40-60%	s l	2-3 c-vc sbk	h	ss ps	I-II	em-es	cs-ci SiO_2 cont	a s	1 vf	n.o.	n.o.	n.o.
2Bkq2b1	44	S7	7.5YR 5/8-5/6	7.5YR 8/6-7/6	10-30%	s l	2-3 m-c sbk	h	ss ps	I-II	em-es	cw-cs SiO_2 cont	a s	1 vf	n.o.	n.o.	n.o.
3Btkb2	55	S6	7.5YR 5/6	7.5YR 6/6-8/4	<5%	cl l	3 f-m pr/sbk	sh-h	s p	I nod	e-es	cw CO^3 cont	d w	1 f-co	2 vf i	n.o.	2 d pf
3Bkb2	90	S6	7.5YR 6/6	7.5YR 8/4-7/6	10-15%	slt l	1 f-m sbk	sh	ss ps	III* lam cap	ev	cw-cs CO_3 disc	c w	1 vf-f	2 f i-t	n.o.	2 d pf
4Kqm1b3	110	S5-2	7.5YR 7/6	7.5YR 8/2	5%	s l	N/a	h	so-ss	III lam	ev	cs $CO_3>SiO_2$ cont	a s	n.o.	1 f-m i between laminae/ matrix	n.o.	n.o.
4Kqm2b3	135	S5-2	7.5YR 7/6	7.5YR 8/2	5-10%	s l	N/a	h	so-ss	III	ev	cs CO_3/SiO_2 cont	a s	n.o.	1 vf-f i between laminae/ matrix	n.o.	n.o.

Table 2. Summary of soil profile descriptions for trench 14D--Continued

Horizon	Depth (cm)	Associated unit	Color[1] Wet	Color[1] Dry	Percent gravel	Texture[2]	Structure[3]	Consistence Dry[4]	Consistence Wet[5]	CO_3 Stage[6]	Efferves-cence (HCl)[7]	Cemen-tation[8]	Horizon boun-dary[9]	Roots[10]	Pores[11]	Rhizo-liths[12]	Clay films[13]
5Bwkqb3	167	S5-2	7.5YR 4/2-4/6	7.5YR 8/4-7/4	15%	s l	2 m-c sbk	h	so po	II	es-ev	cw CO_3	a s	n.o.	1 f-m i cl/peds	2-3 f-m disp	n.o.
6Kqm1b3	212	S5-2	7.5YR 4/2-4/6	7.5YR 8/4-7/4	<5%	slt s	1-2 relic	h	so po	II-III	es-ev	cs CO_3>SiO_2 cont	a w	n.o.	2 f-m v-i matrix	n.o.	n.o.
7Kqm2b3	220	S5-2	7.5YR 6/4-4/4	7.5YR 8/2-7/4	10-40%	l s - s	2 f-c sbk local	h	so po	III-II	ev	CO_3/SiO_2 cont	a s	n.o.	1 f-m i cl	1 vf-m ped	n.o.
7Bwkqb3	249	S5-2	7.5YR 5/6	7.5YR 7/3-7/6	10-40%	l s	1-2 m-c sbk	sh-h	so po	II	em-es	cs CO_3 disc	a w	n.o.	1 f-m v-i matrix	1-2 ? disp	n.o.
8Kqmb4	286	S1	7.5YR 5/4	7.5YR 7/2	60%	s gvl	m	h-vh	so po	III-IV	ev	cs CO_3>SiO_2 cont	n.o.	n.o.	1 m i cl/lam	1 f matrix	n.o.
SP I: south branch south wall (16 m east of main fault zone)																	
Av	0	S16	10YR 4/4	10YR 7/3	<5%	s l	2 f-c pl/sbk	so-sh	ss ps	n/a	eo	n.o.	a s	1 vf-f	1-3 vf-f i	n.o.	n.o.
2Bwkb1	10	S15	10YR 4/6	10YR 6/4 to 7.5YR 6/6 at base	20-30%	s l	1-2 f-c sbk	so-sh	ss ps	I	eo-e	n.o.	a s-w	2-3 vf-m disp	2-3 vf-f v-i disp	n.o.	vf f pf
3Btkb2	42	S11	7.5YR 5/6	7.5YR 7/4	5-10%	s l	2 f-c pr/sbk	sh	ss ps	I-II	em	n.o.	a s	2-3 vf-m disp	2 vf-f i disp	n.o.	vf f pf
4Kqm1b3	60	S9-4	7.5YR 6/6	7.5YR 8/3	5-10%	n/a	n/a	eh	n/a	III-IV	ev	ci CO_3/SiO_2 cont	a-c w	1 vf-f disp	1-2 f-m i disp	n.o.	n.o.
4Kqm2b3	90	S9-4	7.5YR 6/6	7.5YR 8/3	5-10%	n/a	n/a	eh	n/a	III	es-ev	ci CO_3/SiO_2	a-c w	n.o.	1 vf-f i disp	n.o.	n.o.

Table 2. Summary of soil profile descriptions for trench 14D--Continued

Horizon	Depth (cm)	Associated unit	Color[1] Wet	Color[1] Dry	Percent gravel	Texture[2]	Structure[3]	Consistence Dry[4]	Consistence Wet[5]	CO_3 Stage[6]	Efferves-cence (HCl)[7]	Cemen-tation[8]	Horizon boun-dary[9]	Roots[10]	Pores[11]	Rhizo-liths[12]	Clay films[13]
4Bwk + Kqmb3	125	S9-4	7.5YR 7/3(CO_3) 4/6(Bwk)	7.5YR 8/2(CO_3) 7/4(Bwk)	5-10%	l s	1 f-c sbk(Bwk)	h(Bwk)	so po	II-III	e-es	* ci CO_3/SiO_2 *	a-c w	n.o.	1-2 vf-f i disp	n.o.	n.o.
5Bwkqb3	143	S9-4	7.5YR 6/4(CO_3) 5/6(Bw)	7.5YR 8/2(CO_3) 7/4(Bw)	10-15%	l s	2 f-c sbk	h-eh	so po	II-III	vse-em	cs-ci CO_3 disc	a-c w	1 vf local	2 vf-f i disp	1 f-m local	vf f pf
6Bwk + Kqmb3	180	S9-4	7.5YR 7/3(CO_3) 5/4(Bw)	7.5YR 8/1(CO_3) 7/2(Bw)	<5%	s	1-2 f-m sbk	h-eh	so po	II$^+$-III	em-es	ci CO_3/SiO_2 cont	a-c s	n.o.	n.o.	n.o.	n.o.
7Bwkqb3	252	S9-4	7.5YR 7/1(CO_3) 5/4(Bw)	7.5YR 8/1(CO_3) 7/3(Bw)	10-30%	s	1-2 m-c sbk	sh-h	so po	II-III	vse-em	cw-cs * disc	a-c w	n.o.	1-2 f-m i disp	1-3 f-m local	n.o.
8Kqmb4	310	S2	7.5YR 7/3	7.5YR 8/2	10%	n/a	n/a	eh	n/a	III-IV	ev	ci CO_3/SiO_2 cont	not exp	n.o.	1 vf-f i	n.o.	n.o.
SP II: south branch south wall (1 to 0.5 m east of main fault zone)																	
Av	0	S16	10YR 4/3-4/4	10YR 6.5/2	<5%	s l	2 m-c sbk	sh	ss ps	n/a	vse	n.o.	a s	1-2 vf-f disp	3 f v disp	n.o.	n.o.
2Ab1	12	S15	10YR 4/3-4/4	10YR 6/3	<10%	s l	3 c-vc pl	so-sh	ss ps	n/a	vse	n.o.	a s	2 f-co disp	* * v-i disp	2-3 vf-f	n.o.
2Bkb1	21	S15	10YR 5/4	10YR 6.5/3	60%	s l	1-2 f sbk	so	so po	I-II$^-$	vse-e	n.o.	a s	1-2 f disp	2-3 vf-f i	n.o.	n.o.

Table 2. Summary of soil profile descriptions for trench 14D--Continued

Horizon	Depth (cm)	Associated unit	Color[1] Wet	Color[1] Dry	Percent gravel	Texture[2]	Structure[3]	Consistence Dry[4]	Consistence Wet[5]	CO_3 Stage[6]	Efferves-cence (HCl)[7]	Cemen-tation[8]	Horizon boun-dary[9]	Roots[10]	Pores[11]	Rhizo-liths[12]	Clay films[13]
3Bkqb2	30	S14	7.5YR-10YR 8/0(CO_3) 10YR 4/4-4/5	10YR 6/4	<10%	l s	2-3 vc pl/sbk	eh	so po	I	eo-em	cs CO_3/SiO_2 cont	a s	1-2 vf-f disp	1 vf i disp	n.o.	1 f pf
4Btjkb3	88	S13	6.5YR 5/5	7.5YR 5.5/4	70-80%	l s-s	2 f-m abk/sbk	h-eh	so-ss po-ps	I-II	eo-vse	cw-cs CO_3/SiO_2 cont	a s	1 vf-f disp	2-3 m-co i	n.o.	1 f pf
Soil profile description moved laterally to avoid krotovina.																	
5Btk1b4	65	S12	7.5YR 5/6	7.5YR 6/6	50-60%	s l	1 f-m pl/pr/sbk	h-eh	ss-s ps-p	I	eo-vse	cw fines disc	a-c s	1 vf disp	2-3 f-m i disp	n.o.	1-2 d pf
5Btk2b4	82	S12	7.5YR 5/4	7.5YR-10YR 6-7/4	50-60%	s l	1-2 f-c pr/sbk	eh	ss ps	II-I (matrix)	eo-vse	n.o.	c s	1-2 f disp	2-3 f i disp	n.o.	2 d pf
5Btk3b4	103	S12	7.5YR 4/4	7.5YR 6.5/4	50-60%	l s	1 m-c sbk pl(local)	h-eh	so-ss po-ps	II	eo-em	cw CO_3 disc	a s	1-2 vf-f disp	1-3 f-m i disp	n.o.	n.o.
6Btkb5	119	S11	7.5YR 5/4	7.5YR-10YR 7/4	<5%	l s	2 f-m abk/pr	h-eh	so-ss po-ps	I-II	eo-e	n.o.	a s	1-2 vf-f disp	1-2 vf-f i disp	n.o.	n.o.
7Kqm1b6	122	S9-5	7.5YR 6/4-7/4	7.5YR 8/3-8/4	<5%	s	laminar	eh	so po	III-IV	ev	ci CO_3/SiO_2 cont	a-c s	n.o.	1 vf-f i lam	n.o.	n.o.
7Kqm2b6	132	S9-5	7.5YR 6/4-7/4	7.5YR 8/2-8/4	<5%	s	laminar	eh	so po	III	ev	cs-ci CO_3/SiO_2 cont	a s	n.o.	1 f i lam\ooid	n.o.	n.o.
7Bkq1b6	175	S9-5	7.5YR 7/3-7/4(CO_3) 5/6	7.5YR 8/2-8/4(CO_3) 7/4-6/4	<5%	*	2-3 m sbk	sh-eh	so po	II-III	ev	cw-ci CO_3/SiO_2 disc	a s	n.o.	1-2 f i-t lam/ped	1 f matrix	n.o.

Table 2. Summary of soil profile descriptions for trench 14D--Continued

Horizon	Depth (cm)	Associated unit	Color[1] Wet	Color[1] Dry	Percent gravel	Texture[2]	Structure[3]	Consistence Dry[4]	Consistence Wet[5]	CO_3 Stage[6]	Efferves-cence (HCl)[7]	Cemen-tation[8]	Horizon boun-dary[9]	Roots[10]	Pores[11]	Rhizo-liths[12]	Clay films[13]
7Bkq2b6	209	S9-5	7.5YR 6/6	7.5YR 7/4	5-10%	l s	2-3 m-c sbk	h	so po	II	es	cs CO_3 cont	a w	n.o.	1-2 f i	1-2 f	n.o.
8Bwkqb6	240	S9-5	7.5YR 5/6	7.5YR 7/4	20-30%	s l	2-3 m-c sbk	h	so-ss po	I-II	vse-es	cs CO_3/SiO_2 cont	a-c s	n.o.	1 f i	1 f	n.o.
9Bwk + Kqmb6	272	S9-5	7.5YR 8/3 (CO_3) 5/4	7.5YR 8/1-8/2(CO_3) 7/4	<10%	l s	1 f-m sbk	eh	so po	II-III	ev	cs-ci CO_3 cont	not exp	n.o.	1 vf-f i	1-2 f-m	n.o.
SP III: south branch south wall (3 m west of main fault zone)																	
Av	0	S16	10YR 5/4-5/6	10YR 7/3-7/4	<5%	slt l	m-sg f-m pl	lo-so	ss-ps	n/a	vse	n.o.	a s	2 vf-f peds	2-3 f v	n.o.	n.o.
2Bkb1	5	S15	10YR 5/4-5/6	10YR 7/3-7/4	10%	s l	1 f-m pl	so-sh	ss ps	I	vse-e	n.o.	a s	2 f-m disp	1 vf v-i cl	n.o.	n.o.
3Bkqb2	32	S14	10YR 5/4-4/4	10YR 6/3-6/4	<10%	l s	3 m-c sbk	h-vh	so po	I-II	em	cs CO_3/SiO_2 cont	a-c s	1 vf cl/ped	1 vf-f i-t peds	n.o.	vf f pf
4Bkb3	82	S13	7.5YR 4/4	7.5YR 7/4-6/4	40-50%	s l	1-2 vf-m sbk	h	so po	I-II	em	* CO_3/SiO_2 cont	a s	1 vf-f cl	1 f i cl/ped	n.o.	1 f pf/co
5Btk1b4	115	S11	7.5YR 5/6-6/6	7.5YR 6/6	5%	s cl l	2-3 f pr	sh-h	ss-s ps-p	I-II	em	cw CO_3 disc	c s	1 vf-f peds	1-2 vf-f i ped	n.o.	1-2 f-d pf/co
5Btk2b4	140	S11	7.5YR 5/4-4/4	7.5YR 7/4-6/4	5%	l s	2 f pr/sbk	sh-h	ss ps	I-II+	*	cw CO_3 disc	a-c s-w	n.o.	1-2 f i ped	n.o.	1 f pf
5Bkb4	155	S11	7.5YR 5/4-5/6	7.5YR 8/3-8/6	<5%	l s	2 f sbk	sh-h	so po	II-III-	*	cw-cs CO_3	c s	n.o.	1 f i	n.o.	1 f pf

Table 2. Summary of soil profile descriptions for trench 14D--Continued

Horizon	Depth (cm)	Associated unit	Color[1]		Percent gravel	Texture[2]	Structure[3]	Consistence		CO_3 Stage[6]	Efferves-cence (HCl)[7]	Cemen-tation[8]	Horizon boun-dary[9]	Roots[10]	Pores[11]	Rhizo-liths[12]	Clay films[13]
			Wet	Dry				Dry[4]	Wet[5]								
6Kqmb5	167	S9	7.5YR 5/4-5/6	7.5YR 8/2-8/4	<5%	l s?	n/a	h-eh	so po	III	*	cont cs CO_3 cont	n.o.	n.o.	n.o.	n.o.	n.o.

Table 2. Summary of soil profile descriptions for trench 14D--Continued

[1]From Munsell soil color charts, revised edition, 1992.

[2]Texture: l= loam, s=sand, slt= silt.

[3]Structure: grade: m= massive, sg= single grain, 1= weak, 2= moderate, 3= strong; size: vf= very fine, f= fine, m= medium, c= coarse; type: pl= platy, sbk= subangular blocky, abk= angular blocky.

[4]Consistence, dry: lo= loose, so= soft, sh= slightly hard, h= hard, vh= very hard, eh= extremely hard.

[5]Consistence, wet: so= nonsticky, po= nonplastic.

[6]Carbonate stage morphology defined in Birkeland, 1984; lam= laminae.

[7]Effervescence: in cold, dilute hydrochloric acid, vse= very slightly effervescent, e= effervescent, em= moderately effervescent, es= strongly effervescent, ev= very strongly effervescent.

[8]Cementation: CO_3= carbonate, SiO_2= silicate; strength: cw= weak, cs= strong, ci= indurated; type: cont= continuous, disc= discontinuous.

[9]Horizon boundary (lower): not exp= not exposed; distinctness: a= abrupt, c= clear, g= gradual; topography: s= smooth, w= wavy, i= irregular.

[10]Roots: abundance: 1=few, 2= common, 3= many; size: vf= very fine, f= fine, m= medium, co= coarse; location: disp= dispersed, ped= ped faces, cl= clast.

[11]Pores: abundance: 1= few, 2= common, 3= many; size: vf= very fine, f= fine, m= medium, co= coarse; shape: v= vesicular, i= irregular or interstitial; location: cl= clast, disp= dispersed, lam= laminae, ped= ped faces.

[12]Rhizoliths: abundance: 1= few, 2= common, 3= many; size: f= fine, m= medium, co= coarse; location: disp= dispersed, ped= ped faces.

[13]Clay Films: 1= few, 2= common; size: vf= very fine, f= fine, co= coarse.

Day 1, Stop 6

Drilling And Tunneling On The Yucca Mountain Project

Daniel J. Soeder

Underground Facility Construction

A series of tunnels has been excavated under Yucca Mountain during the past few years to provide large scale access to the design repository horizon in the Topopah Spring Tuff. These tunnels are called the "Exploratory Studies Facility" of ESF, and are being utilized to study geologic characteristics, subsurface hydrology and thermal-mechanical properties of the rock. The main ESF tunnel is a U-shaped loop under the east flank of the ridge, which extends nearly 3 km west into the mountain, turns and runs directly south parallel to the ridge for almost 3 km, and then turns again and comes east slightly more than 2 km to the surface. The excavation was started at the North Portal in the spring of 1993. A vertical cut was made in the hillside, and a 60 meter (200 ft) deep "starter tunnel" was excavated using traditional drill and blast methods. The remainder of the tunnel was excavated mechanically with a Tunnel Boring Machine (TBM), sometimes called a "mole." (figs. 1 and 2)

Figure 1. Preliminary Repository Layout.

Figure 2. Pre-Emplacement Development

The TBM utilized for the main tunnel is 7.5 meters (25 feet) in diameter, and was constructed specifically for excavation of the Exploratory Studies Facility under Yucca Mountain. It was built by Construction & Tunneling Services, Inc. (CTS) in Kent, Washington, and was designed for minimal water usage during excavation. Hydraulic oil volume was also kept to a minimum. Early concerns about the ESF excavation focused on the potential for contaminating the site with water or hydraulic fluids. The machine was constructed and tested over a period of about 10 months in Washington state, then disassembled and trucked to the North Portal pad area in the spring of 1994. It took a total of 59 semi-trucks to get the 720 tons of tunnel boring machine to the Nevada Test Site. It was reassembled during the summer of 1994 and moved into the starter tunnel at the North Portal. Mining with the TBM began in September, 1994, and continued until April 25, 1997, when the machine emerged into daylight at the South Portal. The tunnel has a total length of 7877 meters or about 4.9 miles. The average excavation rate of the TBM was approximately 20 meters per day; the record with this machine was 57 meters in a single day. Excavation was done on two shifts, with the third shift reserved for cleanup and maintenance.

Unlike a drill bit, which grinds the rock into small particles, a TBM excavates by mechanically breaking the rock and spalling it off the cut surface. The cutter head on the Yucca Mountain TBM contains numerous cutting wheels made of high carbon steel, which weigh 350 lbs apiece. The cutters are spaced so that their tracks overlap as the head is turned. The entire cutter head was rotated at about 4 RPM by 12 electric motors rated at 250 HP each. The machine

Preliminary Repository Layout

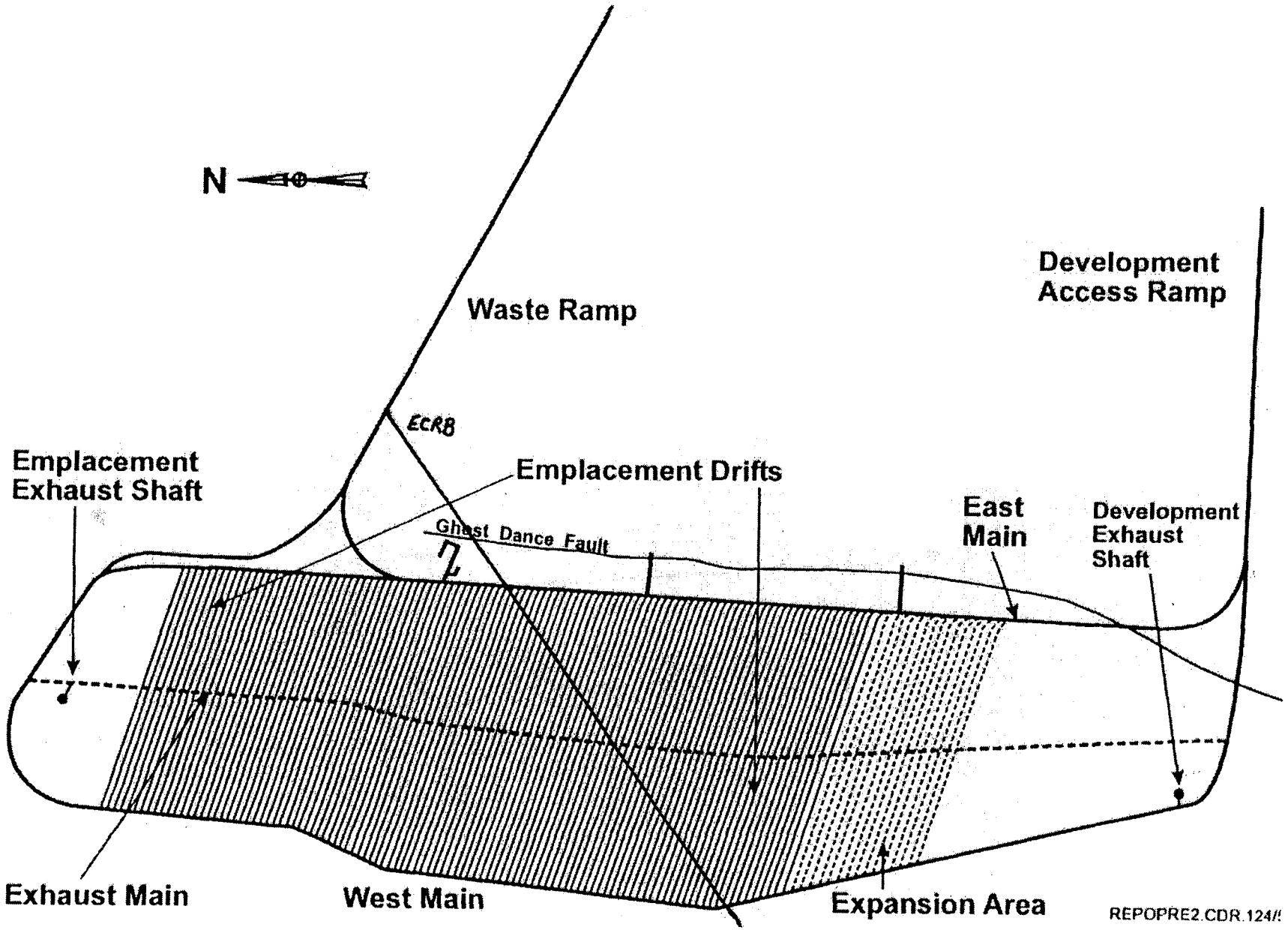

Pre-Emplacement Development

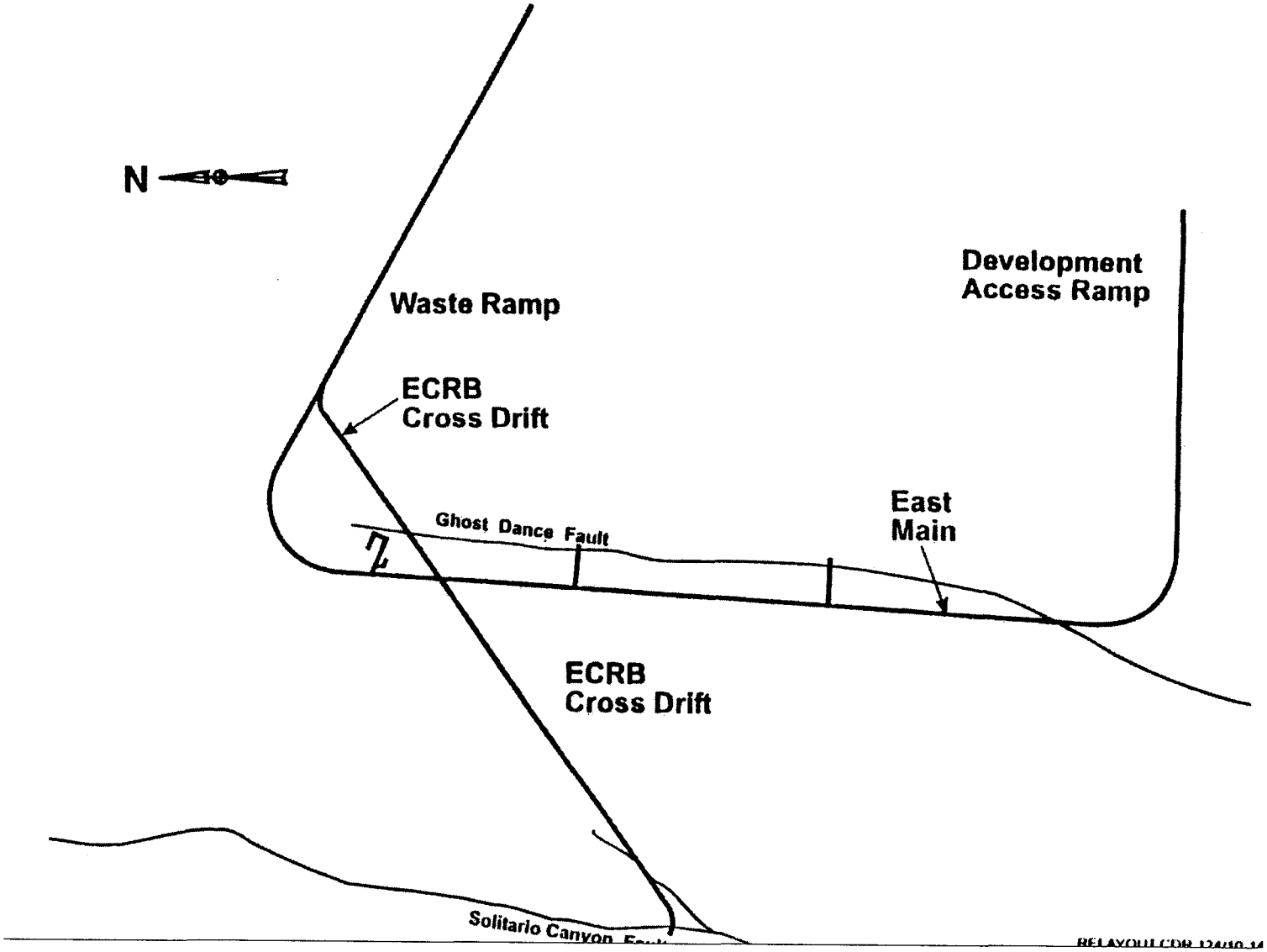

has an operating voltage of 12.47 Kv, and generates up to 3,800 horse power. Behind the cutter head are two independent sets of gripper shoes; one set consists of shoes on either side of the machine, and the other set consists of shoes on the top and bottom. Using powerful hydraulic rams, the gripper shoes can be extended as much as 24 inches to grip the sides of the tunnel with a force of up to 15,000 psi. One set of grippers was used to lock the machine in position while hydraulic rams forced the cutter head against the rock face at pressures as high as 30,000 psi. When the cutter head was rotated under these high pressures, the tensile strength of the rock was exceeded at the wedge-shaped cutting wheels, and the rock spalled off the face in fist-size chunks. The cut rock was gathered by "muck buckets" or scoops spaced at intervals along the rim of the cutter head, and carried to the top of the machine. The muck was then dumped from the buckets into a hopper, which fed it onto a conveyor belt system to remove it from the tunnel. After the machine advanced about a meter, the second set of grippers was engaged and the head continued to cut. The first set was released and pulled forward with the rest of the machine and trailing gear. Thus, the TBM advanced in the manner of an inchworm, cutting continuously all the while. Thirteen work platforms, or trailing decks, were carried along by the machine. These were used for installing ground support, tunnel utilities, and for geologic mapping. The TBM was a surprisingly quiet and vibration-free machine. During excavation operations, the noisiest piece of equipment was the conveyor belt.

Ground support was installed directly behind the TBM "tail shield," which protected the crew working at the cutter head. The idea behind ground support is not for steel ribs or bolts to hold up the entire weight of rock above the tunnel, but rather to secure the rock so it supports itself. Ground failure in a tunnel is typically caused by "ravelling," wherein small, unsecured rocks fall out of the roof, allowing larger blocks to loosen and collapse. Proper ground support holds everything together, and prevents ravelling. Ground quality in the Yucca Mountain tunnel was rated in five different categories, with Category 1 being the best, and 5 the worst. Category 1 support is rock bolts with wire mesh, and was typically employed in relatively unfractured, well-indurated rock. The type of bolts employed were "Super Swellex," which consist of hollow steel tubes 2 inches in diameter by either 10 or 16 feet in length, with a U-shape cross section. These were inserted in drilled holes, and inflated with 4000 psi water pressure. The pressure swelled the bolts, creating a tight friction fit along the length of the hole. Categories 2 and 3 of ground support required the use of sprayed-on concrete, or "shotcrete." The scientific program objected to the use of this material because of concerns over how it might affect geochemical measurements in the tunnel. Of particular concern were CO_2 measurements, especially ^{14}C age-dating of air in the unsaturated zone. Cementitous materials give off CO_2 as they cure, and this could have adversely affected carbon chemistry underground. As such, any ground less stable that Category 1 was treated as Category 4, and supported with 25-foot diameter steel rings called "steel sets." The rings were assembled underground from four sections of curved, six-inch thick, steel I-beams and emplaced at 4 foot intervals in the excavation directly behind the cutter head using a "ring erector." Steel slats called "lagging" were placed between the rings to further support the ground.

Future tunneling at Yucca Mountain will be done using mechanical miners or smaller TBMs. A 5.5 meter (16 foot) diameter machine was used to excavate the 2.8 km long cross-block drift this year, completed in late September. The large TBM used for the main loop excavation will be stored at the South Portal unless someone wants to buy it.

Exploratory Studies Facility Configuration And Experiments

When fully completed, the Exploratory Studies Facility (ESF) is planned to be an underground complex consisting of 14 miles of tunnels, adits, side drifts and test alcoves. The initial portion of the excavation consists of a 25-foot diameter (7.5 meter) tunnel looping approximately 5 miles into and under Yucca Mountain before emerging to the south. This large diameter tunnel will be used for waste emplacement if a repository is eventually constructed at Yucca Mountain. The tunnel consists of the North Ramp, which runs from the portal to the first turn. The first turn starts at about 2100 meters from the North Portal and ends at 2800 meters. The Main Drift runs north-south between 2800 and 5500 meters to the start of the second turn. The South Ramp starts at 5500 meters, at the beginning of the second turn. The second turn ends at about 6600 meters, and the South Ramp is straight from there to the South Portal at 7877 meters. The deepest point in the tunnel is at the end of the first turn near Alcove 5, with approximately 275 meters (900 feet) of overburden. The Cross Block Drift comes off the North Ramp at 2000 meters and angles to the southwest. It extends 2800 meters from the North Ramp to the Solitario Canyon Fault and was completed in September, 1998.

A total of seven test alcoves and two small hydrologic niches were constructed to investigate features of engineering, geological and hydrological importance intersected by the tunnel. These are summarized as follows:

Alcove #	Location (m)	Excavation	Stratigraphy	Investigations
1	00+43	Drill/Blast	Tiva (Tpcpul)	Prototype hydrologic tests
2	01+71	Drill/Blast	Tiva (Tpcpmn)	Hydrology of Bow Ridge Fault
3	07+57	Alpine Miner	Tiva (Tpcpv)	Hydrology of TCw/PTn transition
4	10+28	Alpine Miner	Topopah (Tptrv)	Hydrology of PTn/TSw transition
5	28+27	Alpine+Blast	Topopah (Tptpmn)	Repository rock thermal properties
Niche 1	35+55	Alpine Miner	Topopah (Tptpmn)	Hydrology in fast flowpath zone
Niche 2	36+05	Alpine Miner	Topopah (Tptpmn)	Hydrology in unfractured rock
6	37+37	Alpine+Blast	Topopah (Tptpmn)	Hydrology of Ghost Dance Flt (N)
7	50+64	Alpine Miner	Topopah (Tptpmn/ll)	Hydrology of Ghost Dance Flt (S)

Additional test alcoves are scheduled to be excavated in the Cross Block Drift within the proposed repository block and for hydrologic testing on the Solitario Canyon Fault.

The alcove studies are primarily focused on three areas: 1) hydrologic properties and transport on faults, including pneumatic permeability and contributions of faults to fast pathways through the rock mass; 2) transitional changes in rock matrix properties and state variables between welded and nonwelded hydrogeologic units, including water saturation, air k, Ksat, porosity, and geochemistry; and 3) thermal expansion, mineralogic alteration and hydrologic changes in the rock units of the proposed repository horizon that may be caused by heat from the spent nuclear fuel canisters.

Mapping in the tunnel is being performed by geologists from the U.S. Bureau of Reclamation under an agreement with the USGS. The USBR has an enormous amount of underground mapping experience from water diversion work and dam projects. The fresh rock faces exposed by the large TBM were cleaned with compressed air and mist, and mapping was done on a special gantry carried along on the trailing gear of the mining machine. This allowed the geologists to view the rock without the conveyor belt, ventilation line or utility pipes being in

the way. Three mapping activities were performed in the tunnel: 1) targets were placed on the ribs and roof using a laser surveying device and overlapping stereo photos taken of the entire tunnel, 2) up to 19 attributes (strike, dip, length, aperture, mineralization, terminations, etc.) were measured on fractures greater than 1 meter in length on a detailed line survey run at springline along the right rib of the tunnel, and 3) a full-periphery sketch map was drawn to show engineering features, geology and natural fractures encountered by the tunnel. The data are used for structural geology, hydrologic modeling and engineering design inputs. In the initial 5-mile loop, over 17,000 fractures were measured, 78 maps covering 100 meters of tunnel each have been drawn, and over 25,000 pages of photographic negatives have been archived. Full periphery mapping, detailed line surveys and photography were also done in the Cross Block Drift using an independent mapping platform that was moved along the tracks behind the TBM. The detailed line survey data in this excavation were input directly into "hardened" notebook computers taken underground.

Moisture Monitoring in the ESF: The objectives of this study are to determine the moisture balance within the Exploratory Studies Facility (ESF) and adjacent rock mass in response to water-vapor transport out of the ESF by the operation of the ventilation system. These data provide boundary conditions for the site-scale unsaturated-zone flow model as well as large-scale in situ moisture flow in the rock mass near the ESF. Air pressure, relative humidity, and temperature are monitored at various locations within the ESF. Limited measurements of water loss from the exposed rock surface are being made with time domain reflectrometry (TDR) and heat dissipation probes (HDP).

ESF Drift Scale Flux and Niche Study: The objective of this study is to (1) measure the field scale permeability of repository rock for use in the site-scale model and (2) quantify interaction and monitor fast flow paths and non-fast pathway zones. Following flow threshold testing, the niches will be sealed and allowed to equilibrate back to ambient conditions. The niche, rock surface, and boreholes are being instrumented to monitor the ambient conditions and detect changes associated with potential arrival of fast flow. Air pressure, relative humidity, and temperature are monitored in and out of the niche. Measurements of water loss or gain from the exposed rock surface are being made with time TDR and HDP. The boreholes are being monitored for air pressure and relative humidity using a packer system.

Characterization of Seepage into Alcoves: This activity combines a passive/active surface monitoring program with underground monitoring. Bulkheads in Alcoves 1 and 7 provide a monitoring environment most likely to induce seepage into the alcoves from fracture flow. The objective of the study is to identify and measure the location, timing, and quantities of infiltration and deep percolation fluxes at the potential repository level. Alcove 7 provides a location to investigate hydrologic conditions of the Ghost Dance fault at depth. Alcove 1 is shallow to the surface (37 m), fractured and provides good conditions to test the hypothesis that given a high enough flux, water will flow into and can be detected within emplacement drifts.

Alcove 7: Sensors have been installed at the tuff/alluvium interface and in the fault zone directly over the ESF and Alcove 7 to allow continuous monitoring of the soil moisture conditions and predict the likelihood of water flowing into fractures and/or the fault. Instrumentation installed in the alcove is monitoring relative humidity, temperature, changes of water potential and water content in the walls.

Alcove 1: Alcove 1 will have an infiltration experiment run at the surface that applies a continuous source of water above the alcove for a long period of time. The amount of water

applied will be monitored and environmental conditions estimated so that surface flux can be calculated. Instrumentation within the alcove includes HDP's, TDR, relative humidity, temperature, air pressure, and drip detection.

Surface Drilling Program

Since the late 1970's, a series of both shallow and deep boreholes have been drilled on and around Yucca Mountain to provide subsurface geologic and hydrologic information about the site. One of the first wells in the area was the J-13 water supply well on the east side of Fortymile Canyon, completed in January, 1963 to a depth of 3488 feet. It is producing water from fractured Topopah Spring Tuff at a depth of 1070 to 1301 feet (Doyle and Meyer, 1963). Depth to water measured one month after completion of the well was 928 feet below ground surface, or 2390 feet (728 meters) above sea level. Aquifer test data indicate that Well J-13 is capable of yielding at least 500 gpm, and the yield may be in excess of 700 gpm. This well has been the main water supply for Jackass Flats for the past 35 years. Well J-12, three miles south of J-13, was drilled in 1957 to a depth of 887 feet. It penetrates alluvium from the surface to a depth of 515 feet, and tuff to the bottom. Production is through perforations in the casing from 793 to 868 feet, but sustained yield is only about 95 gpm. Depth to water measured in January, 1960 was 741.4 feet below the ground surface, or 728 meters above sea level. A monitoring hole, designated JF-3, was drilled for the USGS-WRD a short distance south of J-12 in 1992.

Beginning in June of 1978, a series of geologic boreholes, designated UE-25a #1 through UE-25a#7 were drilled in the Midway Valley/Drillhole Wash area of Yucca Mountain for the Nevada Nuclear Waste Site Investigation (NNWSI), the precursor activity to the Yucca Mountain Project (Fenix &Scisson, Inc. 1987). These holes ranged in depth from 500 feet (UE-25a#4) to as deep as 2501 feet (UE-25a#1). The UE-25a#4 hole was instrumented, stemmed and grouted from 499 feet to the surface.

In March of 1980, the first of a series of deep geologic boreholes was begun with USW G-1 in Drillhole Wash. This hole was completed to a depth of 6000 feet, and was cased to 1016 feet. The lower portion of the hole is inaccessible, because a Sandia downhole geophone instrument became lodged at approximately 1100 feet in April, 1982, and remains in place. USW G-1 was drilled using "mud" containing a polymer for stable viscosity. During drilling, a lost circulation zone was encountered in fractured Topopah Spring Tuff, and a substantial quantity (some say as much as a million gallons) of the polymer mud was lost downhole. The hole was completed using foam, and drilling mud has been banned from Yucca Mountain ever since. The polymer material has been found in a perched water body at the base of the Topopah Spring Tuff penetrated by other holes in Drillhole Wash, including USW UZ-1 (drilled 1983), USW UZ-14 (drilled 1993), USW NRG-7/7A (drilled 1993) and USW SD-9 (drilled 1994). Other geologic holes were drilled in 1981 and 1982 at various locations around Yucca Mountain. USW G-2 was drilled to a depth of 6006 feet on Mile High Mesa in 1981-82. USW G-3 was drilled on the southern end of Yucca Crest from January to March, 1982. It was completed to a depth of 2364 feet, but had to be abandoned after a radioactive logging source was lost downhole below 1247 feet. The hole was plugged with cement from 1362 feet to 1160 feet, and a sidetrack hole was drilled from 1144 feet to the planned total depth of 5031 feet. A "geologic unsaturated-zone" hole, USW GU-3 was completed on the same pad as G-3 in June, 1982 to a depth of 2644 feet. A Sandia instrument was lost in this hole in May, 1987. USW G-4 was drilled in Coyote Wash to a depth of 3003 feet in 1983, and an angle hole, USW GA-1, was drilled across the

Solitario Canyon Fault on Mile High Mesa in March, 1981 (Fenix &Scisson, Inc. 1987).

The only hole drilled down through the volcanics into the underlying Paleozoic limestones is UE-25p #1, completed to a depth of 5923 feet in Midway Valley just west of Fran Ridge in May, 1983. This borehole taps both the volcanic aquifer and the much deeper Paleozoic aquifer. Test data indicate that these two aquifers contain water of different chemistry, temperature and hydraulic head (Craig and Johnson, 1984). "Leakage" between aquifers appears to be in an upward direction, i.e., from the Paleozoics into the volcanics. The location of UE-25p#1 was selected using geophysics to be emplaced on a "high" in the Paleozoic platform underlying the Tertiary volcanics. In most places around Yucca Mountain, gravity data indicate that the volcanic rocks are as much as 10,000 to 15,000 feet thick (Snyder and Carr, 1982).

A number of deep holes were drilled into the saturated zone for water level measurements and aquifer testing in the 1980's. These include UE-25b #1, completed to 4002 feet in 1981 in Drillhole Wash and the UE-25c holes, a multiwell set of three closely-spaced boreholes drilled to depths of 3000 feet in the southern end of Midway Valley in 1983-84 (Fenix &Scisson, Inc. 1987). A series of long-term, cross-hole hydraulic and transport tests have been run in the "c" holes since 1995 and are ongoing. Five hydrologic holes were drilled on and around Yucca Mountain in 1982. USW H-1 is in Drillhole Wash near the G-1 hole; it was completed to a depth of 6000 feet, then instrumented and grouted from 5950 to 2207 feet (Fenix &Scisson, Inc. 1987). USW H-3 and USW H-5 are at the south and north ends of Yucca Crest respectively. H-3 is 4000 feet deep, and notable because it has the greatest depth to water in the Yucca Mountain area: nearly 2300 feet. H-5 is also 4000 feet deep. USW H-4 is on the eastern flank of Yucca Mountain in Antler Wash, and USW H-6 is across Solitario Canyon on the east flank of Jet Ridge. Both of these holes are about 4000 feet deep (Fenix &Scisson, Inc. 1987). A series of water table measurement holes, designated WT-1 through WT-18 were drilled in 1983 and 1984 in various locations on and near Yucca Mountain. They range in depth from 1142 feet (WT-1) to 2043 feet (WT-18).

Numerous relatively shallow holes were drilled on Yucca Mountain in the 1980's and 1990's for unsaturated zone hydrologic monitoring and neutron logging of shallow infiltration. One hundred neutron access holes were drilled between 1984 and 1992. Most of these holes are only 30 to 50 feet deep, although a few are as deep as 250 feet (Fenix &Scisson, Inc. 1987). These holes were continuously logged on a monthly basis for a period of 10 years, producing a large infiltration data set.

Eight of the UZ hydrologic monitoring holes were drilled in the mid 1980's, and three more were drilled in the early 1990's. The newer holes were drilled with a special rig called the LM-300, manufactured by Lang Drilling specifically for the Yucca Mountain Project. It uses a dual-wall drill pipe system and compressed air as the circulating fluid. The rig is designed to core and drill with minumum exposure of the cut rock to the circulating air. The compressed air goes downhole through the inner drill string, passes across the bit to cool it and entrain the cuttings, and then returns uphole through the annulus between the inner and outer drill strings. This prevents air and cuttings from passing by rock exposed in the open hole and radically changing the hydrologic conditions. A number of these boreholes have had sensitive instruments in monitoring strings grouted into place. The instrumented UZ holes generally extend at least as deep as the proposed repository horizon, and monitor temperature, barometric pressure and relative humidity at different depths within the rock column. Most of the instrumented holes are located along the alignment of the Exploratory Studies Facility tunnel, to observe hydrologic

changes in the rock induced by the presence of a large "fast pathway" for air represented by the tunnel. Pneumatic connections and passage of a drying front have been observed in several of the monitored holes.

Other boreholes have been drilled by the Yucca Mountain Project to monitor and sample the volcanic aquifer in Crater Flat, collect engineering geology for the ESF tunnel, and gather systematic rock properties data for the site geologic framework model. All told, 230 accessible boreholes have been drilled on the Yucca Mountain Project, including two not yet completed: a systematic drilling hole (USW SD-6) on Yucca Crest, and a water table hole (USW WT-24) north of the repository block on Bleach Bone Ridge. This count does not include the dozens of seismic shot holes drilled on the site for various geophysical experiments in the 1980's and in 1994.

References Cited

Craig, R.W. and Johnson, K.A., 1984, Geohydrology of test well UE-25p#1, Yucca Mountain area, Nye County, Nevada: U.S. Geological Survey Open File Report 84-450, 63 p.

Doyle, Alan C. and Meyer, George L., 1963, Summary of hydraulic data and abridged lithologic log for ground-water test well 6 (J-13), Jackass Flats, Nevada Test Site, Nye County, Nevada: USGS Technical Letter NTS-50, April 26, 1963.

Fenix & Scisson, Inc., 1987, NNWSI drilling and mining sumary: Report DOE/NV/10322-24, July, 1987.

Snyder, D.B., and Carr, W.J., 1982, Preliminary results of gravity investigations at Yucca Mountain and vicinity, southern Nye County, Nevada: USGS Open File Report 82-701, 36 p.

DAY TWO--Saturday, October 10th, West Side of Yucca Mountain

We will leave the campsite at 7:30 am in private four wheel drive vehicles or the vans. Four wheel drive is required. We will not be going back onto the Nevada Test Site.

0.0	0.0	Return to the paved road from the camping area at Big Dune.
1.4	1.4	Turn north (left) on Valley View Dr.
3.6	2.2	Turn northwest (left) on Hwy 95.
3.8	0.2	The south end of Yucca Mountain is on the north side of the road, to the east (right) of the broad gap in the bedrock hills. Here the Crater Flat Tuff is exposed. The southernmost exposures of the Windy Wash fault, the westernmost major Quaternary block-bounding fault, defines the base of the western escarpment. Windy Wash exists from the alluviated gap in the bedrock hills. All of the drainage from western Yucca Mountain, Crater Flat, eastern Bare Mountain, and the mountainous areas to the north of Crater Flat exits through this gap.
6.7	2.9	On your right, near the base of the bedrock ridge to the west of the Windy Wash gap, are the distinctive white outcrops of the Horse Tooth Deposits. This and similar deposits to the south in Amargosa Valley consist of clays, marls, and limestones of paludal origin that yield U-series ages indicative of deposition during the last 2 pluvial periods. (We will visit these deposits on stop 2 of day 3.)
8.4	1.7	Sand Ramps at 3:00 on the flanks of the Will Carr Hills. This bedrock ridge contains complexly faulted Miocene volcanic tuffs intermixed with local slideblocks of highly brecciated Paleozoic sedimentary rocks. The bright white deposit toward the base on the north end is an outcrop of the Bishop ash (730 ka).
9.8	1.4	South side of road, remnants of Q1 alluvium are preserved about the younger Q5 sand that covers the landscape.
10.2	0.4	The dark-colored peak to the north (right) is Black Marble Mountain, a slide block of brecciated Bonanza King (Pz), that in places overlies Tertiary volcanic rocks.
10.7	0.5	Turn right onto the Steve's Pass Rd. into Crater Flat.
12.3	1.6	Steve's Pass-- Nice overview of Crater Flat with the elongate crest of Yucca Mountain in the distance to the east. The dirt road extending eastward along the southern margin of Crater Flat essentially follows the path of the original stagecoach road that was noted in Jackass Flats east of Yucca Mountain and passes through some low hills near the south end of the mountain. The low dark hills in the middle of the basin are early Quaternary (0.7 -1.1 mya) basalt cones.

Page numbers 142-149 skipped

A Quaternary alluvial stratigraphy was developed and mapped independently from the Yucca Mountain mapping program for the State of Nevada by F. Peterson, J. Bell, A. Ramelli and others (see Bell and others, this volume; also Peterson and others, 1995). They defined a chronosequence of six allostratigraphic units in eastern Crater Flat piedmont based on topographic relations, surficial characteristics, and soil stratigraphy. Age control for the units were provided primarily by rock-varnish C^{14} AMS and cation-ratio dating techniques, with support from U-series dating of secondary pedogenic carbonate. The units and ages generally correlate with the Yucca Mountain sequence, except they described and mapped a more prominent unit of latest Pleistocene (late Wisconsin) age. This work will be discussed in stops 1, 2, and 3 (optional).

12.5 0.2 Crossing trace of the Bare Mountain fault.

13.3 0.8 **Stop 1 (8:00-9:00) Crater Flat Quaternary Stratigraphy** The Little Cones unit here is a broad fan-piedmont remnant surrounding the Little Cones basalt flow at 3:00. The Little Cones surface here is little dissected and stands 1-2 m higher than the younger Crater Flat unit to the east. The northern edge of the remnant grades into a slightly higher Late Black Cone remnant along a diffuse, feathered boundary. West of the road, the Bare Mountain piedmont is largely of Crater Flat-age and is inset slightly below the Little Cones surface. Pedon CFP-26 illustrates soil features commonly found in the Little Cones unit. The Av horizon is only 5 cm thick, and it is coarsely vesicular. The Bk horizon is late Stage I that has relatively thick pebble-bottom coatings.

16.2 2.9 Turn east (right) onto road to VH-1 and Solitario Canyon. Just southeast of the junction a pit exposes the Late Black Cone soil which at this location is a calciorthid.

16.6 0.4 Crossing Crater Flat Wash

18.1 1.5 Junction with road to well VH-2; proceed straight passing between Red Cone basalt flow on the south and Black Cone basalt flow on the north.

18.9 0.8 **Stop 2 (9:00-10:30) Crater Flat Quaternary Stratigraphy** Walk north off of road toward Black Cone basalt flow. At this locality, the Late Black Cone unit is an elongate fan-piedmont remnant and is the site of pedon CFP-32. The soil is a haplic durargid formed in volcanic alluvium. It has a moderately thick Av horizon, a minimal argillic horizon with a low clay content, and a weakly cemented haplic duripan containing a single thin lamina.

19.7 0.8 Veer north (left) at the VH-1 drill pad; proceed to northeast across a large Early Black Cone fan-piedmont remnant originating from Solitario Canyon.

21.1 1.4 **Stop 3 (optional)** Junction with road to Windy Wash trenches. On the southwest

corner of the junction, a pit exposes an Early Black Cone soil (pedon CFP-29). This is a good example of an Early Black Cone Typic Durargid that has a strongly reddened (7.5 YR), sticky, plastic, opalized argillic horizon and a cemented duripan.

23.1 2.0 The road crosses a modified scarp developed on the Fatigue Wash fault, which is major Quaternary fault on the west side of Yucca Mountain that merges at either end with the Windy Wash fault. Carbonate cement and breccia in the fault zone is exposed in the road here.

23.6 0.5 Turn southeast (right). There is a nice exposure of the Ranier Mesa tuff (white) in depositional contact with the Tiva Canyon tuff (dark) at 10:00. The Rainer Mesa tuff is typically deposited in sags or grabens formed in the Tiva Canyon tuff in the Yucca Mountain area. Note Big Dune at 2:00.

25.5 1.9 **Stop 3 (10:30-Lunch) Solitario Canyon Fault** Solitario Canyon fault, the largest Quaternary fault on the west side of Yucca Mountain, follows the base of the major bedrock escarpment ahead with the Yucca Mountain crest (stop 1, day 1) on the skyline above. (turn around and park; reset odometer; take your lunch, then walk up the road to the trench on the fault at the base of the escarpment).

> Ramelli--Trench 8--Late Quaternary paleoseismicity of the Solitario Canyon fault; age control on events and trench stratigraphy and soils; basaltic ash in fault fissure (see Ramelli, this volume)

Trench 8 (fig. 7) was originally excavated in the early 1980's and deepened and extended in 1992. Three additional trenches were cut in 1993-94 across the section of the fault beneath the main western escarpment of Yucca Mountain (two can be seen to the south) to help correlate events along the fault trace and provide the best possible exposures of the most recent event. The complete paleoseismic record, consisting of four displacement events and two possible fracturing events, is best expressed in this trench, although many of the events, and particularly event (Y) with the fissure filling basaltic ash, can be identified in all of the trenches. Many of the colluvial units in both hanging wall and foot wall positions in the trenches are very old (middle to early Pleistocene), based on U-series ages of secondary carbonate and opaline silica from dense inner rinds coating clasts in the associated thick petrocalcic soils.

> Whitney, Harrington--Colluvial boulder deposits, evidence of creep, deformed hillslope deposits

We will walk past one of the darkly varnished colluvial boulder deposits on the bedrock escarpment above and to the right of the trench. This is one of the colluvial units described in Whitney and Harrington (1993) with an estimated ages of middle to early Quaternary based on cation-ratio dating of rock varnish.

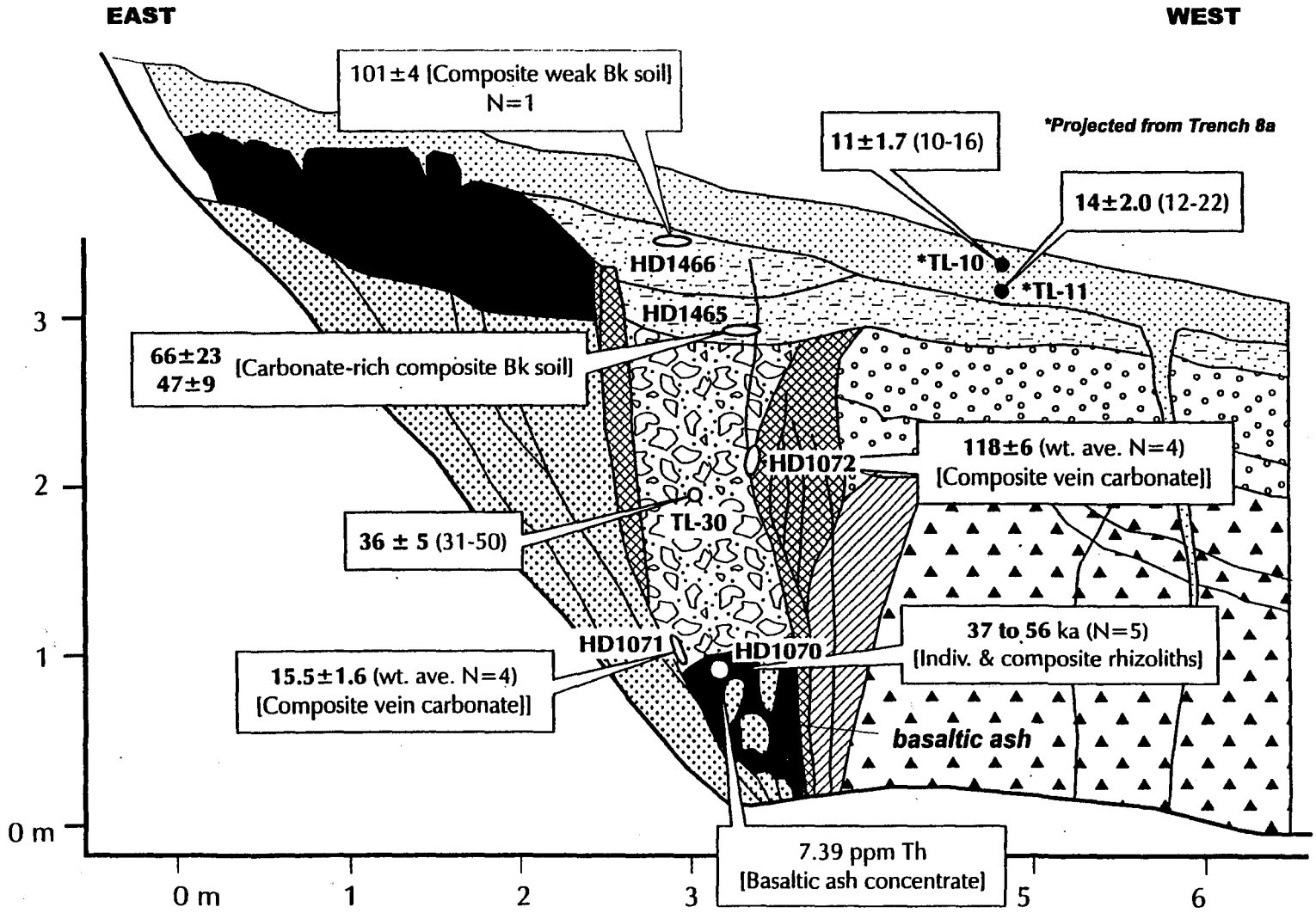

Figure 7: Geologic log for the south wall, Solitario Canyon fault Trench 8, showing fissure event. TL samples are shown for Trench 8a, both from vesicular A horizons. General agreement is shown between the U-series and TL for samples from the fissure event.

The morphology, topographic position and ages of these boulder deposits have been used to infer very slow rates of hillslope erosion in the Yucca Mountain area, an inference supported by subsequent exposure dating of bedrock outcrop and colluvial deposits on the hillslopes (Gosse and others, 1996).

Reheis-- Seismic significance of precariously balanced rocks (see Reheis, this volume); Composition and sources of dust in rock cavities.

J. Brune, J. Whitney, and others have proposed that the presence or absence of precariously balanced rocks erosionally isolated from bedrock outcrops on hillslopes can be used as an indicator of the recency of significant vibratory ground motions. Experimental and theoretical calculations have established that precariously balanced rocks of particular size and geometry will be toppled off their pedestals by ground motion above a threshold acceleration (e.g.., 0.1 g). Observations in seismically active regions of California and Nevada indicate the absence of precarious rocks near large active faults. Conversely, the presence of many varnished precariously balanced rocks in the Yucca Mountain area implies the absence of large ground motion accelerations in at least the past several years. The time since the last ground motions above the indicated threshold can be estimated if the age of the precariously balanced rocks can be determined. Voids and cavities in these rocks also contain fine-grained dust that is compositionally similar to modern sources of dust in the Amargosa Valley.

Return to cars and drive back to the main road that runs along the western edge of Bare Mountain and eventually goes over Steve's Pass.

29.5 4.0 East side of Bare Mountain is straight ahead. Bare Mountain is a relatively small, triangular mountain range roughly 20 km long in a north-south direction and about 10 km wide at its widest point. In contrast to the volcanic terrain that we saw yesterday and this morning at Yucca Mountain, Bare Mountain is composed primarily of late Proterozoic and Paleozoic sedimentary rocks. These rocks are weakly metamorphosed, folded, and faulted, and dip generally northward. Overlying the sedimentary rocks on the north flank of Bare Mountain is a sequence of Tertiary volcanic rocks that were erupted from the Timber Mountain caldera complex about 20 km to the NE (about 4:00). From the east, Bare Mountain has a profile typical of many ranges in the Basin and Range province. It is quite symmetrical with the highest part of the range (elevation 1925 m) located near the center of the range between the Tates Wash area on the north and Steve's Pass at the south. When compared to the volcanic ranges north and east of Bare Mountain, such as Yucca Mountain, both flanks of Bare Mountain are impressively steep, which gives an overall impression of tectonic youthfulness.

34.5 5.0 Turn south (left) on to the main road, toward Steve's Pass.

36.5 2.0 Turn west (right) toward Bare Mountain on the dirt road.

36.8 0.3 Turn south (hard left) on the dirt road.

37.6 0.8 Park and walk east about 0.5 mi to trench 3

Stop 3 (12:30-3:00) The Bare Mountain fault.

Anderson, Klinger, Ferrill, Stamatakos – Bare Mountain fault (see Anderson and Klinger, this volume)

At this stop, we will discuss the geomorphology of the alluvial fans and how their size may reflect fault activity on the Bare Mountain fault, evidence for or against a low slip rate, whether slip varies along strike, fault scarp morphology, and paleoseismic interpretations from trench BMT-3.

Return to the cars and drive straight ahead and over Steve's Pass to Hwy 95.

38.5 0.9 Turn southwest (right) and rejoin main Crater Flat Road

40.3 1.8 Turn north (right) on Hwy 95 toward Beatty.

42.1 1.8 Q1 alluvium at 3:00.

42.5 0.4 Q1 alluvium at 9:00.

43.1 0.6 Turn west (left) into the USA Ecology site.

Stop 4 (3:00-5:00) Hydrogeologic studies at USGS Amargosa Desert Research Site

Andraski, Stonestrom--Unsaturated zone studies; Artificial trenches, effects of disturbance on water movement/balance in the near-surface environment; Liquid and gas flow throughout the 100+ m thick UZ; Tritium and carbon-14 migration (see Andraski and others, this volume)

Andraski, Stonestrom--Stream flow; Thermal detection of stream flows in ungaged arroyos

At this site we will discuss ongoing multidisciplinary collaborative research between the U.S. Geological Survey and other universities, research institutes, and national laboratories concerning the unsaturated zone hydrology in the Amargosa Desert related to interaction with the Beatty low-level radioactive waste burial facility. The overall objective for research at the Amargosa Desert Research Site is to improve understanding of and methods for characterizing mechanisms that control subsurface migration and fate of contaminants in arid environments.

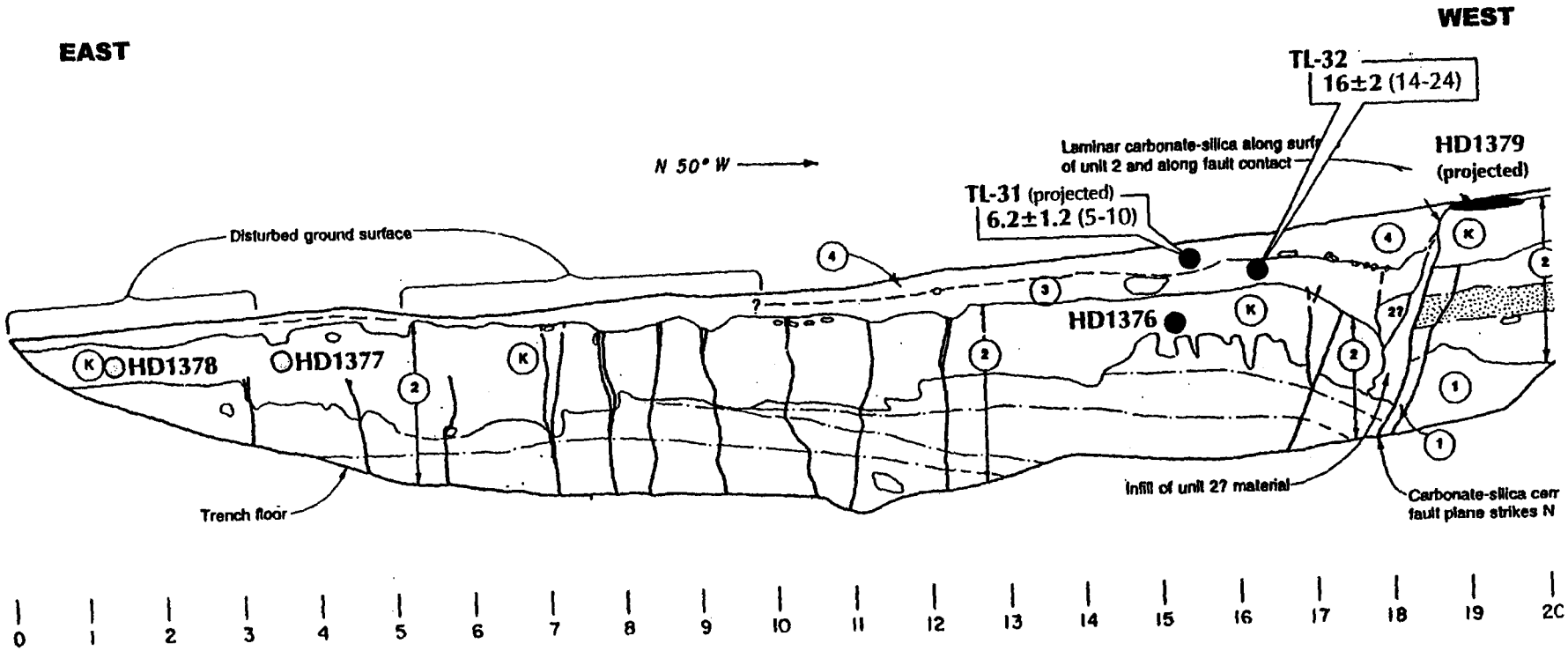

Figure 8: Bare Mountain Fault Trench (BM-T1) sketch of north wall, showing TL samples taken in the vesicular A horizon and Unit 3 of a gravelly-silt rich Pleistocene alluvium. The U-series samples had excess detrital corrections and thus no age could be calculated.

45.7 2.6 Site of Carrara, built to process Carrara Frm marble mined from Bare Mountain. Between 1913 and 1916 the town of Carrara had approximately 40 buildings and even a large water fountain. The town was built to process "marble" quarried from the Carrara Formation at a site about 3 miles east of town up Carrara Canyon. A cable operated railroad (roadbed still visible heading east up the alluvial fan) hauled the marble from the quarry to Carrara where it was processed and loaded on the Las Vegas and Tonapah (TV&T) Railroad or the Tonapah and Tidewater (T&T) Railroad. The LV&T operated between 1906-1918 and the roadbed basically lies beneath Highway 95. The main roadbed for the T&T lies about ½ mile west of Carrara. The ruins located east of the highway (12:00) that many people think are those of Carrara are actually those of a proposed cement operation built by the Elizalde Company in the 1930's that never materialized.

47.4 1.7 **Stop 5 (5:00-end) Beatty Scarp.** At this stop, we will discuss the age and geomorphic significance of the Beatty scarp. The scarp at this location is about the same height as the fault scarps associated with the Bare Mountain fault at Stop 3. At this stop we will also discuss the postulated Carrara fault.

> Yount, Anderson, Klinger-- Beatty Scarp (see Anderson and Klinger, second paper, this volume).
>
> Stamatakos, Anderson, Klinger-- Carrara Fault (see Anderson and Klinger, second paper, this volume).

The Beatty scarp strikes north to north-northwest for about 11 km along the west side of Bare Mountain and parallel and east of to Highway 95. Its apparent down-to-the-west character suggests a possible fault origin, however, the scarp generally follows the contact between the alluvial fans emanating from Bare Mountain and the fluvial deposits of the Amargosa River (8:00 to 11:30). The Beatty scarp was first mapped by Cornwall and Kleinhampl (1961a, 1961b, 1964) and later by Carr (1984), who identified it as a Quaternary fault. Swadley et al. (1986) concluded that the Beatty scarp probably was formed by fluvial erosion, but they also suggested that the feature could be an older fault scarp that had been modified by fluvial erosion. On the surficial geologic map of the Bare Mountain quadrangle by Swadley and Parrish (1988), the Beatty scarp is shown as a fluvial scarp, and in a subsequent article (Swadley *et al.,* 1988), the scarp is reinterpreted to be the direct result of fluvial erosion by the Amargosa River.

The Carrara fault is a proposed primarily strike-slip Quaternary fault (Slemmons, 1997; Stamatokos, 1997) that strikes northwest essentially following the broad distributary channel system of the Amargosa River where it parallels Highway 95 between the Beatty scarps and the south end of Bare Mountain. The presence of some buried fault has been interpreted from detailed gravity and aeromagnetic surveys between the town of Carrara and Steve's Pass road. Quaternary activity on the fault is proposed based on the presence of a series of possible topographic

fault scarps and differential heights of adjoining surfaces ascribed to tectonic uplift. However, most of these ambiguous features occur within or on the margin of the Amargosa River channel system, and thus a nontectonic fluvial origin is equally or more likely.

48.6 1.2 3:00 Beatty scarp again.

50.1 1.5 3:00 Beatty scarp still.

50.4 0.3 3:00 Beatty Scarp Trench (BF-2)

51.2 0.8 Beatty Scarp Trench (BF-1); directly east of Airport Road. The age of the Beatty scarp is constrained by three radiocarbon ages. One of those ages, 10,000±300 C^{14} yrs (10,450 to 12,550 cal yr. B.P.), came from a fragment of carbonized wood fragments recovered from a silt bed interbedded with fluvial sand and gravel in trench BF-1. The maximum scarp height of 29.5 m and a maximum scarp-slope angle of 35° along the Beatty scarp were measured at this site adjacent to the trench.

52.2 1.0 Amargosa River. The Amargosa River is an ephemeral stream that originates near the northern end of Oasis Valley, about 15 km north of the town of Beatty. The river flows south through Oasis Valley before exiting the valley immediately south of Beatty through the Amargosa Narrows (12:00). The Narrows separate the Bullfrog Hills on the west from Bare Mountain on the east..

52.4 0.2 3:00 Beatty scarp

53.1 0.7 Fluorspar Canyon. Low young terrace along the Amargosa River. Large city of Beatty is ahead awaiting your money.

DAY THREE--Sunday, October 11th, Paleodischarge deposits in the Yucca Mountain area

0.0 0.0 Return to the paved road from the camping area at Big Dune.

1.4 1.4 Turn north (left) on Valley View Dr.

2.2 Turn northwest (left) on Hwy 95.

1.6 Turn north (right) off of Hwy 95, through the BLM gate. The low lying white deposits on your right are paleodischarge deposits. We are driving up the southern extent of Windy Wash.

1.2 Stay on the high terrace road, rather than the sandy wash.

0.7 Veer to the left, following the wash into the divide created by the 3.7 my basalt on the north and the light colored Ammonia Tanks Member of the Timber Mountain Tuff on the south. Continue up the main wash until the wash is filled with a trench spoil pile. All surface water from Crater Flat flows through this divide.

0.9 **Stop 1 (8:30-10:00) Southern Crater Flat Discharge Deposits**

Paleoclimatic implications of the deposits and their relationship to regional surface flow and the modern ground water (figs. 12 and 13)

2.8 Return to the cars and drive back to Hwy 95. If you want to see similar paleodischarge deposits, turn north (right). If you want to visit the Lathrop Wells cinder cone and see the stratigraphy and dating sites, turn south (left).

1.7 N **Stop 2 (10:00-End) Horse tooth deposit**

Age control and paleoclimatic implications--Paces and others results (fig

3.4 S **Stop 2 (10:00-End) Lathrop Wells Cinder Cone**

This is an optional stop to informally examine the Lathrop Wells cinder cone, focusing on the long-standing controversies concerning polygenetic vs. monogenetic origin and age of eruption(s) (see earlier summary at mile 1.4 on first day, fig. 14).

DAY THREE--Sunday, October 11th, Paleodischarge deposits in the Yucca Mountain area

0.0 0.0 Return to the paved road from the camping area at Big Dune.

1.4 1.4 Turn north (left) on Valley View Dr.

3.6 2.2 Turn northwest (left) on Hwy 95.

5.2 1.6 Turn north (right) off of Hwy 95, through the BLM gate. The low lying white deposits on your right are paleodischarge deposits. We are driving up the southern extent of Windy Wash.

6.4 1.2 Stay on the high terrace road, rather than the sandy wash.

7.1 0.7 Veer to the left, following the wash into the divide created by the 3.7 my basalt on the north and the light colored Ammonia Tanks Member of the Timber Mountain Tuff on the south. Continue up the main wash until the wash is filled with a trench spoil pile. All surface water from Crater Flat flows through this divide.

8.0 0.9 **Stop 1 (8:30-10:00) Southern Crater Flat Discharge Deposits**

Paleoclimatic implications of the deposits and their relationship to regional surface flow and the modern ground water (figs. 12 and 13)

10.8 2.8 Return to the cars and drive back to Hwy 95. If you want to see similar paleodischarge deposits, turn north (right). If you want to visit the Lathrop Wells cinder cone and see the stratigraphy and dating sites, turn south (left).

1.7 N **Stop 2 (10:00-End) Horse tooth deposit**

Age control and paleoclimatic implications--Paces and others results (fig

3.4 S **Stop 2 (10:00-End) Lathrop Wells Cinder Cone**

This is an optional stop to informally examine the Lathrop Wells cinder cone, focusing on the long-standing controversies concerning polygenetic vs. monogenetic origin and age of eruption(s) (see earlier summary at mile 1.4 on first day, fig. 14).

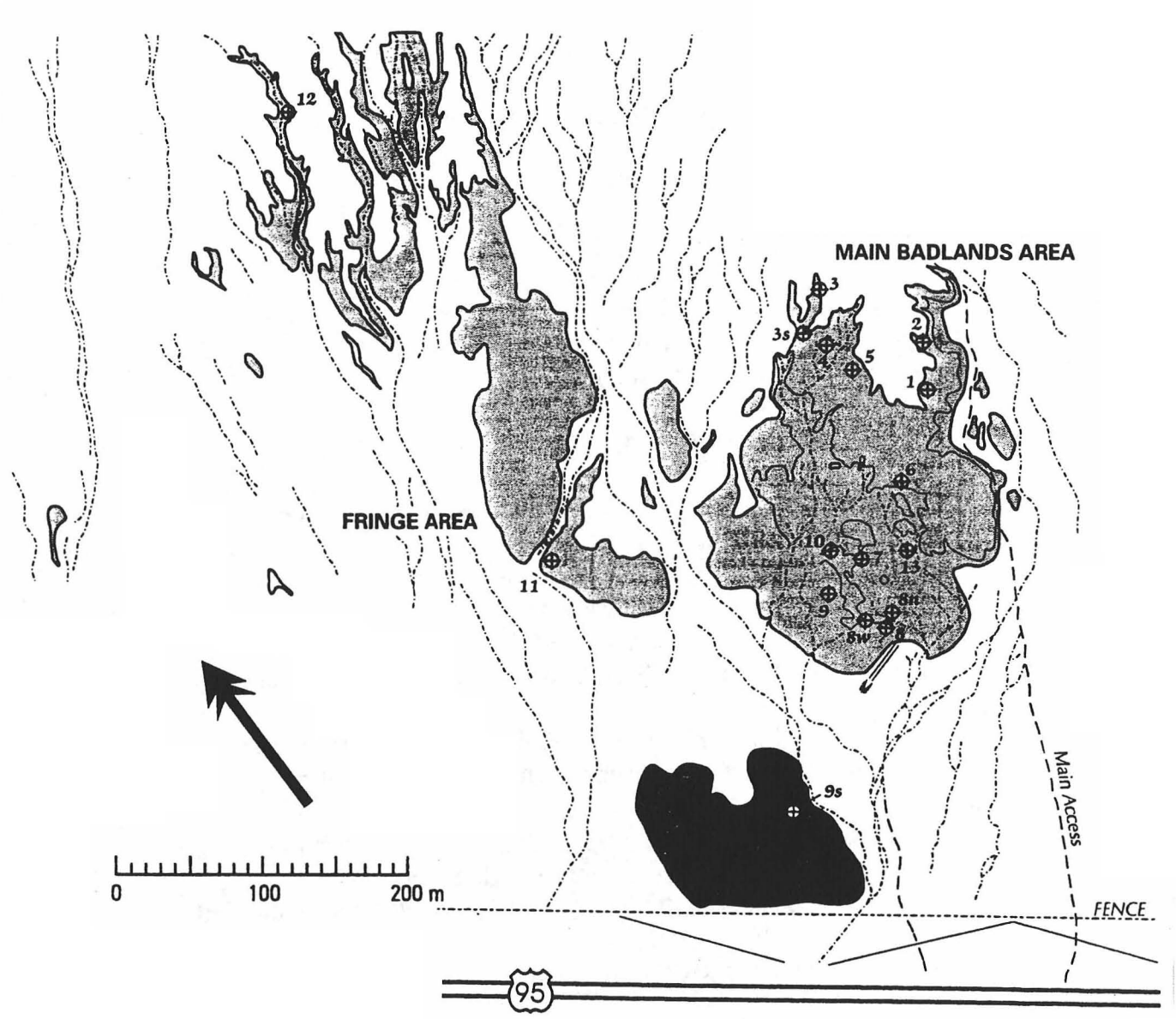

Figure 9: Sketch of air photos showing major morphologic features of the Lathrop Wells Diatomite deposit. Light-colored, fine-grained deposits are shown as light-shaded areas. Area with platy veneer of banded dense limestone shown with darker-shading. Numbered stations are shown with circle/cross symbol. Dash-dot lines represent drainage channels. Light-solid lines within boundary of the main badlands area represent prominent cliffs separating topographically high areas (mostly north half) from low areas (mostly south half).

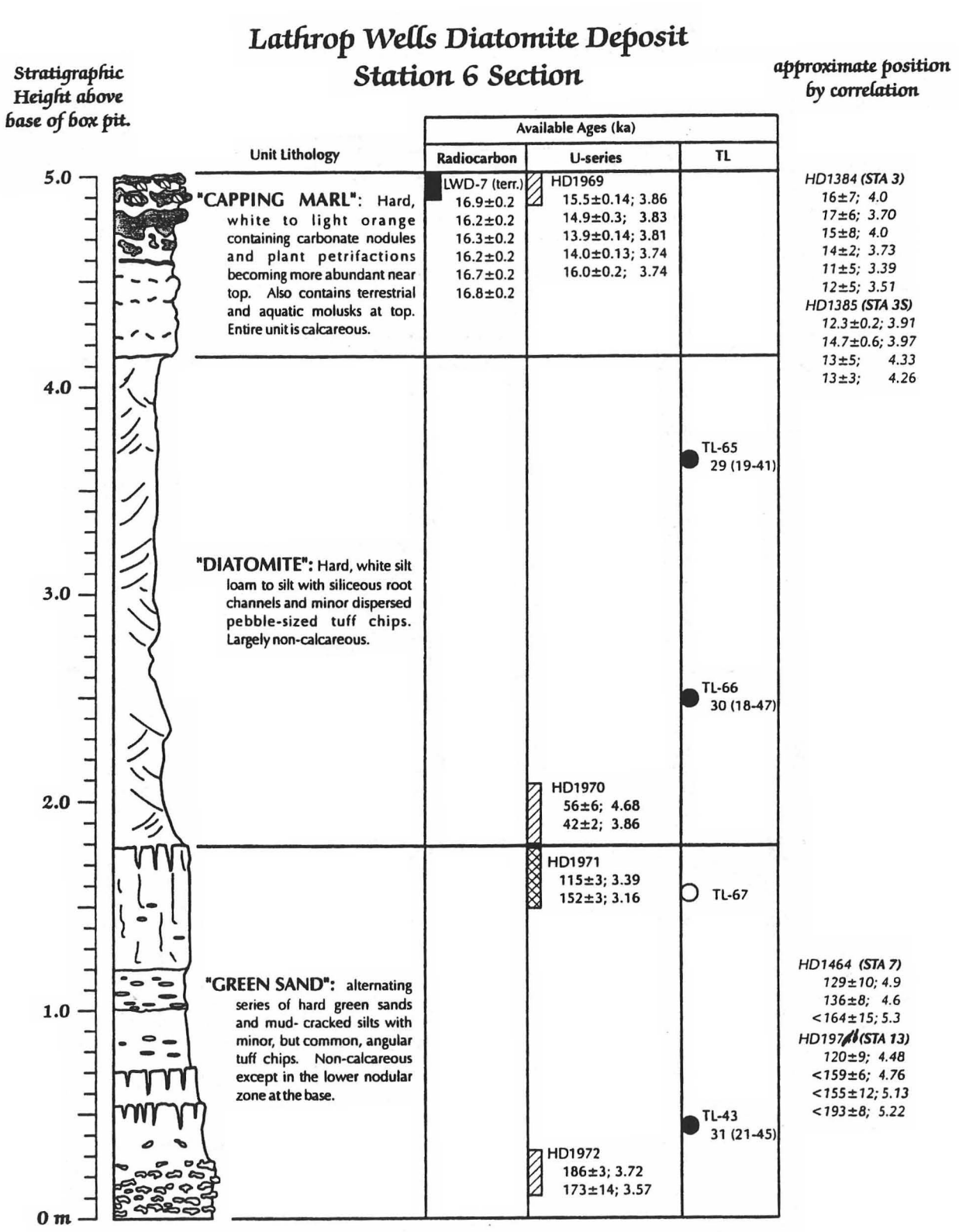

Figure 10: Measured stratigraphic section at LWD Station 6 with age determinations from TL, U-series and radiocarbon. No age was reported for TL-65 as it had unstable luminescence. This could be a result of translocation, incomplete sunlight exposure or bad sampling. All uncertainties quoted at the 95% confidence level. U-series dates to the right of the column are correlated by position within the general stratigraphy.

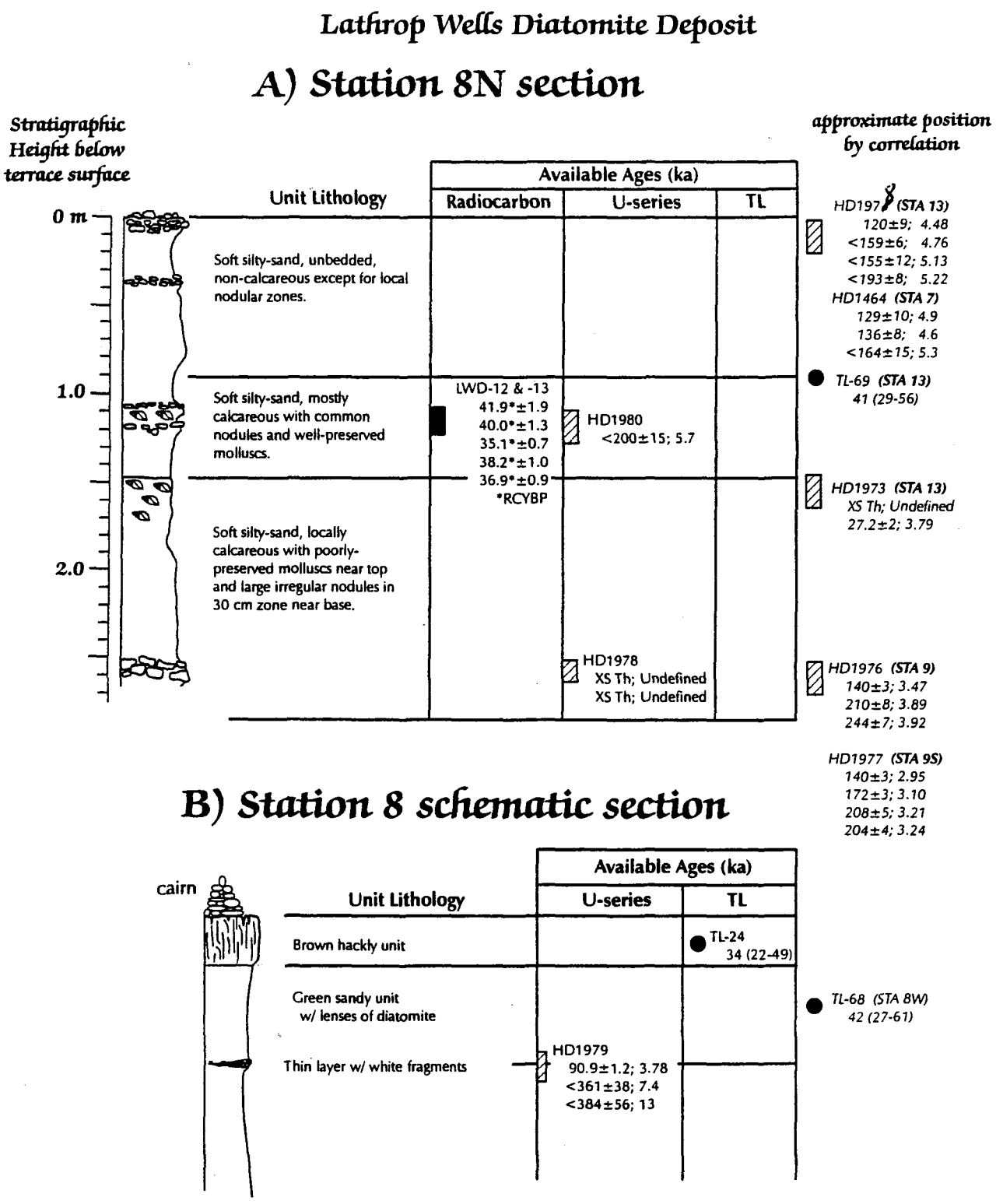

Figure 11: Stratigraphic sections at LVWD stations 8N and 8 with radiocarbon, TL and U-series ages. Radiocarbon ages are given in radiocarbon years before present (RCYBP) and have not been calibrated for the effects of non-linear radiocarbon production rates. A) measured stratigraphic section at station 8N B) schematic section from pit at station 8.

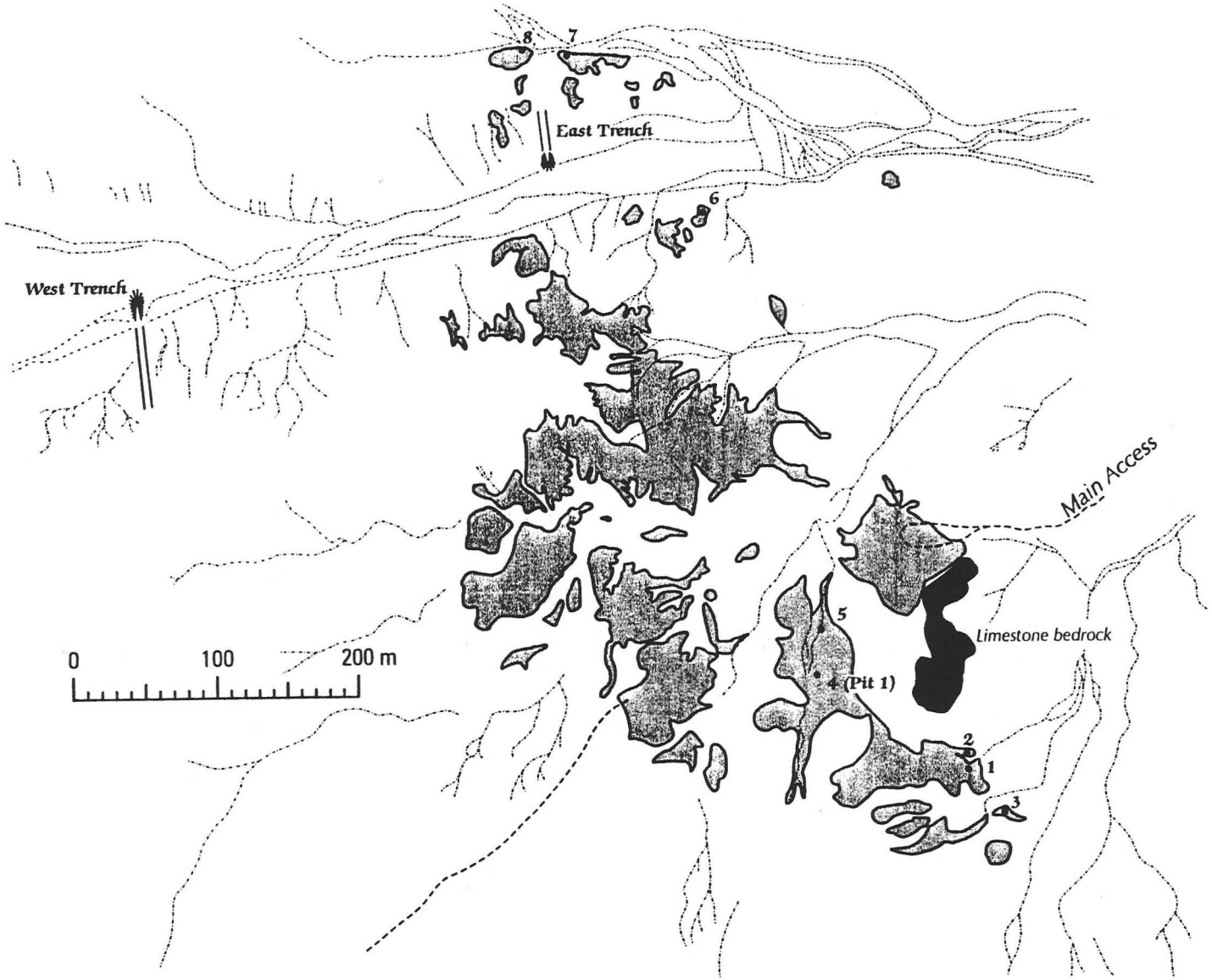

Figure 12: Sketch of air photos showing major morphic features of the Crater Flat Deposit (CFD). Light-colored, fine-grained deposits are shown as light-shaded areas. Numbered sample stations are shown with small black circles. Dash-dot lines represent drainage channels. North is towards top of sketch.

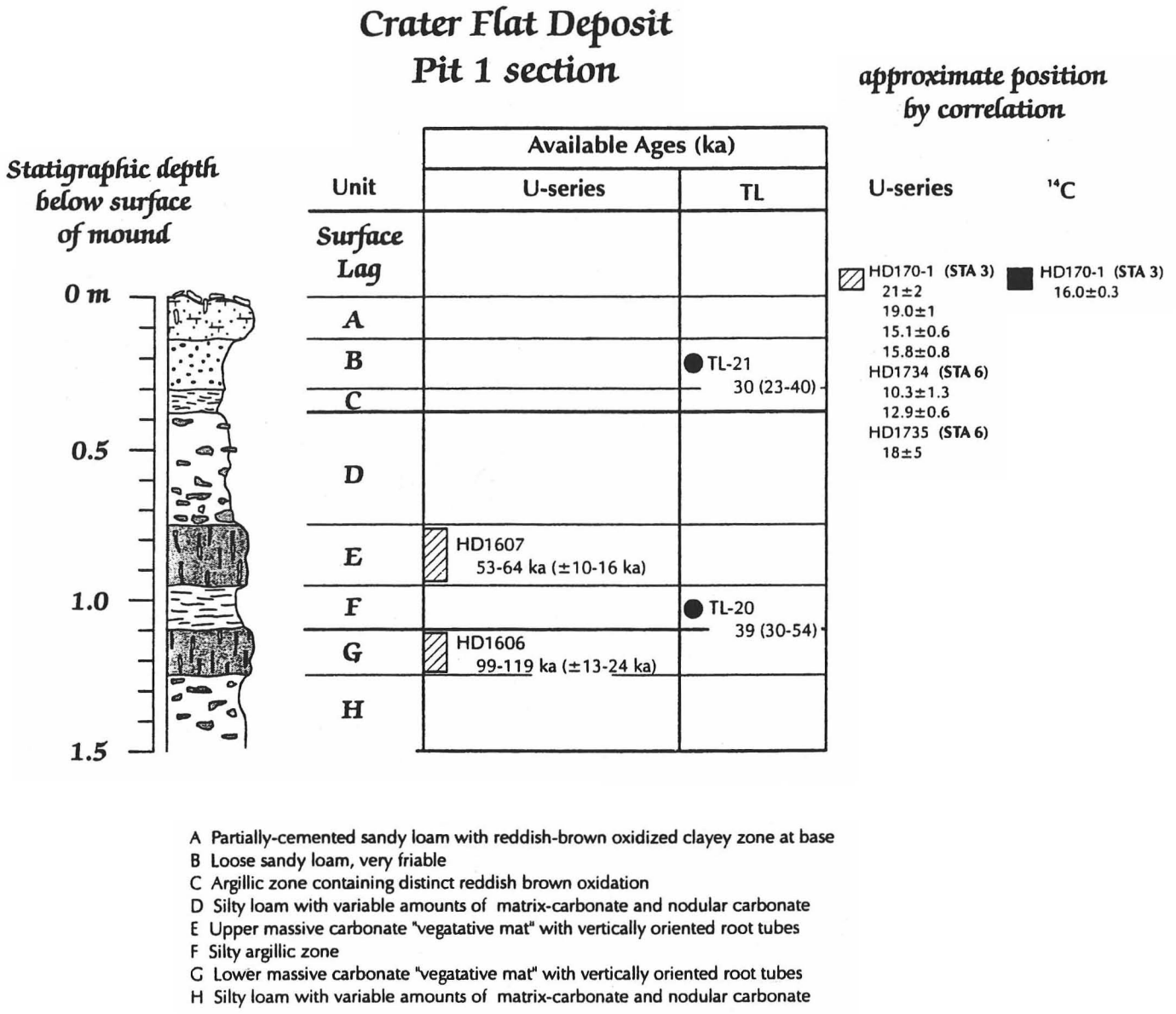

Figure 13: Measured stratigraphic section from Pit 1 at Station 4, CFD, with age determinations. U-series ages for HD1606 and HD1607 are given as a range from five individual determinations on carbonate cement with high detrial-Th corrections and large uncertainties on individual determinations. Age data to the right of the collected by position within the general stratigraphy.

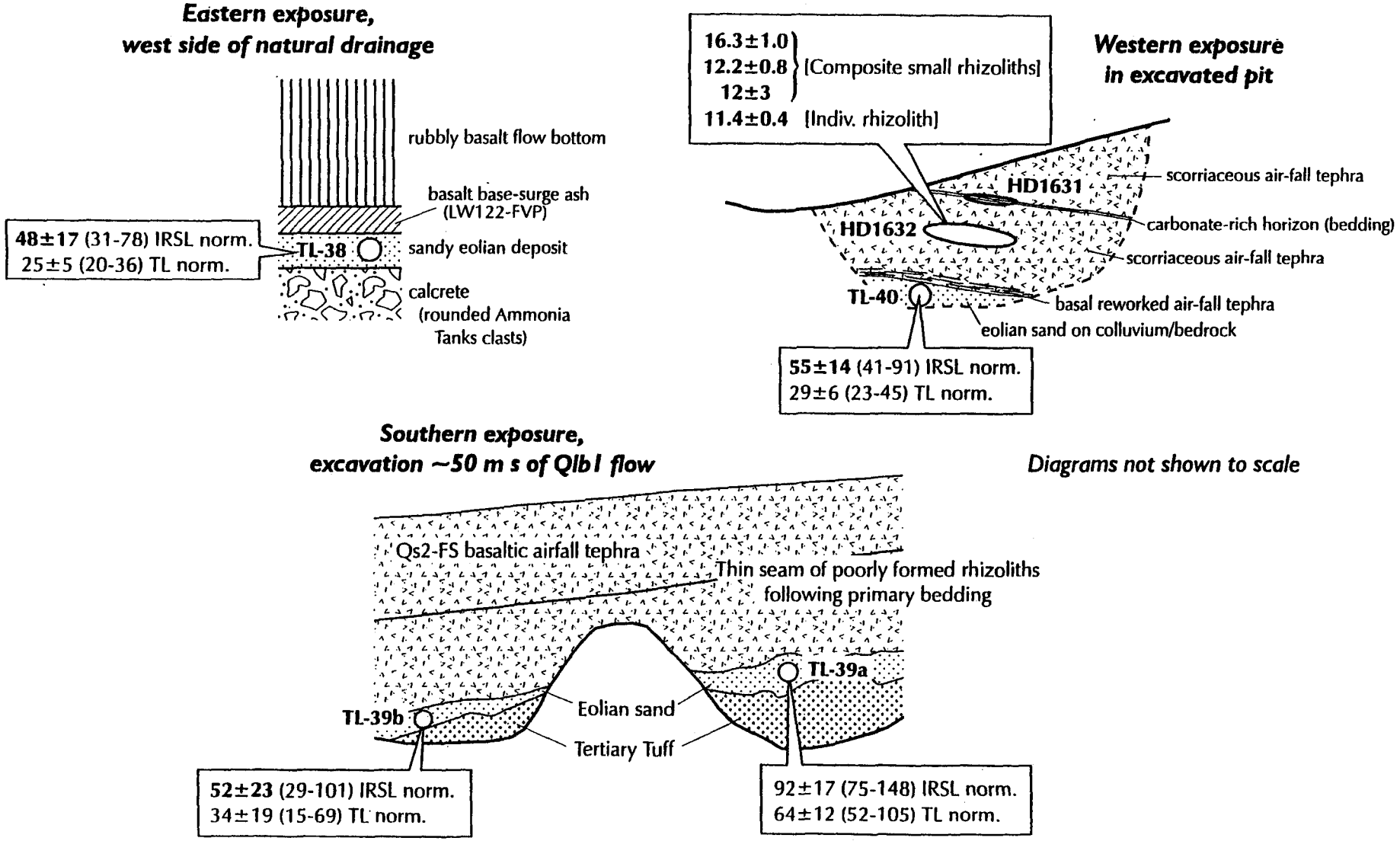

Figure 14: Schematic diagrams showing sample relations associated with Unit Qs2-FS (basaltic airfall tephra event number 2) proximal to Lathrop Wells cinder cone. Samples collected from the three localities described as Eastern, western and Southern exposure.

Day 2, Stops 1, 2 and 3 (optional)

Late Quaternary Geology of Crater Flat

John W. Bell, Fred F. Peterson, Alan R. Ramelli

Geologic Setting

Crater Flat is an alluvium-filled structural basin on the west side of Yucca Mountain (Figure 1). A series of north-trending, west-dipping late Quaternary faults offset the basin alluvium on the east, and the east-dipping Bare Mountain fault bounds the basin on the west. The Quaternary basin fill is predominantly derived from several large drainages originating within the Miocene volcanic tuff rocks comprising Yucca Mountain, with lesser amounts of alluvium originating from the carbonate and metamorphic terrane of Bare Mountain. The central floor of Crater Flat is marked by four Quaternary (0.7-1.1 Ma) basalt cones aligned in a 12-km-long northeast-trending belt.

Figure 1. Location map showing Yucca Mountain, Bare Mountain, and Crater Flat area.

Stratigraphy

We mapped late Quaternary geomorphic surfaces using topographic relations, surficial characteristics, and soils to establish boundaries and to characterize the units as *allostratigraphic units*. A summary of these relations is provided here, and more detailed discussions of these studies are contained in Faulds and others (1994) and Peterson and others (1995).

Six major allostratigraphic units comprise the piedmont slopes and valley floor surfaces of Crater Flat: from youngest to oldest, they are the Crater Flat, Little Cones, Late Black Cone, Early Black Cone, Yucca, and Solitario units (Figure 2). Surficial relations such as inset topography, desert pavement, and rock varnish provide the basis for relative age characterization of the units. In addition, presence or absence and degree of differentiation of six genetic soil horizons help identify and separate the geomorphic surfaces: the vesicular A horizon (*Av*); a recarbonated lower-A subhorizon (*Ak*); a cambic or cambic-like horizon (*Bw*); various argillic horizons (*Bt, Btk, Btkq*); a strongly opalized argillic subhorizon (*Btkq*); and duripans (*Bqkm*). Illustrative pedons are listed in Table 1.

Figure 2. Allostratigraphic map of Crater Flat.

Table 1. Illustrative pedons for Crater flat allostratigraphic units.

Crater Flat Unit

The Crater Flat unit consists of active and recently active washes, inset fans, fan skirts, and fan aprons (landform terms are from Peterson, 1981). It is erosionally inset below all older

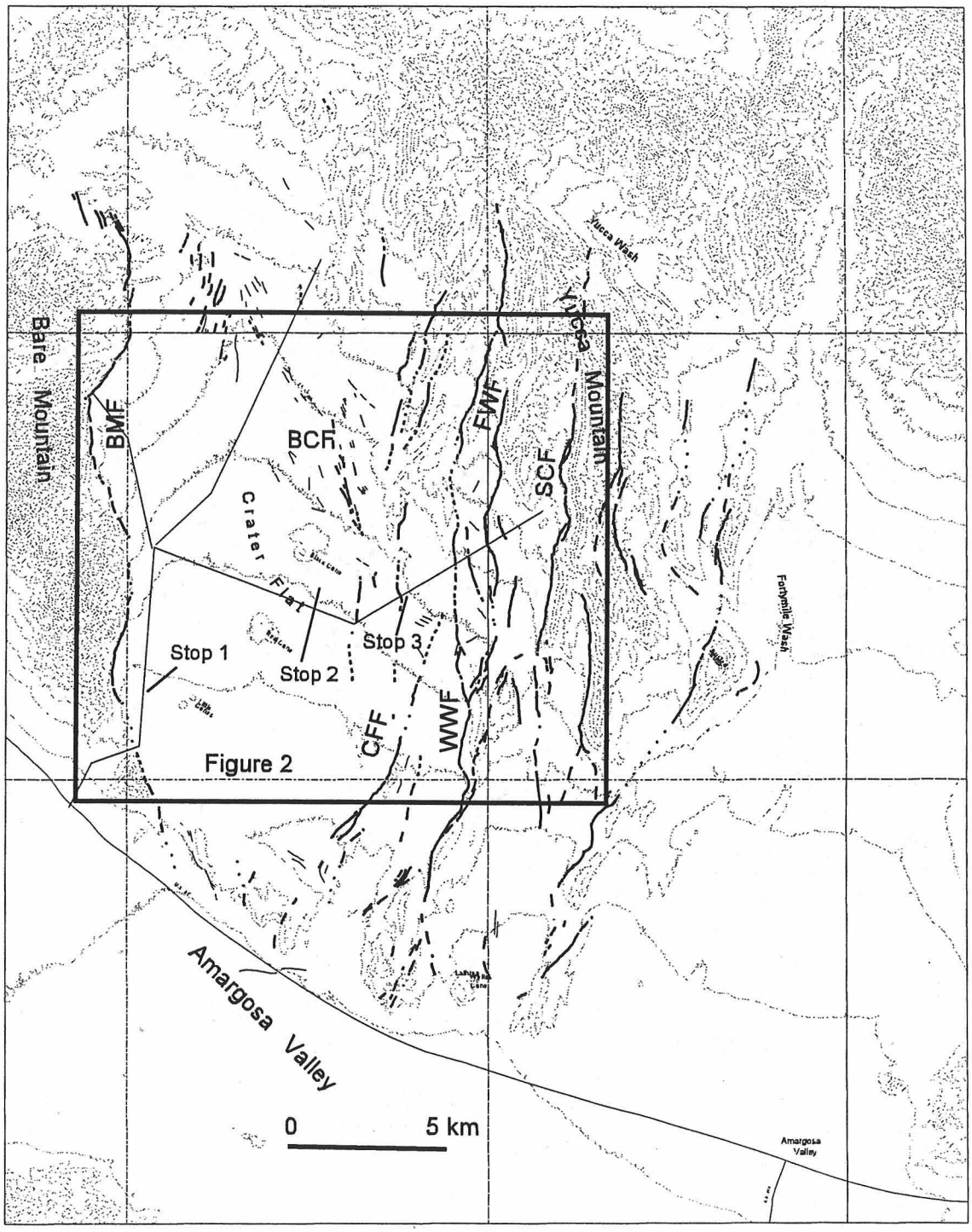

Figure 1. Location map showing Yucca Mountain, Bare Mountain, and Crater Flat area. Base map shows known or suspected regional Quaternary faults. Principal late Quaternary faults include Solitario Canyon (SCF), Fatigue Wash (FWF), Windy Wash (WWF), Crater Flat (CFF), Black Cone (BCF), and Bare Mountain (BMF) faults.

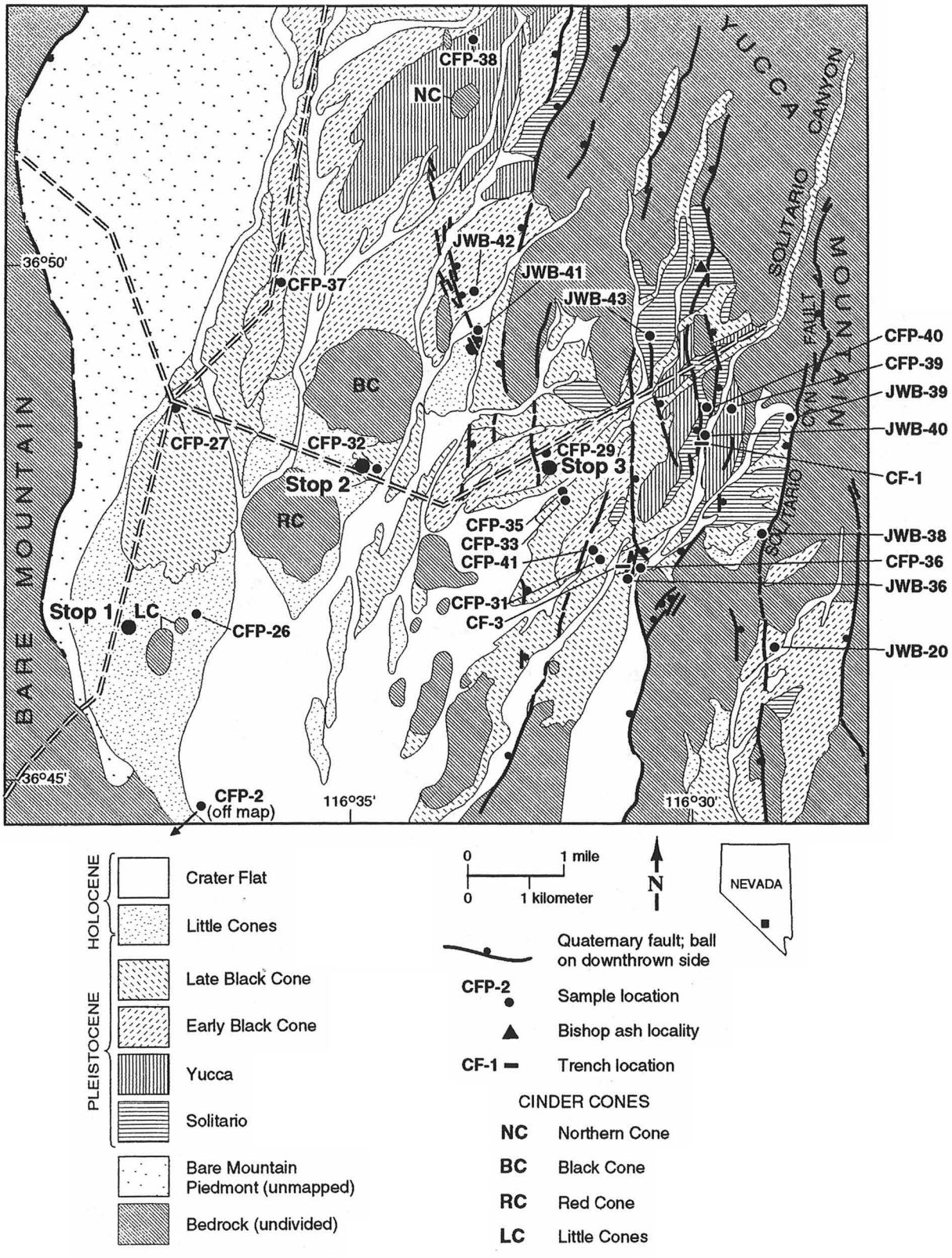

Figure 2. Allostratigraphic map of Crater Flat (from Peterson and others, 1995).

TABLE 1. ILLUSTRATIVE PEDONS FOR CRATER FLAT ALLOSTRATIGRAPHIC UNITS

Horizon	Depth (cm)	Color		Texture	Size (% Vol)			Size (% wt)			Argillans	Structure	Consistency			Cementation	$CaCO_3$ effervescence & morphology	pH	Pores	Roots	Lower boundary
		Dry	Moist		Gravel	Cobble	Stone	Sand	Silt	Clay			Dry	Moist	Wet						
CRATER FLAT UNIT (SITE CFP-41)																					
AC	0-19	10YR 6/2	10YR 4/2	EGS	65	0	0	95	3	2	none	SG	LO	LO	SO/PO	none	EO & E	8.6	no V's	1VF	GW
Ck	19-100	10YR 6/2	10YR 4/2	EGS	65	3	0	95	3	2	none	SG	LO	LO	SO/PO	none	E	8.6	N.D.	1VF-F, v1M	N
LITTLE CONES UNIT (SITE CFP-26)																					
Av	0-5	10YR 7/3	10YR 4/3	GVFSL	20	0	0	58	35	7	none	2VCOPR	SH	VFR	SO/PS	none	ES	8.6	3VF-MV	none	AS
Ak	5-19	10YR 7/3	10YR 5/3	GSL	30	0	0	68	24	7	none	1FSBK	VSH	VFR	SO/PO	none	ES-CISF&SPB	8.8	N.D.	v1VF	CS
Bwk	19-29	10YR 7/3	10YR 5/3	GSL	30	0	0	74	20	6	none	M	SO	VFR	SO/PO	none	EV-CISF&SPB	9.0	N.D.	1VF	GS
Bk	29-54	10YR 7/3	10YR 5/3	VGSL	50	0	0	76	19	5	none	M	SO	VFR	SO/PO	none	EV-CSPB	9.0	N.D.	1VFv1F	CW
2Bk1	54-78	10YR 7/3	10YR 5/3	EGSL	65	0	0	80	15	5	none	M	SO	VFR	SO/PO	none	EV-CSPB	8.4	N.D.	1VFv1F	CW
2Bk2	78-100	2.5Y 7/1	2.5Y 5/2	VGCOS	50	5	0	95	3	2	none	SG	LO	LO	SO/LO	none	ES-CSPB	8.2	N.D.	none	N
LATE BLACK CONE UNIT (SITE CFP-32)																					
Av	0-6	10YR 7/2	10YR 4/3	L	13	0	0	48	40	12	none	2VCOPR	SH	VFR	SS/PS	none	EO	8.6	3VF-FV,2MV	none	AS
Ak	6-15	10YR 6.5/2	10YR 4.5/3	GSL	20	0	0	64	28	8	none	1FPL & 1VFSBK	VSH-SO	VFR	SO/PO	none	ES&EV-D,SPB,SF	9.4	N.D.	1VF-F	CW-I
Bt	15-33	10YR 6/3	8YR 4.5/3	VGSL	50	0	0	60	25	15	INPBC & PO	1VF-FSBK	SH	FR	VSS/VPS	none	EO&E	8.4	N.D.	1VF	CW
Btk	33-51	7.5YR 6/3	7.5YR 4/4	EGSL	68	0	0	70	20	10	NPBCC	1VFSBK	VSH	VFR	VSSPO	none	ES&EV & EO-D,SP	8.4	N.D.	none	AW-I
Bqkm	51-71+	10YR 8/1 & 10YR 6/2	10YR 7/2 & 10YR 4/3	EGLS	65	0	0	N.D.	N.D.	N.D.	none	2VCOPL	EH	EFI	n.a.	CS	EV-D,SP	N.D.	N.D.	none	N
EARLY BLACK CONE UNIT (SITE CFP-37)																					
Av	0-5	10YR 7/2	10YR 4/2	L	10	0	0	45	40	15	none	3COPR	SH	VFR	SS/PS	none	EO & EV	8.4	3FV	none	AS
AB	5-11	10YR 6/2	10YR 4.5/3	GCL	15	0	0	36	35	29	none	3COPR & IMPL	SH	VFR	S/P	none	EO & EV	8.4	1VFV	v1VF	AW
Btk1	11-35	7.5YR 6/4	7.5YR 4/4	VGCL	50	0	0	37	25	38	2NCO	3VFABK	SH	FR	VS/P	none	EO & ES	8.6	N.D.	1VF,v1F	CW
Btk2	35-48	7.5YR 6/4	7.5YR 5/4	EGLCOS	65	2	0	80	15	5	none	1VFSBK	LO	VFR	SO/PO	none	EO & EV	8.8	N.D.	1VF	VAW
Bqkm	48-130	10YR 8/1	10YR 7/3	N.D.	70	5	0	N.D.	N.D.	N.D.	none	M	SH-VH	LO-VFI	n.a.	none-CS	EV	N.D.	N.D.	v1VF-M	N
EARLY BLACK CONE UNIT (SITE CFP-29)																					
Av	0-5	10YR 7/2	10YR 4.5/2	GL	20	0	0	48	40	12	none	2COPR	SH	VFR	SS/SP	none	EO & E	8.8	3VF-MV	none	AS
Ak	5-12	10YR 6.5/3	10YR 4.5/3	SL	10	0	0	74	18	8	none	1VFSBK	SO	VFR	SO/PO	none	ES	8.4	N.D.	1VF	AW
Btqy	12-24	7.5YR 6/3	7.5YR 4/4	GCL	20	2	0	27	35	38	2MKPF & PO	2VFGR-ABK	SO-SH	VFR	S/P	none	EO & ES	8.2	N.D.	none?	AS
Btq	24-47	7.5YR 6/3	7.5YR 4/4	"SL"	50	5	0	n.a.	n.a.	n.a.	INPO & PBC	1COPL & 3FABK	H-VH	VFI	SO/PO	CW	EO	8.2	N.D.	none	CW
Bqkm	47-55+	10YR 8/1 & 10YR 7/2	10YR 7/3 & 10YR 4.5/3	n.a.	60	10	0	n.a.	n.a.	n.a.		M	VH-EH	VFI-EFI	brittle	CS	ES-D,SP,SF	8.2	N.D.	none	N
YUCCA UNIT (SITE CFP-39)																					
Av	0-8	10YR 7/2	10YR 4/2	L	5	0	0	53	35	18	none	3COPR & 1MPL	SH	VFR	SS/P	none	EO & E	8.8	3F-MV	none	AW
Ak	8-17	10YR 6.5/3	10YR 5/3	L	10	0	0	50	35	15	none	1MPL & 2VFSBK	SH	VFR	SS/PS	none	ES-SPB	9.0	N.D.	1VF-F	CW
Bt	17-38	7.5YR 5/4	7.5YR 4/6	VGC	30	10	0	28	30	42	4KPF	3VF-FABK	SH	FR	VS/VP	none	E	8.8	N.D.	v1VF	CS
Btk	38-57	10YR 6/6	10YR 4.5/6	VGC	45	2	0	22	38	40	4KPF & CO	2FSBK	H	FI	VS/VP	none	EO & E-SPB	8.6	N.D.	none	VAW
Bqkm	57-61+	10YR 8/1 & 10YR 7/4	10YR 7/4 & 9YR 5/4.5	n.a.	50	N.D.	0	N.D.	N.D.	N.D.	N.D.	M	EH	EFI	brittle	CS	ES	N.D.	N.D.	none	N
YUCCA UNIT (SITE CFP-38)																					
Av	0-7	10YR 6.5/1	10YR 4.5/2	GL	20	0	0	50	35	15	none	3COPR	H-SH	VFR	S/P	none	EO & E	8.6	3F-MV	v1VF	AW
Ak	7-17	10YR 6/2	10YR 4.5/2	GL	20	0	0	42	40	18	none	1MPF & 2VFSBK	SH	VFR	SS/PS	none	ES-SPB	9.0	N.D.	1VF,v1M	AW
Bt	17-28	7.5YR 6/4	7.5YR 4/6	FG"L"	20	0	0	n.a.	n.a.	n.a.	4KPF,BR,CO	1MPL & 3VFABK	H	FI	SS/P	VCW peds	EO	8.4	N.D.	2VF,1M	VAW
Btqkm	28-72	7.5YR 6/4	7.5YR 4/4	G"LS"	15	0	0	n.a.	n.a.	n.a.	3KPF	3MPL	H	FI	SO/PO	CW	EO & EV	8.4	N.D.	none	VAW
Bqkm	72-77+	10YR 8/1 & 10YR 7/2	10YR 7/3 & 10YR 7/3	n.a.	30	0	0	n.a.	n.a.	n.a.	N.D.	M	VH	EFI	n.a.	CS	EV	N.D.	N.D.	none	N
SOLITARIO UNIT (SITE CFP-40)																					
Av	0-5	10YR 7/2	10YR 4.5/3	VFSL	10	0	0	67	25	8	none	3COPR	SH	VFR	SO/PS	none	E & EO	8.8	3F-MV	none	AS
Ak	5-9	10YR 7/3	10YR 5/3	L	8	0	0	42	35	23	none	3COPR	SH	FR	S/P	none	EV	8.8	N.D.	none	AW-B
Btk	9-19	7.5YR 6.5/4	7.5YR 5/4	VGCL	50	0	0	30	35	35	?	1VFSBK	SH	FR	S/P	none	EO & EV	8.8	N.D.	1VF-F	VAW
Bqkm	19-21+	10YR 8/2-3	10YR 7/3	n.a.	50	0	0	n.a.	n.a.	n.a.	N.D.	M	EH	EFI	brittle	CI	EV	N.D.	N.D.	3VF-F	N

Note: Abbreviations refer to terminology of Soil Survey Staff (1975). N.D. = not determined; n.a. = not applicable.

surfaces in Crater Flat; rough, raw, distrubutive drainage patterns with slightly subdued bar-and-swale microtopography. No organized desert pavement, and little to no rock varnish. The soils of the Crater Flat unit are coarse-textured, thermic, Typic Torriorthents. They have neither significant *genetic* soil horizons (*i.e.*, no Av, cambic or argillic horizons) nor any differentiated horizon of carbonate or opal accumulation. At most, the microtopographic muting of the surface is accompanied by very slight accumulations of pedogenic carbonate as filaments on pebble bottoms at 20-50 cm depths, *i.e.*, Stage I carbonate accumulation (Gile and others, 1966).

Little Cones Unit

The Little Cones unit primarily consists of a large fan-piedmont remnant surrounding the Little Cones basaltic cones in southwestern Crater Flat and several other large remnants around Black and Red Cones. These surface remnants are freshly eroded by the younger, expanding Crater Flat surfaces and are themselves erosionally inset below Black Cone remnants. Compared with the raw, rough, bar-and-swale microtopography of the Crater Flat surface, the Little Cones surface typically is fully-smoothed with abstracted drainageways and a slightly varnished desert pavement on a clearly differentiated soil.

Little Cones soils have minimal but distinct desert pavements and sandy loam Av horizons. Calcareous cambic horizons (Bwk), with some pedogenic carbonate on pebble bottoms, and late Stage I Bk horizons occur under the Av horizons; the Bk does not contain enough pedogenic carbonate to be a calcic horizon, in the sense *calcic horizon* is used in Soil Taxonomy (Soil Survey Staff, 1975). In some pedons, the bottom of the Bwk horizon is too shallow to meet Soil Taxonomy's arbitrary 50-cm depth requirement for a cambic horizon, hence the soils may be identified as either Camborthids (with a cambic horizon) or Torriorthents (without a cambic horizon) depending on where they are examined.

Black Cone Unit

The Black Cone unit consists of small- to medium-sized, fan-piedmont remnants. It has been more closely and more deeply dissected than the Little Cones surface, but less so than the Yucca or Solitario surfaces. Its ubiquitous remnants are broad, flat, microtopographically-muted interfluves covered by darkly varnished, closely spaced desert pavement. Differences in soil development between certain Black Cone remnants are distinct enough that, together with the numerical age relations discussed later, they allow subdivision and mapping of the Black Cone unit as Late and Early Black Cone subunits.

Late Black Cone Subunit

The soils of this subunit have prominent, loam-textured Av horizons under moderately well-varnished desert pavement, have either argillic or cambic horizons, and have haplic (weak or discontinuous) duripans or calcic horizons (stage II-III). The argillic horizons are less clayey than those of Early Black Cone age soils. Near the Bare Mountain piedmont, alluvium of the Late Black Cone subunit contains limestone resulting in the formation of Typic Camborthids rather than Durargids. Because the Late Black Cone Durargids and Calciorthids occur on same-age geomorphic surfaces, they confirm previous work (Nettleton and Peterson, 1983) suggesting that moderate amounts of limestone parent material may prevent the formation of an argillic horizon.

Early Black Cone Subunit

The soils, where formed in volcanic alluvium, are commonly typic durargids having prominent, loam-textured Av horizons under darkly varnished desert pavement, argillic horizons that generally are clay loams, and typic or haplic duripans.

Yucca Unit

The Yucca unit consists of several fairly extensive fan-piedmont remnants which are deeply dissected and narrow but flat-topped. It can be distinguished from the Black Cone, Little Cones, and Crater Flat units by aerial photograph patterns, topographic separation, and soil differences.

Yucca-age soils are Typic Durargids that have darkly varnished desert pavements and loam-textured, strongly crusting Av horizons and Ak horizons that are somewhat thicker than those of younger soils. Their argillic horizons are thicker and more clayey than those of the younger soils, and some have been so strongly opalized (micro-cemented) that the apparent field texture is a loam or loamy sand. The duripans are strongly cemented and apparently thick, as seen exposed in wash cuts.

Solitario Unit

A few ballenas (fully rounded ridge-line fan remnants) comprise the Solitario unit. One at the mouth of Solitario Canyon (Fig. 1) is 1½ m higher than an adjacent, flat-topped, Yucca-age fan remnant that is clearly inset below the Solitario remnant, demonstrating their relative ages. Bedrock spurs up Solitario Canyon-- and in other canyons northeast of Crater Flat-- appear to be bedrock-pediment remnants of a Solitario-age surface once much more extensive. A Solitario remnant in the northeast corner of Crater Flat (Fig. 2) contains reworked Bishop ash (~730 ka) at 5-7 m depth (Marith Reheis, 1991, written communication).

No well-preserved Solitario-age soils were found. Rather, there is a complex of Typic Durorthids with small areas of Typic Durargids on the rounded crests of the ballenas studied. Ballenas form by erosional rounding of formerly flat-topped fan remnants with stripping of A and Bt horizons from the soil of the original fan-remnant summit. Apparently the original soil was a Durargid; subsequent stripping shattered the upper part of the duripan and mixed the detritus with later dust accumulations, leaving a Typic Durorthid.

Age of Crater Flat Stratigraphic Units

We employed the rock-varnish ^{14}C AMS and cation-ratio dating methodologies together with uranium-series dating to numerically date stratigraphic units in Crater Flat (Peterson and others, 1995). A total of 23 rock-varnish samples were analyzed by Ronald I. Dorn, of which 12 were dated by the ^{14}C AMS technique. Six samples of pedogenic carbonate were analyzed by Teh-Lung Ku using the ^{230}Th-^{234}U disequilibrium methodology. Together these age data indicated Holocene to latest Pleistocene ages for the Crater Flat, Little Cones, and Late Black Cone units and older Pleistocene ages for the Early Black Cone, Yucca, and Solitario units (Table 2). In particular, the Late Black Cone unit was interpreted as a late Wisconsin-age deposit likely correlative with other similar glacial/pluvial units in the arid Basin and Range province.

Table 2. Comparison of Crater Flat alluvial chronology with other chronologies in the region.

Crater Flat (this study)	Lower Colorado River (Bull, 1991)	Las Vegas and Indian Springs Valleys (Quade, 1986; Quade and and Pratt, 1989)	Southern Death Valley (Dorn, 1988; Hooke Dorn, 1992)	East-central Mojave (Wells et al., 1990)
Modern (0)	Q4b (0)	Modern (0)	Modern (0)	Modern (Qf9) (0)
Crater Flat (>0.3->1.3)	Q4a (0.1-2)	Unit G (0-4.0)	Q4c (0.5-2.5)	Qf8 (<0.3->0.7)
	Q3c (2-4)	Unit F (4.0-8.0)	Q4b (2.0-4.5)	Qf6,7 (2-8)
	Q3b (4-8)			
Little Cones (>6->11)	Q3a (8-12)	Unit E (8.6-14.0)	Q4a (6-11)	Qf5 (8-15)
Late Black Cone (>17 to >30)	Q2c (12-70)	Unit D (15-30)	Q3 (13-50)	Q4f (<34- >45)
Black Cone (>159 to 201)	Q2b (70-200)	Unit C (>30)	Q2a, Q2b (110-190)	Qf3 (>47->130)
		Unit B (>40->60)		Qf2 (<160- >320)
Yucca (>375)	Q2a (400-730)	Unit A	Qla, Qlb (>500->800)	
Solitario (>433->659 but <730)	Ql (<1200)	Unit A .	Qla, Qlb (>500->800)	Qf1 (<3800)

Note: Listed ages (in ka) are in parentheses.

A recent study by Beck and others (1998) has called into question the accuracy of these rock varnish ^{14}C AMS results based on the presence of coal-like particles in some similar samples submitted by Ronald Dorn. In response, Dorn (1998) argued that these particles were naturally occurring, but agreed that the results must be viewed as ambiguous.

References Cited

Beck, W., Donahue, D.J., Jull, A.J.T., Burr, G., Broecker, W.S., Bonani, G., Hajdas, I., and Malotki, E., 1998, Ambiguities in direct dating of rock surfaces using radiocarbon measurements: Science, v. 280, p. 2132-2135.

Bull, W.B., 1991, Geomorphic responses to climatic change: Oxford University Press, New York, 326 p.

Dorn, R.I., 1988, A rock varnish interpretation of alluvial-fan development in Death Valley, California: National Geographic Research, v.4, p. 56-73.

Dorn, R.I., 1998, Response to "Ambiguities in direct dating of rock surfaces using radiocarbon measurements": Science, v. 280, p. 2135-2139.

Faulds, J., Bell, J.W., Feuerbach, D., and Ramelli, A.R., 1994, Geologic map of part of Crater Flat, southern Nevada: Nevada Bureau of Mines and Geology Geologic Quadrangle Map 101, 1:24,000.

Gile, L.H, Peterson, F.F., and Grossman, R.B., 1966, Morphological and genetic sequences of carbonate accumulation in desert soils: Soil Science, v. 101, p. 347-360.

Hooke, R.LeB, and Dorn, R.I., 1992, Segmentation of alluvial fans in Death Valley, California: New insight from surface exposure dating and laboratory modeling: Earth Surface Processes and Landforms, v. 17, p. 557-574.

Nettleton, W.D., and Peterson, F.F., 1983, Aridisols, *in* Wilding, L.P., Smeck, N.E., and Hall, G.F., eds., Pedogenesis and soil taxonomy Volume II: The soil orders: Elsevier, Amsterdam. p. 165-216.

Peterson, F.F., 1981, Landforms of the Basin and Range Province defined for soil survey: Nevada Agricultural Experiment Station Technical Bulletin 28, University of Nevada, Reno, 52 p.

Peterson, F.F., Bell, J.W., Dorn, R.I., Ramelli, A.R., and Ku, T-L., 1995, Late Quaternary geomorphology and soils in Crater Flat, Yucca Mountain, southern Nevada: Geological Society of America Bulletin, v. 107, no. 4, p. 379-395.

Quade, J., 1986, Late Quaternary environmental changes in the upper Las Vegas Valley, Nevada: Quaternary Research, v. 26, p. 340-357.

Quade, J. and Pratt, W.L., 1989, Late Wisconsin groundwater discharge environments of the southwestern Indian Springs Valley, southern Nevada: Quaternary Research, v. 31, p. 351-370.

Soil Survey Staff, 1975, Soil Taxonomy: Washington, D.C., U.S. Government Printing Office, U.S. Department of Agriculture Handbook 436, 746 p.

Wells, S.G., McFadden, L.D., and Harden, J., 1990a, Preliminary results of age estimations and regional correlations of Quaternary alluvial fans within the Mojave Desert of southern California, *in* Reynolds. R.E., Wells, S.G., and Brady, R.J., eds., At the end of the Mojave: Quaternary studies in the eastern Mojave Desert: San Bernardino County Museum Association, Redlands, California, p. 45-53.

Day 2, Stop 3

Quaternary Stratigraphy And Fault Activity, Solitario Canyon Fault, Yucca Mountain, Nevada

Alan R. Ramelli

The Solitario Canyon fault (SCF), which bounds the main escarpment of Yucca Crest, has a length of at least 18 km and displays a Quaternary scarp that can be traced for about 14 km. Along most of its length, the SCF juxtaposes bedrock against alluvium that is massively cemented by secondary carbonate and silica, especially near the fault. These cemented deposits are inferred to be of early to mid-Quaternary age. At this stop (Trench 8), the massively cemented deposits are buried by a few meters of mid- to late Quaternary gravels. Bedrock and cemented gravels are typically covered by a thin mantle (generally <0.5 m thick) of Holocene/latest Pleistocene eolian material and colluvium.

Four trenches across the SCF reveal mid- to late Quaternary faulting events typically expressed as near-vertical fissures extending upward from a west-dipping bedrock fault. The largest fissures at all four sites contain abundant basaltic ash, suggesting temporal coincidence of faulting with eruptive activity at the Lathrop Wells basalt cone.

Quaternary Stratigraphy

Studies of Quaternary deposits in the Yucca Mountain area (e.g., Swadley, 1983; Swadley and others, 1984; Taylor, 1986; Swadley and Carr, 1987; Swadley and Parrish, 1988; Wesling and others, 1992; Faulds and others, 1994; Peterson and others, 1995; Lundstrom and others, 1995a, 1995b) are based on three stratigraphic schemes (Hoover and others, 1981; Peterson, 1988; and Wesling and others, 1992). Hoover and others (1981) defined three broad alluvial units (Q1, Q2, and QTa) in the area, and further divided units Q1 and Q2 into several subunits. Peterson (1988) defined six soil-geomorphic units in the Crater Flat area (Crater Flat, Little Cones, Late Black Cone, Early Black Cone, Yucca, and Solitario units). Wesling and others (1992) defined a stratigraphy for the Midway Valley area on the east side of Yucca Mountain that included eight numbered surficial units (0-7). General correlations between these schemes are shown in Table 1, although they do not correlate in all respects. For consistency with other paleoseismic studies, the Midway Valley stratigraphy is used here. Table 2 summarizes the stratigraphic relations and correlations between trenches on the Solitario Canyon fault.

Estimated ages (Table 1) are generalized from geochronologic data obtained over the past several years. Ages for the surficial units of Hoover and others (1981) were based primarily on uranium-trend ages that are now discounted (Paces and others, 1995) and are not used here. Ages for the Crater Flat stratigraphy were based on regional correlations, uranium-series ages, and ^{14}C dating of rock varnish (Peterson and others, 1995). Ages for the Midway Valley stratigraphic units (Wesling and others, 1992) are primarily based on uranium-series and thermoluminesence dating (Paces and others, 1995).

Table 1. General correlations between Quaternary stratigraphic schemes developed for the Yucca Mountain/Crater Flat area

Hoover[1]	Peterson[2]	Wesling[3]	Estimated Age (ka)
Q1a	Modern	Q7	0
Q1b	Crater Flat	Q6	0.5-2
Q1c	Little Cones	Q5	5-15
Q2b	Late Black Cone	Q4	20-100
Q2c	Early Black Cone	Q3	150-250
---	---	Q2	?
QTa	Yucca	Q1	300-400
QTa	Solitario	Q1	500->700
QTa	---	Q0	>1000

[1]Hoover and others, 1981 (also Hoover, 1989)
[2]Peterson, 1988 (also Peterson and others, 1995)
[3]Wesling and others, 1992

Trench Investigations of the Solitario Canyon Fault

Trench 8 (T8) exposed the largest observed displacements and the most complete record of faulting. Here, cumulative mid- to late Quaternary slip is estimated at about 2 m, based on vertical separation of an erosional disconformity on bedrock and early Quaternary deposits, and by the extension suggested by fissure openings. Per-event offsets are variable; at T8, the two largest events had estimated dip slip of 1.1-1.3 m and 30-60 cm, and two smaller possible events are estimated at 10-40 cm each. Additional minor events, possibly secondary in nature, are suggested by silt- and carbonate-filled fractures with no obvious displacement.

Carbonate deposition

Stratigraphy and fault relations in the SCF trenches are obscured by extensive carbonate and silica overprinting. Along the SCF and elsewhere in the Yucca Mountain area, carbonate accumulation is greatest at and immediately downslope from faults bounding bedrock hillslopes. This likely occurs for three reasons: 1) enhanced runoff from bedrock hillslopes; 2) a pronounced permeability contrast where alluvium is juxtaposed against bedrock; and 3) fractures that allow relatively deep moisture penetration.

Age Control

Estimated ages of Quaternary deposits along the SCF are largely based on uranium-series (U-series) and thermoluminescence (TL) dating (Paces and others, 1995), and on

correlation to Quaternary stratigraphic schemes developed for the surrounding areas (e.g., Wesling and others, 1992; Peterson and others, 1995; Lundstrom and others, 1995a, 1995b). Geochronologic data from SCF trenches include five U-series ages and three TL ages from T8 and an adjacent shallow pit (T8A), and several U-series ages on four samples from SCF-T3, located 1.3 km south of T8.

Table 2. Summary of stratigraphic relations and correlations - Solitario Canyon fault trenches

Stratigraphic Unit	Trenches present	Unit numbers	Soil[1]	Correlation Unit (East side)[2]	Correlation Unit (Crater Flat)[3]
Eolian silt/colluvium	SCF-T3	11-12	Av	Q5	Little Cones
	SCF-T4	9-10			
	SCF-T2	10-11			
Eolian silt/gravel	T8	15	Stage I+ $CaCO_3$	Q5	Little Cones
	SCF-T1	20-22			
Gravelly silt	T8	14	Bw/Bt	Q4	Late Black Cone
	SCF-T4	8			
	SCF-T2	8-9			
Gravel	SCF-T1	12-19	Bt/Btk	Q4	Late Black Cone
Stratified gravel	T8	5-9	Bqkm	Q3	Early Black Cone
Silty gravel	T8	2-4	Bq	Q3?	E. Black Cone?
Gravel	T8	1	K	Q1	Solitario
	SCF-T1	1-8			
	SCF-T3	1-9			
	SCF-T4	1-6			
	SCF-T2	1-7			

[1]Selected soil characteristics
[2]Wesling and others (1992)
[3]Peterson (1988)

Trench 8

Trench 8 (T8) is located at the head of an alluvial fan emanating from a small drainage basin formed where the Iron Ridge fault splays from the SCF (figs. 1 and 2). One of several original trenches excavated for the Yucca Mountain project, T8 was deepened in mid-1993 to provide better exposure of older faulted deposits.

Figure 1. Generalized map of the Solitario Canyon fault and other nearby Quaternary faults at Yucca Mountain, with locations of exploratory trenches. Bedrock areas are shaded light gray and Quaternary basalts dark gray. Balls are on downthrown sides of faults. SCF - Solitario Canyon fault; IRF - Iron Ridge fault; WWF - Windy Wash fault; FWF - Fatigue Wash fault; PCF - Paintbrush Canyon fault; SRF - Stagecoach Road fault.

Figure 2. Surficial geology at the T8 site along the Solitario Canyon fault (after Lundstrom and others, 1995b). Stratigraphic nomenclature is after Wesling and others (1992).

T8 exposes a west-dipping bedrock fault bounding a 3- to 5-m-wide, flaring-upward fault zone comprised of laminar and massive carbonate and silica, carbonate-cemented gravel, slivers of tuff, and extensional fissures filled with silt, gravel, and basaltic ash.

The shallow pit adjacent to T8 (T8A), was excavated to further assess the recency of faulting. Relations in T8A are similar to those in the equivalent (upper) part of the south wall of T8. Two thermoluminesence ages from T8A (TL-10: 11 $\pm$ 1.7 ka, and TL-11: 14 $\pm$ 2 ka) indicate a late Pleistocene age for the mantling colluvium and eolian material. The two ages are reversed stratigraphically, but their uncertainties overlap.

Stratigraphy

Trench 8 (fig. 3) exposes alluvium downthrown against welded tuff. The hanging wall deposits are divided into five age groups, most, if not all, of which are present as surficial units on the alluvial fan at this site (fig. 2). On the footwall, bedrock is covered only by a thin deposit of young eolian silt and colluvium.

Figure 3. Log of the south wall of Trench 8.

Unit 14: Silty gravel about 1 m thick; present only downslope from the fault zone; soil consists of a fairly thin vesicular A (Av) horizon, cambic (Bw) horizon, and Stage I-I+ carbonate. Soil development suggests an early Holocene or latest Pleistocene age; correlated to Q5.

Unit 13: Eolian silt and fine sand, and some gravel; contains a weak argillic (Btj) soil, and exhibits soil catena characteristics, where soil development increases downslope. TL ages from T8A (TL-10 and TL-11: 11 $\pm$ 1.7 ka and 14 $\pm$ 2 ka, respectively) indicate a latest Pleistocene age; correlated to Q4 and/or Q5.

Units 10-12: Deposits within and overlying a fissure formed during the largest late Quaternary faulting event. Basal fissure fill (unit 10), south wall: bottom meter is filled by nearly pure basaltic ash and mixed volcanic and carbonate clasts; lack of other material indicates ash was deposited soon after faulting, and ash grains are very angular, indicating minimal transport. North wall: bottom of fissure is filled with ash-free pebbly silt (unit 5-6?) that likely collapsed into the fissure during surface faulting. Upper fissure fill (unit 11) is mostly fine sand with some gravel clasts and reworked basaltic ash; ash content decreases

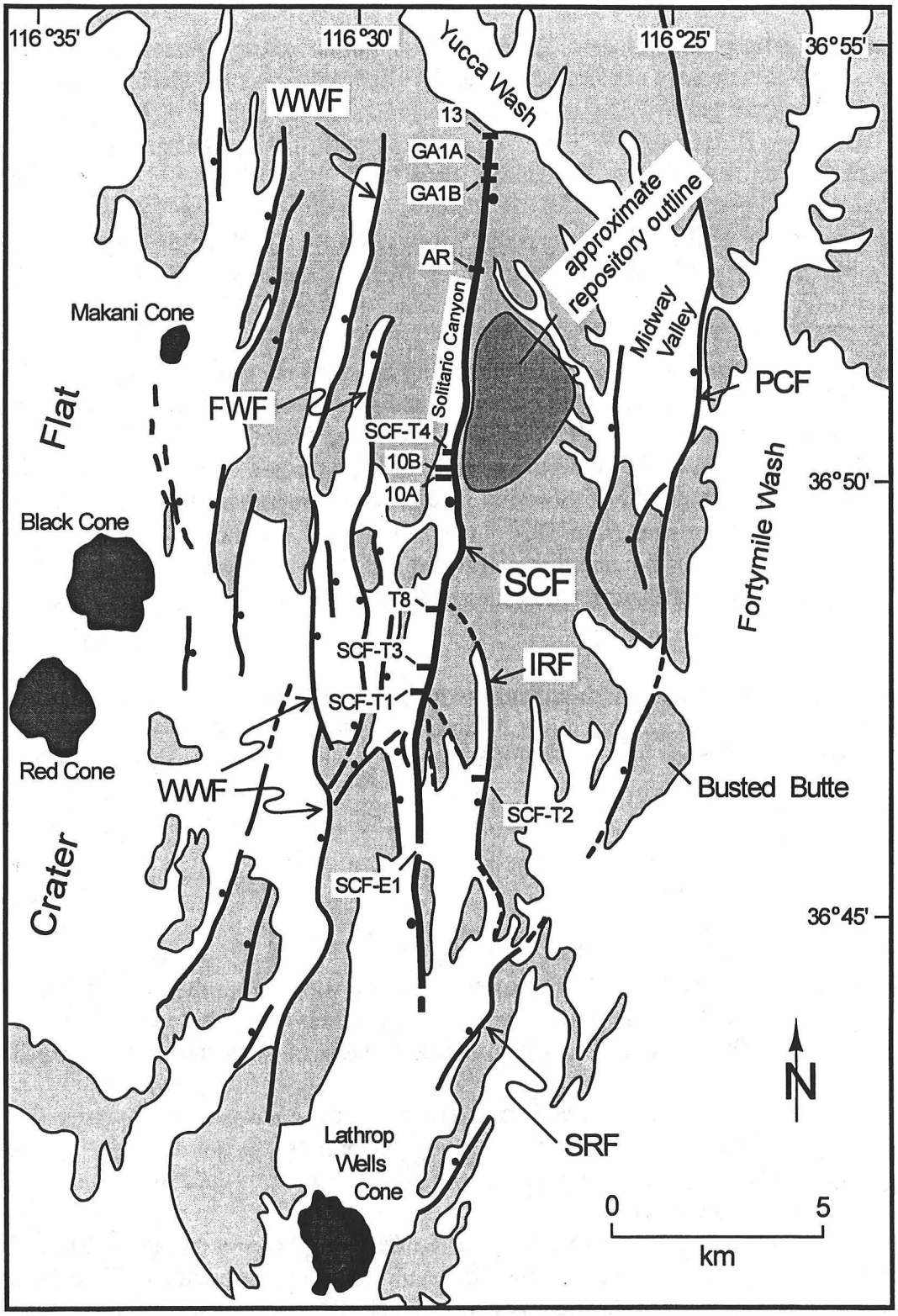

Figure 1. Generalized map of the Solitario Canyon fault and other nearby Quaternary faults at Yucca Mountain, with locations of exploratory trenches. Bedrock areas are shaded light gray and Quaternay basalts dark gray. Balls are on the downthrown sides of the faults. SCF, Solitario Canyon fault; IRF, Iron Ridge fault; WWF, Windy Wash fault, FWF, Fatigue Wash fault, PCF, Paintbrush Canyon fault; SCR, Stagecoach Road fault.

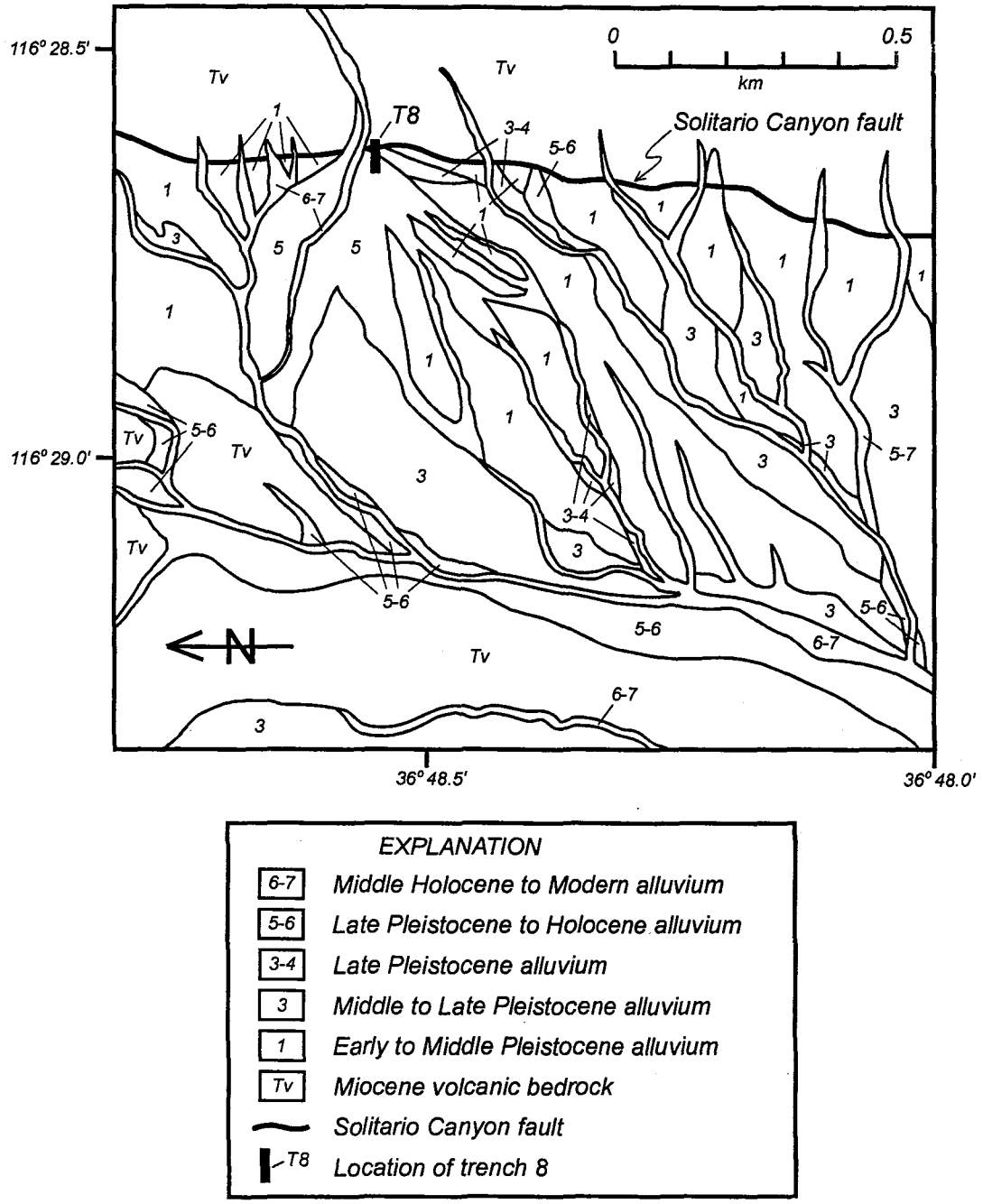

Figure 2. Surficial geology at the T8 site along the Solitario Canyon fault (after Lundstrom and others, 1995b). Stratigraphic nomenclature is after Wesling and others (1992).

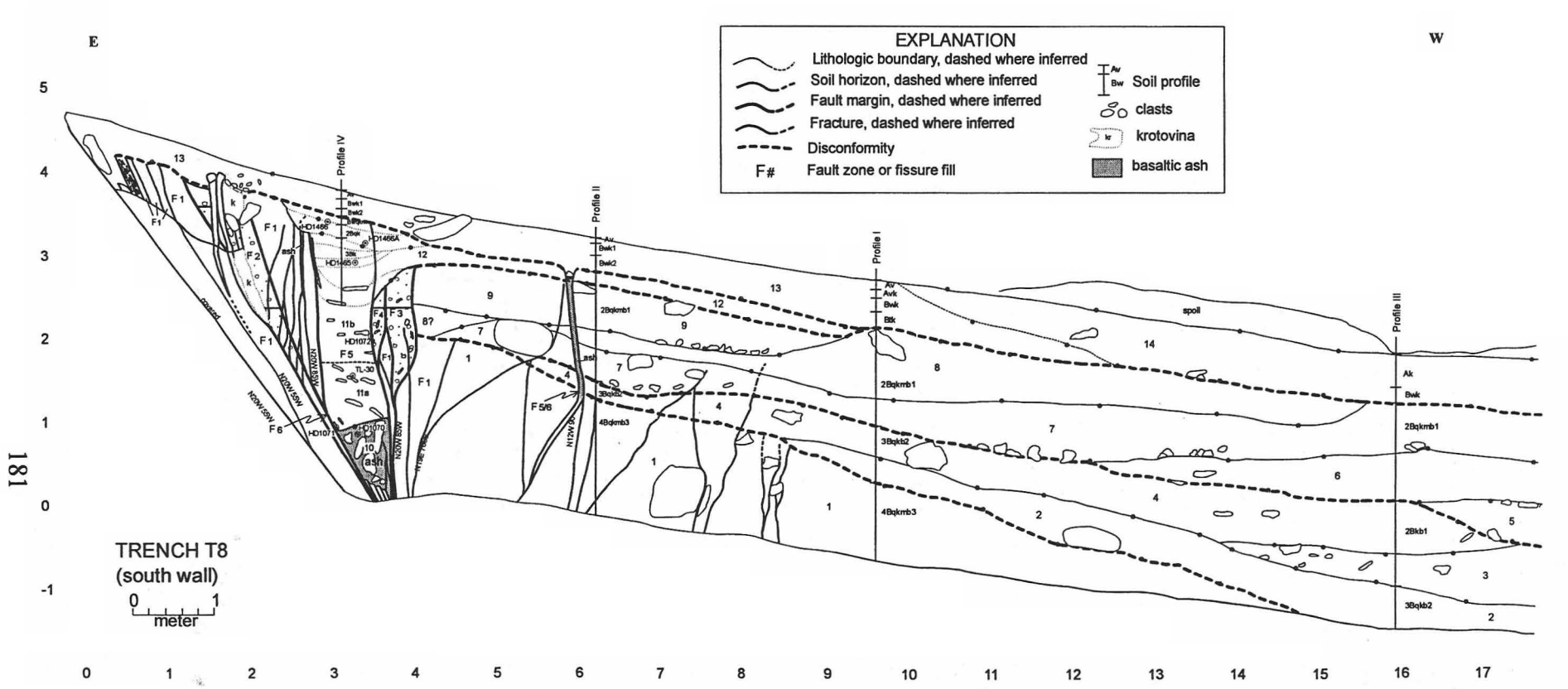

Figure 3: Log of the south wall of Trench 8.

upward. Unit 12 has indistinct contact with unit 11, but is distinguished based on position (i.e., downslope-tapering wedge of material deposited after fissure was filled). Fissure fill contains Stage II+ $CaCO_3$. A maximum age for the fissuring event comes from a U-series age (HD1072: 118 $\pm$ 6 ka) on older fissure carbonate. Minimum ages include U-series ages (HD1070: 37 to 56 ka) on rhizoliths within unit 10, a TL age (TL-30: 36 $\pm$ 5 ka) on the middle of unit 11, U-series ages (HD1465: 47 $\pm$ 9 and 66 $\pm$ 23 ka) on secondary carbonate within lower unit 12, and a U-series age (HD1071: 15.5 $\pm$ 1.6 ka) on vein carbonate crosscutting basaltic ash. Secondary carbonate from upper unit 12 (HD1466: 101 $\pm$ 4 ka) provides an apparent minimum age, but is discounted due to poor sample quality and inconsistency with other results. Geochronologic data (Paces and others, 1995), carbonate accumulation, and stratigraphic position indicate a late Pleistocene age (within range of 40-100 ka), and correlation to the largest eruption at the Lathrop Wells basalt cone suggests an age of 70-80 ka (Perry and Crowe, 1996).

Units 5-9: Moderately stratified and sorted gravels that reflect a period of alluviation not evident at the other SCF trench sites; contain a well-developed petrocalcic horizon ($CaCO_3$ Stage III-IV), but carbonate/silica accumulation significantly less than in unit 1 and sedimentary fabric is not obliterated; upper soil horizons eroded prior to deposition of younger material. Stratigraphic position, carbonate accumulation, and a U-series age (sample HD1072; 118 $\pm$ 6 ka) on fracture-filling carbonate that crosscuts these deposits suggest a middle to late Pleistocene age; correlated to Q3, and likely within or close to an age range of 150-250 ka.

Units 2-4: Gravel deposits with a distinctive silica-cemented brown silt matrix; thicker in north wall, so apparently channelized in vicinity of active wash just north of the trench. The only constraint on age is stratigraphic position; likely closer in age to overlying deposits, which are correlated to Q3, and thus probably middle Pleistocene in age (a few hundred ka).

Unit 1: Bouldery gravels best exposed low in south wall; entirely engulfed in carbonate and silica ($CaCO_3$ Stage III-V), largely obliterating original sedimentary fabric and contacts; upper soil horizons associated with this petrocalcic horizon were eroded. Based on cementation and stratigraphic position, correlated with the oldest deposits generally present in the area (Q1); at least middle Pleistocene, and probably early Pleistocene, in age (probably $>>500$ ka). These deposits dominate the southern part of the alluvial fan in this area (fig. 2).

Structure

The SCF is a mostly singular fault with an average strike of about N5°E and a west dip of 50°-60°. Predominantly normal slip has displaced Miocene tuffs (Tiva Canyon and Topopah Spring members of the Paintbrush Tuff) by an estimated 500-700 m in the vicinity of T8, based on cross sections (Scott and Bonk, 1984) and lithologic logs for well WT-10, located about 700 m west of the surface trace of the fault (Nelson and others, 1991). A subordinate component of left-lateral displacement is suggested by bedrock striations in various locations along the fault (rakes generally range from 50° to 70°; Simonds and others, 1995), but it's unclear whether these striations represent Quaternary slip.

Late Quaternary offsets have occurred primarily as subvertical fissure openings that sole into a west-dipping bedrock fault. Displacements cannot be directly measured, because the fault juxtaposes bedrock against alluvium, but they can be estimated from downthrow of hanging wall deposits, vertical separations of erosional disconformities, and fissures widths. At T8, vertical separation of a disconformity on the fault zone and older gravels suggests

about 1.8 m cumulative mid- to late Quaternary vertical offset (2.1 m dip slip).

Sequence of Events

The following outline of Quaternary activity is largely based on relations in T8, where five events are apparent; four of these occurred during the mid- to late Quaternary, whereas the fifth is significantly older (additional older events are probable, but are difficult to recognize due to carbonate and silica overprinting) (Table 3).

Table 3: Estimated displacements associated with mid- to late Quaternary surface faulting events along the SCF

Event	Age (ka)	SCF-T4	T8	SCF-T3	SCF-T1	Comments
?	5-15	0	0?	0?	np	Silt-filled openings
?	15-25	0?	0	np?	np?	Cemented fracture
Z	20-30	0-10?	10-20	0-10?	?	Minor fissure; fractures in event-Y fissure fill; dragged event-Y ash
Y	70-80	20-40	110-130	60-120	50-120	Largest event; fissures contain basaltic ash
X	120-200	0?	20-40	?	?	15-cm wide fissure in T8
W	150-250	15-30	30-60	20-40	?	2nd largest event
Cummulative offset		60-80	180-260	80-130	150-250	

Fracturing events Two fracturing "events" with no apparent offset postdate the most recent displacement. Uncemented, silt-filled fractures in the south wall of T8, and in both walls of T8A, but not in the north wall of T8, suggest a minor Holocene event. However, these are not conclusively of tectonic origin; proposed origins include: 1) primary offsets associated with a moderate-sized earthquake; 2) response to shaking from a nearby earthquake; 3) sympathetic slip triggered by a nearby or regional earthquake; 4) aseismic fault creep; 5) bioturbation; 6) $CaCO_3$ dissolution; 7) root wedging; 8) downslope mass movement; 9) compaction; and 10) shrink/swell processes. Similar features occur in many locations in the Yucca Mountain area, and likely have various origins. In many cases, such features remain problematic, although similar fractures exposed in wash cuts throughout eastern Crater Flat are spatially associated with known Quaternary faults (Ramelli and others, 1989).

A silt-filled opening in the south wall (@ 2 m on fig. 3) appears to be an animal burrow; it has an irregular width (ranging from 0 to 20 cm) and does not noticeably displace an older gravel-filled fissure. Narrow silt-filled openings upslope from this appear due to soil creep caused by collapse into the burrowed area. In the south wall, these are present only near the ground surface, and they do not occur in the north wall where there is no similar evidence

of burrowing.

A single carbonate- and silica-cemented fracture in the south wall (@ 3.5 m on fig. 3) cuts all cemented deposits; it is older than the silt-filled fractures, yet cuts deposits capping the events discussed below. The narrow, even width suggests extensional opening, but still leaves several possible origins. Similar fractures of various age have likely occurred at all of the trench sites, but are masked by carbonate overprinting.

Event Z The most recent event with displacement (F6 on fig. 3) is indicated by: 1) carbonate-cemented fractures that cut the ash-filled fissure discussed below; 2) basaltic ash dragged along the fault; and 3) a narrow (10-15 cm wide) silt- and ash-filled fissure exposed in the north wall (@ 3.5 m on fig. 4), all of which suggest an offset of 10-20 cm. This presumably occurred during an event subsequent to event Y, but afterslip associated with event Y cannot be precluded. The basaltic ash suggests this event was associated with eruptive activity at the Lathrop Wells basalt cone, similar to event Y, but reworking of ash into this fissure is also possible. A U-series age (sample HD1071: 15.5 $\pm$ 1.6 ka) from vein carbonate provides an apparent minimum age for event Z; a maximum age is difficult to define, but it probably postdates the secondary carbonate within the event-Y fissure (U-series ages ranging from 37 to 66 ka). Event Z likely occurred between 20 and 30 ka.

Event Y All four trenches across the central SCF expose prominent fissures containing abundant basaltic ash. At each site, these ash-bearing fissures reflect the largest Quaternary offsets, are bracketed by generally similar-aged deposits, and contain similar secondary carbonate, so they are assumed to represent a single event (Y). In T8, event Y (F5 on fig. 3) is indicated by a prominent, 60-70 cm wide silt- and ash-filled fissure in both walls and the bench in the middle of the trench. Based on geometry, the width of this fissure suggests dip slip of 1.1-1.3 m (0.9-1.1 m vertical displacement). In the south wall, the bottom meter of this fissure is filled with jumbled tuff and carbonate clasts in a matrix of loose, nearly pure basaltic ash. A lack of other detrital material indicates the ash was deposited soon after the fissure opened, and suggests faulting and volcanism were essentially contemporaneous. In the north wall, this fissure is less obvious and lacks the nearly pure ash; the bottom of the fissure is filled with ash-free pebbly silt quite similar to material (unit 5-6?) underlying a tilted block of calcrete (unit 9); these apparently collapsed into the fissure before the ash was deposited, likely during surface faulting. The upper fissure fill in the north wall is a mixture of silt, ash, and gravel similar to that in the south wall. The fault slip suggested by this fissure, which splays subvertically from the dipping bedrock fault plane at a depth of about 4 m, can be estimated from the fault dip (58°) and extensional opening (consistently 60-70 cm), suggesting dip slip of 1.1-1.3 m (0.9-1.1 m vertical displacement). The moderately developed soil in the upper fissure fill ($CaCO_3$ Stage II+ to incipient Stage IV; typically capped by a 1- to 3-mm-thick silica layer) indicates an age of at least a few tens of thousands of years. Minimum ages for event Y are provided by U-series ages from rhizoliths in unit 10 (HD1070: 37 to 56 ka) and from secondary carbonate in unit 12 (HD1465: 47 $\pm$ 9 ka and 66 $\pm$ 23 ka), and by a TL age (TL-30: 36 $\pm$ 5 ka) from unit 11. A U-series age (HD1072: 118 $\pm$ 6 ka) from vein carbonate predating this event provides a single maximum age. The materials from which the younger ages are derived are directly related to the faulting event, whereas the maximum age is not, suggesting the event is closer to the younger ages. These limiting ages are similar to the estimated 70-80 ka age of the principal eruptive phase of the Lathrop Well basalt cone (Perry and Crowe, 1996), and are supportive of a correlation between faulting and volcanism.

Event X In T8, an apparent gravel-filled fissure (F4 on fig. 3) sandwiched between the event-Y and event-W fissures has a jumbled fabric with aligned clasts. There is no clear expression of event X at the other trench sites. There is little constraint on the offset associated with this possible event, but the width of the apparent fissure (about 15 cm) suggests dip slip of 20-30 cm. A U-series age (HD1072; 118 $\pm$ 6 ka) from fracture-filling carbonate in T8 provides an apparent minimum age for event X.

Event W The oldest event cutting all cemented deposits (W) is evidenced by a wedge of gravel (F3 on fig. 3) extending downward into older, massively carbonate-cemented fault zone. All four trenches expose distinct gravel-filled fissures that are smaller than, and predate, the ash-filled fissures — these probably occurred during the same event (W). The age of event W is constrained by the estimated age of the deposits it cuts in T8 (150-250 ka) and by the U-series age apparently associated with event X (118 $\pm$ 6 ka).

Early to Mid-Quaternary Hiatus in Activity

At all of the SCF trench sites, extremely cemented alluvium is present very near the ground surface on the downthrown side of the fault, indicating that prior to the events discussed above, little, if any, offset occurred over a period spanning at least several hundreds of thousands of years. At SCF-T3, a colluvial deposit that yielded U-series ages of 700-900 ka caps most of the fault zone and is offset only by the mid- to late Quaternary events, which thus appear distinctly clustered in time relative to a lower long-term rate.

Prior events

The broader fault zone indicates prior activity, but carbonate overprinting precludes defining a complete event sequence or precise event ages.

A gravel-filled fissure in T8 (F2 on fig. 3), which indicates an earlier event of similar size as event W, is highly fractured and cut by 1- to 2-cm-thick silica veins, but is not obviously displaced by the crosscutting fractures. The secondary carbonate and silica within this fissure indicates a relatively old age. This is the only feature within the older fault zone in T8 that retains recognizable sedimentary fabric, so it likely reflects the most recent significant displacement predating the above events. Similar, albeit less distinct, features are present within the fault zone in SCF-T3.

Earlier activity is better preserved at other trench sites. At SCF-T1, older alluvium is faulted and backtilted across a wider fault zone than that which cuts overlying deposits, which are also massively cemented. SCF-T4 exposes evidence of at least three episodes of prior activity, including a fissure capped by the upper petrocalcic horizon (possibly the same event apparent in T8 and SCF-T3) and by an apparent colluvial wedge cut by that fissure.

Recurrence interval

The occurrence of three or four events over an estimated time period of about 200 ka suggests average recurrence of 50-70 ka over the mid- to late Quaternary. These events may have occurred over a period as short as about 150 ka, suggesting average recurrence of 35-60 ka. Recurrence of about 35 ka is considered to be a maximum (two events within the past 70-80 ka, and four within the past 150 ka). Minimum recurrence of about 100 ka is suggested by considering only the two most definitive (and largest) events, and averaged over a 200 ka time period (the presumed age for the faulted Q3 deposits in T8).

Slip rate

Most of the uncertainty in slip rate estimates stems from age control; displacement uncertainties are generally relatively small. The average slip rate (dip slip) along the SCF over the mid- to late Quaternary appears to be on the order of 0.01-0.02 mm/yr, considering 2.1 m slip over 200 ka and 1.4 m slip over 70-80 ka. Using current estimates of displacement and time over which the observed events have occurred (1.8-2.4 m and 150-250 ka, respectively), the average mid- to late Quaternary slip rate for the SCF is considered to be within the range of 0.007-0.016 mm/yr, with a preferred rate of 0.011 mm/yr. Averaging slip over the past 900 ka (i.e., the age of faulted colluvium in SCF-T3 based on U-series dating) suggests a longer-term average rate of 0.002-0.003 mm/yr, but this is likely less representative of the fault's current character.

Possible Volcanic-related Fault Activity

The largest fissures at all four trench sites along the main trace of the SCF contain abundant basaltic ash. In all of these trenches, a relative lack of other material indicates the ash was deposited very soon after the fissure opened, and suggests temporal coincidence of surface faulting and a nearby basaltic eruption. Historical earthquakes show that such extensional openings begin to fill with detrital material during the first significant rainfall, and invariably contain noticeable fill within weeks to months.

Lack of rounding of the basalt fragments indicates minimal transport and implies a local source. Trace-element chemistry indicates the source to be the Lathrop Wells cinder cone located 11-16 km to the south (Perry and Crowe, 1996). Some geochronologic data (^{39}Ar-^{40}Ar and cosmogenic ^{36}Cl) suggest the ash in the trenches is too old to be associated with the Lathrop Wells cone, and more likely came from one of the ~1 Ma Crater Flat cones (Marek Zreda, University of Arizona, and Brent Turrin, University of California at Berkeley, written communication, 1996). The Crater Flat cones seem an unlikely source, however, because soil development, stratigraphic correlation, several U-series ages, and one TL age all indicate a late Pleistocene age for the fissure-filling material. The possibility of ash from one of the Crater Flat cones being preserved and then emplaced in the fissures during a late Pleistocene faulting event seems unlikely due to the ash's presence at multiple trench sites.

A connection between faulting and volcanism was previously suggested by ash identified in trenches on four different fault traces (Swadley and others, 1984), including T8, but in all of these the ash was present in narrow (2 mm to 2 cm) vertical fractures. The ash exposed in the newer SCF trenches more definitively established a temporal association between faulting and volcanism, and indicates both greater fault slip and a greater volume of ash than could be inferred from the previous exposures.

Temporal clustering of events, combined with apparent association of faulting and volcanism, suggests the mid- to late Quaternary activity on the SCF may be genetically linked with volcanic activity at the Lathrop Wells basalt cone. The simplest association would involve basalt intrusion intersecting the down-dip projection of the southern end of the SCF, but the southern SCF is significantly less active than the central SCF and the ash-filled fissures are well removed from the cinder cone. Activity could be related in a more indirect manner, with both responding to broader tectonic deformation.

Discussion

Fault relations along the SCF are complicated by extensive carbonate overprinting and by relatively small surface offsets. Colluvial wedges (i.e., material shed from and deposited against fault scarps) are commonly observed along normal faults, but are generally lacking along the SCF due to three factors. First and foremost, surface offsets have occurred largely as extensional opening of vertical fissures splaying from a dipping bedrock fault. Colluvial wedges can be formed only after the fissures have been filled. Second, surficial erosion subsequent to faulting is evident at all sites, as indicated by missing soil horizons, truncated fissures, and truncated stratigraphic contacts, and colluvial wedges could thus be partially removed. In all cases, Q5 deposits rest on these disconformities, suggesting erosion occurred during the latest Pleistocene/early Holocene. Third, small vertical displacements ($\leq$0.5 m) are not conducive to formation of obvious colluvial wedges.

Single-event displacements range from fracturing with no obvious offset to possibly more than 1 m of slip associated with the largest event; most of the offsets are relatively small (no more than a few 10s of centimeters). Similarly, the limited age data suggest events have not occurred over regularly spaced time intervals. The apparent mid-Quaternary hiatus in activity further suggests noncharacteristic behavior, and adds uncertainty to forecasting future activity.

Rather than behaving independently, the faults at Yucca Mountain may rupture together during individual seismic events or sequences. Such distributive behavior is suggested by a high degree of fault interconnection and by the presence of basaltic ash in fractures along multiple faults. The faults around Yucca Mountain can be considered to comprise one or more complex fault systems, rather than numerous, independent faults. Historical earthquakes show that small displacements are often highly discontinuous; such events may cause significant offsets in some locations and little or no offset in others. Uncertainties in age control and fault relations will likely always limit how well events can be correlated between faults, or even along individual fault traces.

References Cited

Faulds, J.E., Bell, J.W., Feuerbach, D.L., and Ramelli, A.R., 1994, Geologic map of the Crater Flat area, Nevada: Nevada Bureau of Mines and Geology Map 101, w/text and cross sections, scale 1:24,000.

Hoover, D.L., Swadley, W.C., and Gordon, A.J., 1981, Correlation characteristics of surficial deposits with a description of surficial stratigraphy in the Nevada Test Site region: U.S. Geological Survey Open-file Report 81-512, 27 p.

Lundstrom, S.C., Mahan, S.A., and Paces, J.B., 1995a, Preliminary map of the surficial deposits of the northwest quarter of the Busted Butte 7.5' quadrangle, Nye County, Nevada: U.S. Geological Survey Open-file Report 95-133, scale 1:12,000.

Lundstrom, S.C., Whitney, J.W., Paces, J.B., Mahan, S.A., and Ludwig, K.R., 1995b, Preliminary map of the surficial deposits of the southern half of the Busted Butte 7.5' quadrangle, Nye County, Nevada: U.S. Geological Survey Open-file Report 95-311, scale 1:12,000.

Nelson, P.H., Muller, D.C., Schimschal, U., and Kibler, J.E., 1991, Geophysical logs and core measurements from forty boreholes at Yucca Mountain, Nevada: U.S. Geological Survey Geophysical Investigations Map GP-1001.

Paces, J.B., Mahan, S.A., Ludwig, K.R., Kwak, L.M., Neymark, L.A., Simmons, K.R., Nealey, L.D., Marshall, B.D., and Walker, A., 1995, Progress report on dating Quaternary surficial deposits, 1995 Milestone Report 3GCH510M.

Perry, F.V. and Crowe, B.M., 1996, Geologic setting of basaltic volcanism in the Yucca Mountain region: *in* Volcanism Synthesis Report, Crowe and others, Los Alamos report to the U.S. Department of Energy, chapter 2.

Peterson, F.F., 1988, Soil geomorphology studies in the Crater Flat, Nevada, area: in Evaluation of the geologic relations and seismotectonic stability of the Yucca Mountain area (NNWSI), Quaternary geology and active faulting at and near Yucca Mountain, Appendix B, unpublished Final Report to the Nevada Nuclear Waste Project Office, 45 p.

Peterson, Frederick F., Bell, John W., Dorn, Ronald I., Ramelli, Alan R., and Ku, Teh-Lung, 1995, Late Quaternary geomorphology and soils in Crater Flat, Yucca Mountain area, southern Nevada: Geol. Soc. Amer. Bull., v. 107, no. 3.

Ramelli, A.R., Sawyer, T.L., Bell, J.W., Peterson, F.F., Dorn, R.I., and dePolo, C.M., 1989, Preliminary analysis of fault and fracture patterns at Yucca Mountain, southern Nevada: American Nuclear Society Proceedings FOCUS '89 - Nuclear Waste Isolation in the Unsaturated Zone, Las Vegas, NV, September 18-20, 1989.

Scott, R.B. and Bonk, J., 1984, Preliminary geologic map of Yucca Mountain, Nye County, Nevada, with geologic sections: U.S. Geological Survey Open-file Report 84-494, 9 p., 3 pl.

Simonds, F.W., Whitney, J.W., Fox, K.F., Ramelli, A.R., Yount, J.C., Carr, M.D., Menges, C.M., Dickerson, R.P., and Scott, R.B., in press, Map showing fault activity in the Yucca Mountain area, Nye County, Nevada: U.S. Geological Survey Map I-2520.

Swadley, W.C., 1983, Map showing surficial geology of the Lathrop Wells quadrangle, Nye County, Nevada: U.S. Geological Survey Miscellaneous Investigations Map I-1361, scale 1:48,000.

Swadley, W.C. and Carr, W.J., 1987, Geologic map of the Quaternary and Tertiary deposits of the Big Dune quadrangle, Nye County, Nevada, and Inyo County, California: U.S. Geological Survey Miscellaneous Investigations Map I-1767.

Swadley, W.C., Hoover, D.L., and Rosholt, J.N., 1984, Preliminary report on late Cenozoic

faulting and stratigraphy in the vicinity of Yucca Mountain, Nye County, Nevada: U.S. Geological Survey Open-file Report 84-788, 42 p., 1 pl.

Swadley, W.C. and Parrish, L.D., 1988, Surficial geologic map of the Bare Mountain quadrangle, Nye County, Nevada: U.S. Geological Survey Map I-1826, scale 1:48,000.

Taylor, E.M., 1986, Impact of time and climate on Quaternary soils in the Yucca Mountain area of the Nevada Test Site: unpublished M.S. thesis, University of Colorado, Boulder.

Wesling, J.R., Bullard, T.F., Swan, H.F., Perman, R.C., Angel, N.N., and Gibson, J.D., 1992, Preliminary mapping of surficial geology of Midway Valley, Yucca Mountain, Nye County, Nevada: Sandia National Laboratory Report 91-0607.

Day 2, Stop 3

Eolian Dust from Natural Traps on Yucca Mountain

Marith Reheis, Jim Brune, Jim Yount, and Jim Budahn

Fine grained deposits fill vugs (cavities) formed by weathering in the rhyolite tuffs of Yucca Mountain. Samples of some of these deposits were collected from vugs formed in precariously balanced rocks along the west side and crest of Yucca Mountain where deposition by alluvial or slope processes is precluded by the positions of the rocks. The precarious rocks, and thus the vugs, have been in position for at least the last several thousand years (Bell and others, 1998). Thus the vugs serve as long-lived dust traps for the Yucca Mountain region. The vug fills are composed of calcareous, silt-rich sediment that must have been deposited by eolian processes. The samples were compared to samples of modern dust, alluvium of various compositions, and playa deposits, all collected in the Amargosa region around Yucca Mountain. We used instrumental neutron activation analysis (INAA) to determine the chemistry of the vug-filling deposits. (The initial intent of the study was to examine the samples petrographically for shards of volcanic glass that might constrain the length of time that the rocks had been balanced in their present positions, but not enough shards were found for tephrochronologic analysis.) Results of this cursory petrographic examination are presented in Table 1.

Table 1. Petrographic examination of dust samples from vugs within precarious rocks near Yucca Mountain. [r, rare; c, common; --, not observed]

	Silt Fraction (<63μ)			Fine Sand Fraction (<250μ)			
Precarious Rock Locality[1]	Glass shards[2]	Carbonate + clay clots	Angular quartz	Sub-angular quartz	K-spar	Plagioclase	Mafics
Lathrop Point	r	r	r	c	--	--	c
Tripod Point	--	--	r	c	r	--	--
Trench 8	r	c	r	r	--	r	c
Above Trench 8	r	r	c	r	--	--	c
Green Flag Point	--	c	c	c	r	--	c

[1]Locality names not standard. Informal names amongst investigators do not correspond to named locations on maps of the Yucca Mountain area.

[2]Isotropic, angular, clear fragments. Distinctly different than hydrated cloudy fragments of Miocene-aged welded tuff. Presumed to be fragments of Quaternary-aged tephra.

For most of the elements examined (Figs. 1A, B), the vug-filling deposits are nearly identical to, or overlap with, samples of modern eolian dust collected from sites in the Amargosa region. The examples in Figure 1 show elements that reflect different source types: (A) Sr is associated with Ca and reflects playa deposits and, to a lesser extent, carbonate-rich alluvium. Rb is associated with K and is indicative of felsic rocks and clay minerals. (B) Eu and Ce are rare

earth elements that concentrate in heavy minerals which tend to be winnowed out during eolian transport. (C) As and Sb are found in a variety of geologic settings, including concentrated amounts in ore deposits, and are also used in atmospheric studies as tracers of industrial pollutants. The vug fills and the modern dust are probably mixtures of sediment deflated mainly from local alluvial sources and playas (Fig. 1; Reheis and Kihl, 1995; Reheis and Budahn, 1998). Some of the vug fills (henceforth referred to as "old dust") are slightly enriched in some elements such as K, Rb, and rare earths (Figs. 1A, 1B) with respect to modern dust. We interpret this enrichment to be caused by additions of K-rich weathered tuff from the vug walls. Sand-size sub-angular quartz, K-feldspar, and mafic fragments seen in petrographic examination (Table 1) confirm the presence of vug wall contaminants in the dust.

Figure 1. Plots of trace-element concentrations of dust and source samples measured by INAA.

Some of the vug fillings were subsampled by depth (vug fills are as much as 6 cm thick) to see if they are stratified. Comparison of samples from the tops and bottoms of these fillings (not shown) indicates little difference in trace-element content with depth, except that some of the elements associated with heavy minerals (e.g. Fe, Zr, Cs, and most rare earths) are slightly more concentrated on the bottoms of the fillings. These relations indicate that either there has been little change through time in the composition of dust accumulating in the vugs, or that the fillings are well mixed by burrowing insects and by wetting and drying.

Most interesting is the discrepancy in contents of As and Sb between samples of old dust from Yucca Mountain and of modern dust from the Amargosa region (fig. 1C); old dust is depleted in As and Sb relative to modern dust. Preliminary interpretations of these data combined with those from dust and dust-source samples elsewhere in the Mojave Desert suggest that southern Owens Valley, including Owens (dry) Lake (artificially desiccated due to water diversions by Los Angeles early in the 1900's), is the source of the dust enriched in As and Sb (triangles, fig. 1C; Reheis and Budahn, 1998). Sb in dust above the lake bed is 7-11 ppm and increases to as much as 14 ppm in Owens Valley south of the lake bed; As shows a similar pattern (Reheis and Budahn, 1998). Because the As and Sb enrichment doesn't seem to be solely derived from the lake bed, we suspect the ultimate or additional sources are the mining districts along the Inyo Range east of Owens (dry) Lake, some of which contain As- and Sb-bearing ores (Merriam, 1963).

The old dust on Yucca Mountain would have accumulated over a long time span, perhaps thousands of years, during which Owens Lake (then full of water) and the unmined ore deposits would not have been dust sources. The calculated silt-plus-clay (dust) accumulation rate from Holocene soils at Yucca Mountain is about 6 $g/m^2/yr$ and the modern rate is about 7 $g/m^2/yr$ (Reheis and others, 1995). Because modern dust-deposition rates are only a little larger than the Holocene rates, the old dust would be dominated by dust from sources with little As and Sb, in contrast to modern dust.

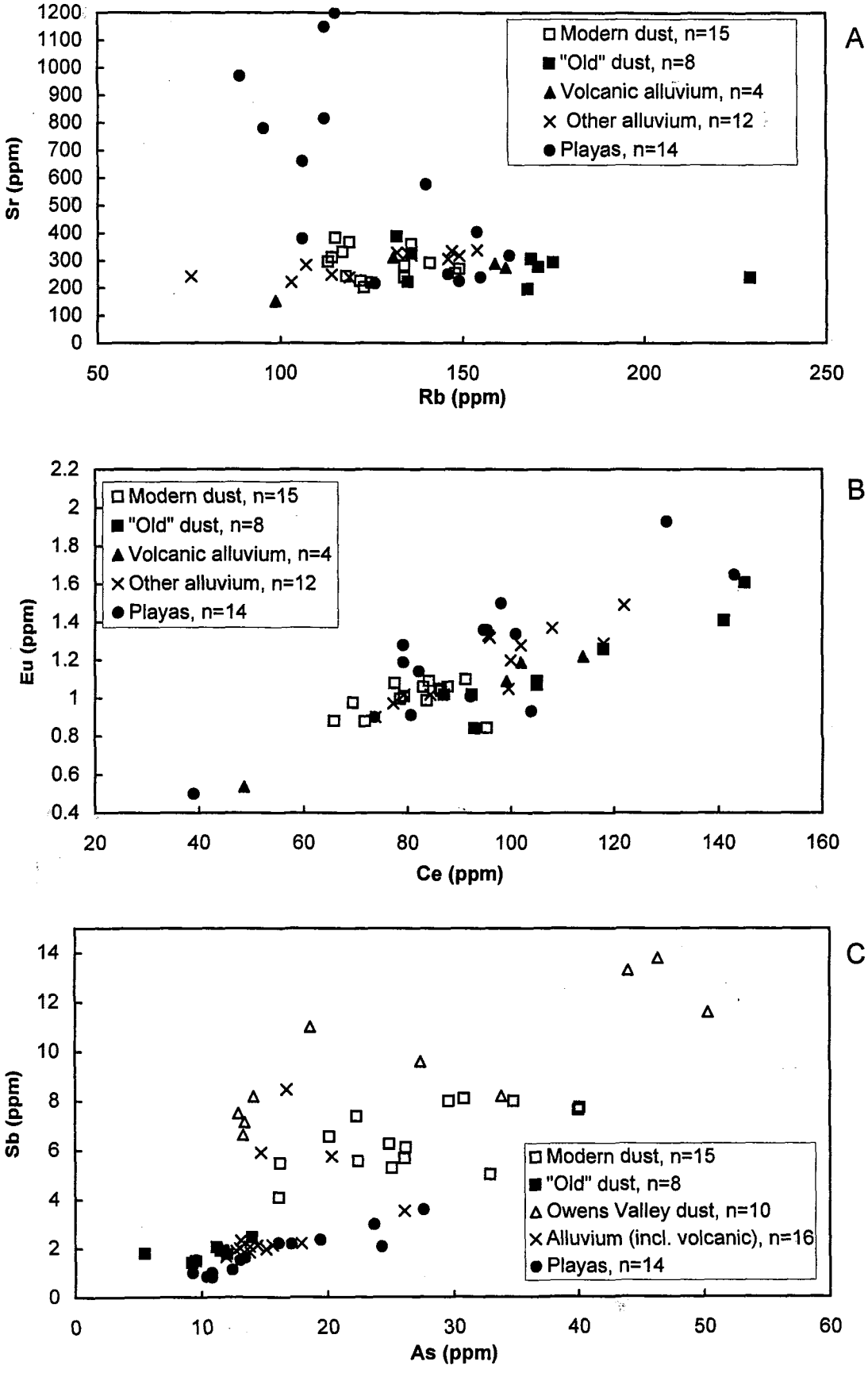

Figure 1. Plots of trace-element concentrations of dust and source samples measured by INAA

References Cited

Bell, J.W., Brune, J.N., Liu, Tanzhuo, Zreda, Marek, and Yount, J.C., 1998, Dating precariously balanced rocks in seismically active parts of California and Nevada: Geology, v. 26, p. 495-498.

Merriam, C.W., 1963, Geology of the Cerro Gordo mining district, Inyo County, California: U.S. Geological Survey Professional Paper 408, 83 p.

Reheis, M.C., and Budahn, J.R., 1998, Geochemical evidence for sources of dust in the southwestern Great Basin, U.S.A.: Abstract for 3rd International Conference on Aeolian Research, Oxford, England, July 1998.

Reheis, M.C., Goodmacher, J.C., Harden, J.W., McFadden, L.D., Rockwell, T.K., Shroba, R.R., Sowers, J.M., and Taylor, E.M., 1995, Quaternary soils and dust deposition in southern Nevada and California: Geological Society of America Bulletin, v. 107, p. 1003-1022.

Reheis, M.C., and Kihl, Rolf, 1995, Dust deposition in southern Nevada and California, 1984-1989: Relations to climate, source area, and source lithology: Journal of Geophysical Research, v. 100, no. D5, p. 8893-8918.

Day 2, Stop 4

Bare Mountain Fault

Larry W. Anderson and Ralph E. Klinger

Bare Mountain is a relatively small, triangular mountain range roughly 20 km long in a north-south direction and about 10 km wide at its widest point (Fig. 1). In contrast to the volcanic terrain at Yucca Mountain, Bare Mountain is composed primarily of late Proterozoic and Paleozoic sedimentary rocks. These rocks are weakly metamorphosed, folded, and faulted, and dip generally northward (Monsen et al., 1992). Overlying the sedimentary rocks on the north flank of Bare Mountain is a sequence of Tertiary volcanic rocks that were erupted from the Timber Mountain caldera complex about 20 km northeast of Bare Mountain. As viewed from the east (Fig. 2), Bare Mountain has a profile typical of many ranges in the Basin and Range province. The range is quite symmetrical with the highest part of the range (elevation 1925 m) located about halfway between the Tates Wash area and Steves Pass. A major difference from most other ranges in the Basin and Range is that Bare Mountain is relatively short, being only about 18-20 km in length. Also, when compared to the volcanic ranges north and east of Bare Mountain, such as Yucca Mountain, both flanks of Bare Mountain are impressively steep, which gives an overall impression of tectonic youthfulness. It is interesting however, that both the east and southwest sides of the range are equally steep, with slopes averaging about 14-22°.

Figure 1. Vertical aerial photograph mosaic of Bare Mountain area.

The Bare Mountain fault is a 20-km-long, east-dipping normal fault that bounds the east side of Bare Mountain. Cornwall and Kleinhampl (1961a) were the first to suggest the presence of a major range-bounding structure along the east side of Bare Mountain. They inferred Quaternary activity on this fault because of the sharp, straight range front; the small, relatively undissected alluvial fans along the east side of the range; and the linear alignment of Pleistocene volcanic cones in Crater Flat. Swadley et al. (1984) were the first to refer to this structure as the Bare Mountain fault. Mapping by Swadley and Parrish (1988) shows the range-front fault displacing early Pleistocene deposits, but being buried by younger, late to middle Pleistocene deposits. In contrast, Reheis (1988) and Monsen et al. (1992) indicate that deposits as young as Holocene are faulted at several locations along the range.

Anderson and Klinger (1996a) conducted a detailed paleoseismic study of the Bare Mountain fault as part of site characterization for Yucca Mountain. Data gathered through a program of surficial geologic mapping (Fig. 3; table 1), descriptions of representative soil profiles (table 2), topographic profiling of fault scarps (Fig. 4, table 3), excavation and mapping of trench exposures across the fault (Figs. 5 and 6), and numerical dating of deposits exposed in trenches indicate that the fault can best be characterized as a fault with a low slip rate (on the order of 0.01 mm/year) and infrequent, moderate to large-magnitude earthquakes (return periods of about 100,000 years). Anderson and Klinger (1996a) also concluded that the most recent surface-rupturing event associated with the Bare Mountain fault occurred no more recently than about 16-21 ka, but could be old as 100 ka.

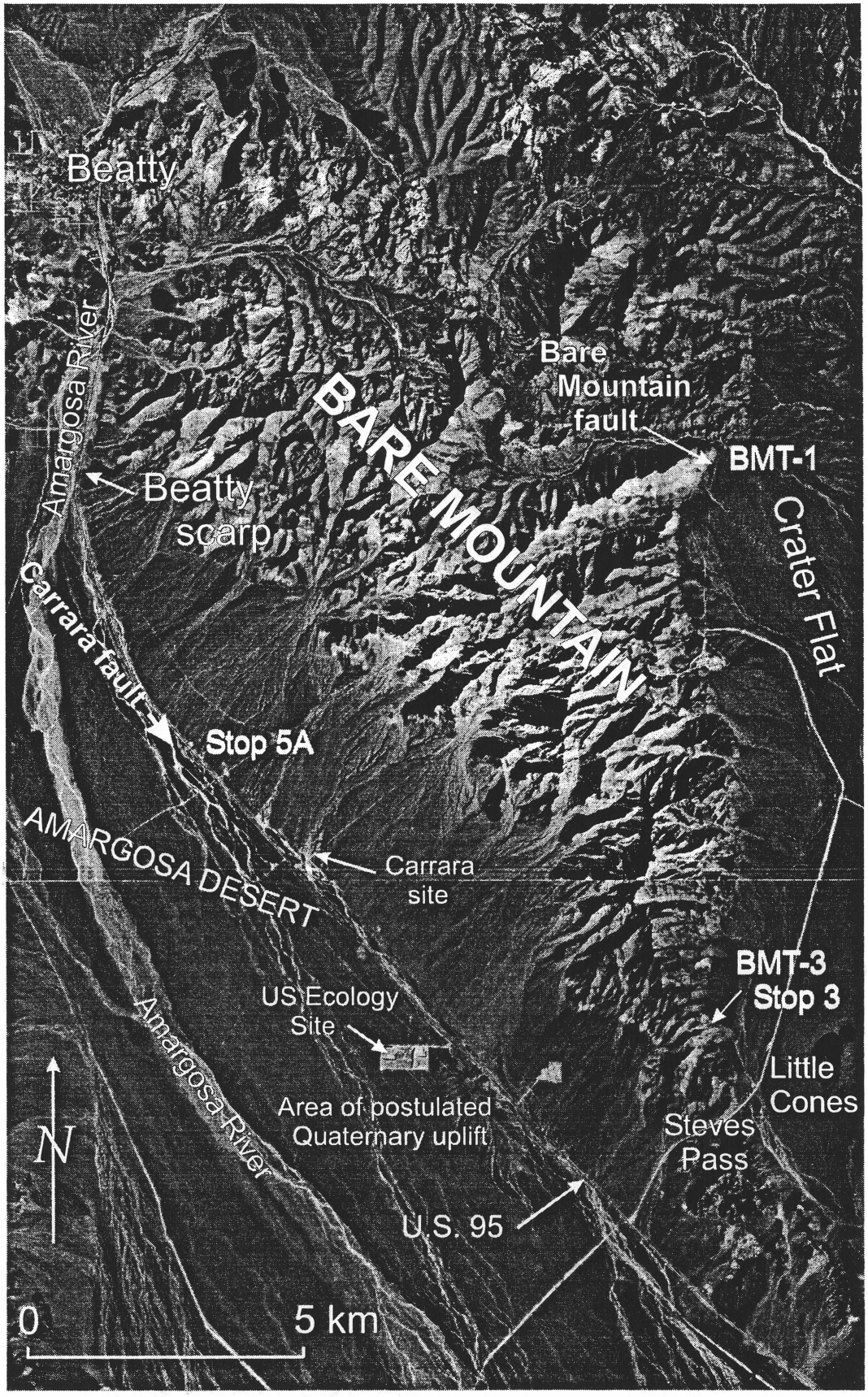

Figure 1 - Vertical aerial photograph mosaic of Bare Mountain area

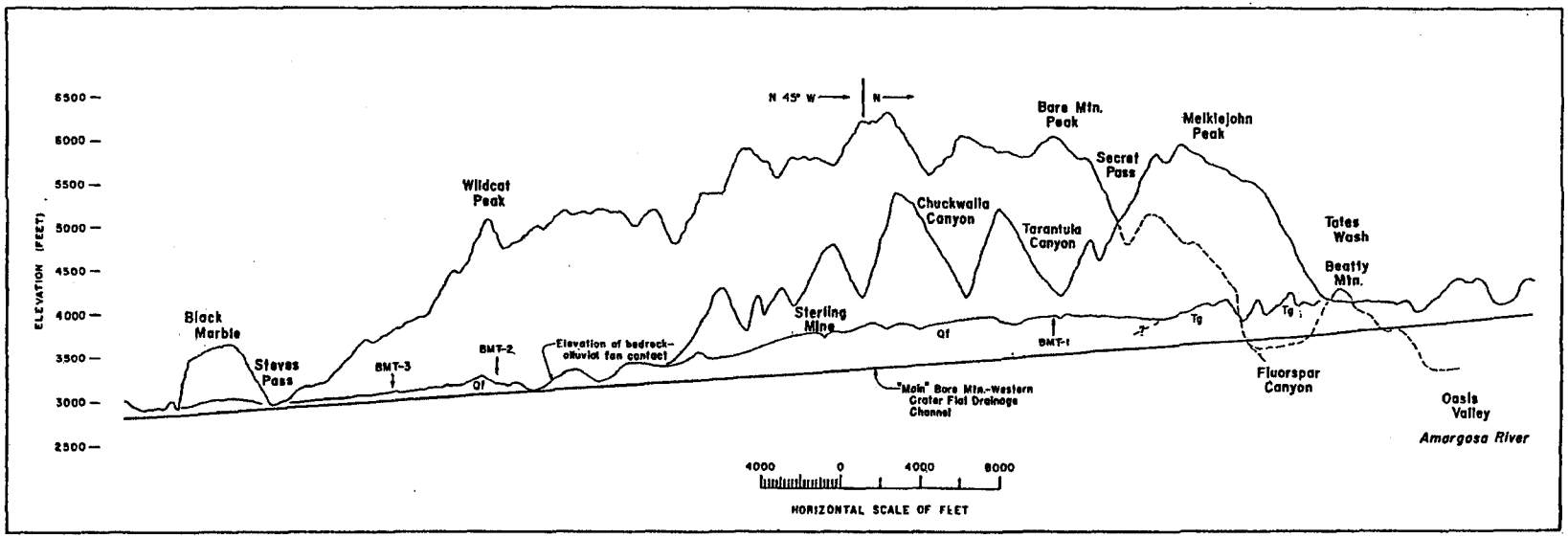

Figure 2. Topographic profile of Bare Mountain looking west from Crater Flat. The profile that starts near Black Marble is the western-most crest of the range. The profile that starts near the Sterling Mine is the eastern-most crest. The dashed line is the profile of the western crest hidden behind Melkejohn Peak. The lowest profile is the bedrock-alluvium contact at the range front. Vertical exaggeration is about 4X. BMT-1 (Tarantula Canyon site), BMT-2 (Wildcat Peak site), BMT-3 (Stirling site) are trench locations; Qf - Quaternary alluvial fans; Tg - Tertiary gravel.

Table 1. Surface characteristics utilized for the subdivision of surficial deposits and geomorphic surfaces along the Bare Mountain fault. The characteristics listed in this table may not depict the age of underlying deposits or reflect sedimentological properties related to its depositional history.

Unit	Soil	Pavement	Desert Varnish	Topography
Q5	May have weak Av/C profile; Av<1 cm thick	Generally absent; local incipient packing and horizontal orientation of clasts	None	High-relief bar and swale
Q4	Thin Av horizon (several cm thick)	Poorly packed	Weakly developed on quartzite clasts	Bar and swale is distinct but subdued; bars are coarser grained than adjacent swales.
Q3	Moderately developed Av horizon (5-10 cm thick)	Moderately to well packed on bars	Moderately developed on quartzite clasts	Bar and swale subdued; transition between bars and swales diffuse
Q2	Well developed Av horizon (>10 cm thick)	Moderately to well packed pavement; $CaCO_3$ rinds on clasts, fragments common in pavement	Well developed on surface clasts	Little or no evidence of bar and swale; surface is nearly smooth
Q1	Av horizon may or may not be present depending on topographic position	Moderately to well packed; pavement is being degraded; underlying petrocalcic horizon is locally exposed	Moderately to well developed on some surface clasts; sometimes lacking	Surface is dissected; small rills and drainages common
QTa	Gravel completely cemented with carbonate or silica, or both; in places, surface veneered by younger unconsolidated deposits	None	None	No original surfaces preserved

---

Table 2. Field Descriptions of Soil Profiles.

FIELD DESCRIPTIONS OF SOIL PROPERTIES

[This profile was described in support of Yucca Mountain Site Characterization Activity 8.3.1.17.4.3.4 following procedures outlined in USGS Technical Procedure GP-17, Rev 1. Horizon nomenclature and soil property abbreviations follow Soil Survey Staff (1994) and Birkeland and others (1991)]

Profile No. BMT-3 Described by Ralph E. Klinger Date 06/13/95 Time 8A

Parent Material(s) Late Proterozoic quartzite alluvium Surficial Unit Q2 Slope 8-11° Aspect E

Location Station 8.25 in the northwall of fault trench BMT-3 (see plate 5)

Quadrangle Carrara Canyon Provisional 7½' Longitude 116°37'50" Latitude 36°46'26" Elevation 3120'

Horizon	Depth (Thickness)	Boundaries	Structure	Clay Films	Wet Consistence Stickiness	Wet Consistence Plasticity	Dry Consistence	Texture	$CaCO_3$ Morphology	Gravel %	Color
Av	0-11 (11)	as	sg to 1m-cpl-sbk	none	so	po	so	S	no reaction	10	10YR 6/3d 10YR 4/3m
2Avbk	11-26 (15)	cw	2csbk	v1fpf	ss	po	so	SL	es, II+	25	10YR 7/3d 10YR 5/3m
3Btbkb	26-44 (18)	cw	gr to 2fsbk	1dpf	ss	po	sh to h	SL	es, I	50	7.5YR 6/4d 7.5YR 5/6m
3Btbkb2	44-86 (42)	cw	3c-vcabk to pr	3dpf	s	p	vh	SCL	es, II	50	7.5YR 6/4d 7.5YR 5/6m
3Btbkb3	86-102 (16)	cw	gr to 1-2m-csbk	1dpf-po	s	ps	sh to h	SCL	es, I	50	7.5YR 6/4d 7.5YR 5/6m
3BKb	102-184 (82)	cw	sg to 1fsbk	none	so	po	lo	S	ev, II+ to III	>75	10YR 7/3d 10YR 5/4m
4Abkb	184-197 (13)	cw	sg to 1fsbk	none	so	po	lo to so	S	es, II to II+	50	10YR 7/3d 10YR 5/4m
4Btbkb	197-228 (31)	cw	2fsbk	1dpf	ss	ps	h to vh	SL	e-ev, II	50	7.5YR 6/4d 7.5YR 5/4m
5BKb	228-284+ (56)	none	sg	none	so	po	lo	S	es, I+ to II	>75	10YR 7/3d 10YR 5/4m

NOTES:

This profile is a composite with the upper meter of the soil profile being described on the north wall of the trench and the lower part of the profile being described on the south wall. While the horizon sequence of this profile is not technically buried as defined by the Soil Survey Staff (1994), numerous properties of underlying horizons are related to soil forming processes not associated with current climatic conditions and buried horizon nomenclature has been used to emphasize these characteristics and their importance relative to landscape development and timing of fault activity. The Av horizon is developed on fine-grained eolian sand derived from nearby Crater Flat Wash. There is no source of sand upslope. Colluvial processes downslope have apparently incorporated the desert pavement to contribute gravel found in horizon. The Avbk horizon is developed on eolian silt as opposed to eolian sand, thus the designated change in parent material. The B horizons are formed on quartzite alluvium. The lack of fine-grained material in the upslope drainage basin suggests that the bulk of the fine-grained material in the argillic horizons is pedogenic. Calcium carbonate development in the 3Btbkb2 horizon appears to be overprinted onto an older argillic horizon. Calcium carbonate morphology reaches maximum development in this horizon with maximum argillic development. Calcium carbonate morphology in the 3BKb horizon is strongest at the upper boundary. Weak laminar morphology, near continuous filaments, and rinds are several millimeters thick are present. Patchy morphology of rinds suggests possible inheritance of morphology. The buried 4Abkb horizon designation based on horizon position relative to the underlying argillic horizon and the similarity in color and texture to surface A horizon. No vesicular structure was observed. The change in parent material is based on higher percentage of fine-grained material. Calcium carbonate nodules in the 4Btbkb horizon are common forming mottles up to 10 centimeters in diameter. The 5BKb horizon is developed on clast-supported quartzite alluvium.

FIELD DESCRIPTIONS OF SOIL PROPERTIES

[This profile was described in support of Yucca Mountain Site Characterization Activity 8.3.1.17.4.3.4 following procedures outlined in USGS Technical Procedure GP-17, Rev 1. Horizon nomenclature and soil property abbreviations follow Soil Survey Staff (1994) and Birkeland and others (1991)]

Profile No. BMT-3-1 Described by Ralph E. Klinger Date 06/13/95 Time 3P

Parent Material(s) Late Proterozoic quartzite alluvium Surficial Unit Q2 Slope 18° Aspect E

Location West end of the north wall of fault trench BMT-3 (see plate 5)

Quadrangle Carrara Canyon Provisional 7½' Longitude 116°37'50" Latitude 36°46'26" Elevation 3120'

Horizon	Depth (Thickness)	Boundaries	Structure	Clay Films	Wet Consistence Stickiness	Wet Consistence Plasticity	Dry Consistence	Texture	$CaCO_3$ Morphology	Gravel %	Color
Av	0-2 (2)	as	1fpl	none	so	po	so	SL	slight	none	10YR 6/3d 10YR4/3m
2Avk	2-15 (13)	as	3c-vcsbk	3d-ppf/po	vs	vp	so	SiL to SiCL	es, II	10	10YR 7/3d 10YR5/4m
3Bt	15-37 (22)	as	2c-vcabk	3d-ppf/po	vs	vp	sh to h	CL to C	e	25	7.5YR6/6d 7.5YR5/6 m
3BK	37-120 (83)	as	m to 1mpl	none	so	po	eh	S	es, IV	75	10YR 8/2d 10YR6/3m
Bedrock	120+	none	m	none	-	-	-	-	es, III	rock	10R 8/2 to 5R 4/6

NOTES:

The A horizon is developed on fine-grained eolian sand. The thickness of the horizon is highly variable along the length of the trench thickening slightly across the topographic scarp. The 2Avk horizon is developed on eolian silt. This horizon similarly thickens across the topographic scarp. The B horizons are developed on quartzite alluvium. The lack of calcium carbonate development in the argillic horizon as seen elsewhere is believed to be due to the compressed nature of the profile and the position of the horizon relative to the surface. The 3BK horizon is completely cemented with calcium carbonate displaying weak platey structure in the upper 5-10 centimeters. The bedrock is the lower quartzite member of the late Proterozoic/early Cambrian Wood Canyon Formation. The red color of the bedrock reflects hydrothermally altered and highly sheared nature of the rock. Upper part of the bedrock adjacent to boundary with calcic horizon is completely impregnated with calcium carbonate.

FIELD DESCRIPTIONS OF SOIL PROPERTIES

[This profile was described in support of Yucca Mountain Site Characterization Activity 8.3.1.17.4.3.4 following procedures outlined in USGS Technical Procedure GP-17, Rev 1. Horizon nomenclature and soil property abbreviations follow Soil Survey Staff (1994) and Birkeland and others (1991)]

Profile No. BMT-3-2 Described by Ralph E. Klinger Date 06/27/95 Time 7A

Parent Material(s) Late Proterozoic quartzite alluvium Surficial Unit Q2 Slope 8-11° Aspect E

Location Station 22.5 in the south wall of fault trench BMT-3 (see plate 5)

Quadrangle Carrara Canyon Provisional 7½' Longitude 116°37'50" Latitude 36°46'26" Elevation 3120'

Horizon	Depth (Thickness)	Boundaries	Structure	Clay Films	Wet Consistence Stickiness	Wet Consistence Plasticity	Dry Consistence	Texture	CaCO3 Morphology	Gravel %	Color
Av	0-8 (8)	cw	sg to 3mpl	none	so	po	so	LS	no reaction	10	10YR 6/3d 10YR 4/3m
2Avbk	8-22 (14)	as	2msbk	2ppo	s	p	so to sh	L	es to ev, II to II+	10	10YR 7/3d 10YR 5/4m
3Btbkb	22-56 (34)	aw	2-3cabk	3ppf	vs	p	h to vh	CL	e to es, I+	50	7.5YR 6/6d 7.5YR 5/6m
3BKb	56-107 (51)	aw	m to 1fsbk	none	so	po	so to sh	S	es, III+ to IV	50	10YR 7/2d 10YR 6/4m
Bedrock	107+	none	m	none	-	-	-	-	es, III	rock	10R 8/2 to 5R 4/6

NOTES:

The Av horizon is developed on fine-grained eolian sand. Horizon has poorly developed vesicular structure. Horizon color influenced by organic content. Very well developed vesicular structure exists in 2Avbk horizon. The horizon is also developed on eolian silt, but the upper boundary marked by stone line formed by buried desert pavement. The 3Btbkb horizon has a very well developed argillic horizon. Calcium carbonate filaments are present adjacent to clasts. The matrix is only slightly whitened and effervesces slightly. The upper part of the 3BKb horizon is marked by thin laminar calcium carbonate and recemented pendants (incipient stage IV morphology). The horizon has an overall mottled appearance with occasional pockets of reddened matrix laterally (relict argillic horizon?). The lower quartzite member of the late Protozoic/early Cambrian Wood Canyon Formation outcrops in the bottom of the trench. The upper part of the outcrop adjacent to lower boundary of overlying calcic horizon is completely impregnated with calcium carbonate.

Table 3. Bare Mountain fault scarp profile data. Scarp height, surface offset, maximum scarp-slope angle, and surface-slope angle measured by hand and from computer-generated plots of the profiles. Profiles 1-9 measured at the Tarantula Canyon site. Profiles 11-15 measured at the Stirling site. Profiles 1, 3, and 5 measured with hand level and stadia rod; profile 15 measured with hand level and 0.5-m-long rod; all other profiles measured with electronic surveying equipment (total station). No scarp was observed in profiles 8 and 9. Profile 3 was measured along axis of trench BMT-1 before excavation. Profile 4 was measured immediately south of trench BMT-1.

Profile	Scarp height (meters)	Surface offset (meters)	Maximum scarp-slope angle (degrees)	Surface-slope angle (degrees)
1	2.0	1.6	5.5	1.0
2	1.4	0.9	7.0	2.0
3	2.2	1.5	6.0	1.5
4	2.4	1.9	10.0	1.5
5	1.9	1.5	6.0	1.0
6	1.8	1.1	8.5	2.0
7	1.1	0.4	7.5	3.0
8	-	-	-	-
9	-	-	-	-
10	1.2	0.8	14.0	5.0
11	2.5	1.1	18.0	9.5
12	2.3	1.1	17.5	8.5
13	1.3	0.5	18.0	8.5
14	2.7	0.9	15.0	8.5
15	3.3	0.8	20.0	11.0

Figure 3. Surficial geologic map of the Stirling site.

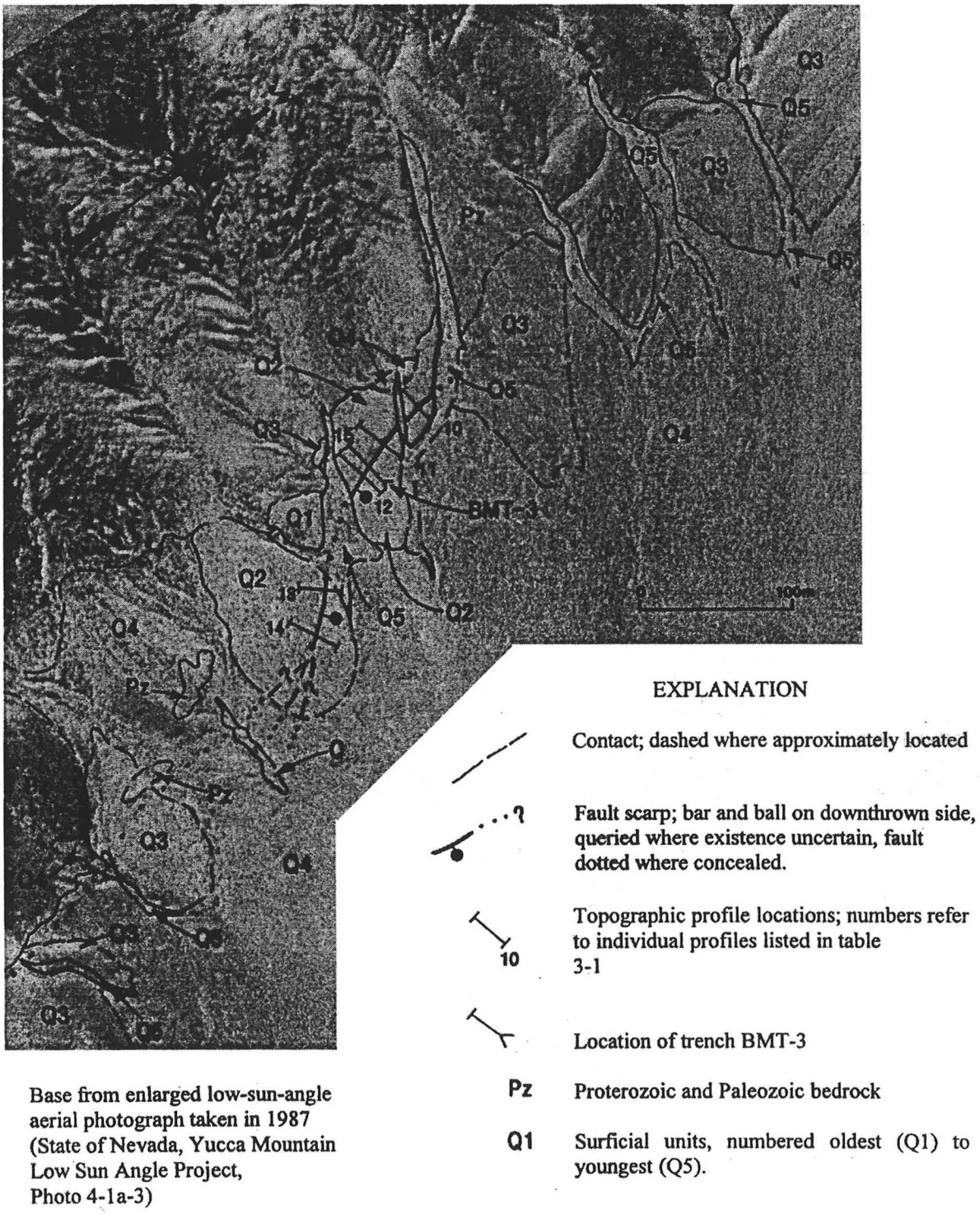

Base from enlarged low-sun-angle aerial photograph taken in 1987 (State of Nevada, Yucca Mountain Low Sun Angle Project, Photo 4-1a-3)

Figure 3. Surficial geologic map of the Stirling site.

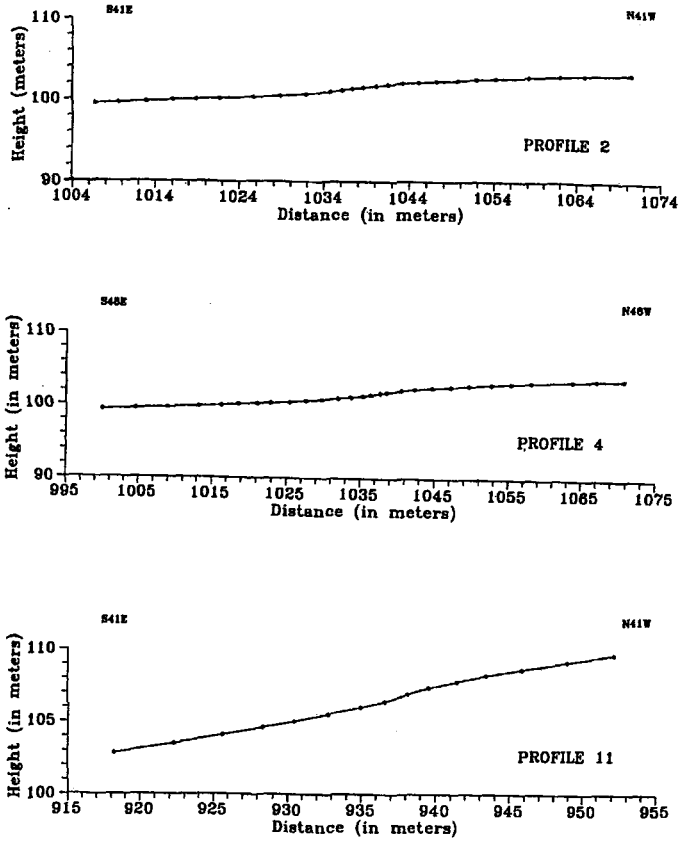

Figure 4. Representative scarp profiles of the Bare Mountain fault.

Figure 5. Log of trench BMT-3.

Trench BMT-3 - Stirling Site

This site is informally named after the Stirling Quartzite which is the source for the monolithologic alluvial fans in the area. The Bare Mountain range-front at the Stirling site is quite low, with only about 200 m of relief (Fig. 2). This suggests that displacement on Bare Mountain fault is less at the Stirling site than it is near Tarantula Canyon, where the relief approaches 700 m.

The alluvial fan deposits at this site are relatively thin in places, overlying bedrock of the Late Proterozoic Wood Canyon Formation. The Q2 alluvial fan surface is fairly steep (average slope of 8-11°), has subdued bar-and-swale topography, and has moderately-developed desert pavement. Many of the quartzite clasts have moderate to dark rock varnish and many clast bottoms are reddened. The middle Pleistocene age for the Q2 alluvial fan is based on the collective characteristics of the surrounding alluvial fans (table 1) and the correlation to dated deposits in the area.

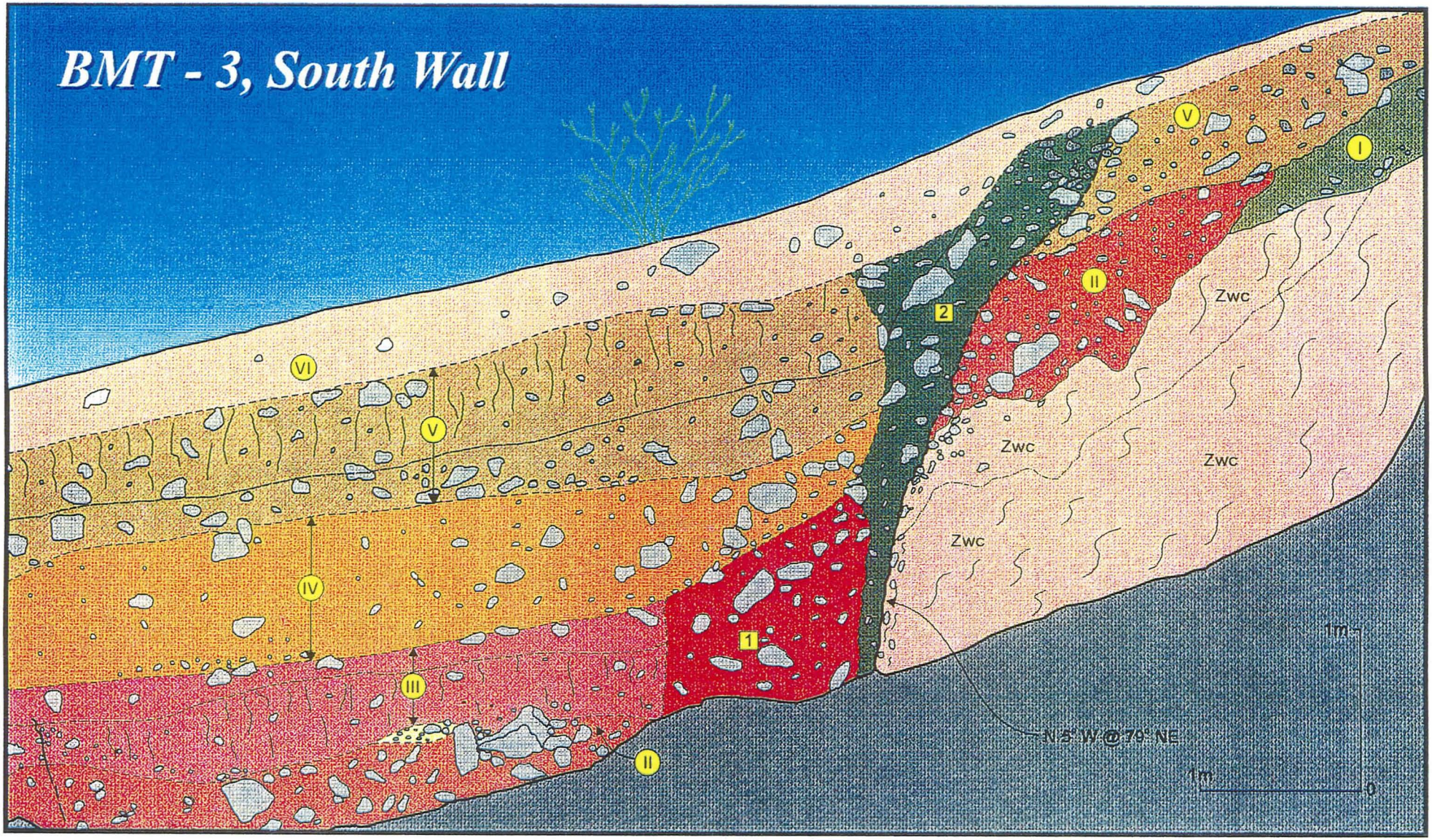
BMT - 3, South Wall
VI
V
IV
III
II
I
II
V
2
1
Zwc
Zwc
Zwc
Zwc
N 5° W @ 79° NE
1m
1m
0

Scarp Profiles

The scarp at the Stirling site is slightly arcuate, is approximately 250 m long, and strikes nearly north-south to about N40W (Fig. 3). The scarp is about 1-3 m high and is present on remnants that are interpreted to be a middle Pleistocene Q2 alluvial fan (Fig. 3; table 3). Six topographic profiles were measured across the scarp at the Stirling site (Fig. 3; profiles 10-15). Maximum scarp angles range from 15° to 20° and maximum scarp heights range from 1.3 m to 3.3 m (table 3). Data for the Stirling scarp are plotted against the data for the dated Beatty scarp (Anderson and Klinger, 1996b), the regressions of Bucknam and Anderson (1979), and the data for the Tarantula Canyon scarp (fig. 7). Although scarp heights for the Stirling scarp and the Tarantula Canyon scarp are very similar (about 1-3 m), maximum scarp angles for the Stirling scarp are higher than those for the Tarantula Canyon scarp and are more similar to those for the Beatty scarp. The difference between the Tarantula Canyon scarp and the Stirling scarp suggests that the Stirling scarp is younger than the Tarantula Canyon scarp. However, no scarps have been identified on Q3 and Q4 age alluvial fans to the north and south of the scarp at the Stirling site (fig. 3). We believe the steep alluvial fan surface at the Stirling site (8.5-11° slopes verses 1-3° for the Tarantula Canyon alluvial fan) results in steeper maximum scarp-slope-angles (see Hanks and Andrews, 1989). If the effect of far-field slope is taken into consideration, the scarp characteristics between the two sites are very similar.

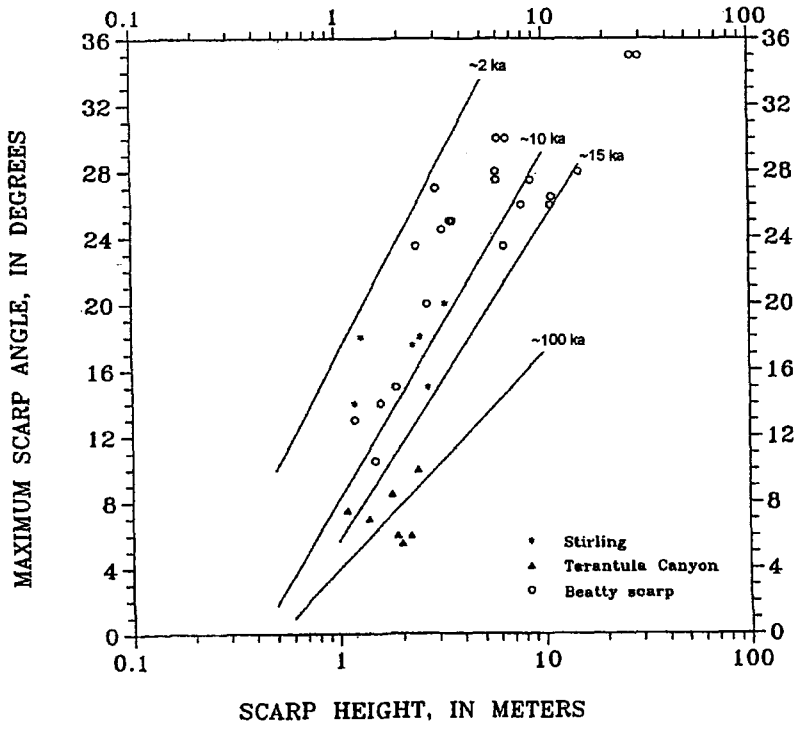

Figure 7. Plot of scarp heights and maximum scarp-slope-angles for the Bare Mountain scarp profiles compared to those for the Beatty scarp (from Anderson and Klinger, 1996b) and to the regression lines for scarps of known age in the Basin and Range (modified from Bucknam and Anderson, 1979).

Trench Interpretation

An obvious fault zone is exposed in BMT-3, coincident with the base of the surface scarp (Fig. 5). Strata and structures exposed in BMT-3 indicate that at least two surface-rupturing earthquakes associated with the Bare Mountain fault have occurred at this location in the middle to late Quaternary. The Wood Canyon Formation (Zwc) and units II, III, and IV, V are clearly faulted. Although unit VI thickens near the fault, this unit overlies the fault zone with no obvious evidence of being faulted. However, because unit VI is interpreted to be the Av horizon associated with the underlying Bt and Bk horizons of units IV and V, the base of unit VI must have been faulted by the most recent surface-rupturing event. The lack of clear evidence of being faulted and the thickening of the unit across the scarp probably reflects the time-transgressive nature of the unit, subsequent pedogenesis, and the relative mobility of the fine-grained sediment on the alluvial fan surface.

The earliest geologic event recorded in the strata at BMT-3 is the erosion or pedimentation of the Wood Canyon Formation and subsequent deposition of unit I. A faulting event (event A), probably occurred following the deposition of unit I, but there is no direct geologic evidence (colluvial wedge or correlative unit I on the hanging wall) for this in the trench exposure. Sometime later, the package of sediment represented by units II and III was deposited across the fault. A period of landscape stability followed deposition of these units as evidenced by the development of the B horizon on unit III (the correlative unit does not appear on the footwall side of the fault apparently being eroded before or during deposition of units IV and V. A faulting event (event B), then occurred, displacing units II and III. The subsequent shearing and fracturing associated with this event, and erosion of these units produced fissure fill 1. Faulting event B is clearly post-dated by the deposition of units IV and V across the fault. The amount of displacement associated with this event is difficult to measure, but appears to be about 1.5 m. Unit III appears to be significantly backtilted towards the fault, resulting in an apparent vertical separation of nearly 3 m if one projects the top of unit III towards the former ground surface. This assumes the top of a B horizon of similar thickness to the B horizon developed on unit III was associated with unit I and that unit III had a slope similar to that of unit V and the present ground surface (about 8-11°). Restoring unit III to that position results in the net slip from this event of roughly 1.5 m.

Following the penultimate event (event B), the stratigraphic package represented by units IV, V and VI was deposited across the fault zone. A significant period of landscape stability followed as evidenced by formation of the well developed Bt horizon on units V and the Bk horizon on units II and IV. These units were subsequently displaced by the most recent surface-rupturing event (event C). Measurements on unit V indicate the net slip for event C is about 0.8 m. This value was measured by projecting the surface of unit V towards the fault zone from a point about 7 m on their respective sides of the fault and using a slope of 11°. The detailed scarp profile (fig. 4; profile 15) shows a relatively constant far-field slope of 11° at this location. This projection was also made to account for the backtilting of unit V on the hanging wall and the apparent erosion of unit V near the fault on the foot wall. The net slip of 0.8 m determined from the faulted strata agrees with the surface offset of 0.8 m measured from the scarp profile.

Shearing and fracturing associated with event C, and the subsequent erosion of units II, IV, and V produced fissure fill 2 and resulted in the thickening of unit VI on the downthrown side of the fault. Faulting event C was also followed by calcium carbonate horizon (stage I+ to II morphology) development in unit V and fissure fill 2, and deposition of a thin unit across the

scarp (north wall). The formation of the calcic horizon on unit V following the most recent event is supported by the fact that the lower boundary of the horizon parallels the ground surface and has formed on fissure fill 2. This relationship of the Bk horizon to the fault is similar to the relationship between the Bk horizon and the fault in trench BMT-1. The upper part of fissure fill 2, displays significant clay accumulation and a greater degree of rubification characteristic of argillic (Bt) horizons in late Pleistocene soil profiles in the area (table 2), but these soil properties are not as strongly developed as those in unit IV. Our interpretation is that the upper part offissure fill 2 is composed in large part of former unit V material or that the B horizon development represents post-faulting pedogenesis on the fissure fill.

Slip Rate for the Bare Mountain Fault

Recently, Ferrill et al.(1996) have suggested that by examining the age and distribution of alluvial fan sediments around Bare Mountain from literature and topographic maps, they can provide alternative constraints on the slip history of the Bare Mountain fault to those provided by detailed field studies. We strongly disagree with their methods and their conclusions (Anderson et al., 1997). Ferrill et al. (1996) claimed they analyzed alluvial fan sedimentation, while in essence, they only calculated alluvial fan areas and use the reported age of the alluvial fan surfaces. Alluvial fan volume is the important factor if one is truly analyzing alluvial fan sedimentation. In the Yucca Mountain area (as in many areas), the alluvial fan surfaces are clearly much younger than most of the alluvial fan deposit. It is also important to remember that the accommodation space for alluvial fans is not solely limited to tectonic subsidence.

More recently, Stamatakos et al. (in press) have determined that Little Cones, about 2 km east of trench BMT-3, may be the same age (0.76-1.1 Ma) as the much larger Red Cone and Black Cone which are located some 3-5 km further north-northeast. The size difference is believed by them to be due to partial burial of Little Cones by up to 25 m of alluvium, suggesting that the southern part of Crater Flat in the vicinity of Little Cones has subsided more than the northern part. Thus, the greater degree of subsidence is cited as additional evidence for increasing slip to the south on the Bare Mountain fault. We also strongly disagree with this more recent assessment. Little Cones may be partially buried, but it is being buried by the alluvial fans headed in the large Tarantula Canyon and Chuchwalla drainages and northern Crater Flat, not by alluvial fans originating from drainages directly to the west of Little Cones at the southern end of Bare Mountain. Regardless, using the youngest numerical estimate for Little Cones and assuming the 25 m of sediment burying the cone is due solely to the of tectonic subsidence of Crater Flat, yields a subsidence rate of only 0.03 mm/yr. This is essentially equivalent to the slip rate estimate of 0.01 mm/yr of Anderson and Klinger (1996a) derived for the Bare Mountain fault at trench BMT-3 given the resolution of the dating and confidence level in displacement measurements.

References Cited

Anderson, L. W. and R. E. Klinger, 1996a, Evaluation and characterization of Quaternary faulting--Bare Mountain fault zone, Nye County, Nevada: U.S. Bur. Recl. Seis. Rept. 96-5, 78 pp.

Anderson, L.W., and Klinger, R.E., 1996b, The Beatty scarp in Nye County, Nevada - An important late Quaternary morphologic datum: Bull. Seis. Soc. Am., v. 86, p. 1650-1654.

Anderson, L.W., R.E. Klinger, and D.S. Anderson, 1997, Quaternary slip history of the Bare Mountain fault (Nevada) from the morphology and distribution of alluvial fan deposits

(Comment): Geology, v. 25, p. 189.
Buckram, R. C. and R. E. Anderson, 1979, Estimation of fault-scarp ages from a scarp-height-slope-angle relationship: Geology, v. 7, p. 11-14.
Cornwall, H. R. and F. J. Kleinhampl, 1961a, Geology of the Bare Mountain Quadrangle, Nevada: U.S. Geol. Surv. Geol. Quad. Map.
Ferrill, David A., Stamatakos, John A., Jones, Sidney M., Rahe, Bret, McKague, H. Lawrence, Martin, Ronald H., and Morris, Alan P., 1996, Quaternary slip history of the Bare Mountain fault (Nevada) from the morphology and distribution of alluvial fan deposits: Geology, v. 24, no. 6, p. 559-562.
Hanks, Thomas C, and Andrews, D.J., 1989, Effect of far-field slope on morphologic dating of scarplike landforms: Journal of Geophysical Research, v. 94, p. 565-573.
Monsen, S. A., M.D. Carr, M. C. Reheis, and P. P. Orkild, 1992, Geologic map of Bare Mountain, Nye County, Nevada: U.S. Geol. Surv. Misc. Inv. Ser. Map 1-2201.
Reheis, M. C., 1988, Preliminary study of Quaternary faulting on the east side of Bare Mountain, Nye County, Nevada, *in* M.D. Carr and J. C. Yount, eds., Geologic and Hydrologic Investigations of a Potential Nuclear Waste Disposal Site at Yucca Mountain, Southern Nevada: U.S. Geol. Surv. Bull. 1790,
Swadley, W.C., D. L. Hoover, and J. N. Rosholt, 1984, Preliminary report on late Cenozoic faulting and stratigraphy in the vicinity of Yucca Mountain, Nye County, Nevada: U.S. Geol. Surv. Open-File Rept. 84-788.
Swadley, W.C., and Parrish, L.D., 1988, Surficial geologic map of the Bare Mountain quadrangle, Nye County, Nevada: U.S. Geological Survey Miscellaneous Field Studies Map
Anderson, L. W. and R. E. Klinger, 1996a, Evaluation and characterization of Quaternary faulting--Bare Mountain fault zone, Nye County, Nevada: U.S. Bur. Recl. Seis. Rept. 96-5, 78 pp.

Day 2, Stop 5

Hydrogeologic Studies at the USGS Amargosa Desert Research Site

Brian J. Andraski and David A. Stonestrom

In 1976, the U.S. Geological Survey (USGS) began studies of unsaturated-zone hydrology in the Amargosa Desert in support of the USGS Low-Level Radioactive Waste Program. In 1983, agreements with the Bureau of Land Management and the State of Nevada established two field study areas: a 16-ha area adjacent to a waste-burial facility 17 km south of Beatty and a 0.1-ha area about 3 km farther south (fig. 1A). The study areas are collectively known as the Amargosa Desert Research Site (ADRS). Investigations at the ADRS have provided long-term benchmark information about hydraulic characteristics and soil-water movement for undisturbed conditions and for simulated waste-site conditions in arid environments. In 1995, as a result of unexpectedly finding high concentrations of tritium and carbon-14 in the unsaturated zone beneath the ADRS, the scope of research was broadened to include the study of processes affecting radionuclide transport. The ADRS was incorporated into the USGS Toxic Substances Hydrology Program in 1997. Research at the site is a multidisciplinary, collaborative effort that involves scientists from the USGS, universities, research institutes, and national laboratories. The overall objective for research at the site is to improve understanding of and methods for characterizing mechanisms that control subsurface migration and fate of contaminants in arid environments.

Figure 1. Location of Amargosa Desert Research Site (ARDS) study areas near Beatty, Nevada.

Annual precipitation at the ADRS averages about 108 mm. Annual pan evaporation is about 1,900 mm (Nichols, 1987). Air temperatures average 3 °C during December and 33 °C during July (Andraski and others, 1995). Vegetation in the area is sparse; creosote bush [*Larrea tridentata* (DC.) Cov.], an evergreen shrub, is the dominant species. Soils and sediments are typically coarse textured and highly stratified (Andraski, 1996). Sediments in the area are primarily fluvial and alluvial-fan deposits that are at least 170 m thick. Depth to the water table ranges from 85 to 115 m (Nichols, 1987; Fischer, 1992).

Different experimental sites at the ADRS have been established over the years to support research of flow and transport processes. An instrument shaft was installed in 1983 to facilitate emplacement and maintenance of monitoring devices in undisturbed sediments in the upper 13 m of the unsaturated zone (figs. 1B and 2; Fischer, 1992). Three disturbed sites established in 1987 allowed comparison of arid-site hydrology under undisturbed, vegetated soil (fig. 2), devegetated soil, and simulated waste-trench conditions (figs. 1B and 3; Andraski, 1990). Ground-water level has been monitored at well MR-3 (fig. 1B). Deep test holes drilled near the instrument shaft and at the 0.1-ha study area have been used for measurements of temperature, water potential, and air pressure, and for collection of soil gas samples throughout the thick unsaturated zone (Fischer, 1992; Prudic and Striegl, 1995; Andraski and Prudic, 1997). The presence of radioactive contaminants (tritium and carbon-14) beneath the 16-ha research area was determined on the basis of gas samples collected during 1994-95 from test hole UZB-2 (fig. 1B). An array of soil-gas probes in undisturbed, near-surface sediments was installed in 1997 to allow for

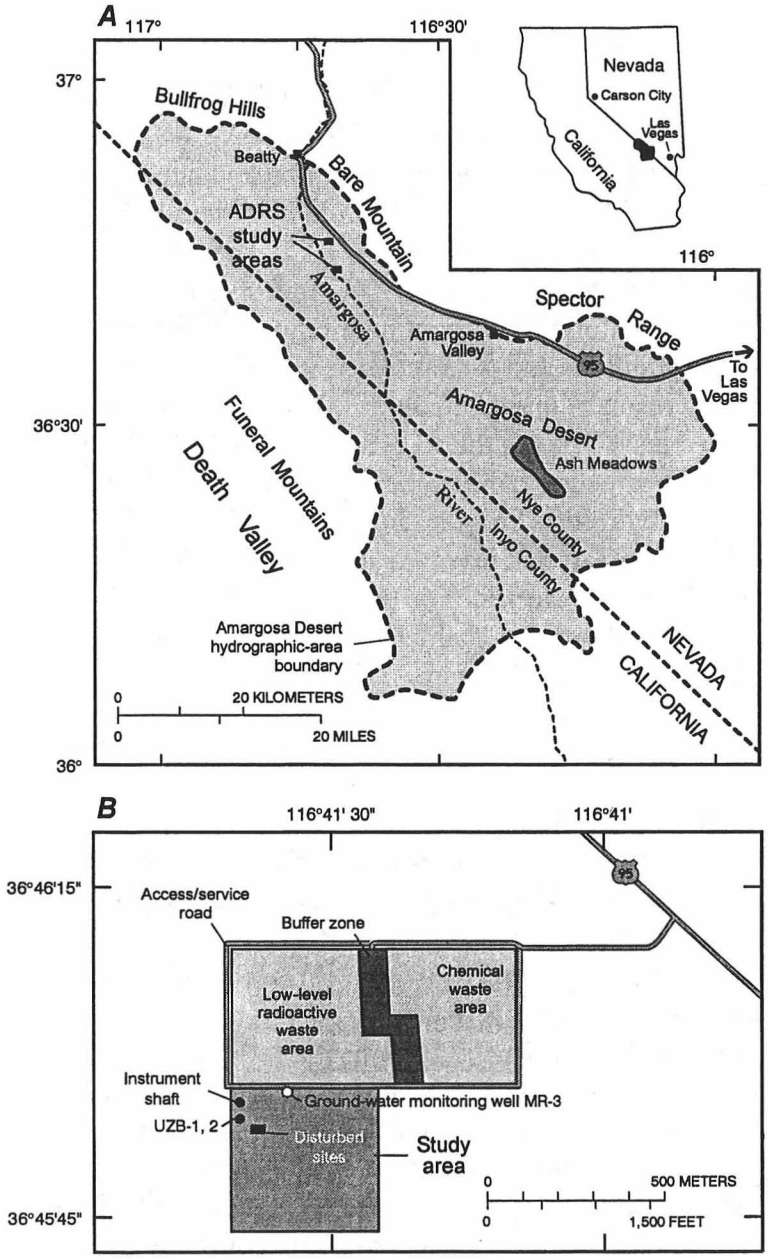

Figure 1. Location of (***A***) Amargosa Desert Research Site (ADRS) study areas near Beatty, Nev., and (***B***) 16-hectare study area adjacent to waste-burial facility. The instrument shaft and unsaturated-zone boreholes UZB-1 and UZB-2 are located in undisturbed sediments.

periodic collection and analysis of the chemical composition of unsaturated zone air (Striegl and others, 1998).

Figure 2. Diagram of instrument shaft used to study hydrologic processes under undisturbed conditions.

Figure 3. Diagram of instrumentation used to study hydrologic processes under devegetated soil and simulated waste-trench conditions.

The following summaries present some significant findings from the ADRS. Additional information is available on the ADRS web page at http://nevada.usgs.gov/adrs/.

■ Data from beneath undisturbed, vegetated areas have provided a conceptual understanding of moisture and gas movement through the unsaturated zone:

- Chloride mass-balance estimates suggested that percolation of precipitation below a depth of 10 m has been minimal or nonexistent for at least 6,000 (Fouty, 1989) to 16,000 years (Prudic, 1994).
- Water-potential gradients between depths of 9 and 48 m and the geothermal gradient indicated upward driving forces for water flow (Fischer, 1992; Prudic, 1994; Andraski and Prudic, 1997).
- Distribution of carbon dioxide suggested degassing from ground water and upward movement of carbon dioxide gas to land surface (Prudic and Striegl, 1994).
- Profiles of deuterium and oxygen-18 concentrations in soil-pore water were consistent with the hypothesis of upward movement and evaporative discharge of ground water at land surface (Prudic and others, 1997).

■ Multiple-year field and laboratory investigations indicated the degree to which features of the natural system can be altered by installation of a waste-disposal facility:

- Test-trench construction significantly altered properties and variability of the natural site environment; results demonstrated that the lower limit to which hydraulic characterization data normally are measured (−1.5 MPa) is not adequate for nonirrigated, desert soils and plants (Andraski, 1996).
- Under devegetated waste-site conditions, continued accumulation and shallow (1–2 m) downward penetration of infiltrated water was observed during a 5-year test period. In contrast, native plants in an undisturbed setting effectively removed available moisture to the extent that the potential for deep percolation of precipitation was limited; episodic, deep drying during periods of below-average precipitation further limited the potential for deep percolation (Gee and others, 1994; Andraski, 1997).

■ Data are being collected to improve understanding of factors and processes that control transport of radioactive contaminants through the unsaturated zone:

- Initial gas samples collected from test hole UZB-2 (fig. 1B) show elevated tritium concentrations in water vapor to a depth of 108.8 m and elevated carbon-14 concentrations in carbon dioxide gas to a depth of 34 m; tritium concentration in ground water collected from UZB-2 at the time of drilling was below detection (Prudic and

Striegl, 1995; Striegl and others, 1996). Gas samples collected in 1997 indicate that tritium concentrations in the upper 50 m of the unsaturated zone have stabilized and tritium concentrations in soil gas below 50 m have increased since they were last sampled (Striegl and others, 1998).

- Tritium concentrations in gas samples collected in 1997 from a coarse gravel layer (1-2 m deep) within 300 m of the waste burial area indicate a general trend of increasing concentrations toward the burial area; values range from 16 ± 9 to 36,900 ± 300 tritium units. The coarse gravel layer is thought to provide a preferential pathway for radionuclide movement (Striegl and others, 1998).

References Cited

Andraski, B.J., 1990, Water movement and trench stability at a simulated arid burial site for low-level radioactive waste near Beatty, Nevada: La Grange Park, Ill., American Nuclear Society, Nuclear Waste Isolation in the Unsaturated Zone, Las Vegas, Nev., September 1989, Proceedings, p. 166-173.

——1996, Properties and variability of soil and trench fill at an arid waste-burial site: Soil Science Society of America Journal, v. 60, p. 54-66.

——1997, Soil-water movement under natural-site and waste-site conditions--A multiple-year field study in the Mojave Desert, Nevada: Water Resources Research, v. 33, no. 9, p. 1901-1916.

Andraski, B.J., and Prudic, D.E., 1997, Soil, plant, and structural considerations for surface barriers in arid environments--Application of results from studies in the Mojave Desert near Beatty, Nevada, *in* Barrier Technologies for Environmental Management, Summary of a Workshop: Washington, D.C., National Academy Press, p. D50-D60.

Andraski, B.J., Prudic, D.E., and Nichols, W.D., 1995, Waste burial in arid environments--Application of information from a field laboratory in the Mojave Desert, southern Nevada: U.S. Geological Survey Fact Sheet FS-179-95, 4 p.

Fischer, J.M., 1992, Sediment properties and water movement through shallow unsaturated alluvium at an arid site for disposal of low-level radioactive waste near Beatty, Nye County, Nevada: U.S. Geological Survey Water-Resources Investigations Report 92-4032, 48 p.

Fouty, Suzanne, 1989, Chloride mass-balance as a method for determining long-term ground-water recharge rates and geomorphic surface stability in arid and semi-arid regions--Whiskey Flat and Beatty, Nevada: Tucson, University of Arizona, unpublished M.S. thesis, 130 p.

Gee, G.W., Wierenga, P.J., Andraski, B.J., Young, M.H., Fayer, M.J., and Rockhold, M.L., 1994, Variations in water balance and recharge potential at three western desert sites: Soil Science Society of America Journal, v. 58, no. 1, p. 63-72.

Nichols, W.D., 1987, Geohydrology of the unsaturated zone at the burial site for low-level radioactive waste near Beatty, Nye County, Nevada: U.S. Geological Survey Water-Supply Paper 2312, 57 p.

Prudic, D.E., 1994, Estimates of percolation rates and ages of water in unsaturated sediments at two Mojave Desert sites, California-Nevada: U.S. Geological Survey Water-Resources Investigations Report 94-4160, 19 p.

Prudic, D.E., Stonestrom, D.A., and Striegl, R.G., 1997, Tritium, deuterium, and oxygen-18 in

water collected from unsaturated sediments near a low-level radioactive-waste burial site south of Beatty, Nevada: U.S. Geological Survey Water-Resources Investigations Report 97-4062, 23 p.

Prudic, D.E., and Striegl, R.G., 1994, Water and carbon dioxide movement through unsaturated alluvium near an arid disposal site for low-level radioactive waste, Beatty, Nevada [abs.]: Eos, American Geophysical Union Transactions, v. 75, no. 16, p. 161.

——1995, Tritium and radioactive carbon (^{14}C) analyses of gas collected from unsaturated sediments next to a low-level radioactive-waste burial site south of Beatty, Nevada, April 1994 and July 1995: U.S. Geological Survey Open-File Report 95-741, 7 p.

Striegl, R.G., Healy, R.W., Michel, R.L., and Prudic, D.E., 1998, Tritium in unsaturated zone gases and air at the Amargosa Desert Research Site, and in spring and river water, near Beatty, Nevada, May 1997: U.S. Geological Survey Open-File Report 97-778, 13 p.

Striegl, R.G., Prudic, D.E., Duval, J.S., Healy, R.W., Landa, E.R., Pollock, D.W., Thorstenson, D.C., and Weeks, E.P., 1996, Factors affecting tritium and ^{14}carbon distributions in the unsaturated zone near the low-level radioactive-waste burial site south of Beatty, Nevada: U.S. Geological Survey Open-File Report 96-110, 16 p.

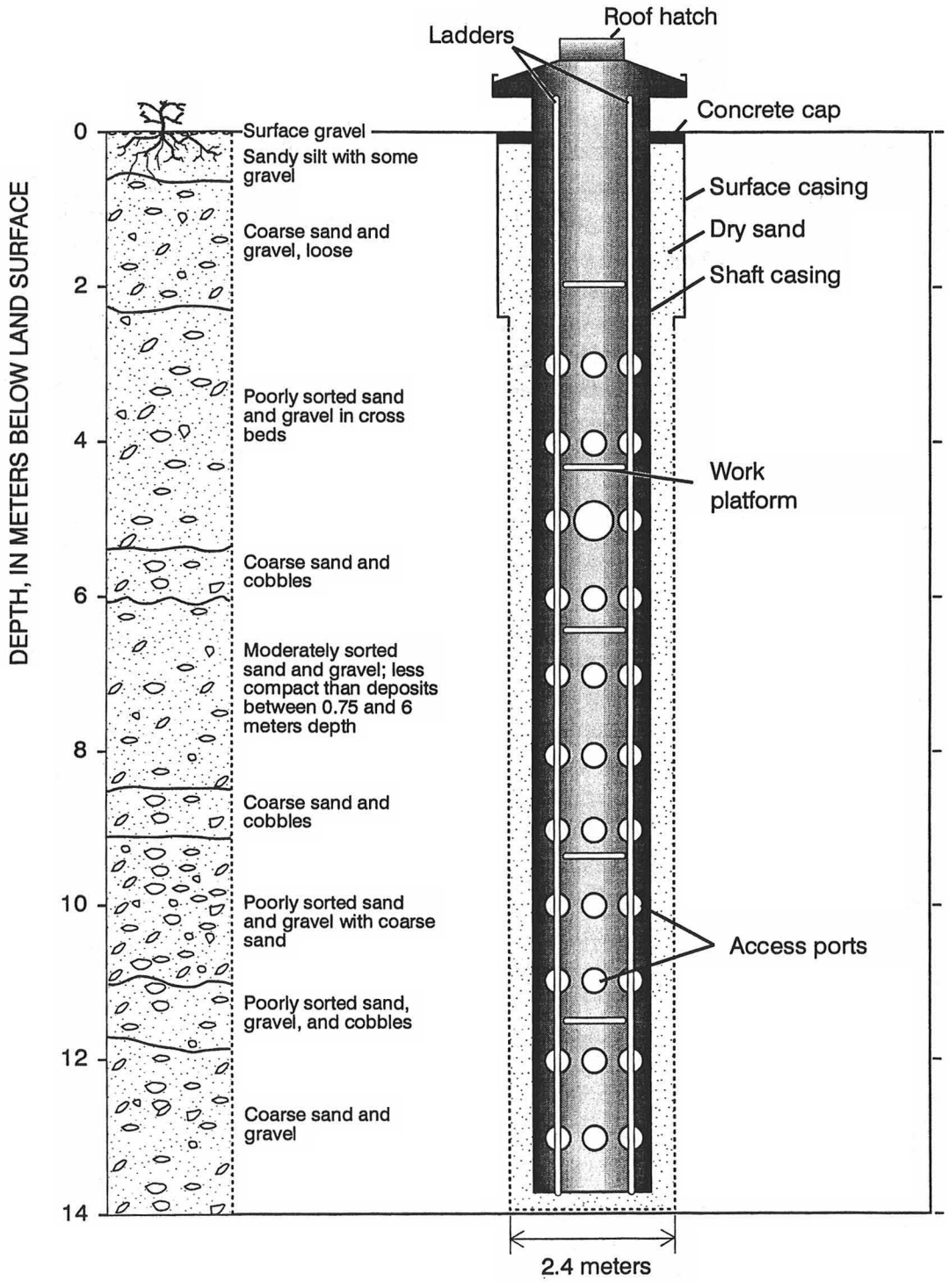

Figure 2. Diagram of instrument shaft used to study hydrologic processes under undisturbed conditions.

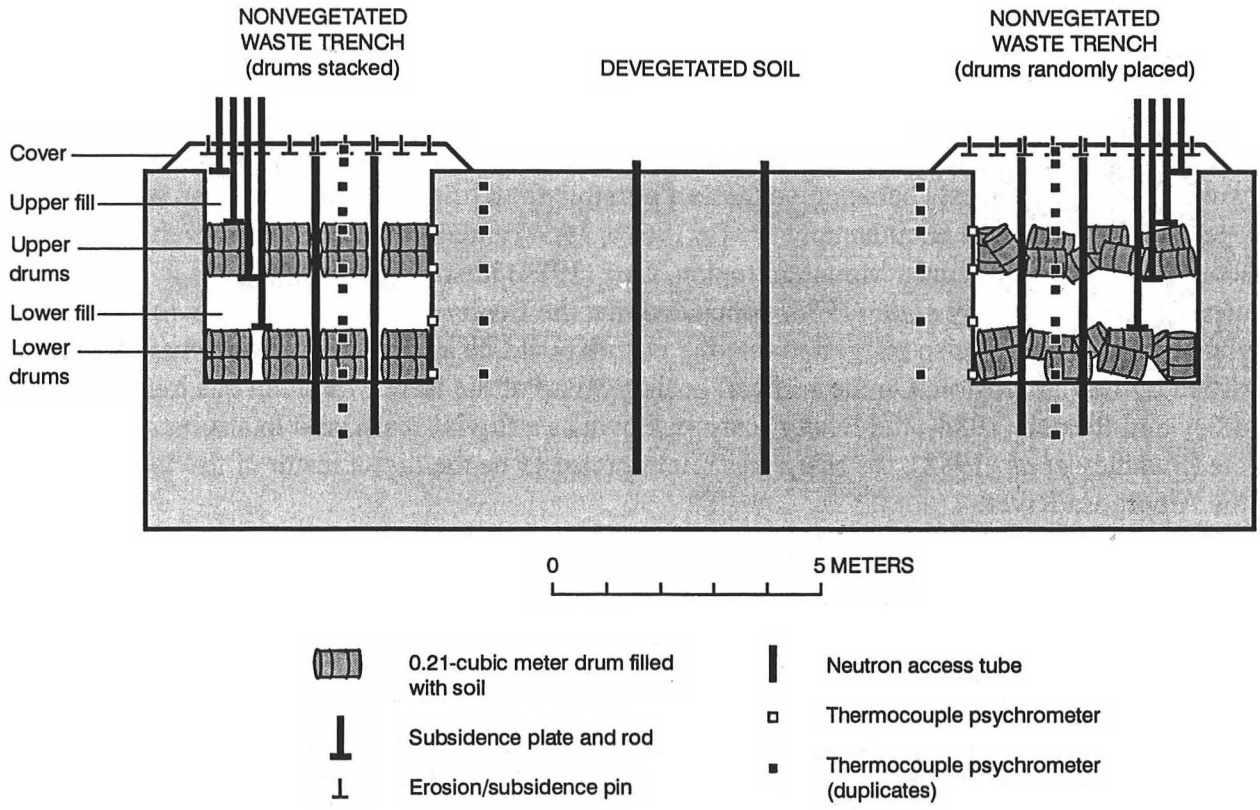

Figure 3. Diagram of instrumentation used to study hydrologic processes under devegetated soil and simulated waste-trench conditions.

Day 2, Stop 6

Beatty Scarp

Larry W. Anderson and Ralph E. Klinger

The Beatty scarp strikes north to north-northwest for 11 km along the west side of Bare Mountain immediately east of Highway 95 (Fig. 1, Anderson and Klinger, this volume). The scarp generally follows the contact between the alluvial fans emanating from Bare Mountain and the fluvial deposits of the Amargosa River. The Amargosa River is an ephemeral stream that originates near the northern end of Oasis Valley, about 15 km north of Beatty. The river flows south through Oasis Valley before exiting the valley immediately south of Beatty through a canyon termed the Amargosa Narrows. The Narrows separates the Bullfrog Hills on the west from Bare Mountain on the east. After emerging from the Narrows, the river continues south to southeast across the Amargosa Desert.

The trend of the Beatty scarp, subparallel to the Bare Mountain range front with an apparent down-to-the-west character, suggests a possible fault origin. The feature was first mapped by Cornwall and Kleinhampl (1961a, 1961b, 1964) and, in the description of the structural setting of the Yucca Mountain region, Carr (1984) identified this feature as a Quaternary fault. Swadley *et al. (1986)* concluded that the Beatty scarp probably was formed by fluvial erosion, but they also suggested that the feature could be an older fault scarp that had been modified by fluvial erosion. On the surficial geologic map of the Bare Mountain quadrangle by Swadley and Parrish (1988), the Beatty scarp is shown as a fluvial scarp, and in a subsequent article (Swadley *et al.,* 1988), the scarp was reinterpreted to be the direct result of fluvial erosion by the Amargosa River.

Age control

The age of the Beatty scarp is constrained by three radiocarbon ages. In a trench (BF-1) across the scarp, carbonized wood fragments from a silt bed interbedded with the fluvial sand and gravel at the base of the scarp yielded a radiocarbon age of 10,000±300 yr (10,450 to 12,550 cal yr B.P.; 2σ confidence), while a sample of charcoal from the same stratigraphic horizon exposed 1 km southwest of trench BF-1 yielded a radiocarbon age of 9800±300 yr (10,150 to 12,350 cal yr B.P.; 2σ confidence) (Swadley *et al.,* 1986). A third radiocarbon age of 8300 ±75 yr (9000 to 9440 cal yr B.P.;2σ confidence) was obtained on charcoal from similar fluvial deposits 2 km south of Beatty (Swadley *et al.,* 1984). The three radiocarbon ages on fluvial deposits associated with formation of the Beatty scarp provide a minimum age for the formation of the scarp of about 9 ka.

Ages on spring deposits in the area indicate that the last pluvial maximum in southern Nevada began about 14 ka (Quade *et al.,* 1995). Considering that the Amargosa River probably responded to these same environmental conditions, and given the range of the radiocarbon ages, the Beatty scarp probably formed sometime between 9000 and about 13,000 yr ago.

Scarp Morphology

Topographic profiling has been widely used in the western United States to approximate the ages of fault scarps and other scarp-like features (Wallace, 1977, 1984; Bucknam and

Anderson, 1979; Hanks *et al.*, 1984; Nash, 1984; Machette and Personius, 1984; Pierce and Colman, 1986). Anderson and Klinger (1996b) measured 22 scarp profiles across the main trace of Beatty scarp using electronic surveying equipment. Measurements of scarp height, scarp offset, maximum scarp-slope angle, and far-field-slope angle were derived from computer-generated plots of these profiles (Fig. 2). The maximum scarp height measured on the Beatty scarp is 29.5 m, and the maximum scarp-slope angle is 35° (Table 1). The maximum scarp height was measured north of the middle of the scarp (south of Fluorspar Canyon; Fig. 1, profile 8), and the lowest scarp height was measured at the south end of the scarp near the site of Carrara (profile 22; near FOP Stop 5).The maximum scarp-slope angle and scarp height of the 22 Beatty scarp profiles are plotted (Fig. 3a). The regression of maximum scarp-slope angle (θ) on the log of scarp height (H) results in a line with the equation

$$\theta = 14.1 + 14.6 \log (H)$$

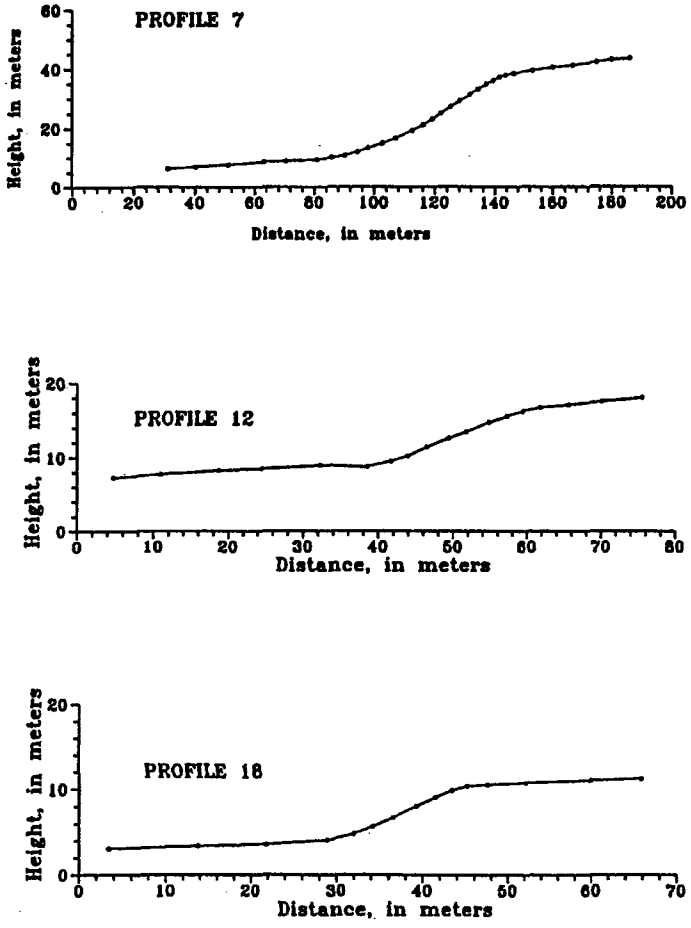

Figure 2. Representative scarp profiles of the Beatty scarp.

Table 1: Beatty Scarp Profile Data[†]

Profile	Scarp height[‡] (meters)	Scarp offset[§] (meters)	Maximum scarp-slope angle[*] (degrees)	Far-field slope angle[#] (degrees)	
				Upper	Lower
1	10.8	9.0	26.0	6.0	3.0
2	11.0	9.5	26.5	5.0	1.5
3	6.4	5.0	23.5	4.5	3.5
4	8.0	6.5	27.5	4.5	4.0
5	5.9	5.0	28.0	3.5	3.0
6	15.0	12.0	28.0	6.5	4.5
7	27.0	22.5	35.0	7.0	4.0
8	29.5	27.0	35.0	7.0	-1.0
9	5.9	5.0	27.5	3.0	3.0
10	7.3	6.5	30.0	3.5	2.5
11	3.5	3.0	25.0	4.0	3.0
12	3.0	2.5	27.0	3.0	5.0
13	3.2	3.0	24.5	0.5	1.0
14	6.0	5.5	30.0	2.0	0
15	6.8	6.0	26.0	1.5	1.0
16	3.6	3.2	25.0	1.5	1.0
17	2.4	2.2	23.5	1.0	1.0
18	2.7	2.4	20.0	2.5	1.0
19	1.6	1.5	14.0	1.5	1.5
20	1.5	1.2	10.5	2.0	0.5
21	1.8	1.4	15.0	2.5	2.0
22	1.2	1.0	13.0	3.0	1.0

[†]All values for scarp characteristics were measured from computer-generated plots of the profiles. Errors associated with these measurements are ±0.1 meters and ±0.5 degrees respectively. Terminology used follows Hanks *et al.*, (1984). The location of the profiles are shown on Figure 1 and are listed from north to south.

[‡]Scarp height - vertical distance between the projections of the basal and crestal slopes at the mid-point of the scarp.

[§]Surface offset - the vertical distance separating the crestal and basal slopes. Because the crestal and basal slopes are not always parallel, the surface offset is measured at the midpoint of the scarp.

*Maximum scarp-slope angle - the maximum slope angle measured between the crest and base of the scarp.

#Far-field-slope angle - the slope angle of the ground surface adjacent to the scarp and is assumed to be the slope of the ground surface prior to the formation of the scarp. Steeper far-field-slopes influence the surface offset measurements and affect the rate of scarp degradation. In the case of the Beatty scarp, the basal (lower) and crestal (upper) slopes differ significantly in some cases. Therefore, both the upper and lower far-field-slopes are listed.

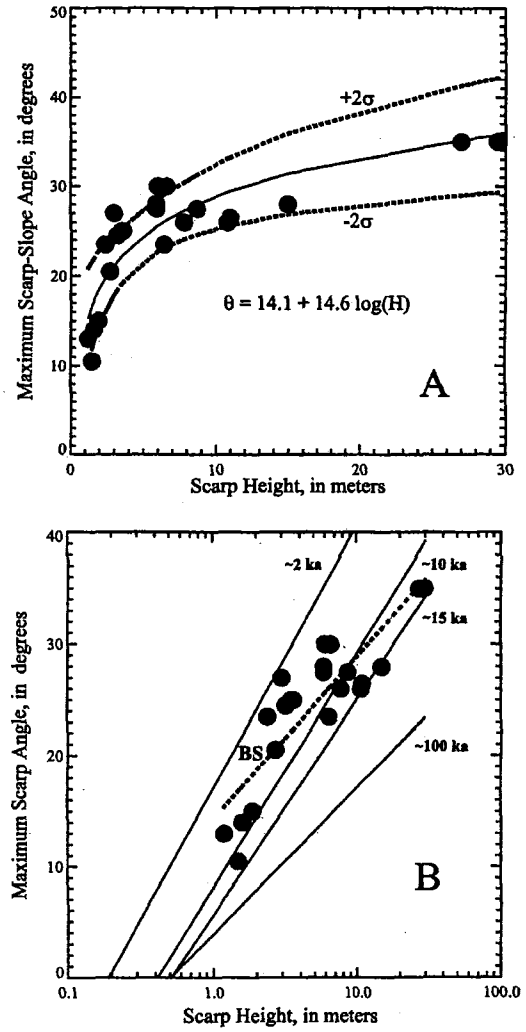

Figure 3. Plots of scarp profile data for the Beatty scarp. (A) Plot of scarp height (H) versus maximum scarp-slope angle (θ) for the Beatty scarp. (B) Scarp height versus maximum scarp-slope angle for the Beatty scarp)BS, dashed line) compared to the linear regressions for dated scarps in the Basin and Range [modified from Bucknam and Anderson (1979); ages from Bucknam *et al.*, (1989), Crone (1983), and Machette (1989)].

For comparison, the Beatty scarp data also are plotted (Fig. 3b) against the regressions of Buckram and Anderson (1979). The position of the Beatty scarp data with respect to the 10-ka regression line of Bucknam and Anderson (1979) is in agreement with the previously discussed radiocarbon ages that range between 9000 and 12,550 cal yr B.P. However, the slope in the equation for the Beatty scarp is less than that of similar-aged scarps described by Bucknam and Anderson (1979) and may reflect differences in aspect, climate, parent material, or the processes responsible for their formation.

Carrara Fault

The Carrara fault was originally described by D. B. Slemmons (memorandum to Rich Quittmeyer dated February 3, 1997; Slemmons, 1997a) and most recently discussed by Stamatakos et. al. (1997) and Slemmons (1997b). As currently postulated, the Carrara fault is a northwest-striking fault that follows the general alignment of U.S. Highway 95, extending from the general vicinity of Beatty, to the southern end of Bare Mountain (Fig. 1) and possibly as far as the southern end of Yucca Mountain near Fortymile Wash. The distance between the farthest-most points is almost 50 km. Recently acquired geophysical data, the presence of suspected Quaternary fault scarps, and areas of suspected Quaternary uplift are cited as evidence for Quaternary activity on the fault. This has important implications for the earthquake hazards and tectonic characterization of Yucca Mountain and vicinity.

Bedrock geology, geophysical data, structural, and geomorphic relationships strongly support the presence of faults in the Amargosa Desert along the southwest side of Bare Mountain. Such a structural feature or features is needed to explain Bare Mountain, the structural relationship between Proterozoic, Paleozoic, and Tertiary volcanic rocks west of Bare Mountain, the structural trough through which the Amargosa River currently flows, and the apparent southern truncation of the faults at Yucca Mountain.

From Beatty, south to the site of Carrara, the Amargosa River flows essentially due south and the dominant geomorphic features are the Beatty scarp and the alluvial fans shed off of the southwest flank of Bare Mountain. From the south end of Bare Mountain to Fortymile Wash near the south end of Yucca Mountain, a distance of about 15 km, drainages flow south to southwest. Quaternary alluvial deposits in this area are young (latest Pleistocene to Holocene) and are covered by a thin veneer of Holocene eolian sand. No topographic features or lineaments with west or northwest trends have been observed in this area. On the basis of preservation of the Beatty scarp, this indicates that the age of most recent activity on the Carrara is at least pre-Holocene and perhaps pre-latest Pleistocene. Thus, the recurrence of surface faulting events is long (i.e., > 10,000 yrs).

Clear geomorphic evidence for the Carrara fault in the approximately 15-km-long section between the site of Carrara and south end of Bare Mountain is the most problematic. In this area, the strike of the Carrara fault is parallel to the broad anastomosing stream channel of the Amargosa River. This is also the area where most of the evidence for Quaternary activity of the Carrara fault has been cited (Slemmons, 1997a, 1997b). This evidence consists of "possible fault scarps" and "uplifted Quaternary deposits" identified during aerial overflights or from analysis of aerial photographs. On the basis of extensive field observations and aerial photograph analysis made during the study of the Beatty scarp, it is believed that many of the features identified as possible fault scarps are most likely of fluvial origin.

A series of low, gravel capped hills are also present south of the site of Carrara and near

the U.S. Ecology site. These hills have been interpreted by Slemmons (1997a, 1997b) to be the result of possible Quaternary uplift. The hills, mapped as QTa by Swadley and Parrish (1988), occupy a small part of the 2-mile-wide, slightly topographically higher area between the main Amargosa River floodplain and the alluvial fans along the west side of Bare Mountain. Most of this topographically higher area consists of early Holocene Q1 deposits (Swadley and Carr, 1987; Swadley and Parrish, 1988; ^{14}C age of 9-13 kyrs B.P.). This "uplifted area" is not anomalous and is probably not the product of late Quaternary uplift. Similar features exist along the west side of the Amargosa River and throughout the region. We believe that this area of older deposits above younger deposits is more easily explained by normal fluvial processes. Large anastomosing streams like the Amargosa River exhibit periods of aggradation, lateral migration, and incision producing areas of higher and older deposits. It also is interesting to note that the present Amargosa River is incised into, and essentially flows down the center of the Amargosa Desert and does not appear to be affected by any recent tectonic activity in the vicinity of Highway 95.

In conclusion, the evidence cited for Quaternary activity of the Carrara fault is ambiguous at best and can easily be explained by normal fluvial processes. If the Carrara fault, or any other fault in the Amargosa Desert has experienced Quaternary activity, the rate of that activity is low enough that the geomorphic expression is very poor.

References Cited

Anderson, L.W., and Klinger, R.E., 1996b, The Beatty scarp in Nye County, Nevada - An important late Quaternary morphologic datum: Bull. Seis. Soc. Am., v. 86, p. 1650-1654.

Anderson, L.W., R.E. Klinger, and D.S. Anderson, 1997, Quaternary slip history of the Bare Mountain fault (Nevada) from the morphology and distribution of alluvial fan deposits (Comment): Geology, v. 25, p. 189.

Buckram, R. C. and R. E. Anderson, 1979, Estimation of fault-scarp ages from a scarp-height-slope-angle relationship: Geology, v. 7, p. 11-14.

Bucknam, R. C., A. J. Crone, and M. N. Machette, 1989, Characteristics of active faults, *in* National Earthquake Hazards Reduction Program, Summaries of Technical Reports, 28, U.S. Geol. Surv. Open-File Rept. 89-453, 117 p.

Carr, W. J., 1984, Regional structural setting of Yucca Mountain, southwestern Nevada, and late Cenozoic rates of tectonic activity in part of the southwestern Great Basin, Nevada and California: U.S. Geol. Surv. Open-File Rept. 84-854, 109 pp.

Cornwall, H. R. and F. J. Kleinhampl, 1961a, Geology of the Bare Mountain Quadrangle, Nevada: U.S. Geol. Surv. Geol. Quad. Map GQ-157.

Cornwall, H. R. and F. J. Kleinhampl, 1961b, Preliminary geologic map and sections of the Bullfrog Quadrangle, Nevada-California: U.S. Geol. Surv. Min. Inv. Map MF-177.

Cornwall, H. R. and F. J. Kleinhampl, 1964, Geology of the Bullfrog Quadrangle and ore deposits related to Bullfrog Hills caldera, Nye County, Nevada and Inyo County, California: U.S. Geol. Surv. Prof. Pap. 454-J, 25 pp.

Crone, A. J., 1983, Amount of displacement and estimated age of a Holocene surface faulting event, eastern Great Basin, Millard County, Utah, *in* A. J. Crone, ed., Paleoseismicity along the Wasatch Front and Adjacent Areas, Central Utah: Utah Geol. and Min. Surv. Spec. Studies 62, p. 49-55.

Hanks, T. C., R. C. Bucknam, K. R. Lajoie, and R. E. Wallace, 1984, Modification of wave-cut and faulting-controlled landforms: J. Geophys. Res., v. 89, p. 5771-5790.

Machette, M. N., 1989, Slope morphometric dating, *in* S. L. Forman, ed., Dating Methods Applicable to Quaternary Geologic Studies in the Western United States: Utah Geol. and Min. Surv. Misc. Publ. 89-7, p. 30-42.

Machette, M. N. and S. F. Personius, 1984, Map of Quaternary and Pliocene faults in the eastern part of the Aztec 1 o by 2° Quadrangle and the western part of the Raton 1° by 2° Quadrangle, northern New Mexico: U.S. Geol. Surv. Misc. Field Studies Map MF-1465-B.

Nash, D. B., 1984, Morphologic dating of fluvial terrace scarps and fault scarps near West Yellowstone, Montana: Geol. Soc. Am. Bull., v. 95, p. 1413-1424.

Pierce, K. L. and S. M. Colman, 1986, Effect of height and orientation (microclimate) on geomorphic degradation rates and processes, late-glacial terrace scarps in central Idaho: Geol. Soc. Am. Bull., v. 97, p. 869-885.

Quade, J., M.D. Mifflin, W. L. Pratt, W. McCoy, and L. Burckle, 1995, Fossil spring deposits in the southern Great Basin and their implications for changes in water-table levels near Yucca Mountain, Nevada, during Quaternary time: Geol. Soc. Am. Bull., v. 107, p. 213-230.

Slemmons, D.B., 1997a, Memorandum to Rich Quittmeyer, Yucca Mountain aerial reconnaissance on January 10, 1997 by David B. Slemmons and Norma Bigger, geologists, and Cady Johnson, pilot and geologist, dated February 3, 1997, 17 p.

Slemmons, D.B., 1997b, Carrara fault in southern Nevada from paleoseismic, geologic and geophysical evidence: Implications to the earthquake hazards and tectonics near Yucca Mountain, Nevada (abs.): EOS, Transactions, AGU, v. 78, no. 18, p. F453.

Stamatakos, et. al., 1997, The Carrara fault in southwestern Nevada revealed from detailed gravity and magnetic results: Implications for seismicity, volcanism, and tectonics near Yucca Mountain, Nevada (abs.): EOS, Transactions, AGU, v. 78, no. 18, p. F453.

Swadley, W.C., and Carr, W.J., 1987, Geologic map of the Quaternary and Tertiary deposits of the Big Dune quadrangle, Nye County, Nevada, and Inyo County, California: U.S. Geological Survey Miscellaneous Field Studies Map I-1767.

Swadley, W.C., D. L. Hoover, and J. N. Rosholt, 1984, Preliminary report on late Cenozoic faulting and stratigraphy in the vicinity of Yucca Mountain, Nye County, Nevada: U.S. Geol. Surv. Open-File Rept. 84-788.

Swadley, W.C., H. E. Huckins, and E. M. Taylor, 1986, Logs of trenches across the Beatty scarp, Nye County, Nevada: U.S. Geol. Surv. Misc. Field Studies Map MF-1897.

Swadley, W.C., and Parrish, L.D., 1988, Surficial geologic map of the Bare Mountain quadrangle, Nye County, Nevada: U.S. Geological Survey Miscellaneous Field Studies Map I-1826.

Swadley, W.C., J. C. Yount, and S. T. Harding, 1988, Reinterpretation of the Beatty scarp, Nye County, Nevada, *in* M.D. Carr and J. C. Yount, eds., Geologic and Hydrologic Investigations of a Potential Nuclear Waste Disposal Site at Yucca Mountain, Southern Nevada: U.S. Geol. Surv. Bull. 1790, p. 113-119.

Wallace, R. E., 1977, Profiles and ages of young fault scarps, north-central Nevada: Geol. Soc. Am. Bull., v. 88, p. 1267-1281.

Wallace, R. E., 1984, Fault scarps formed during the earthquakes of October 2, 1915, in Pleasant Valley, Nevada, and some tectonic implications in faulting related to the 1915 earthquakes in Pleasant Valley, Nevada: U.S. Geol. Surv. Profess. Pap1274-A.